MECH

STRIBUTION S
pproved for P
Distribution

Book of Abstracts

19-23 November 2000
Eindhoven University of Technology
The Netherlands

AF FOR-04-0051

EFMC2000
LOCAL ORGANISING COMMITTEE

- G.J.F. van Heijst
  (chairman)
- H.J.H. Clercx
  (scientific secretary)
- M.E.H. van Dongen
- C.C.M. Rindt
  (treasurer)
- A.A. van Steenhoven
- A.M.E.H. Peeters
  (EFMC2000 Conference Office)
- M.C.J. Tielemans
  (EFMC2000 Conference Office)
- C. Damsma
  (University Congress Office)

phone: *+ 31 40 247 3110*
or *+ 31 40 247 2140*
fax: *+ 31 40 246 4151*
or *+ 31 40 243 3445*
e-mail: *info@efmc2000.tue.nl*
web: *http://www.efmc2000.tue.nl*

EUROMECH
FLUID MECHANICS CONFERENCE
COMMITTEE

P. Blondeaux, Genoa
D.G. Crighton, Cambridge
(deceased on 12 April 2000)
H.H. Fernholz, Berlin
G.J.F. van Heijst, Eindhoven
E.J. Hopfinger, Grenoble
P.A. Monkewitz, Lausanne
T.J. Pedley, Cambridge
L. van Wijngaarden, Enschede
(chairman)

CIP DATA
LIBRARY TECHNISCHE
UNIVERSITEIT EINDHOVEN

Abstracts of papers presented at the 4th EUROMECH Fluid Mechanics Conference, held 19-23 November 2000 in Eindhoven, The Netherlands.
ISBN 90-386-2652-5
NUGI 841

The 4th EUROMECH Fluid Mechanics Conference

EUROMECH - the European Mechanics Society - is an international non-governmental non-profit scientific organisation.

The objective of the Society is to engage in all activities intended to promote in Europe the development of mechanics as a branch of science and engineering. Mechanics deals with motion, flow and deformation of matter, be it fluid or solid, under the action of applied forces, and with any associated phenomena.

The 4th EUROMECH Fluid Mechanics Conference is held at Eindhoven University of Technology, Eindhoven, The Netherlands from 19 to 23 November 2000.
The objective of the Conference is to bring together fluid dynamicists active inside or outside Europe, to provide a platform for discussion, exchange of expertise and experience to further incite research activities.

Like the previous ones (Cambridge 1991, Warsaw 1994, Göttingen 1997) this Conference comprises the whole field of Fluid Mechanics: turbulence, computational fluid dynamics, multiphase flow, compressible flow, transport and mixing, industrial applications etc.

The Conference starts on Sunday 19 November at 13.30 hrs. The on-site Conference Desk is opened from 11.00 hrs onwards. The programme contains 11 plenary keynote lectures, 3 mini-symposia, and about 300 contributed papers presented in lecture and poster sessions.

DISTRIBUTION STATEMENT A
Approved for Public Release
Distribution Unlimited

20010108 058

AQ F01-04-0689

DTIC QUALITY INSPECTED 3

Programme Overview

Sunday 19 November 2000

11.00 – 13.30	Registration					
13.30 – 13.40	OPENING					
13.40 – 14.15	Memorial addresses in honour of George K. Batchelor and David G. Crighton by H.H. Fernholz, H.K. Moffatt and T.J. Pedley					
14.15 – 14.20	Intermission					
14.20 – 15.20 (3 x 20 min.)	BDP-1 (see pp. 13-15)	Tu-1 (see pp. 31-33)	SNM-1 (see pp. 47-49)	BL-1 (see pp. 61-63)	EFM-1 (see pp. 75-77)	Wa-1 (see pp. 95-97)
15.20 – 15.50	Break					
15.50 – 16.50 (3 x 20 min.)	BDP-1 (cont'd) (see pp. 16-17)	Tu-1 (cont'd) (see pp. 34-36)	SNM-1 (cont'd) (see pp. 50-52)	BL-1 (cont'd) (see pp. 64-66)	EFM-1 (cont'd) (see pp. 78-80)	Wa-1 (cont'd) (see pp. 98-99)
16.50 – 17.50	G.I. Barenblatt: Fluid Mechanics in the 20th Century (see p. 1)					
17.50 – 18.15	Escort to the MUZIEKCENTRUM FRITS PHILIPS					
18.15 – 20.00	WELCOME RECEPTION					

REPORT DOCUMENTATION PAGE

Form Approved OMB No. 0704-0188

Public reporting burden for this collection of information is estimated to average 1 hour per response, including the time for reviewing instructions, searching existing data sources, gathering and maintaining the data needed, and completing and reviewing the collection of information. Send comments regarding this burden estimate or any other aspect of this collection of information, including suggestions for reducing this burden to Washington Headquarters Services, Directorate for Information Operations and Reports, 1215 Jefferson Davis Highway, Suite 1204, Arlington, VA 22202-4302, and to the Office of Management and Budget, Paperwork Reduction Project (0704-0188), Washington, DC 20503.

1. AGENCY USE ONLY (Leave blank)	2. REPORT DATE	3. REPORT TYPE AND DATES COVERED
	November 2000	Conference Proceedings

4. TITLE AND SUBTITLE

EUROMECH Fluid Mechanics Conference (EFMC2000)

5. FUNDING NUMBERS

F61775-01-WF002

6. AUTHOR(S)

Conference Committee

7. PERFORMING ORGANIZATION NAME(S) AND ADDRESS(ES)

Eindhoven University of Technology
Den Dolech
Eindhoven 5600 MB
The Netherlands

8. PERFORMING ORGANIZATION REPORT NUMBER

N/A

9. SPONSORING/MONITORING AGENCY NAME(S) AND ADDRESS(ES)

EOARD
PSC 802 BOX 14
FPO 09499-0200

10. SPONSORING/MONITORING AGENCY REPORT NUMBER

CSP 01-5002

11. SUPPLEMENTARY NOTES

12a. DISTRIBUTION/AVAILABILITY STATEMENT

Approved for public release; distribution is unlimited.

12b. DISTRIBUTION CODE

A

13. ABSTRACT (Maximum 200 words)

The Final Proceedings for EUROMECH Fluid Mechanics Conference (EFMC2000), 19 November 2000 - 23 November 2000

The Conference will cover various topics of field of Fluid Mechanics such as: Turbulence, Computational Fluid Dynamics, Multiphase Flows, Compressible Flow and Industrial Applications.

14. SUBJECT TERMS

EOARD, Fluid Mechanics, Aerodynamics, Combustion, Gas Dynamics

15. NUMBER OF PAGES

291

16. PRICE CODE

N/A

17. SECURITY CLASSIFICATION OF REPORT	18. SECURITY CLASSIFICATION OF THIS PAGE	19. SECURITY CLASSIFICATION OF ABSTRACT	20. LIMITATION OF ABSTRACT
UNCLASSIFIED	UNCLASSIFIED	UNCLASSIFIED	UL

Monday 20 November 2000

08.00 – 09.00	Registration					
09.00 – 09.45	D. Barthès-Biesel: Cell and Capsule Mechanics (see p. 2)					
09.45 – 10.30	J. Magnaudet: Some Recent Advances in the Understanding of Bubbly Flows (see p. 3)					
10.30 – 11.00	Break					
11.00 – 12.40 (5 x 20 min.)	BDP-2 (see pp. 18-22)	MD-1 (see pp. 109-113)	BFM-1 (see pp. 119-123)	St-1 (see pp. 143-147)	EFM-2 (see pp. 81-84)	MPF-1 (see pp. 163-167)
12.40 – 14.00	Lunch					
14.00 – 14.45	P. Luchini: Excitation Mechanisms of Boundary Layer Instabilities (see p. 4)					
14.45 – 16.05 (4 x 20 min.)	BDP-3 (see pp. 23-26)	RFVD-1 (see pp. 183-185)	BFM-2 (see pp. 124-127)	BL-2 (see pp. 67-69)	EFM-3 (see pp. 85-88)	SNM-2 (see pp. 53-55)
16.05 – 16.30	Break					
16.30 – 17.15	Oral summaries of posters (in 3 parallel Sessions: see pp. 213-248)					
17.15 – 18.00	POSTERS					
18.00 – 20.00	POSTERS + Drinks					

Tuesday 21 November 2000

09.00 – 09.45	L. Kleiser: Direct and Large-Eddy Simulation of Wall-Bounded Turbulent Flows (see p. 5)					
09.45 – 10.30	A. Dillmann: On the Internal Structure of Steady Cylindrical Supersonic Free Jets (see p. 6)					
10.30 – 11.00	Break					
11.00 – 13.00 (6 x 20 min.)	NN-1 (see pp. 195-200)	Tu-2 (see pp. 37-42)	BFM-3 (see pp. 128-133)	St-2 (see pp. 148-153)	Wa-2 (see pp. 100-104)	MPF-2 (see pp. 168-172)
13.15 – 14.15	Lunch in bus to Antwerp (Belgium)					
14.15 – 18.00	Social Programme in Antwerp (Belgium)					
18.00 – 22.00	Conference Banquet Alta Ripa (Oud Turnhout, Belgium)					

Wednesday 22 November 2000

09.00 – 09.45	H.I. Andersson: Effects of Rotation on Wall-Bounded Flows (see p. 7)					
09.45 – 10.30	A. Provenzale: Dispersion in Quasi-Geostrophic Flows (see p. 8)					
10.30 – 11.00	Break					
11.00 – 12.40 (5 x 20 min.)	NN-2 (see pp. 201-205)	MD-2 (see pp. 114-118)	RFVD-2 (see pp. 186-190)	St-3 (see pp. 154-158)	EFM-4 (see pp. 89-91)	MPF-3 (see pp. 173-176)
12.40 – 14.00	Lunch					
14.00 – 14.45	D.H. Peregrine: Water Waves at Sea Walls (see p. 9)					
14.45 – 16.05 (4 x 20 min.)	BDP-4 (see pp. 27-30)	RFVD-3 (see pp. 191-193)	BFM-4 (see pp. 134-137)	BL-3 (see pp. 70-73)	EFM-5 (see pp. 92-94)	Wa-3 (see pp. 105-108)
16.05 – 16.30	Break					
16.30 – 17.15	Oral summaries of posters (in 3 parallel Sessions: see pp. 249-285)					
17.15 – 18.00	POSTERS					
18.00 – 20.00	POSTERS + Drinks					

Thursday 23 November 2000

09.00 – 09.45	A. Liñan: The Role of Fluid Dynamics on Combustion in Unpremixed Systems (see p. 10)					
09.45 – 10.45 (3 x 20 min.)	BDF-1 (see pp. 207-209)	Tu-3 (see pp. 43-45)	BFM-5 (see pp. 138-140)	St-4 (see pp. 159-161)	SNM-3 (see pp. 56-58)	MPF-4 (see pp. 177-179)
10.45 – 11.15	Break					
11.15 – 11.55 (2 x 20 min.)	BDF-1 (cont'd) (see pp. 210-211)	Tu-3 (cont'd) (see p. 46)	BFM-5 (cont'd) (see p. 141)	St-4 (cont'd) -	SNM-3 (cont'd) (see p. 59)	MPF-4 (cont'd) (see pp. 180-181)
11.55 – 12.00	Intermission					
12.00 – 12.45	F.T.M. Nieuwstadt: Experiments and Simulations in Turbulence Research (see p. 11)					
12.45 – 13.00	EUROMECH PRIZES + CLOSURE					
13.00 – 14.00	Lunch					

ABSTRACTS
KEYNOTE LECTURES

Fluid Mechanics in the 20^{th} Century

G.I Barenblatt

Miller Institute for Basic Research in Science, University of California, Berkeley,
United States of America

Abstract

Highlights of fluid dynamics development in the XX century will be presented and discussed. Some perspective branches of fluid dynamics born in the XX century will be outlined.

CELL AND CAPSULE MECHANICS

D. Barthès-Biesel,
UMR CNRS 6600, Université de Technologie de Compiègne, France.
Email :dbb@utc.fr

A capsule consists of an internal medium (pure or complex liquid), enclosed by a deformable membrane that is usually semi-permeable. Capsules are frequently met in nature (cells, eggs) or in industrial processes (biomedical, pharmaceutical, cosmetic or food industry). Capsules are found in a variety of sizes from a few microns (liposomes, living cells) to a few millimetres (artificial capsules). They may take different rest shapes (e.g., discoïdal geometry of a red blood cell), and the mechanical properties of the internal medium and of the membrane may vary widely.

The membrane is usually so thin that it is approximated by an elastic or viscoelastic 2D surface isotropic in its plane. If only small deformations are involved, a linear 2D Hooke law is appropriate. In the domain of large deformations, the proper choice of the membrane constitutive law is an open problem. A homogeneous gelatine membrane (commonly selected for its biocompatibilty) may be treated as a very thin sheet of a volume incompressible material. This leads to a Mooney-Rivlin law. Polymerised interfaces, such as nylon membranes, are well described by a Skalak law (Skalak et al. 1973) that accounts separately for the shear deformation and for the area dilatation of the material. The red blood cell membrane is almost area incompressible and this constraint regulates the cell response to stress. It follows that the interpretation of experiments designed to measure the mechanical properties of a capsule depends strongly on the law that is selected except in the range of small deformations.

Cells and many artificial capsules are usually suspended into another liquid subjected to flow. It is then important to be able to predict the motion and deformation of the particle under stress and the eventual occurrence of break-up. This involves the solution of two free surface flow problems (motion of the internal liquid and of the suspending fluid) in the range of low Reynolds numbers. Furthermore the large deformations of the elastic membrane must also be computed. This is a case of fluid-structure interactions in the range of very viscous flows. The coupling between fluid and solid mechanics is kinematic (no slip condition at the interface) and dynamic (equilibrium between viscous and elastic stresses on the membrane). An efficient method for solving such problems consists in recasting the Stokes equations in integral form and in using the boundary integral technique. This method has been successfully applied to different flow situations.

Axisymmetric elongational flow is simple and useful to assess the role of the intrinsic physical parameters on the capsule response to viscous stresses. An axisymmetric capsule of known properties is freely suspended in a pure straining motion and its transient response to the sudden start of the flow is computed until a steady state is reached. The model predicts that a capsule with a Mooney-Rivlin membrane will always burst through the process of continuous elongation when the flow strength exceeds a critical value. Conversely, a capsule with a Skalak type membrane reaches an asymptotic deformation and burst only if a failure criterion of the membrane material is exceeded. Such predictions are in qualitative agreement with experimental data obtained on artificial capsules freely suspended in a plane hyperbolic flow..

Similarly, the axisymmetric flow of a cell or of a capsule in a small pore has been computed. This model allows the interpretation of filtration experiments of a dilute suspension of red blood cells. It can also be used to explain the erythropoiesis, i.e., the process by which newly formed cells are ejected from the bone marrow into the blood flow.

Some recent advances in our understanding of bubbly flows: From local bubble hydrodynamics to "real" bubbly flows

JACQUES MAGNAUDET
Institut de Mcanique des Fluides de Toulouse, UMR CNRS/INPT/UPS 5502
2, avenue Camille Soula 31400 Toulouse FRANCE magnau@imft.fr

During the last decade, our understanding of bubble hydrodynamics and bubbly flows has progressed tremendously due to a combination of new experimental techniques, analytical derivation of asymptotic results, and systematic use of direct numerical simulations. In the first part of this talk I shall consider those of these progresses concerning isolated bubbles. In particular, I shall discuss hydrodynamic forces acting on clean and contaminated bubbles in unsteady and/or inhomogeneous flows, dynamics of bubble wakes in the high-Reynolds-number regime, and bubble-bubble or bubble-wall interactions. In the second part I shall try to show how these local informations can be used to understand the characteristics of the disturbances produced by the presence of many bubbles (with however a low volume fraction) in a given flow. I shall focus on some "simple" situations, especially those in which bubbles are randomly injected either in a stagnant liquid layer or in a free shear layer. I shall show how some physical processes involved in these situations can be explained in terms of basic instability mechanisms and dynamical system theory, and how the predictions of simple models compare with experiments.

Excitation mechanisms of boundary layer instabilities

Paolo Luchini
Dipartimento di Ingegneria Aerospaziale
Politecnico di Milano, Italy
Email: paolo.luchini@polimi.it

Keywords - Boundary layer - Stability - Receptivity - Transient growth

Abstract -

The practical need to describe, predict and hopefully influence transition to tu rbulence, on an airplane wing for instance, has kept the interest high for studies of boundary-l ayer stability. The elongated character of the boundary layer gives a sequential spatial structure to the evolution of disturbances, with a linear amplification region where disturbances build up, followed by a transition proper, in which nonlinearities rapidly produce breakup to turbulence, and preceded by a receptivity region in which sensitivity to external disturbances is highest.

Most efforts have been traditionally devoted to the linear amplification region, where a relatively general analysis can be performed by representing a disturbance as a superposition of modes. In fact, practically all the techniques and numerical methods still today employed for transition prediction simplify the effect of the receptivity and breakup regions to the point of establishing fixed amplitudes at the beginning and exit of the linear region. These are the so-called "e^N" methods. There are, however, a number of important advances th at have been made in relatively recent times in the comprehension of boundary layer stability, and these should definitely be incorporated in the prediction methods .

First, the discovery of transient growth has radically changed the picture of fl uid motion instabilities. Actually it is hard to call it a discovery: researchers ha ve known all along that dynamical systems ruled by a non-symmetric (or, more generally, non-self-adjoint or non-normal) evolution operator have non-orthogona l and possibly degenerate eigenvectors. However, it was not realized for a long time (except by a few researchers under the lead of Marten Landahl) how deep the effects of non-normality can be in the context of fluid mechanics. In a boundary layer, this type of disturbances has a structure very similar to Görtler vortices, but with the added difficulty that they never acquire a separable structure, not even far downstream. Interestingly enough, in the small-wavenumber limit algebraic growth in a boundary layer becomes a true instability, no longer a transient. But, above all, algebraic instabilities can grow in a Reynolds number range where other disturbances do not grow at all, and can therefore explain a few phenomena of subcritical transition. It is today possible to characterize the algebraic transient growth in a boundary layer completely, but this knowledge st ill waits to be incorporated in the transition-prediction techniques. There is still no algorithm for the analysis of wings that considers other than modal disturbances.

The other important advance that has occurred in relatively recent times is the development of adjoint methods for the calculation of receptivity. In fact, transition is a sensitive phenomenon that can be influenced by external factors in several ways; character izing this sensitivity is the receptivity problem, and the sensitivity itself, once quantitatively defined, can be given the name of receptivity. The adjoint method enables us today to determine the receptivit y and maximum growth of both classical (modal) and non-modal disturbances, and to compare their relative importance. Adjoint methods are just beginning to be incorporated in practical tools for transition prediction.

Direct and Large-Eddy Simulation of Wall-Bounded Turbulent Flows

L. Kleiser,
N.A. Adams, T. Maeder, S. Stolz

Institute of Fluid Dynamics
ETH Zurich
CH-8092 Zurich, Switzerland

An overview is given on recent progress made with direct and large-eddy simulation (DNS and LES) of wall-bounded turbulent flows.
In our group, we have considered a set of successively more complex building-block flows. Cases to be reported include incompressible channel flow, compressible (supersonic) flat plat boundary layers, and a supersonic compression ramp flow with shock-turbulence interaction.

In DNS all relevant turbulent scales are resolved by the numerical grid employed. This necessitates the use of very fine grids and thus limits DNS to relatively low Reynolds numbers, often orders of magnitude below those of practical problems. Higher Reynolds numbers can be attained with LES, where the effect of the non-resolved scales is taken into account by a sub-grid scale (SGS) model. In recent years new, non-eddy-viscosity type SGS models have appeared which avoid some of the problems of traditional SGS models.

In our group the approximate deconvolution model (ADM) was developed which is based on an approximate defiltering of the computed (filtered) quantities. LES performed with ADM gives results in excellent agreement with DNS data at a fraction (order one percent) of the cost of DNS for the afore-mentioned flow cases. We believe that ADM represents a significant improvement over previous models and has a large potential for future applications.

References

N.A. Adams
Direct simulation of the turbulent boundary layer along a compression ramp at M=3 and Re_theta=1685. J. Fluid Mech. 420:47-83, 2000.

T. Maeder, N.A. Adams, and L. Kleiser
Direct simulation of turbulent supersonic boundary layers by an extended temporal approach.
J. Fluid Mech., 2000, to appear.

S. Stolz and N.A. Adams
An approximate deconvolution procedure for large-eddy simulation. Phys. Fluids 11:1699-1701, 1999.

S. Stolz
Large-eddy simulation of complex shear flows using an approximate deconvolution model. Ph.D. thesis, Diss. ETH No. 13861, 2000.

On the Internal Structure of Steady Cylindrical Supersonic Free Jets

Based on linear potential theory, the problem of steady supersonic flow inside a cylindrical free jet is treated by analytical methods. The presence of shocks in the flow leads to non-uniform convergence of the obtained series solutions, which thus are unsuitable for direct numerical computation. This practical difficulty is overcome by an analytical method based on Kummer's series transformation. Several basic solutions are discussed, and it is shown that cylindrical jets exhibit a rather complex cellular structure, which is completely different from the corresponding plane flow field. Theoretical Mach-Zehnder interferograms are calculated by analytical integration of the density field, whose excellent agreement with experiment proves the validity of linear theory even close to singularities and far downstream the nozzle orifice. Furthermore, it is shown that the well-known formula of Pack for the wavelength of the shock cell structure is inconsistent; the correct formula is derived and excellent agreement with experiment is found.

Prof. Dr.rer.nat. Dr.-Ing. habil. A. Dillmann
Technische Universität Berlin
Hermann-Föttinger-Institut für Strömungsmechanik
Straße des 17. Juni 135, 10623 Berlin, Germany.

Effects of rotation on wall-bounded flows

H.I. Andersson
Division of Applied Mechanics, Department of Mechanical Engineering
Norwegian University of Science and Technology, Trondheim, Norway
E-mail: helge.i.andersson@mtf.ntnu.no

Keywords - System Rotation - Coriolis Force - Secondary Flow - Turbulence

Abstract - Fluid flows in rotating frames-of-reference are encounterd not only in nature (e.g. atmospheric boundary layers and ocean currents) but have also a variety of industrial applications, notably in rotating appliances such as centrifuges, compressors, pumps and turbines. General characteristic features of rotating flows are addressed in the book edited by Hopfinger (1992), whereas Johnston (1998) focused on those effects of rotation that are particularly relevant in turbomachinery. The Coriolis body force, which arises from imposed system rotation, have important implications both on laminar and turbulent flow fields. Since most flows of practical interest are turbulent, the presentation will primarily be concerned with turbulent flows. The turbulence is typically genereated by the presence of mean flow shear, like in the flow in a boundary layer along a solid wall or the flow in ducts and channels. The simplest of these flows are two-parameter problems characterized by a Reynolds number and a rotation number, the latter which is the inverse of the Rossby number used in geophysical and astrophysical applications.

A particularly notewothy feature of rotating wall-bounded flows are the occurrence of counter-rotating streamwise-oriented vortical structures, some of which are generated by the presence of side-walls and others from an inherent instability mechanism analogous to the Görtler instability arising from the centrifugal force due to streamline curvature. The orientation of the imposed rotation vector with respect to the mean flow vorticity vector can be shown to be of fundamental importance. In particular, when these two vectors are antiparallel, i.e. the rotation is anticyclonic, the flow is susceptible to a roll-cell instability. Such vortical cell patterns have been observed both in laboratory and computer experiments, see e.g. Johnston (1998) for an overview, and the organized cellular motion has a substantial effect on the overall transport and mixing. The turbulence is also affected by the imposition of a Coriolis force, both directly through additional Reynolds-stress generation terms and indirectly by the sole presence of the roll cell pattern (Andersson 1999). Since laboratory experiments in rotating systems are difficult to perform, a better understanding of rotational-induced flow phenomena and their underlying physical mechanims can be achieved by means of direct numerical simulations (DNS). Sample results will be shown and explained for plane Poiseuille flow (Kristoffersen & Andersson 1993), plane Couette flow (Bech and Andersson 1996, 1997) and a rotor-stator-type flow (Lygren & Andersson 2000).

In spite of its many outstanding features, DNS is obviously too costly and inflexible for industrial and environmental applications. For most flows of practical interest, the number of grid points required to solve all the essential scales of the turbulence are far beyond the capabilities of today's computers. Computerized flow analysis will therefore in the foreseeable future be based on mean flow equations (RANS) and a suitable turbulence model. The ability of a second-moment closure to predict the three-componential mean flow which results when a plane Couette flow is subjected to weak and moderate anticyclonic rotation will be demonstrated (Pettersson Reif & Andersson 2000). In this approach, the counter-rotating roll cells are treated as an integral part of the mean motion governed by the RANS equations and the turbulence model is thus left to account only for the real turbulence.

References

Andersson, H.I. (1999) Organized structures in rotating channel flow. In: *Simulation and Identification of Organized Structures in Flows*, Kluwer, pp. 81-90.

Bech, K.H. & Andersson, H.I. (1996) Secondary flow in weakly rotating turbulent plane Couette flow. *J. Fluid Mech.* **317**, 195-214.

Bech, K.H. & Andersson, H.I. (1997) Turbulent plane Couette flow subject to strong system rotation. *J. Fluid Mech.* **347**, 289-314.

Hopfinger, E.J. (ed) (1992) *Rotating Fluids in Geophysical and Industrial Applications*, CISM, Springer.

Johnston, J.P. (1998) Effects of system rotation on turbulence structure: a review relevant to turbomachinery. *Int. J. Rotating Machinery* **4**, 97-112.

Kristoffersen, R. & Andersson, H.I. (1993) Direct simulations of low-Reynolds-number turbulent flow in a rotating channel, *J. Fluid Mech.* **256**, 163-197.

Lygren, M. & Andersson, H.I. (2000) Turbulent flow between a rotating and a stationary disk, *J. Fluid Mech.*, in print.

Pettersson Reif, B.A. & Andersson, H.I. (2000) Prediction of longitudinal roll cells in rotating plane Couette flow. *Theoret. Comput. Fluid Dynamics* **14**, 89-108.

DISPERSION IN QUASI-GEOSTROPHIC FLOWS

Antonello Provenzale, ICGF-CNR, Torino

Whenever turbulent geophysical flows have been observed with sufficient resolution, long-lived coherent structures have been detected. In rotating flows, coherent structures often take the form of intense localized vortices that can dominate the dynamics of the system. Examples include the Great Red Spot on Jupiter, Gulf Stream Rings in the Atlantic Ocean, the lenses of salty Mediterranean water called "Meddies", the polar stratospheric vortex, and some types of tropospheric cyclones.

Coherent vortices play an important role in determining mesoscale transport processes in the ocean and the atmosphere. In particular, vortices trap fluid particles and passive tracers in their cores, and generate transport barriers that can lead to anomalous dispersion phenomena. Moreover, the velocity distributions induced by an ensemble of coherent vortices are usually non-Gaussian, a fact that invalidates the standard approach to the stochastic parameterization of turbulent dispersion. Analogously, a simple description of tracer transport based on advection diffusion equations is not capable of capturing the dynamics associated with the presence of intense mesoscale vortices.

In this talk I review some of the transport properties generated by coherent vortices in quasi-geostrophic flows. To this end, I consider both numerical simulations and laboratory experiments in a large rotating tank. In particular, I discuss how the presence of vortices can affect the dynamics of advected tracers such as plankton, and show that the velocity distribution induced by the coherent vortices is non-Gaussian. Finally, I discuss a novel parameterization of dispersion in vortex-dominated flows.

Abstract for Invited Lecture at 4th EUROMECH Fluid Mechanics Conference, 19-23 November 2000 in Eindhoven.

Water waves at sea walls

D. Howell Peregrine

School of Mathematics, Bristol University,
University Walk, Bristol BS8 1TW, England.
d.h.peregrine@bris.ac.uk

Sea walls and breakwaters are constructed to protect land and shelter harbours from the destructive power of water waves incident from the open sea. It is not unusual for the most exposed breakwaters to suffer damage due to the violent nature of wave impacts. The most violent wave impacts are the topic of the lecture. These occur when breaking or near-breaking waves hit the structure.

The traditional, and successful, model for water waves is inviscid irrotational flow with constant pressure at the free surface. Suprisingly, this model is sufficient to describe impact pressures as high as any that are measured in the laboratory (Cooker & Peregrine, 1990). Near-singular flows can be computed and are still being investigated. However, for prototype conditions other real fluid effects become important, especially the role of air. In storm waves and at wave breaking air is entrained into the water. Also when a wave breaks at a wall a "pocket" of air can be trapped. In both cases the compressibility of the air is important. The general impression is that this "cushions" wave impacts. Although there are indications that peak pressures are reduced, the total impulse due to an impact may be increased (Wood, Peregrine & Bruce, 2000).

Cooker, M.J. & Peregrine, D.H. (1990) Computations of violent motion due to waves breaking against a wall, *Proc. 22nd Internat. Conf. Coastal Engng.* Delft. A.S.C.E. **1**, pp.164-176.

Wood, D.J. Peregrine, D.H. & Bruce, T. (2000) Study of wave impact against a wall with pressure-impulse theory: Part 1, Trapped air. *J. Waterway, Port, Coastal & Ocean Engng.*, A.S.C.E. in press.

THE ROLE OF FLUID DYNAMICS IN COMBUSTION IN UNPREMIXED SYSTEMS

Amable Linan

The combustion reactions which are exothermic and have reaction rates strongly dependent on temperature occur only after vaporization or gasification of the fuels and mixing with the oxygen of the air. In an large fraction of the combustion systems the reactants are unpremixed when entering the combustion chamber. They may partially mix before leaving the chamber without effects of the chemical reaction or they may react in thin layers the diffusion flames that separate the reactants at a rate controlled by diffusion.

In most applications the flow has Reynolds numbers such that mixing is restricted to thin mixing layers or slender Jets. These are typically turbulent with an important role played by coherent structures affected by the heat release. If the diffusion flame is attached to the rim of the fuel injector the reaction is diffusion controlled everywhere leading to a problem of pure heat and mass transfer with an important role played by the fluid dynamics and the diffusivities of the species and heat.

The high sensitivity of the chemical reactions with temperature is responsible for the phenomena of flame extinction and ignition. For example by straining the mixing layers the flame can be locally extinguished when we try to increase the rate of mixing or equivalently the rate of burning of fuel per unit flame surface above a critical value. In the combustion chamber we often encounter regions of low temperature near the injectors where the reactants mix without chemical reaction effects. These regions of chemically frozen flow are separated by thin premixed flames with rich and lean branches from regions of near chemical equilibrium flow where the reactants do not coexist outside trailing thin diffusion flames. We shall describe the role of these triple flame fronts in the ignition and lift off of diffusion flames and their role on the structure of the leading edge of the diffusion flames in the anchoring of the flames in the near wake of the fuel injector.

The combination of numerical simulation and experiment to study turbulence

F.T.M. Nieuwstadt
J.M. Burgers Centre
Delft University of Technology

Numerical simulation of turbulence has progressed to a stage where its quality and detail can compete with data obtained in experiments. However, numerical simulations remain limited in the flow geometry and flow conditions that can be simulated, e.g. the flow domain is always limited and it is frequently not obvious how to specify correct boundary and initial conditions. On the other hand experimental data are usually limited either in their spatial or time resolution. Therefore a combination of experiment and numerical simulation is the most promising method to study a turbulent flow in detail. Here, we shall discuss the results of such a combination applied to the problem of turbulent mixing of a scalar.

In the two figures shown below we illustrate the problem of turbulent mixing obtained on the left side from a computation and on the right side from an experiment. The computation is has been carried out for an isotropic turbulent flow in which scalar fluctuations were generated by imposing a mean scalar gradient. The experiment of scalar mixing was carried in a turbulent jet where the concentration patterns were made visible by means of Laser Induced Fluorescence (LIF).

The numerical simulation allowed us to study in detail how the mechanism of scalar mixing takes place. We have found that mixing occurs in intermittent events in which a strong scalar gradient is produced by a combination of a compressive strain and an alignment of this strain with the scalar gradient vector. The time scale of these events has been found to be proportional to the Kolmogorov time scale, irrespective of the diffusivity or the Schmidt number. Moreover the topology of these mixing events takes the shape of sheets, which are clearly visible, both in the concentration patterns of the computed and measured scalar field.

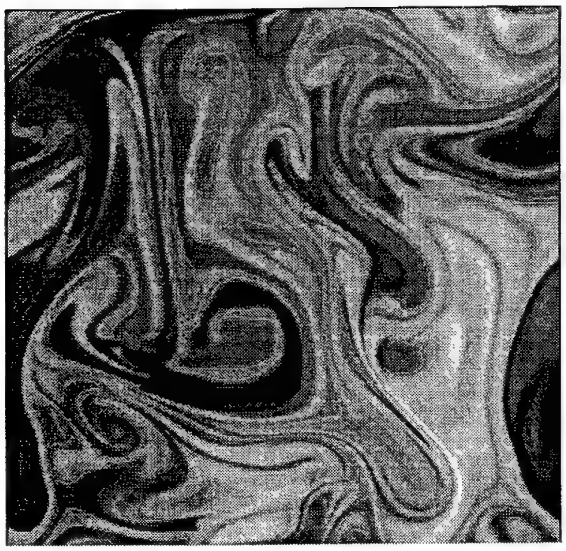

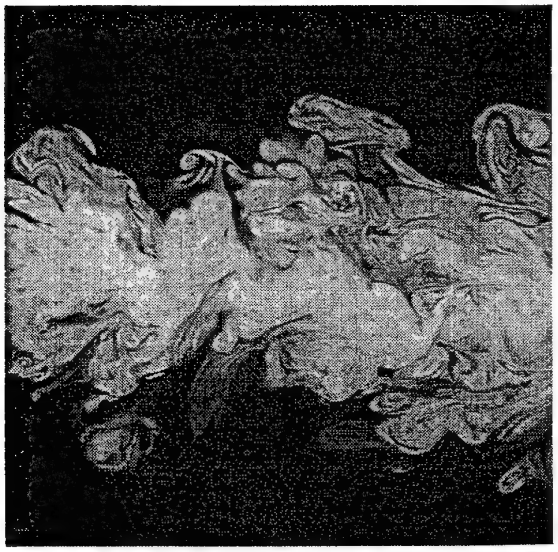

ABSTRACTS
LECTURES

Bubbles, Droplets & Particles

Collision of drops with inertia effects in strongly sheared linear flow fields

F. Pigeonneau[1,2] and F. Feuillebois[1]
1. PMMH, ESPCI, 10, rue Vauquelin, 75005 Paris, France.
2. C.E.A.-Saclay, D.R.N./D.M.T./S.E.M.T./L.T.M.F.
91191 Gif sur Yvette Cedex, France.
E-mail : feuillebois@pmmh.espci.fr

Keywords - Drops - Hydrodynamic interactions - Collisions

Abstract - The relative motion of drops in shear flows is responsible for collisions leading to the creation of larger drops. The collision of liquid drops in a gas is considered here. Drops are small enough for the Reynolds number to be low (negligible fluid motion inertia), yet large enough for the Stokes number to be possibly of order unity (non-negligible inertia in the motion of drops).

General expressions are first presented for the drag forces on two interacting drops of different sizes embedded in a general linear flow field. These expressions are obtained by superposition of solutions for the translation of drops and for steady drops in elementary linear flow fields (simple shear flows, pure straining motions). Earlier solutions adapted to the case of inertialess drops (by Zinchenko, Davis and coworkers) are completed here by the solution for a simple shear flow along the line of centres of the drops. A solution of this problem in bipolar coordinates is provided ; it is consistent with another solution obtained as a superposition of other elementary flow fields.

The collision efficiency of drops is calculated neglecting gravity effects, that is for strongly sheared linear flow fields. Van der Waals attractive forces are taken into account. Results are presented for the cases of a simple linear shear flow and an axisymmetric pure straining motion. It is found that the collision efficiency in a simple shear flow becomes negligible below some value of the ratio of radii, for any value of the drops inertia. The combined effects of drops inertia and attractive van der Waals forces also induce anisotropic shapes of the collision cross-section and two different regimes in the variation of the collision efficiency with the Stokes numbers. By comparison, results for the collision efficiency in an axisymmetric pure straining motion are more regular. In that case, the collision cross-section is axisymmetric and drops inertia and attractive van der Waals forces combine in a simpler way.

Dynamics of bubble growth and detachment in a shear flow

C. Colin and G. Duhar
Institut de Mécanique des Fluides de Toulouse UMR-CNRS/INP-UPS 5502
Allée du Professeur Camille Soula
31 400 Toulouse, France
Email : colin@imft.fr

Keywords – bubble, bubble detachment, forces balance.

Abstract – The prediction of the bubble growth and detachment at the wall is crucial in many industrial situations. Indeed, the bubble size controls the mass, momentum and energy transfers between the phases and with the wall. This study presents some results concerning the growth and the detachment of isolated bubbles at the wall of a shear flow. Bubbles are created either by air injection through a hypodermic needle traversing the lower wall of a channel or by vaporisation of the liquid on a heated wall, on an artificial nucleation site. Different fluids are used: water and silicone oil for the experiments with air injection and n-pentane for the experiments with boiling. These experiments are carried out for air or vapour flow rates between 3 and 50 mm^3/s and for shear rates near the wall between 0 and 50 s^{-1}.

High-speed video pictures of the bubbles growing at the wall are taken. After image processing the temporal evolution of the bubble morphology is characterised: its outline, the position of its centre of mass, an equivalent radius of the bubble.

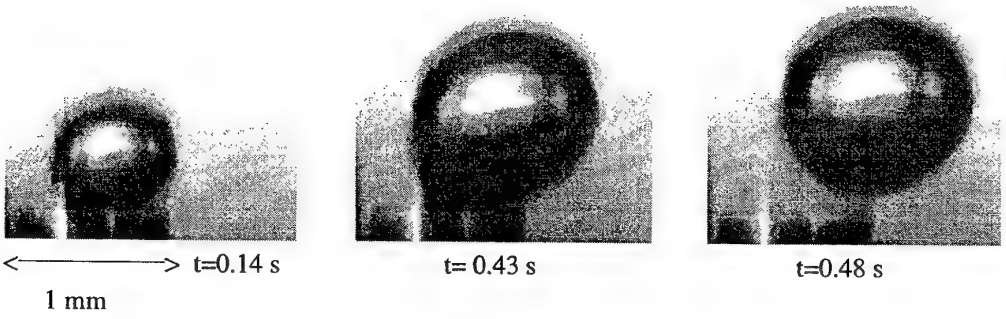

Air bubble growth and detachment in silicone oil with an air flow rate of 3 mm^3/s, and a shear rate of 10 s^{-1}.

A mechanistic model is also developed. The experimental results are used to estimate the different forces acting on the bubble during its growth, in order to write a forces balance. The main forces playing a role are the surface tension, the buoyancy, the viscous drag, and the lift forces. The added mass force is weak in these experiments with air injection or boiling at atmospheric pressure. At low shear rate (<5 s^{-1}), the detachment of the bubble is perpendicular to the wall. It occurs when the buoyancy force becomes greater than the surface tension force. For greater shear rates, the viscous drag force is responsible for the bubble detachment. A criterion based on the forces balance is derived to predict the bubble size at their detachment.

Creeping motion of a sphere along the axis of a closed axisymmetric container

N. Lecoq[1], K. Masmoudi[1], F. Feuillebois[2], R. Anthore[1] and F. Bostel[1]
1. U.M.R. 6634 C.N.R.S. Université de Rouen,
76821 Mont Saint Aignan, France.
2. PMMH, ESPCI, 10, rue Vauquelin, 75005 Paris, France.
Email: Nicolas.Lecoq@univ-rouen.fr

Keywords - Creeping flow - Sphere - Cylinder - Cone

Abstract - The motion of a particle embedded in a viscous fluid in creeping flow is influenced by nearby container walls. These hydrodynamic interactions cannot be avoided in closed containers. However, even the simplest container geometries have not been studied in sufficient detail. Two types of containers are considered here: circular cylinders closed by planes at both ends and cones closed by a base plane. The axis of the container is set in a vertical position. The particle is solid and spherical and it is settling along the container axis. Thus, the motion is axisymmetric. The hydrodynamic interactions are studied both theoretically and experimentally.

The Stokes flow problem was solved numerically, using a technique pioneered by Bourot (1969) and used thereafter in a number of problems by Coutanceau and coworkers. The solution of Stokes equation for the fluid velocity is written as a series in spherical coordinates around the sphere and the boundary condition on the sphere is applied exactly. The boundary condition on the walls of the container then is applied in the sense of least squares: the quantity to minimise is written as an integral of the squared difference between the approximated velocity and the exact boundary condition to be enforced. The minimisation provides the coefficients in the series. On the experimental side, several containers (cylinders and cones) of typical size 5 cm were used. They were filled with a very viscous silicon oil. The sphere was a steel bead a few millimeters in diameters (several sizes were used). The Reynolds number based on the sphere radius was typically of the order of 10^{-5}. The displacement of the sphere was measured with laser interferometry, allowing a minute accuracy of 50 nm.

Calculated streamlines patterns for a small sphere in a cylinder are in agreement with results by Blake (1979) for a Stokeslet in a cylinder. Various sets of eddies appear in cylinders and cones, depending upon the geometry and the sphere position. Results are in agreement with earlier works about eddies in close containers and corners when in Stokes flow (Moffatt 1964, O'Neill 1983). With a standard computer accuracy, the present numerical technique applies when the gap between the sphere and the nearby wall is larger than about one radius. The numerical results for the drag force are in excellent agreement with the experimental ones both for the cylindrical and the conical containers. For a sphere in the vicinity of any of the plane walls, our results also match with the analytical solution of Brenner (1961) and Maude (1961). That solution is in excellent agreement with our experimental results at small distances from the wall (typically less than a diameter, depending on the sphere size). Experiments show that the motion towards the apex of a cone is much slower than that towards a plane. This is because of the hindered back flow. In the limit of small gaps normalised with the radius, $\varepsilon \ll 1$, the drag force in a cone varies like $\varepsilon^{-5/2}$, in agreement with the lubrication result (Masmoudi et al, 1998), whereas it varies like ε^{-1} close to a plane.

The optimal charge for drops in electric fields

A.J. Mestel
Department of Mathematics, Imperial College, London SW7 2BZ, UK

Email: j.mestel@ic.ac.uk

Keywords - Electrospraying, charged drops

Abstract - Many printing and spraying devices involve the guidance of electrically charged drops using external electric fields. The speed of such processes depends on the force which can be exerted on each drop, which varies as the product of the drop charge and field strength. However, for given surface tension, too strong a field or too large a charge causes the drop to break up, either by fragmentation into smaller drops or by the emission of thin jets. The drops tend to elongate in the direction of the field. The critical field strength for an uncharged drop is known, as is the maximum drop charge in the absence of a field (the "Rayleigh limit.")

When both field and charge are present the drop accelerates, giving rise to an effective hydrostatic pressure in the fluid. This paper calculates numerically the equilibrium shapes and the critical relationship between charge and field. The results are compared with an extension of the known spheroidal approximation to the case of accelerating, charged drops. It is found that the optimum charge is about 56% of the Rayleigh limit.

Air resistance is considered, both for low and high Reynolds number, R. The results for $R << 1$ do not differ greatly from those for freely accelerating drops, but the asymmetry introduced by the wake for $R >> 1$ leads to a more oblate shape, and different field criteria. It is estimated that in practice the Reynolds number is high, but that air resistance may be neglected over distance of order 1cm.

Unsteady drag on a sphere in a rectilinear motion at small Reynolds number

Evgeny S. Asmolov
Central Aero-Hydrodynamic Institute
Zhukovsky, Moscow region, 140160, Russia
Email: aes@an.aerocentr.msk.su

Keywords - Unsteady Oseen Force

Abstract - Unsteady flow induced by a small sphere at the distances large compared with its radius a is considered. At the distances from the sphere of order a and small particle Reynolds number, $\mathrm{R} = aU_c/\nu$, based on a characteristic particle velocity, the disturbance flow to the leading order is governed by creeping-flow equations. Their solution gives a Stokes drag on the sphere. At the distances compared with Oseen length, $l'_O = \nu/U_c \gg a$, inertial terms in Navier-Stokes equations become of the same order as the viscous ones. When the timescale of particle velocity variation is of the order of Oseen timescale, $t'_O = \nu/U_c^2$, the unsteadiness of the flow should also be taken into account. As a result the disturbance velocity field in far region differs from Stokeslet field. A first-order force on a sphere also differs from the classical Basset history force. Ockendon (1968) used singular perturbation methods and Fourier transform of disturbance field to solve the unsteady Oseen equations for rectilinear particle motion and to obtain the equation for unsteady drag to $O(\mathrm{R})$. Lovalenti & Brady (1993) extended analysis to arbitrary time-dependent particle velocity and to particles of arbitrary shape. They expressed the history force for the general case using reciprocal theorem in terms of double integral.

In the present work the previous results are refined for rectilinear motion. New concise expressions for disturbance field and history force are derived in terms of a single history integral. The three-dimensional Fourier transform of velocity field (Ockendon 1968) is integrated over Fourier space in order to obtain dimensionless velocity field. Unsteady Oseen force (history force) comes from the homogeneous part of disturbance velocity at the particle position. As a result it can be expressed in terms of particle displacement $z_p = \int_{-\infty}^{t} V_p(s)\,\mathrm{d}s$ as

$$F_O = \frac{9\pi^{1/2}}{4}\mathrm{R}\int_{-\infty}^{t}\left[\frac{4\Delta\tau}{\Delta z_p}\frac{\mathrm{d}\exp\left(-\frac{\Delta z_p^2}{4\Delta\tau}\right)}{\mathrm{d}\tau} - V_p(t)\right]\frac{\mathrm{d}\tau}{\Delta\tau^{3/2}}.$$

Here $\Delta z_p = z_p(t) - z_p(\tau)$, $\Delta\tau = t - \tau$, the particle V_p is scaled by U_c, space coordinates by l'_O, and time by t'_O.

Different types of particle velocity variation $V_p(t)$ were considered previously. We study the new class of start-up problem. For some dependences $V_p(t)$ the self-similar solutions for velocity fields are obtained.

The research was supported by Russian Foundation for Fundamental Research (Grant No. 99-01-00419).

References

LOVALENTI, P. M. & BRADY, J. F. 1993 The hydrodynamic force on a rigid particle undergoing arbitrary time-dependent motion at small Reynolds number. *J. Fluid Mech.* **256**, 561–606.

OCKENDON, R. J. 1968 The unsteady motion of a small sphere in a viscous liquid. *J. Fluid Mech.* **34**, 229–239.

Upscaling Sonoluminescence

R. Toegel and D. Lohse
Section Fluid Dynamics and Heat Transfer, Department of Applied Physics
University of Twente, The Netherlands
Email: r.toegel@tn.utwente.nl

Keywords - Single Bubble Sonoluminescence - Sonochemistry

Abstract - Sonoluminescence is the conversion of sound into light:
A small gas bubble – usually filled with argon – is trapped in a standing acoustical wave and forced into strongly nonlinear radial oscillations. During the rapid compression phase the bubble volume changes by a factor of 10^6 on a time scale of microseconds. Therefore the heat exchange with the surrounding liquid – usually water – becomes neglegible and hence the bubble is heated considerably. By this means temperatures of up to $20000K$, i.e., typical energies of a few eV, can be achieved: The bubble starts to glow as bright as to be visible to the naked eye.

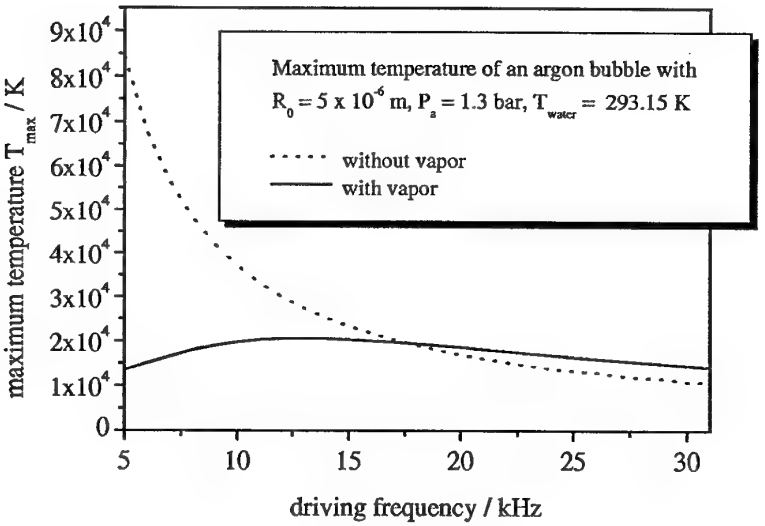

Figure 1: Maximum temperature of an argon bubble with $R_0 = 5\mu m$, $P_a = 1.3bar$ and $T_0 = 293.15K$. Dotted line: without diffusion of vapor, solid line: with diffusion of vapor.

It has been suggested that this extraordinary energy focusing mechanism even can be upscaled (temperatures up to $100000K$) by lowering the frequency of the acoustical field. We present experimental results as well as a theoretical model which show that these predictions are only valid under the constraint of zero vapor pressure of the liquid. In reality however, vapor will diffuse into the bubble – the more the lower the frequency of the acoustical field – and will lower the final temperature. Figure 1 shows as one example result from our model the frequency dependence of the maximum temperature for an argon bubble in water. The dotted line corresponds to the zero vapor pressure case, the solid line takes diffusion of vapor into account. Significant deviations occur reflecting the experimental results.

Analytical and numerical prediction of deformation and motion of a bubble near a plane wall

C.W.M. van der Geld and J.G.M. Kuerten
Department of Mechanical Engineering
Technische Universiteit Eindhoven, The Netherlands
Email: c.w.m.v.d.geld@wtb.tue.nl

Keywords - Bubble - Deformation

Abstract - In the presence of a solid wall, the hydrodynamic forces acting on a bubble not only displace the center of mass but also tend to deform the bubble. In the present study, the Lagrangian formalism is applied to predict the motion and deformation of a bubble in a perfect fluid near a plane, infinite wall. Although only axisymmetric cases are considered, the extension of the analysis to the general case is straightforward. The bubble radius is represented by a series

$$R(\theta,t) = R_0[1 + \sum_{i=1}^{\infty} b_i(t) P_i(\cos\theta)],$$

where θ denotes the angle with the normal to the wall, and P_i the Legendre polynomial of degree i. The kinetic energy of the two-bubble system, T, is expressed as a function of b_i and $\dot{b}_i$. Each generalized coordinate b_i yields a differential equation, $\frac{d}{dt}\frac{\partial T}{\partial \dot{b}_i} - \frac{\partial T}{\partial b_i} = 0$, and these coupled equations have to be solved in order to predict the evolution of the bubble shape and the trajectory of the center of mass. The analysis is analytical up to the point where the set of ordinary differential equations has to be solved. This is done by means of the method of reduction and a standard Runge-Kutta method for the integration in time.

The shape and displacement history predictions are compared with BEM computations. Boundary element techniques are well known for their applicability to potential flow problems with interface deformation. Given the velocity potential at the surface of the bubble, the normal component of the velocity can be calculated. To this end the interface is divided in higher-order elements which are parameterized with piecewise C^2 cubic B-splines. The integrals over the interface are approximated with higher order Gauss quadrature, using a quadratic transformation to remove the singularities. The evolution of the shape and velocity potential are predicted using the kinematic and dynamic boundary conditions. Integration in time is performed with the standard fourth-order Runge-Kutta method.

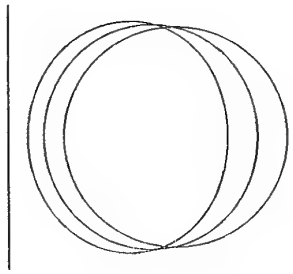

A bubble approaching the wall calculated with the BEM *method*

Response of rising bubbles to a sudden depressurization

C. D. Ohl and A. Prosperetti*
Department of Applied Physics, University of Twente, Enschede, The Netherlands
Email: c.c.m.rindt@wtb.tue.nl
*Also: Department of Mechanical Engineering, The Johns Hopkins University, Baltimore U.S.A.

Keywords - Vertical Rising Bubble - Response to Depressurization -

Abstract - The response of single rising bubbles in a stagnant pressurized vertical tube is investigated experimentally. The bubble is subjected to a rapid depressurization from a few atmospheres to ambient pressure. The translational and radial dynamics are recorded by means of high speed video and analyzed with digital image processing techniques. In particular, the onset and the frequency of the radial oscillation and its coupling to the translational acceleration are investigated. Additionally, the onset of path instabilities which are triggered by the volume increase are considered. The observed bubble behavior is compared to a model taking into account buoyancy, added mass and the drag forces. The bubble dynamics is recorded at a speed up to 2000 frames/s with a CCD camera (Kodak HG2000, 512 × 384 pixels). The pictures are transferred to a computer for digital image processing. The steps consist of edge detection, thresholding and tracking of closed contours. From the contour data, the diameter and centroid are calculated. This makes it possible to track the shape, size and position of the bubble without user intervention. Depending on the rise velocity of the bubble (determined by the bubble size), and the magnification used, the bubble can be tracked for several hundred pictures.

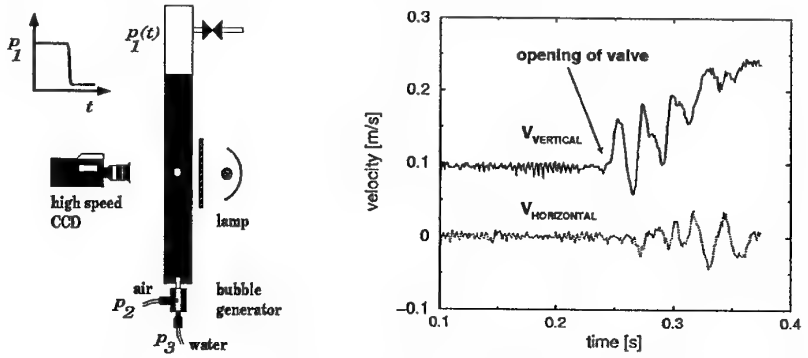

The experimental set-up (left) and the vertical and horizontal velocity component of a rising bubble subjected to a pressure change from $p_i = 4$ bar to $p_f = 1$ bar. (right)

This experiment allows one to vary the bubble volume by decreasing the pressure from p_i to p_f during the rise. Assuming a slow volume change (compared to the natural frequency of the bubble) the bubble radius will increase from a smaller initial radius R_i to a larger radius $R_f = R_i \sqrt[3]{p_i/p_f}$, neglecting surface tension. It is known that in water bubbles smaller than 0.7 mm in radius rise rectilinearly, while larger bubbles exhibit a zig-zag or spiraling motion. The experimental setup allows to investigate the onset of the spiraling motion as a consequence of the volume increase. As shown in the Figure at time $t = 0.24$ s, the valve is opened and due to the volume increase the bubble is accelerated upwards; 20 ms after the pressure decrease the bubble shows a non-zero horizontal velocity and a transition to a zig-zag motion. These first experimental results suggest that it will be possible to investigate in detail the response of bubbles for Reynolds numbers between 100 to 1000.

Acknowledgement - This work is supported by the Dutch Foundation for Fundamental Research on Matter (FOM).

Free rising and bouncing bubbles

A.W.G. de Vries, A. Biesheuvel and L. van Wijngaarden
Section Engineering Fluid Dynamics, Department of Mechanical Engineering
University of Twente, The Netherlands
Email: a.w.g.devries@wb.utwente.nl

Keywords - Bouncing Bubble Dynamics - Wake Effects - Experimental - Bubbly Flows

Abstract - Above a certain volume gas bubbles rising in clean water perform unsteady irregular motions. Our experiments suggest that there is an intimate relationship between the observed type of motion and the structure of the wake behind the bubble. We use 3D Schlieren optics to visualize the wake. Bubble motion distorts an initial temperature stratification and the associated variations of the refractive index of the water enables visualization of the flow. Two perpendicular views are recorded simultaneously making it possible to determine the instantaneous 3D position, velocity and shape of the bubble and the structure of the wake.

For spiraling bubbles the wake deforms into a pair of helicoidal vortices, which farther downstream interact. For zigzagging bubbles the filaments deform into segments that first 'twist' at regular intervals and farther downstream interact, as for the spiraling case, into what resembles 'Crow instability'. The zigzag-motion is not due to regular vortex shedding, as is often believed, but appears to be a consequence of the twisting of the filaments. The 'twisting' of the trailing vortices results in a change of sign of the velocity induced on the bubble, forcing it in the zigzag motion. From the measured path of a spiraling bubble the force on the bubble can be estimated with help of the equation of motion of the bubble. This force can also be estimated from the momentum conservation of the system bubble and wake. Both results agree satisfactorily.

As bubbles approach a vertical wall the flow becomes even more complex and the influence of the wake is more pronounced. Initially a bubble is attracted to the wall, due to hydrodynamic interaction, and subsequently bounces off the wall, during which a vortical structure is left behind near the wall. This determines, together with the trailing vortices in the wake of the bubbles, the dynamics of the bounce and the path subsequently followed by the bubble.

Describing these vortical structures as Hill's Spherical Vortices (HSV), a tentative model is proposed to predict the excess turbulent energy in bubbly liquids. This calculation shows that shed vorticity has a great effect on the turbulence. The configuration of the produced vorticity is not necessarily a HSV, however one can expect that also with otherwise shaped vorticity the result for the excess turbulent energy will be of the same order of magnitude.

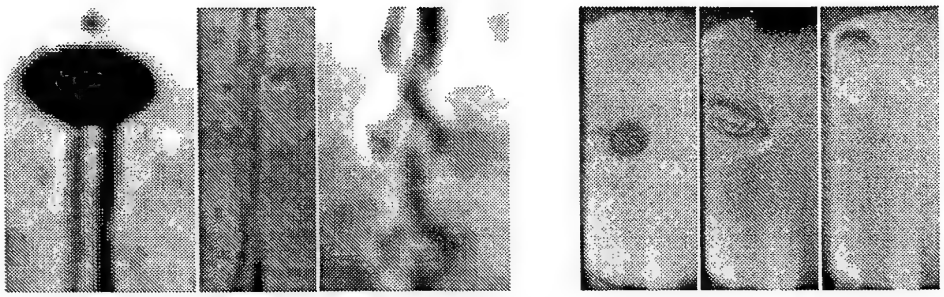

On the left two the wake at different distances behind a zigzagging bubble ($r_{eq} = 1.00mm$). Clearly visible the twisting and interaction of the filaments is. On the right the formation of a vortical structure of a bouncing bubble ($r_{eq} = 0.85mm$)

Excitation of nonlinear shape oscillations of a resonant gas cavity in an acoustic field

D. Zardi[1], G. Rampanelli[1] and G. Seminara[2]
[1] Department of Civil and Environmental Engineering, University of Trento, Italy
[2] Department of Environmental Engineering, University of Genova, Italy
Email: Dino.Zardi@ing.unitn.it

Keywords - Bubble - nonlinear oscillation - stability - acoustic wave - resonance

Abstract - A single gas cavity in a liquid irradiated by an acoustic wave of small amplitude ϵ performs forced radial pulsations around its equilibrium radius. However also shape oscillations can be excited, through coupling with the basic radial motion, under suitable conditions.
Indeed the linear stability of this oscillations has been widely explored, both experimentally and theoretically, in the case of non resonant basic radial flow, i.e. when the angular frequency of the acoustic wave Ω is far enough from the resonance frequency Ω_0 of the radial oscillations. In fact both the shape distortion and the perturbed flow may be described as a superposition of normal modes through an expansion in spherical harmonics. The time evolution of each mode amplitude turns out to be governed by a Mathieu equation, which explains the appearance of a subharmonic mode response when the angular frequency of the acoustic wave and the proper frequency of the excited mode are nearly in a ratio of 2:1, or a synchronous one when that ratio is 1:1. A weakly-nonlinear analysis (Hall & Seminara, 1980) shows that linearly unstable modal amplitudes do not grow indefinitely, but reach finite values.
In the present work we extend the latter analysis to the case when the basic flow resonates displaying typical nonlinear features as multiple solutions and hysteresis phenomena. Again the amplitude evolution in the linear regime turns out to be governed by a Mathieu equation, but peculiar and reacher features arise from nonlinearity of the basic flow. A weakly nonlinear analysis shows a nonlinear feed-back of the shape oscillations on the radial flow: the evolution of the amplitude of both radial and distortion modes turns out to be modulated by slowly varying amplitudes (denoted as $\mathcal{R}$ for the radial mode and Z for the distortion mode) whose coupled evolution is governed by the following nonlinear dynamical system:

$$\frac{d\mathcal{R}}{d\tau} = - i\lambda_0\mathcal{R} + a_0 i\mathcal{R}^2\mathcal{R}^* - b_0\mathcal{R} + if_0 + c_0 iZ^2\mathcal{R}^* + d_0 iZZ^*\mathcal{R} + e_0 iZ^2Z^*$$

$$\frac{dZ}{d\tau} = - i\lambda_2 Z + a_2 iZ^2Z^* - b_2 Z + c_2 iZ^2\mathcal{R}^* + d_2 iZZ^*\mathcal{R} + e_2 i\mathcal{R}\mathcal{R}^*Z + f_2 i\mathcal{R}^2Z^*$$

where τ is a slow time variable, i is the imaginary unit, λ_0, λ_2 are detuning parameters, b_0, b_2, are damping coefficients, and an asterisk denotes complex conjugate. The solution of the latter system is in progress and appears to have a rich behaviour including the possibility of chaotic response, as found in Zardi & Seminara (1995).

References

Hall, P. & Seminara, G. 1980. Nonlinear oscillations of non spherical cavitation bubbles in acoustic fields, *J. Fluid Mech.*, **101**, 423-435.
Zardi, D. & Seminara, G., 1995, Chaotic mode competition in the shape oscillations of pulsating bubbles, *J. Fluid Mech.*, **286**, 257-276.

Vertical and glancing drop impact: two opposite conditions with respect to the dynamics at the fluid surfaces

R. Koehler & G. Leneweit

Carl Gustav Carus-Institut in der Gesellschaft zur Förderung der Krebstherapie, Am Eichhof, D-75223 Niefern-Öschelbronn, Tel: ++49-7233-68-411, Fax:++49-7233-68413, e-mail: physik.carus@t-online.de

Vertical drop impact has been investigated in great detail [1]. Regarding the surface motions of drop and target fluid the results obtained can be summarized as follows: The momentum transfer at the very small contact area at the time of impact produces a high pressure maximum during a short time interval which drives a thin lamella out of the drop volume and generates a crater with an uprising crown in the target fluid (Fig. 1). In this process the bottom side of the lamella coalesces with the crater surface. Thereby the fluid velocities are so high that the surfaces of the lamella and the crater are freshly formed from inner fluid while the surfaces of drop and crater neighbourhood of the target fluid persist nearly in their original state. This description is supported by the experiments of LOEHR [2], who investigated the formation of the lamella and of ENGEL [3], who studied the crater kinematics.

In contrast to vertical impact completely different phenomena can be found during glancing drop impact (Figs. 2 and 3), with many of the phenomena being not yet described in the literature. For Weber numbers We > 20, higher than the boundary to cause coalescence and drops of 1.2 to 2 mm in diameter of a glycerol/water mixture (with $\nu = 0.1$ cm²/s; $\sigma/\rho = 58$ cm³/s²) we found:

1. For glancing drops with an angle of incidence $\alpha \leq 16°$ no formation of a lamella or crater is visible (Fig. 2). The drop slides over the target fluid surface and formes a thin layer of drop fluid on the target surface which is not engulfed by the target fluid as in the case of vertical impact, where a ring vortex is formed in the succeeding process.

2. The sliding drop causes a horizontal circulation in the near surface volume of the target fluid, indicated by a wave like surface rise at its front with local surface compression and a surface depression at the rear with local surface expansion. After 15 ms (impact at We = 119 and $\alpha = 16°$) the sliding drop volume has slowed down below the velocity of the front wave which drifts away, while the drop volume is spread out in a harpoon-like form (Fig. 3). It seems likely that the rolling drop front presses its surface on the target surface and thereby returns to the inner fluid volume.

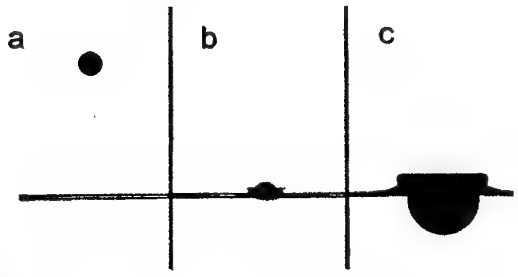

Fig. 1a,b,c: Vertical impact at We = 260, drop diameter 4 mm. **a** approaching drop, **b** formation of a thin lamella of the drop fluid,**c** formation of crater and crown out of the target fluid.

Fig. 2 a, b: Glancing impact at We = 117, $\alpha = 12°$, drop diameter 2 mm, lateral view. **a** 0.42 ms before impact, **b** 3.74 ms after impact.

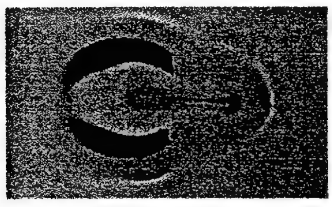

Fig. 3: Glancing impact at We = 119, $\alpha = 16°$, drop diameter 1.85 mm. View from top, 23 ms after impact.

This work was funded by the Rudolf Steiner Fonds für wissenschaftliche Forschung, Nürnberg.

[1] Rein M (1993) Phenomena of liquid drop impact on solid and liquid surfaces. Fluid Dyn Res **12**: 61-93

[2] Loehr KF & Lasek A (1990) Splashing of water drops. Arch Mech **42**,4-5: 507-513

[3] Engel OG (1966) Crater depth in fluid impacts. J Appl Phys **37**,4: 1798-1808

The Thermocapillary flow of a viscoelastic fluid past a bubble

J. Jiménez-Fernandez and A. Crespo
Dpto. Ingeniería Energética y Fluidomecánica
E.T.S.I.I., Universidad Politécnica de Madrid (Spain)

Email: jajimenez@enerflu.etsii.upm.es

Keywords - Bubble - Thermocapillary Flow - Viscoelastic Fluid

Abstract - The steady thermocapillary flow of a spherical bubble in a linear temperature gradient is analyzed by considering that the continuous phase is a weak viscoelastic fluid. Convective heat and momentum transfers are ignored but the action of gravity is taken into account. The problem is formulated by means of a retarded motion expansion analysis. In dimensionless terms this is equivalent to assume that the Weissenberg number $Wi = \lambda/t$ where λ is the relaxation time of the fluid and t the scale time of the flow, is small compared to unity. Thus, the corresponding boundary value problem is solved following a perturbation procedure by regular expansions of the kinematic and stress variables in powers of Wi. Velocity fields as well as the force exerted by the fluid upon the bubble are determined at second order in Wi for a general third order fluid and numerical results are obtained for a 4-constant Oldroyd fluid. The analysis performed shows that elongational and memory effects have a similar quantitative influence for both, isothermal and purely thermocapillary flows past a bubble. However, when the motion is driven by buoyancy in the presence of surface tension forces of a comparable order of magnitude, the velocity fields are strongly affected. Unlike the newtonian case where the recirculation region generated is symmetrical, in a non-newtonian fluid memory effects produce a breaking of symmetry, so that this region is enhanced and shifted in the downstream direction. The analysis also provides the temperature gradient needed to hold the bubble at rest in terms of the characteristic viscoelastic parameters.

Surface tension driven flow in a slender cone

S.P. Decent and A.C. King
School of Mathematics and Statistics,
The University of Birmingham, United Kingdom
Email: spd@for.mat.bham.ac.uk

Keywords - Surface tension - Liquid bridge

Abstract - Peregrine, Shoker & Symon (1990) photographed the breaking of a water drop away from its parent body of liquid. Just before the drop breaks off, a thin column of liquid called the *liquid bridge* connects the drop to the rest of fluid. At the moment of bifurcation, when the drop is at the point of breaking away from the rest of the water mass, the liquid bridge is observed to be approximately conical close to the bifurcation point. After the bifurcation has occured, surface tension gives rise to an impulse at the tip of the conical liquid bridge which causes rapid recoil and strong free-surface deformation. A smaller spherical blob is observed to form on the tip of the recoiling liquid bridge immediately following the bifurcation of the droplet, and capillary waves accelerate upwards from the tip of the liquid bridge.

In this presentation, we examine the evolution of an ideal fluid which is initially conical. The only force acting on the fluid is due to surface tension. We find an asymptotic solution to the problem in terms of the aspect ratio of the cone which is assumed to be small. The flow is found to be self-similar. We find an inner asymptotic region close to the tip of the evolving free-surface. Here the free-surface is found to be a slowly modulated strongly nonlinear wave. At leading-order this wave is found to be a series of linked spheres, with a slowly varying radius. An outer asymptotic region, far from the tip of the fluid, is also identified. Here the free-surface is a slender jet with weakly nonlinear capillary waves. The inner and outer regions are matched using a multiple scales methodology, similar to Kuzmak's method. The results are compared to a computational solution of the initial value problem, and good agreement is found.

Secondary Bjerknes Forces and the Phenomenon of Acoustic Streamers

Nikolaos A. Pelekasis[1], Alexandra Gaki[1], Alexander Doinikov[2]
and John A. Tsamopoulos[1]

[1] Laboratory of Computational Fluid Dynamics
Department of Chemical Engineering, University of Patras
Patras 26500, GREECE
E-mail: pel@chemeng.upatras.gr, tsamo@chemeng.upatras.gr

[2] Institute of Nuclear Problems, Byelorussia State University,
11 Bobruiskaya Str. MINSK
220050, BELARUS
E-mail: doinikov@inp.minsk.by

Keywords - Cavitation - Acoustic streamer - Transient/Steady Oscillations

Abstract - Cavitating bubbles in liquid solutions that are insonated at very high amplitude, are often seen to form filamentary structures where each one of them is moving rapidly, while the distance between them remains constant and much larger than their average radius. These structures are called acoustic streamers and the mechanism of their formation is not fully understood, especially since the bubbles that form them are particularly small, <10μm, and they are driven below resonance, $\omega_f < \omega_{0i}$; ω_f, ω_{oi}, denote the forcing frequency and the fundamental frequencies of the two bubbles, respectively. In the present study the translational velocities of two spherical air bubbles that are oscillating in water in response to a large disturbance in the static pressure field, are calculated. The two bubbles are assumed to be located far enough so that shape oscillations be negligible in comparison with volume oscillations and their translational velocities remain much smaller than their radial ones, thus decoupling the translational from the radial part of their motion. Viscous effects are accounted for, Re=O(1), due to the small size of the bubbles. In this context the translational velocity, which is a direct measure of the secondary Bjerknes force between the two bubbles, of each bubble is calculated for sound intensities as large as the Blake threshold.

When two bubbles of unequal size with radii in the order of 100 μm are subjected to a sound wave with, roughly, half their eigenfrequency and amplitude P_A<0.5 atm their translational velocity is seen to change from attractive to repulsive as P_A increases from 0.05 to 0.1 due to the second harmonic, $2\omega_f$, of the forcing frequency which grows as a result of nonlinear interaction. Then, as is well known for secondary Bjerknes forces between two bubbles, when $\omega_{01} < 2\omega_f < \omega_{02}$ the two bubbles repel each other. However, as the amplitude of sound further increases, P≈0.5 atm, the two bubbles are again seen to attract each other due to the growth of even higher harmonics that fall outside the range defined by the eigenfrequencies of the two bubbles.

The case of much smaller bubbles was also examined, radii in the order of 5 μm, driven well below resonance, $\omega_f=2\pi\times20$ KHz, at very large sound intensities, $P_A\approx1$ atm, which is a more realistic representation of prevailing conditions in an acoustic streamer. Then both viscosity and nonlinearity play an important role in determining the interaction forces. An asymptotic solution, valid for any sound intensity in the limit t<<Re was found that accounts for viscous dissipation of the translational motion. Thus, it was found that the translational velocities of the two bubbles eventually reach a steady oscillation determined by the forcing frequency. Numerical simulations verify this result and show that the forces between the two bubbles tend to be attractive except for a narrow region of bubble sizes corresponding to a nonlinear resonance, thus allowing for sign inversion of the secondary Bjerknes forces as the distance between them decreases and partly confirming previously obtained inviscid results. As a presiminary conclusion we note that this mechanism seems to be closer to the dynamic behavior of bubbles in acoustic streamers.

PS: The authors wish to acknowledge support by the INCO program of DG 12 (N° IC15-CT98-0141).

Acoustically levitated drops: Drop oscillation and break-up driven by ultrasound modulation

A. L. Yarin[1], D. A. Weiss[2], G. Brenn[3], and D. Rensink[3]

[1]Faculty of Mechanical Engineering, Technion - IIT, Haifa 32000, Israel

[2]DaimlerChrysler, Research and Technology, P. O. Box 23 60, D-89013 Ulm
Email: daniel.weiss@daimlerchrysler.com

[3]Lehrstuhl für Strömungsmechanik (LSTM), University of Erlangen-Nürnberg, D-91058 Erlangen

Keywords – Drop dynamics – Ultrasonic levitation

Abstract - The behaviour of drops in an acoustic levitator is simulated numerically. The ultrasound field is directed along the axis of gravity, the motion of the drop is supposed to be axisymmetric. The flow inside the drop is assumed inviscid and incompressible. Computational results are compared with experimental findings.

For a stationary ultrasound wave we observe that stable drop equilibrium shapes exist for acoustic Bond numbers (which relate acoustic radiation pressure to capillary pressure) up to a critical value. The critical value depends on the dimensionless wave number of the ultrasound. Beyond the critical value, we still observe equilibrium drop shapes, but they are not purely convex and found to be unstable.

For the case of an ultrasound wave modulated with a small modulation amplitude and with a frequency, which is comparable to the first few drop resonance frequencies, simulations and experiments are performed and compared. The agreement found is very good. More generally, for an arbitrary modulation frequency (still comparable to the first few drop resonance frequencies, yet), a very rich drop dynamics is obtained; a resonant drop break-up can be triggered by an appropriate choice of the modulation frequency. The drop then disintegrates although the acoustic Bond number remains below its critical value.

Finally a window containing the drop's first eigenfrequency is swept over by the modulation frequency. For small modulations the range of oscillation grows linearly with the modulation amplitude. For larger modulations, however, a substantial increase in the oscillation range of the drop equatorial radius is observed in the case of down-sweep; the increase does not occur in up-sweeps of the modulation frequency. The results are compared with experiments and in particular the so-called jump phenomenon, as well as with experimental and numerical results from the literature.

References

E. Trinh and T.G. Wang: „Large-amplitude free and driven drop-shape oscillations: experimental observations"; J. Fluid Mech. **122** (1982), pp. 315-338.

A. L. Yarin, D. A. Weiss, G. Brenn, and D. Rensink; submitted to J. Fluid Mech.

A kinematic model for cloud droplet motion and growth

C. Pasquero M. Manuguerra, A. Provenzale
ICG - Consiglio Nazionale delle Ricerche. Torino. Italy
Email: claudia@icg.to.infn.it

Keywords - Cloud droplets - -

Abstract - The size distribution of cloud droplets has been extensively studied because of its importance in the determination of the absorption and reflection properties of the atmosphere, which largely affect the heart climate.

Basing on the argument that during their early stage droplets grow mainly by diffusion of water vapor, the expected distribution should be very narrow. Conversely, observative data show broader, and eventually multimodal, distributions.

In the past decades many efforts have been devoted to the understanding of the observed spectra. The basic idea is that droplets follow paths along which the integral of the supersaturation is different, due to variations in any of the involved dynamical or thermodynamical properties (vertical fluid velocity, temperature, humidity). Those fluctuations have been associated either with entrainment of dry air processes or with different concentration of droplets due to inertial effects.

In this study, we choose a different, and maybe complementary, view, focusing on the different velocities droplets may have due to tiny differences in their size. We use the bidimensional convective structure introduced by Stommel (1949) as stationary solution of the equation of motion. We advect droplets in such a flow. When their inertia is taken into account, complicated patterns and eventually chaotic motion may arise. Neverthless, we restrict our study to a region in the parameter space where no chaotic motion of droplets occurs, to show that the process we describe does not depend on the irregular motion of droplets.

We show that droplets with a small different initial size may experience very different growths, due to the solely presence of fixed points in the flow field, whose stability properties depend on the mass of the advected droplets. We show that droplets of a critical radius spend a long time in the vicinity of neutrally stable fixed points. When introducing condensation through a given growth rate for droplets, small initial differences may thus be enhanced, and a broad, and eventually bimodal, size distribution is obtained.

Ball suspension by a thin liquid jet

A.M.Frank
Institute of Computational Modelling SB RAS, Krasnoyarsk, Russia
Email: frank@icm.krasn.ru

Keywords - Ball Suspension - Jet Flow - Discrete Models

Abstract - The stable suspension of a rigid ball by a thin liquid upright jet in a presence of gravity force is obtained numerically by the use of a discrete model of inviscid incompressible fluid. Some kinematic characteristics of the motion are studied. It is obtained, in particular, that the period of a ball oscillations has a minimum at certain jet to ball radii ratio. The dependence of a period on the ball density is weak. The results are compared with an experiment, and a new explanation of the nature of retracing force is discussed.

After 1870, when Osborne Reynolds studied the suspension of a ball by a vertical water jet, this effect became well known as a classical example of the interesting hydrodynamical phenomena. Still only few works concerning this problem appeared ever since. Some theoretical background was given by M.A.Lavrentyev [1], where the explanation of the retracing force appearance was suggested, based on the analysys of two-dimensional steady state jet flow arround a cylinder. As far as the flow was supposed to be inviscid and potential, some additional hypotheses on the detachment point position had to be introduced in order to select the unique solution. Namely, it was assumed that the detachment point is always diametrically opposite to the attachment point. This was explained as being caused by viscous forces, and the fact of such behaviour was observed in experiments by Vilgelmi [3]. In [2] the similar principle was postulated that the total circulation on the cylinder s urface must be equal to zero. In these works the question of stability of a real time-dependent flow was not considered. It is important because the system is not conservative and so just the presence of a retracing force is not sufficient for the stable oscillations. Experimental investigation of a ball suspension by a submerged jets was made in [4].

Two-dimensional inviscid simulation of a cylinder motion in a thin upright jet gave the effect of stable cylinder oscillations in a range of parameters provided the Lavrentyev's condition on detachment point position had been imposed [5]. The present 3D discrete model is a simplified version of the method [5] and, unlike the latter, it gives only a weak approximation of fluid mechanics equations. On the other hand it allowed to simulate this complicated phenomenon on Pentium PC. The simulations gave a stable ball motion in a range of jet to ball radii ratio, density ratio and Froud number. A simple experiment was made and a computed period of ball oscilations appeared to be in a fairly good agreement with measurements. Calculations confirmed the hypotheses that in 3D case neither viscosity nor the additional assumptions about detachment point position are required. A purely inertial mechanism of the phenomenon is discussed.

References

1. M.A.Lavrentjev *Prikl. Matem. Mekh.* (1966) **30**, No.1, 177-182 (in Russian).
2. M.A.Goldshtik *Vertex flows.* Nauka, Novosibirsk, 1981(in Russian).
3. T.A.Vilgelmi *Zh. Prikl. Mekh. Tekhn. Fiz.* (1969), No.5, 76-80. (in Russian).
4. J.Feng, D.D.Joseph *J. Fluid Mech.*(1996) **315**, 367-385.

Formation of drops: singularity, its origin and removal

Y. D. Shikhmurzaev
Department of Applied Mathematics, University of Birmingham,
Edgbaston, Birmingham, U.K.
Email: yulii@for.mat.bham.ac.uk

Keywords - Drop Formation - Singularity - Cusp

Abstract - Breakup of liquid jets leading to the drop formation, coalescence and breakup of drops are examples of fluid motion where the flow domain undergoes a topological transition. Mathematical modelling of these flows is a formidable problem which remains in the focus of intensive research. A number of theoretical works published in the last decade examine several different self-similar regimes of pinchoff in the framework of the slender-jet approximation [1]. A common feature of these works is that the solution has a singularity at the point where a liquid volume breaks into two. This, by continuity, leads to physically unrealistic values of parameters, in particular the pressure, in a finite region adjacent to this point over a finite time interval embracing the moment of breakup. Since these features are unacceptable from the physical point of view, the models require a microscopic "cut-off" to stop the solution on its way to the singularity, thus reducing the modelling to a semi-empirical level.

The goal of the present work is to examine the origin of the singularity and develop an approach which would allow one to remove it in a physically satisfactory and mathematically self-consistent way. As is shown, the singularity appears not as a result of the slender-jet approximation and is inherent in the problem formulation itself. Its origin is an assumption that the interface remains smooth up to the very moment of the topological transition so that the standard kinematic boundary condition together with an assumption that the flow in the final stage of breakup is self-similar couple the scales for lengths and velocities. Then, if the pressure in the liquid is finite, the problem becomes overdetermined; otherwise the pressure has to be singular. An alternative approach developed in the present work is to abandon the above assumption and allow for a cusp on the free surface [2] forming before the topology change and "severing" the liquid thread connecting the two separating volumes. Then, the scales for lengths and velocities are no longer coupled and the singularity disappears. Furthermore, in contrast to what the existing models suggest, the free surface becomes smooth again after the topology change. The problem is considered on the basis of an earlier developed theory [3], which treats cusping as a particular case of the interface disappearance-formation process. A self-similar solution is found and analysed.

References:

1. J. Eggers, *Rev. Mod. Phys.* **69** (1997) 865.
2. D. D. Joseph *et al., J. Fluid Mech.* **223** (1991) 383.
3. Y. D. Shikhmurzaev, *J. Fluid Mech.* **359** (1998) 313.

Turbulence

Analysis of the turbulent/non-turbulent interface in a far-wake DNS

D.K. Bisset[1,3], J.C.R. Hunt[2] and M.M. Rogers[1]
1 Center for Turbulence Research, Stanford University, USA
2 Dept of Space and Climate Physics, University College London, UK
3 *Present Address:* SMME, University of Surrey, Guildford UK
Email: d.bisset@surrey.ac.uk

Keywords - turbulent shear flow - entrainment - vorticity detection

Abstract - In general, a turbulent shear flow includes interface regions that separate the free stream(s) from the fully turbulent zones. The properties of such interfaces are particularly interesting because the flow entrains free stream fluid through the interface, and the fluid becomes vortical and turbulent. In this work, vorticity surfaces are detected in data from DNS of two turbulent far-wakes of a parallel flat plate carried out by R.D. Moser, M.M. Rogers & D.W. Ewing, *J Fluid Mech* **367**, pp255–289; the data include a passive scalar of values 1.0 and 0.0 in the upper and lower free-streams respectively. The first wake is unforced, but in the second simulation, two-dimensional modes are forced (amplified) initially, doubling the growth rate through

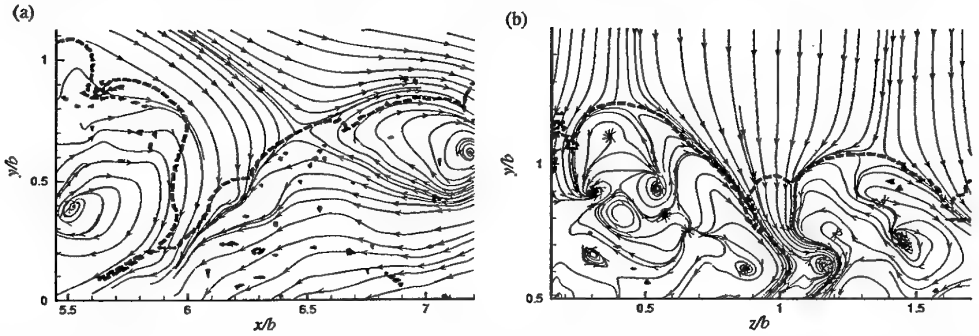

Fig. 1. *Sectional streamlines relative to vorticity surfaces (heavy dashed lines). (a) Part of an (x, y) plane, forced wake. (b) Part of a (z, y) plane, unforced wake.*

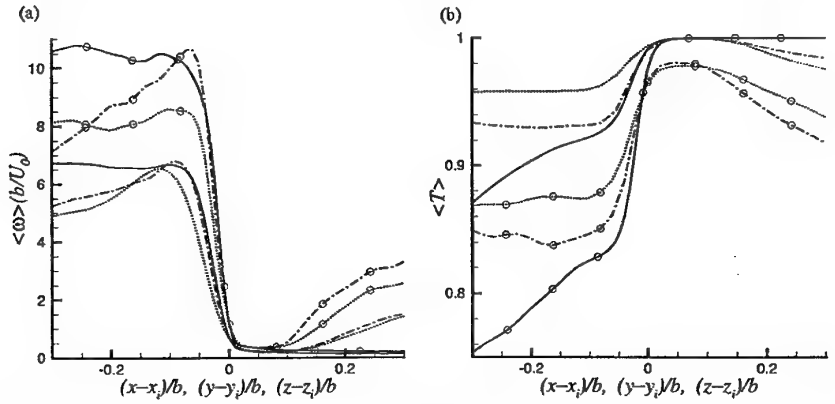

Fig. 2. *Conditional averages of (a) vorticity magnitude and (b) passive scalar in forced (with circles) and unforced wakes. Surfaces face ·····, downstream; ——, vertically; – · –, spanwise.*

increased entrainment. Detection of surfaces is based on ω, the magnitude of the vorticity vector, and the detection level is the lowest value that is consistently above numerical noise in the free stream. We found that the edge of the wake is quite well-defined in the sense that moderate increases in detection level produced only small changes in surface position. Two examples of flow patterns around the vorticity surface are given in Figure 1. Conditional averages of many quantities relative to the detected surface show sharp changes initially (for about 6% to 8% of the wake half-width) and are then constant (Fig 2a, vorticity) or slowly changing (Fig 2b, scalar). This pattern corresponds to a distinct interface enclosing a well-mixed turbulent region. Further analysis has been carried out for the main paper.

Modelling the flow and eddy structure in conductive fluids subjected to magnetic field

S. Kenjereš and K. Hanjalić
Department of Applied Physics, Thermo-Fluids Section
Delft University of Technology, The Netherlands
Email: kenjeres@ws.tn.tudelft.nl, hanjalic@ws.tn.tudelft.nl

Keywords - MHD Turbulence - Modelling - Numerical Simulations - Eddy Capturing

Abstract - In many turbulent flows of industrial and environmental relevance, large-scale eddy structures are the major carrier of momentum, heat and species. In such flows the transport processes can be best controlled by affecting the coherent eddy structure, either by imposing an external force, or by control of boundary topology or its physical conditions. The present papers reports on recent developments in modelling and eddy structure capturing of turbulent magnetohydrodynamics (MHD) flows. The effects of Lorentz force on turbulence are represented with a new model within framework of second-moment and eddy-viscosity closure. First, the model performances have been tested on an isothermal steady flow of liquid metal in a rectangular duct entering and leaving imposed magnetic field, causing very complex magnetohydrodynamical interactions. The proposed model reproduced the formation of a characteristic 'M' shaped velocity profile in a close agreement with the experimental results of Tananev (1978), Fig.1. Next, the model was tested in framework of time-dependent Reynolds-Averaged Navier-Stokes ('TRANS') approach for the case of magnetic Rayleigh-Bénard convection. The TRANS approach is based on the triple-decomposition where the large scale periodic-like motion is fully resolved in time and space, whereas the unresolved stochastic contribution is modelled by a conventional single-point eddy-viscosity or second-moment closure model. In contrast to LES, in the TRANS approach the contribution of both modes (resolved and modelled) to the turbulence fluctuations are of the same order of magnitude. In wall boundary layers the TRANS model accounts almost fully for the turbulence statistics, with a marginal contribution of the resolved motion. It is demonstrated that the imposed magnetic field significantly reduces heat transfer and cause a reorganisation and reorientation of large eddy structures. Two eddy structure capturing methods have been used for this purpose: the classical vorticity/helicity approach and the critical point theory (the kinematic vorticity number, the second invariant of the velocity gradient tensor, the discriminant of characteristic equation). The effect on imposed magnetic field (aligned with the gravitational vector) on reorientation of large eddy structures is shown in Fig.2.

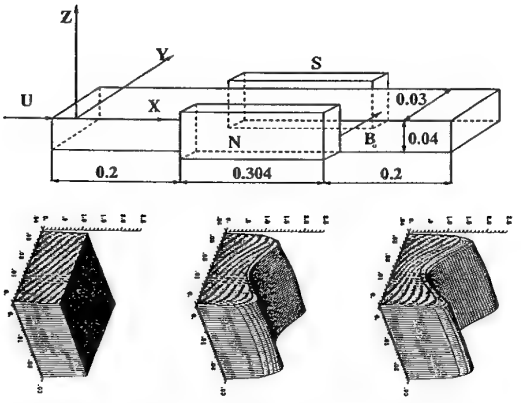

Fig.1. Velocity profiles in a 3D MHD flow in a rectangular duct, Re=2×10^5, Ha=700, N=2.45, experiment by Tananev (1978)

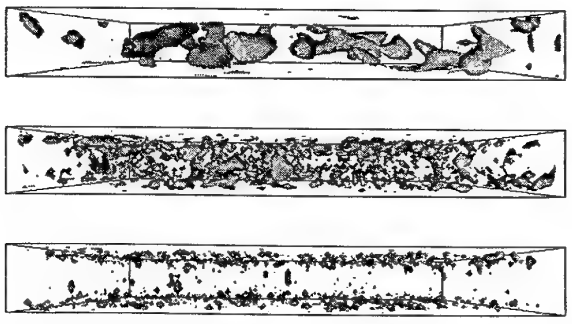

Fig.2. Effects of magnetic field ($B_i||g_i$,Ha=$0, 20, 100$) on the spatial reorganisation of coherent structures in magnetic RB convection, $\mathcal{N}_k$=3,Ra=10^7

Direct simulation of turbulent flow in a pipe with annular cross-section

Maurizio Quadrio and Paolo Luchini
Dipartimento di Ingegneria Aerospaziale
Politecnico di Milano, Italy
Email: maurizio.quadrio@polimi.it

Keywords - Wall Turbulence - Navier–Stokes Equations - Cylindrical Coordinates

Abstract - The turbulent flow in a pipe of annular cross-section is studied by means of direct numerical simulation (DNS) of the Navier–Stokes equations in cylindrical coordinates. Wall turbulent flows in cylindrical geometry are common in engineering applications, but they have received less attention in the literature, because of the additional complexities implied by the cylindrical coordinate system, compared to the cartesian case. The effects of transversely curved boundary layers have been studied by Neves, Moin & Moser (Journal of Fluid Mechanics v.272, 1994), but via a model problem and for large curvatures; we are unaware of a DNS study of turbulent flow in an annular pipe.

The numerical method employed in the present work is a pseudo-spectral method which extends to the cylindrical case a highly efficient solution of the Navier–Stokes equations in cartesian geometries, by writing only two scalar equations for the radial components of velocity and vorticity. The other velocity components can be easily recovered when a Fourier expansion is used in the homogeneous directions. Finite differences are used for the radial discretization.

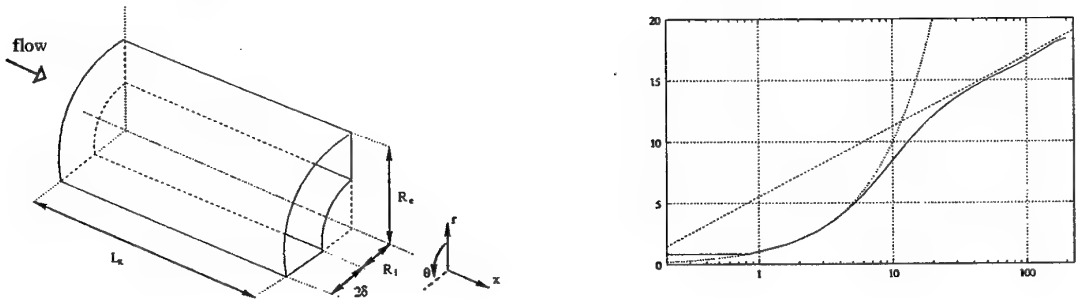

The flow geometry and coordinate system (left) and the mean velocity profile in wall units over the outer wall (right)

The simulated flow is characterized by a Reynolds number (based on the friction velocity and half the annular gap) of approximately 180. The radius of the inner cylinder is 360 wall units: this puts the present case into the mild-curvature range. The Reynolds number, the dimensions of the computational domain, the spatial resolution and the integration time interval have been chosen such as to be similar to those commonly used in the study of plane turbulent channel flow. Results will be shown in terms of turbulence statistics, in order to assess the basic characteristics of this flow, and to compare it with its planar counterpart and the turbulent pipe flow. A detailed comparison of the flow over the convex and concave wall will be reported.

2D turbulence in a bounded domain

A.H. Nielsen[1], H.J.H. Clercx[2] and E.A. Coutsias[3]
[1]Association EURATOM-Risø National Laboratory,
Optics and Fluid Dynamics Department, DK-4000 Roskilde
[2]Eindhoven University of Technology, Department of Technical Physics,
Fluid Dynamics Laboratory, P.O. Box 513, 5600 MB Eindhoven, The Netherlands
[3]Mathematics and Statistics, University of New Mexico,
Albuquerque, NM 87131, USA
Email: anders.h.nielsen@risoe.dk

Keywords - turbulence - computer simulations - bounded flows

Abstract - During the last decades two-dimensional turbulence in unbounded (double periodic) domains, in Navier-Stokes fluids and plasmas has been investigated intensively by means of numerical simulations. The presence of an inertial range in the energy spectrum of these flows has been well documented. As two-dimensional flows exhibit an inverse cascade in the energy, coherent structures comparable with the size of the periodic domain will eventually emerge. Thus, the presence of boundaries and especially the conditions imposed on these will play a significant role in the evolution of the turbulence and the coherent structures, see e.g. [1,2].

In this contribution we present numerical investigations of forced flows in circular geometries. These results are compared with results obtained in double periodic domains. The model equations are the Navier-Stokes equations. For the circular domain we have solved the equations using a pseudo spectral method based on a Chebyshev-Fourier expansion of the solutions. As boundary condition we employ the no-slip condition resulting in strong boundary layers that inject small-scale structures into the interior of the domain. The Reynolds number accessible for our code is in the range $2,000 - 10,000$. For the double periodic domain we have used a standard code based on Fourier expansion.

As forcing we have used a random flow field. From a double periodic squared box, with the same length as the radius of the disk, we initialize a random vorticity field with a specific length scale. The forcing is then transformed into Fourier space. For the double periodic code this term can consequently be used directly. For the circular domain the flow field is spectrally interpolated onto each collocation point of our domain.

We observe that the presence of a no-slip boundary changes the flow evolution significantly. Only initially is there some similarity between the time evolution of the bounded and unbounded flows. Whereas the unbounded flow quickly organizes into two stable monopolar vortices the bound flow creates temporary monopoles, tripoles and quatropoles as a strong boundary layer is continuously created and becomes unstable.

[1] S. Li, D. Montgomery and W.B. Jones, JPL (1996) vol. 56, part 3 pp. 615-639.
[2] H.J.H. Clercx, S.R. Maassen and G.J.F. van Heijst, Phys. Fluids (1999) vol. 11 pp. 611-626.

Turbulence modelling in a single normally impinging jet

L. Thielen and K. Hanjalić
Thermofluids Section , Department of Applied Physics
Delft University of Technology, The Netherlands
Email: luuk@ws.tn.tudelft.nl

Keywords - Turbulence modelling - Impinging flows - CFD

Abstract - Impinging fluid jets are widely used for heating and cooling of solid surfaces. While in most cases a significant heat transfer can be achieved, the optimum performance depends on a number of parameters, primarily on the jet nozzle distance from the wall, targeted solid wall, level of turbulence in the jet and the configuration of the set-surface assembly. Various ways of enhancing the heat transfer have been proposed, such as jet inclination, swirl, forced or self-induced acoustic excitation,special nozzle forms. Because of a number of parameters that need to be considered for optimal design, computer simulation with Reynolds-averaged approach seems an attractive and rational method, provided that the applied models of flow, turbulence and heat transfer are trustable.

We report here on our computational study of a single normally impinging jet flow and heat transfer using different turbulence models: the standard $k-\varepsilon$ model with wall functions, $k-\varepsilon-\overline{v^2}-f$ model and a second-moment closure with wall functions.

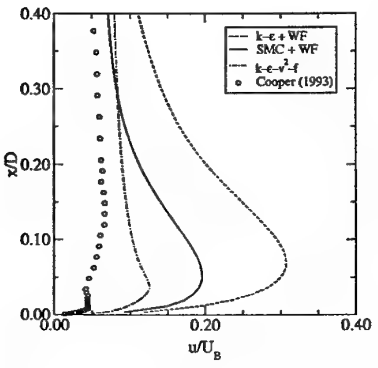

Figure 1: Velocity fluctuation normal to the wall at r/D=0

The $k-\varepsilon$ model is known to produce excessive turbulence energies in the stagnation region. This is a fundamental deficiency and arises from the use of the eddy viscosity stress-strain law to represent normal stresses. Reynolds-stress models give somewhat better results. Also the use of wall functions is not appropriate, since the flow is not in equilibrium, especially in the stagnation region.

The $k-\varepsilon-\overline{v^2}-f$ model, while robust and convenient for engineering applications, seems to possess a potential. This because of the use of $\overline{v^2}$ as a velocity scale, elliptic relaxation, which accounts for non-viscous wall blockage effects, and the switch of the scales from energy-containing to Kolmogorov, to account for viscosity effects very close to a wall.

Symmetry-preserving discretisation of turbulent flow

R.W.C.P. Verstappen and A.E.P. Veldman
Research Institute for Mathematics and Computer Science
University of Groningen, P.O.Box 800, 9700 AV Groningen, The Netherlands
Email: verstappen@math.rug.nl, veldman@math.rug.nl

Keywords - Direct Numerical Simulation - Turbulent Flow and Heat Transfer - Cartesian Grid Method

Abstract - We propose to perform turbulent flow simulations in such manner that the difference operators do have the same symmetry properties as the corresponding differential operators. That is, the convective operator is represented by a skew-symmetric difference operator and the diffusive operator is approximated by a symmetric, positive-definite matrix. Mimicing crucial properties of differential operators forms in itself a motivation for discretising them in a certain manner. We give it a concrete form by noting that a symmetry-preserving discretisation of the Navier-Stokes equations is stable on any grid, and conserves the mass, momentum and kinetic energy if the dissipation is turned off.

We have performed a fourth-order direct numerical simulation (DNS) of the turbulent flow and heat transfer in a channel with surface mounted cubical obstacles. Here, one of the cubes is heated. The temperature is treated as a passive scalar. The Reynolds number (based on the channel width and the mean bulk velocity) is equal to 13,000; the Prandtl number equals 0.71. Both the incompressible Navier-Stokes equations and the energy equation are discretised such that the symmetries of the differential operators are preserved. First- and second-order statistics of the DNS are compared to the available experimental data. The profiles of the mean streamwise velocity and the mean-square of the fluctuating streamwise velocity are in good agreement with the experiments. The same holds for the time-averaged temperatures and heat fluxes.

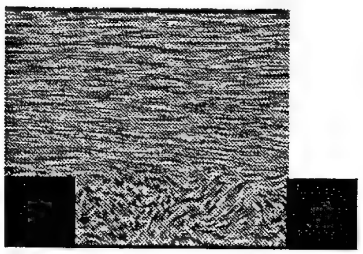

We have extended the symmetry-preserving discretisation method to flow problems in domains with complicated boundaries. We discretise these problems on a Cartesian grid. The simple structure of the Cartesian grid allows to retain much of the basics of our numerical approach. The major issue is: how to discretise the flow in the irregular cells that are cut by the boundary of the flow domain? We address this issue by discretising the convective operator in irregular boundary cells in such a way that the skew-symmetry is preserved. The resulting discrete operator can be integrated explicitly in time for Courant numbers up to 1. In other words, the discretisation is such that small boundary cells do not lead to a sharpening of the convective stability restriction. Diffusion through cut-cells is approximated by a symmetric, positive-definite coefficient matrix. Severe diffusive stability restrictions to the time step are bypassed by treating the diffusive flux partially implicit in time. The method is tested for an incompressible, unsteady flow around a circular cylinder at $Re = 100$. The first results show that the bulk quantities (the Strouhal number, the drag coefficient, the lift and the separation angle) are in fair agreement with the available experimental data.

Premixed flame propagation in isotropic incompressible turbulence

B. Favini and L. Bognetti
Dip. Meccanica e Aeronautica, Universiti Roma, La Sapienza
Email: bfavini@caspur.it

Keywords - Flamelets - DNS

Abstract - The aim of the present research is the analysis of the laminar flamelet regime in forced isotropic turbulence. Incompressibility constraint could appear a severe modification of the true phenomenology, but experimental measurements confirm that the major effects of flame surface wrinkling by turbulence are adequately described by the constant density model (see Lee et al.). This subject has been considered often in the past but still it deserves some attention. In particular flame front behaviour in strongly homogeneous turbulence hasn't yet been analyzed. Among other open questions, the conditions under which the eikonal term, whose role it is to stabilize the flame, affects the scalar dynamics is waiting for a clear answer: a question connected with the possibility of adopting the alternative approach of the passive scalar model. As preliminary results we have performed LES simulations of forced isotropic triperiodic flows at $Re_\lambda = 80$, with a rms fluid velocity two times the laminar flame speed, and a diffusivity $\mathcal{D}$ four times the fluid viscosity. The time history of the turbulent flame speed $s_T =< s_L|\nabla G| >$, where the brackets denote the volume average, is presented in fig. 1; after an initial transient the s_T reaches a stationary state, oscillating around the value of 3.6. The spectra of the turbulent energy and of the scalar are shown together in fig. 2. Because of the roughness of the adopted resolution (32^3) the inertial range reduces to few modes. However it can be noticed that scalar spectra behaves like turbulent energy spectra, except for the higher modes were diffusion becomes relevant which means that front propagation effects are hidden by the flow field advection. These results are in excellent agreement with those of Im et al.

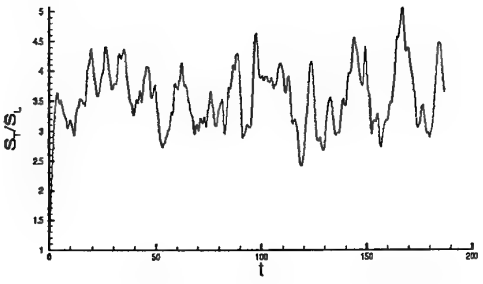

Figure 1

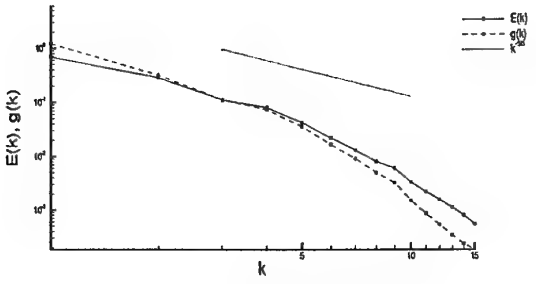

Figure 2

More information about the scalar field can be obtained by tha analysis of its structure functions S_n^i: the i index relates to the physical directions 1,2,3 respectively x,y,z, and n the order of the structure function. The obtained values almost coincide with the exponent of the passive scalar structure functions. In the full paper direct numerical simulation at higher Re_λ and also different diffusivity will be presented. The effect of Lewis number will be also analysed.

1-d Turbulence Spectra in a Shear Flow

B. R. Pearson[‖], P. -Å. Krogstad[⊤] & W. v .d. Water[‖]
[‖] Fluid Dynamics Laboratory, Dept. Applied Physics
University of Technology, Eindhoven. The Netherlands
[⊤]Dept. Thermo- and Fluids Dynamics
Norwegian University of Technology, Norway
Email: w.v.d.water@tue.nl

Keywords - Anisotropic Turbulence - Spectra

Abstract - The 1-dimensional longitudinal $\phi_u(k_1)$ and transverse [$\phi_v(k_1)$ and $\phi_w(k_1)$] turbulent velocity spectra are examined in a modified grid flow. A shear flow is generated by a *NORMAN* grid, a geometry which is composed of a perforated plate superimposed over a square mesh grid. Figure 1 shows the *NORMAN* grid geometry. The u velocity direction is out of the page; the v velocity direction is parallel to the normal Y axis and mean shear gradient. The w velocity direction is parallel to the spanwise Z axis and free of shear. 2-component velocity measurements, using the constant temperature anemometry technique, are made in the resulting anisotropic flow using an $X-$ wire probe (e.g. $u-v$ and $u-w$) over a considerable R_λ ($\equiv u'\lambda/\nu$, u' is the root-mean-square of the turbulent longitudinal variance $\equiv \langle u^2 \rangle^{1/2}$; λ is the Taylor microscale $\lambda \equiv u'/\left\langle (\partial u/\partial x)^2 \right\rangle^{1/2}$) range of 190 to 1200. The measurement station, located 40 mesh heights downstream, is on the mean velocity centreline.

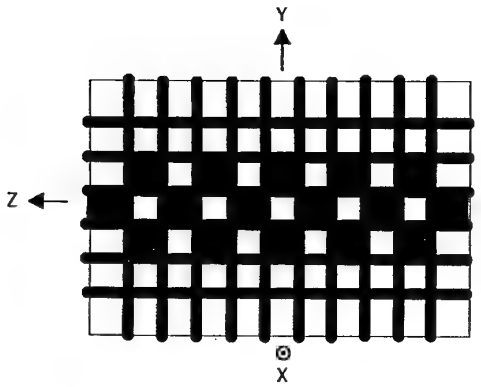

Fig 1: *NORMAN* grid geometry

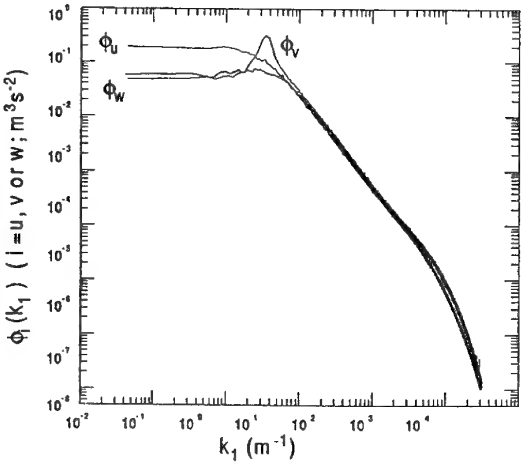

Fig 2: 1-d spectra, $R_\lambda \approx 825$

A preliminary analysis of the spectra (Figure 2) indicates that large spanwise vortices are alternately shed from the upper and lower levels of the perforated plate - giving us the opportunity to study the effect of a localized forcing on the inertial and dissipative range structures over a considerable R_λ range. The aim of the current investigation is to compare the effect of this large scale perturbation on $\phi_v(k_1)$ and $\phi_w(k_1)$ with respect to $\phi_u(k_1)$. In particular we will analyze inertial range scaling and anisotropies using the method of Mydlarski and Warhaft (1996) - a technique yet to be applied to shear flow. We will also discuss cospectra.

Generation of large scale zonal flows over topography by forced turbulence

J. van de Konijnenberg, V. Naulin, J. Juul Rasmussen, and B. Stenum
Risø National Laboratory, OFD-129,
P.O. Box 49, DK-4000 Roskilde, Denmark
Email: jens.juul.rasmussen@risoe.dk

Keywords - Large scale flows - Potential vorticity - Turbulence

Abstract - Generation of large scale mean flows by turbulent mixing at smaller scales is of great importance in various situations as, e.g., geophysical flows. These so called zonal flows will regulate the turbulence by suppressing the small scale fluctuations and set up transport barriers. A relatively simple description of the generation of zonal flows is provided by the idea of homogenization of Lagrangian invariants, here the potential vorticity.

We have performed laboratory experiments in a rotating tank with sloping bottom to investigate the formation of large-scale flows by mixing and homogenization of the potential vorticity. Specifically we consider a tank with radial symmetric bottom topography and a rigid lid. The bottom has a constant slope in the radial direction, which may be either negative (the shallowest part is at the center) or positive (the deepest part is at the center). As is well known, this topography is equivalent to the varying Coriolis parameter for flows on a rotating planet. The shallowest part corresponds to the pole on the planet. The potential vorticity for this system is $PV = \omega + \beta r$ and is a Lagrangian conserved quantity, ω is the relative vorticity and β is proportional to the slope of the bottom. Thus, an effective mixing that homogenizes PV will – for $\beta < 0$ – lead to replacing the high PV near the center with low PV from the outside, and this will appear as an anti-cyclonic mean flow around the center, the pole. Thus, ω in the center will be lower than near the wall. For $\beta > 0$, on the other hand, a cyclonic flow will appear.

In the experiment the mixing is forced by periodical pumping near the outer boundary of the tank at two azimuthally opposite positions. Thus, the azimuthally averaged forcing is zero. The velocity field is measured by particle tracking in the horizontal plane. After a transient time of several tens of forcing periods, we observe the formation of a zonal velocity in the anti-cyclonic direction (for $\beta < 0$). The zonal velocity peaks in the region away from the forcing regime, in the latter a slight cyclonic flow is observed. This is in agreement with the discussion above. As a control case, we checked that no zonal flow appeared in the case of a flat bottom.

We have numerically modeled the experiment by solving the quasi-geostrophic vorticity equation in the β-plane approximation on a disk. The forcing is modeled by localized vorticity sources. Using the parameters of the experiment, we find satisfactory agreement. In addition, we are employing the numerical model to investigate the influence of varying parameters, as, e.g., the Ekman friction, on the structure of the zonal flows, their radial scale size and strength. Finally, by generalizing the numerical model we consider the influence of a finite radius of deformation (Rossby radius) on the formation and structure of the zonal flow.

Experimental study of the nonlinear stress-strain relation for a complex axisymmetric turbulent flow

F. Schmitt and Ch. Hirsch
Department of Fluid Mechanics
Vrije Universiteit Brussel, Belgium
Email: francois@stro.vub.ac.be

Keywords - Turbulence models - constitutive relation - invariants

Abstract - Nonlinear constitutive equations linking the stress tensor to the strain and vorticity tensors have been proposed to overcome the limitations of linear eddy-viscosity models to describe complex turbulent flows. These new equations have been mainly indirectly compared to experimental data, through the outputs of numerical models. It is proposed here to experimentally study the constitutive equation itself, using a 3 terms development recently proposed by Jongen and Gatski (*Int. J. Eng. Sci.*, 36, 739, 1998). Using a projection method onto the tensor basis, the scalar coefficients of this development are explicitely written as function of invariants of the flow. With the experimental determination of the invariants, the constitutive equation can then be studied.

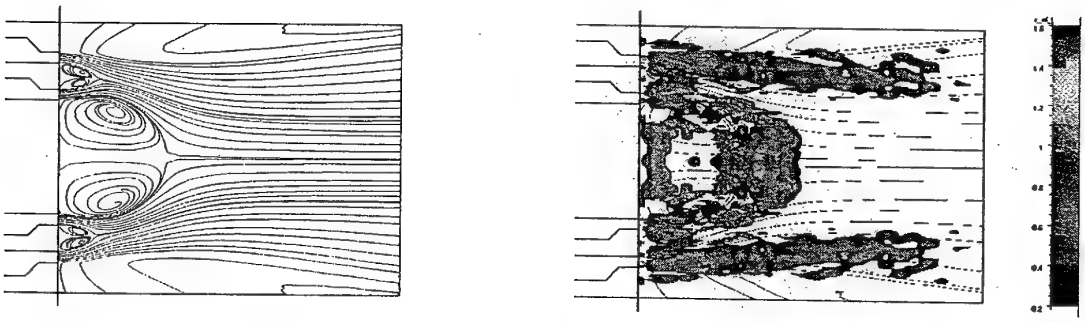

Streamlines of the flow computed from experimental data (left) and a map of the ratio of linear to nonlinear terms in the constitutive relation (right); blank region correspond to a ratio less than 1/5, where the nonlinear terms are dominant, and for gray regions, the linear and nonlinear terms have the same order of magnitude.

The test case chosen is a complex axisymmetric flow generated by a double annular burner. Measurements have been taken on a fine grid (5,500 grid points), enabling the local experimental estimate of the stress and strain tensors. Invariants are then estimated, and the relative values of the different components of the tensor development are evaluated for different regions of the flow. The constitutive equation is also studied considering the "angles" of the traceless stress tensor with the different terms of the tensor basis. It is then experimentally shown that the linear term (which is the only one considered in the classical k-ϵ modelization) of the constitutive equation is dominant only in a very limited region of this complex flow; for other parts of the flow, nonlinear terms are clearly needed. Finally, the different invariants are also used to experimentally estimate the eddy-viscosity ν_T, and since the kinetic energy k is also known, the adimensionnal dissipation can be estimated as $\epsilon/C_\mu = k^2/\nu_T$. This novative post-processing approach can also be applied to fully 3D flows; it is expected to help to significantly improve the efficiency of eddy-viscosity turbulence models to describe complex flows.

PIV in single and multiple impinging jets at high Reynolds numbers

L.F.G. Geers & prof. K. Hanjalić
Thermofluids Unit, Department of Applied Physics,
Delft University of Technology, The Netherlands
Email: leon@ws.tn.tudelft.nl

Keywords - PIV - Impinging jet - High Reynolds number

Abstract - Velocity distributions are measured in single and multiple impinging jets using PIV (particle image velocimetry). For the single impinging jet set-up, a steel pipe (diameter D=35.9 mm, 2.74 m= 76D long) was aligned perpendicular to a flat steel plate (1 m x 1 m) at a distance of 2D. This set-up was used to test the PIV system by comparing the results to those from hot-wire measurements of Cooper et al. [1]. Some preliminary results are presented in Figure 1, more results will be presented in the full paper.

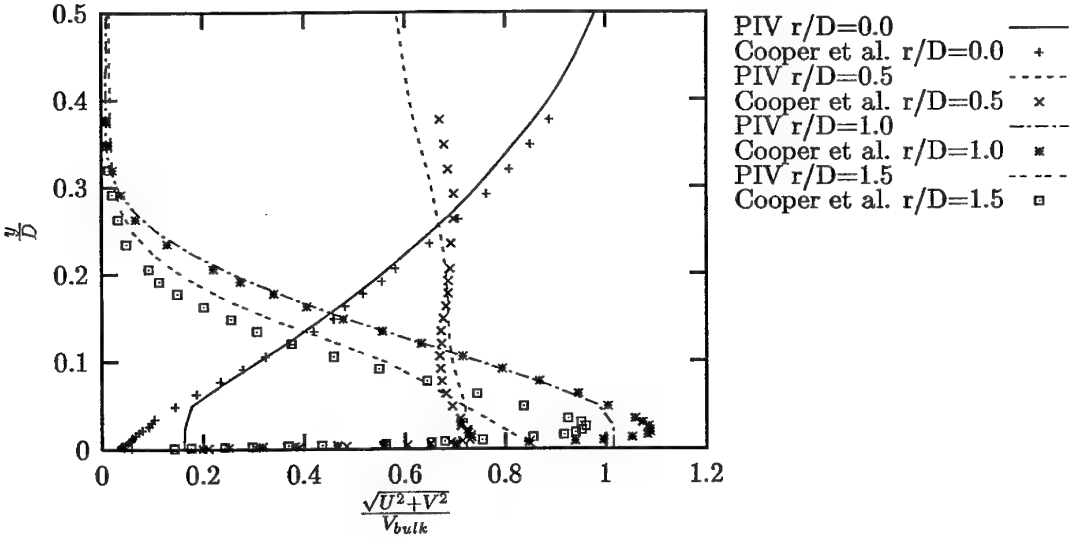

Figure 1: Mean velocity magnitude in single impinging jet

For the multiple impinging jets measurements an open wind tunnel was constructed. Different kinds of nozzle plates can be attached to the output of the wind tunnel contraction to produce different kinds of jets. A glass plate will be used as impingement surface, so PIV measurements can be done in planes both parallel and perpendicular to the jets.

The velocity distributions from both the single jet set-up and the multiple jets set-up can be used for identification of coherent structures in the flow. Different methods of structure identification will be tested with PIV results.

References

[1] D. Cooper, D. C. Jackson, B. E. Launder, and G. X. Liao. Impinging jet studies for turbulence model assessment — I. flow-field experiments. *Int. J. Heat Mass Transfer*, 36:2675–2684, 1993.

The effect of large free-stream turbulence on highly accelerated turbulent boundary layers

B. Stefes and H.H. Fernholz
Hermann-Föttinger-Institut für Strömungsmechanik
Technische Universtät Berlin
Email: stefes@obiwan.pi.tu-berlin.de

Keywords - large free-stream turbulence - relaminarization - retransition

Abstract - Highly accelerated turbulent boundary layers with large free-stream turbulence levels ($Tu \simeq 15 - 20\%$) are usually found in the flow field of turbomachines. The behavior of highly accelerated turbulent boundary layers with low free-stream turbulence undergoing relaminarization and retransition is well known, as well as the effect of very high free-stream turbulence on boundary layers with zero pressure gradient. High acceleration of boundary layers and large free-stream turbulence are two phenomena which have opposite effects on a boundary layer. In the present study measurements have been made in a highly accelerated turbulent boundary layer with relaminarization and retransition influenced by large free-stream turbulence levels ($Tu_\delta \simeq 10 - 20\%$). The maximum acceleration parameter $K \leq 4 \cdot 10^{-6}$ and the starting value of the Reynolds number is $Re_{\delta_2} = 1045$.

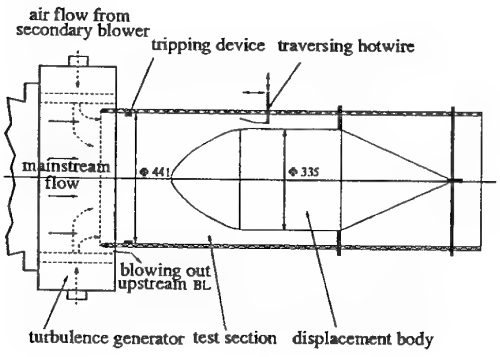

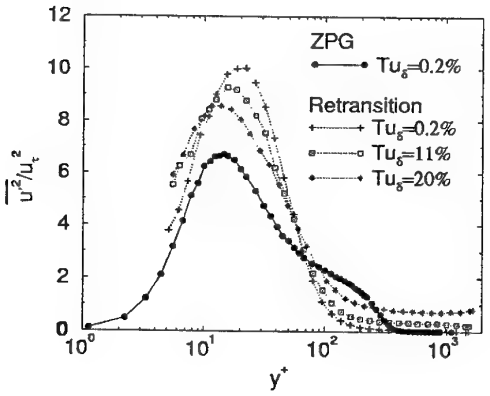

Fig.(1) The experimental set-up. Fig.(2) Normalized profiles of velocity fluctuations in the ZPG boundary layer and in the retransitional boundary layer.

Large free-stream turbulence levels were generated injecting high-velocity jets normal to the mainstream at the beginning of the test section. Acceleration of the mean flow was achieved by mounting an axisymmetric displacement body into the center of the test section. The upstream boundary layer was blown out at the entry of the test section. Hot-wire and LDA measurements were performed in the free-stream and in the boundary layer and skin friction was measured by a wall hot-wire probe. The computed statistics cover mean and rms velocities, velocity correlation coefficients, power spectra and length scales. The profiles of the mean velocity in the accelerated boundary layer are little affected by the free-stream turbulence. However, the velocity fluctuations and their higher moments are strongly influenced by the free-stream turbulence levels (Fig.2), indicating a much faster retransition of the boundary layer compared with the case of low free-stream turbulence.

Intermittency in turbulent boundary layers

Federico Toschi[1], Emmanuel Levêque[2] and Gerardo Ruiz-Chavarria[3]
[1]Department of Applied Physics, University of Twente, The Netherlands
and INFM-Unitá di Tor Vergata, Italy.
[2]Laboratoire de Physique CNRS, ENS de Lyon, France.
[3]Departamento de Física, Facultad de Ciencias, UNAM, Mexico.
Email: f.toschi@tn.utwente.nl

Keywords - Turbulence, Intermittency, Wall Bounded Flows, Channel Flow.
Abstract - Much efforts have been devoted in the recent past towards a better understanding of the phenomenology of homogeneous and isotropic turbulence (in particular from the point of view of intermittency). Here we address the problem of the influences on intermittency of non homogeneities of the flows. We define the following Integral Structure Functions (ISF):

$$\tilde{S}_p(r) = \left\langle (\delta v(r)^3 + r \cdot \mathcal{S} \cdot \delta v(r)^2)^{p/3} \right\rangle \tag{1}$$

The rationale behind these structure functions being that the energy, in presence of shear, is not only transferred to small scale but also is advected spatially by means of the average velocity. In general we expect that there will be a length scale ($L_{\mathcal{S}}$, shear length scale) at which the two contributions will be of the same order of magnitude. In general:

$$\tilde{S}_p(r) \simeq S_p(r) \qquad \text{for} \quad r \ll L_s \tag{2}$$

$$\tilde{S}_p(r) \simeq (r\mathcal{S})^{p/3} S_{2p/3}(r) \quad \text{for} \quad r \gg L_s \tag{3}$$

The shear length scale being defined by the condition $\frac{\delta v(L_{\mathcal{S}})}{L_{\mathcal{S}}} = \mathcal{S}$ can be estimated (neglecting intermittency) as $L_{\mathcal{S}} = (\epsilon/S^3)^{1/3}$ (ϵ being the energy dissipation rate). We report here one test

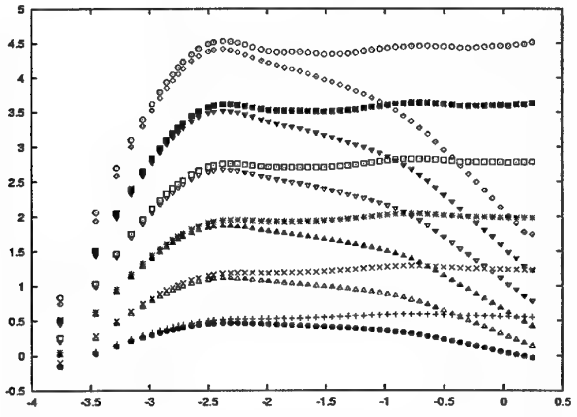

Figure 1: From experimental data at $y^+ = 102$. From bottom to top, in log-log scale, $\tilde{S}_p(r)/r^{\zeta_p}$ as compared to $S_p(r)/r^{\zeta_p}$, for p=1...6.

on experimental data coming from the recirculating wind tunnel of ENS-Lyon. At a distance $y^+ = 102$ from the wall, we have computed the ordinary structure functions, $S_p(r)$, and the ISF, $\tilde{S}_p(r)$. The value of the shear S at our distance from the wall is estimate from the well-established log-law for the average velocity in a turbulent boundary layer.
In Figure 1 we show the normal structure functions compensated by the expected homogeneous/isotropic power law behavior, $S_p(r)/r^{\zeta_p}$ and the ISF compensated by the same intermittency exponents of homogeneous/isotropic turbulence, $S_p(r)/r^{\zeta_p}$ for several values of p. While $S_p(r)/r^{\zeta_p}$ show a definite tendency to decrease at inertial range separations, the $S_p(r)/r^{\zeta_p}$ show a clear *plateau*.

Towards lowering dissipation bounds in turbulent shear flows using a smoothness constraint

R.R. Kerswell
Department of Mathematics
Bristol University, United Kingdom
Email: R.R.Kerswell@bris.ac.uk

Keywords - turbulence - bounds

Abstract - In the continued absence of any fundamental theory of turbulence, there is considerable interest in examining the possible scaling of global transport properties with control parameters. In boundary-driven turbulence, it remains an open question whether the viscous dissipation rate ϵ becomes independent of the fluid's viscosity ν as $\nu \to 0$. So far, all upper bounds on the dissipation rate (e.g. Busse 1970, Doering & Constantin 1992) display this asymptotic independence yet the tempting possibility exists that a tighter bound incorporating more dynamical information may not. We examine the effect of a physically plausible extra 'smoothness' condition on existing upper bounds ϵ_{bound} for the viscous dissipation rate ϵ in turbulent Plane Couette flow. If the minimum lengthscale allowed *parallel* to the plates (separation distance h) is $\ell = O(Re^{2\alpha-1}h)$, then we find that $\epsilon_{bound} = O(Re^{-\alpha})$ as $Re \to \infty$ (measured in units of V_0^3/h where $Re = V_0 h/\nu$, V_0 is the velocity differential and ν is the kinematic viscosity). This implies that transverse lengthscales down to $O(Re^{-1}h)$ must be included in numerical simulations to avoid prejudicing dissipation scalings. In particular, if ℓ is the order of the Kolmogorov scale $(\nu^3/\epsilon)^{1/4}$, then $\epsilon_{bound} = O(Re^{-1/7})$.

Concept of turbulence on the basis of the Boltzmann equation and the structure of a supersonic unstable jet

V.V.Aristov
Computing Center of the Russian Academy of Sciences, Moscow, Russia
Email: aristov@ccas.ru

Keywords - Turbulence - The Boltzmann equation - Free supersonic jets

Abstract - The kinetic approach for description of turbulence in a gas is developed. The main assumption is that the notion of the molecular chaos is valid in a wide range of regimes including unstable ones and the Boltzmann equation is an adequate apparatus (in contrast to some other kinetic conceptions of turbulence). The features intrinsic to turbulence at macroscopic scales can appear as a result of correlations between different parts of a flow due to the distribution function is disturbed and nonequilibrium. We search for the bifurcations in the solutions of the Boltzmann equation and the transition to the unstable nonequilibrium distribution when the outer parameter (Knudsen number) tends to zero. From the mathematical point of view this investigation is made for the dynamical system (with a small parameter) which is obtained after the descritization of the Boltzmann equation in velocity space. The conservative splitting implicit scheme of the direct method of solving the Boltzmann equation with parallel computing is used. It is emphasized that the Chapman-Enskog formalism is valid for the stable kinetic solutions for which the molecular heat and stress are small. If at a certain small Knudsen number the solution of the Boltzmann equation is unstable then it can be expected that the Chapman-Enskog relationships are broken. The large dissipation for this unstable nonequilibrium distribution function is associated with the so-called turbulent stress and heat. In the numerical solutions [1] instabilities in a jet have been observed. In the present study results of the numerical analysis are compared with the experimental data concerning the streamwise vortex structure of the unstable supersonic jet [2]. The underexpanded free jets are considered for the characteristic Reynolds numbers varied in the range: $Re_L = 10^4 - 10^6$. The Goertler-Taylor type of the instability is observed in the computations. Special attention is paid to the character of the spatial structure of the jet flow from the initial section to the downstream areas. Farther downstream there is the transition to a flow with chaotic features where the increase of the dissipation is obtained. We note that the amplitudes of the dissipative values begin to grow in a range of the characteristic Reynolds number between $Re_L = 10^3$ and $Re_L = 3 \cdot 10^3$ that is in accordance with the critical Reynolds number from experiments. The frequencies of density pulsations obtained in computations ($\sim$ 100kHz) are within the unstable zone of the spectra fluctuations presented in the experimental data [3].

This work was supported by the Russian Foundation of Basic Investigations, Grant No. 98-01-00443.

1. Aristov V.V. Study of stable and unstable jet flows on the basis of the Boltzmann equation. Fluid Dynamics. 1998, Vol.33, N2, pp. 280-283. 2. Arnette S.A., Samimy M. and Elliot G.S. On stream vortices in high Reynolds number supersonic axisymmetric jets. Phys. Fluids A. 1992, Vol. 5, pp. 187-202. 3. Novopashin S.A. and Perepelkin A.L. Turbulence in rarefied gases. Rarefied Gas Dynamics, Beylich A. ed., Weinheim, VCH, 1991, pp. 877-883.

On the Gradient Hypotheses for Turbulence Fluid Flow

J.J.H. Brouwers
Section Process Technology, Department of Mechanical Engineering
Technische Universiteit Eindhoven, The Netherlands
Email: j.j.h.brouwers@wtb.tue.nl

Keywords - gradient hypotheses - turbulent fluid flow - Fokker-Planck equation - diffusion limit - asymptotic analysis - stochastic process.

Abstract -The Fokker-Planck equation for the probability density of fluid particle position in inhomogeneous unsteady turbulent flow is derived. The equation is obtained starting from the general kinematic relationship between velocity and displacement of a fluid particle and applying exact asymptotic analysis. For (almost) incompressible flow the equation reduces to the convection diffusion equation and the equation pertaining to the scalar gradient hypothesis. In this way the connection is established with widely used eddy diffusivity models. It is further shown that within the accuracy of the approximation scheme of the diffusion limit, diffusion constants can equally be based on coarse-grained Lagrangian statistics as defined by Kolmogorov or on Eulerian statistics in a frame that moves with the mean Eulerian velocity as proposed by Burgers.

Presented results of diffusion theory are the leading terms of asymptotic expansions. Truncated terms are higher order spatial derivatives of the probability density or of the scalar mean value withcoefficients based on cumulants higher than second order of fluid velocities and their derivatives. The magnitude of these terms has been assessed employing scaling rules of turbulent flows in pipes and channels, turbulent boundary layers, turbulent jets, wakes and mixing layers, grid turbulence, convective layers and canopy turbulence. It reveals that a true diffusion limit does not exist. Although truncated terms can be of limited magnitude, a limit process by which these terms become vanishingly small and by which the diffusion approximation would become exact does not occur for any of the cases of turbulent flow considered. Applying the concepts of diffusion theory resorts to employing approximate methods of analysis.

Simulations & Numerical Methods

Numerical simulation of coupled liquid-solid dynamics

J. Gerrits and A.E.P. Veldman
University of Groningen, Department of Mathematics
P.O. Box 800, 9700 AV Groningen, The Netherlands
Email: j.gerrits@math.rug.nl

Keywords - Coupled Dynamics - Free-Surface Flow - Flat Spin

Abstract - Nowadays, theoretical and experimental studies of fluid behaviour are more and more accompanied by computer simulations. For a fluid under micro-gravity conditions theoretical and experimental results of its motion are often not available since the behaviour of a fluid in an extra-terrestrial environment is physically not well understood yet and experiments in such an environment are very expensive. Thus, in extra-terrestrial fluid flow, Computational Fluid Dynamics (CFD) has become an essential, and because of the ongoing increase of computer resources as well as the improvement of numerical algorithms, a reliable development tool.

Also from a computational point of view, fluid behaviour under micro-gravity conditions is more complicated than under terrestrial conditions: the fluid has a tendency to undergo large topological changes, requiring an accurate and robust method for free-surface advection. Further, if the fluid is contained in a cavity such as a satellite then the motion of the satellite is influenced by the sloshing liquid: the dynamics of the solid-body motion and the liquid motion are coupled.

In our paper we present a method for simulating coupled liquid-solid dynamics. The liquid dynamics is solved by discretizing the Navier-Stokes equations on a Cartesian grid. The incorporation of a so-called cut-cell approach allows the solid body, in which the liquid is contained, to have complex shape. Transportation of the free surface is based on the well-known VOF-method. However, by introducing a local height function, we changed this method slightly in order to avoid the (numerical) creation of "flotsam" and "jetsam". The coupling between the solid-body motion and the liquid motion is achieved by solving (each time step) equations for the linear and angular momentum of the solid body. In these equations terms appear that represent the force and torque exerted upon the solid body by the liquid. On the other hand terms accounting for the solid-body motion are added to the Navier-Stokes equations making the coupling complete. Some care has to be taken in integrating the coupled equations in order to keep the coupling numerically stable for arbitrary liquid/solid mass ratios.

For the validation of our method we study the coupled dynamics of a container that is (partially) filled with liquid. If the coupled system, initially, is rotating around the long axis (which is unstable), then, because of the interaction with the liquid motion, the system will settle itself into a steady state in which it is rotating around the (stable) short axis. This phenomenon is known as flat spin. We show the results of several flat-spin simulations with different liquid/solid mass ratios.

Analytical Solution of a 3-D Flow by the Lattice Boltzmann Method

D.Valougeorgis
Department of Mechanical & Industrial Engineering
University of Thessaly, Pedion Areos, GR-38334 Volos, Greece
Email: diva@mie.uth.gr

Keywords - Computational Fluid Dynamics - Numerical Schemes

Abstract - The Lattice Boltzmann Method (LBM) is a relatively new computational approach that utilizes parallel computers to study transport phenomena (Chen & Doolen 1998). The method is based on the discrete Boltzmann equation or simplified kinetic model equations and it has been proved capable to describe macroscopic average properties and to simulate efficiently fluid flows. There is great interest in the method due to its potential to solve complex physical systems that are problematic for conventional methods. For this reason a large portion of the present effort is towards a thorough quantitative investigation of the method trying to place it on a rigorous theoretical foundation. It is well known that instability problems may arise, while the implementation of the hydrodynamic boundary conditions is still under investigation. A number of analytical LBM solutions have been derived to provide exact representation of simple flows. It has been indicated that the analytical solutions for these flows are still to simple to use as a general guidance for boundary condition analysis. Further studies on more complicated flows for additional benchmarking and verification are necessary.

In the present work an analytical LB solution is derived for the three dimensional square duct flow subject to a fifteen velocity model. Analytical expressions for the distribution functions are derived, based on the LBBGK equation, the corresponding equilibrium distribution functions and the geometric and physical properties of the fully developed flow in a rectangular channel. The analytical solutions are functions of the lattice size, the collision relaxation parameter and a characteristic velocity related to the constant pressure gradient in the axial direction. The analytical LBM solution is verified by the well known macroscopic analytical solution, while the results of an independent LBM numerical simulation for various relaxation time parameters and lattice sizes are compared with the analytical solutions. The above results are valid in the interior of the flow domain.

Using these analytical solutions explicit expressions for the distribution functions at the boundaries are obtained. Then different schemes for the application of certain heuristic and hydrodynamic boundary conditions are analyzed and the order of accuracy of these schemes is obtained. Numerical simulation is carried out for different implementation of boundary conditions for stationary walls including the bounce back rule, the modified bounch back rule, the no slip boundary condition and the bounch back scheme with half way wall. The simulation results are verified with the corresponding theoretical ones. An investigation is made to whether the occasional break down of the LBM scheme is due to high time relaxation values or the application of non suitable boundary conditions.

It is hoped that the present approach, gives guidance in applications regarding the implemented discretization schemes, helps to develop better boundary conditions of general purpose and in general enhance our understanding of the method.

References

Chen S. and Doolen G.D., *Annu. Rev. Fluid Mech.*, **30**, 329-364 (1998).

Simulation of green water loading using the Navier-Stokes equations

G. Fekken, A.E.P. Veldman
University of Groningen, Department of Mathematics
P.O. Box 800, 9700 AV Groningen, The Netherlands
Email: g.fekken@math.rug.nl

Keywords - Green water - Cartesian grid - Volume of Fluid

Abstract - Simulating viscous flows with a free surface causes special difficulties, since its position will change continuously. Therefore, besides solving the Navier-Stokes equations, the position of the free surface must be determined every time step. In the present method, the Navier-Stokes equations are solved on a three-dimensional Cartesian grid. A Volume-of-Fluid function is used for the position of the fluid. Since the method is able to handle arbitrary forms of the geometry, many types of industrial flow problems can be simulated.

One of the applications of this method is the simulation of *green water*. Green water is the water which flows on the deck in high waves when the relative wave motion around the bow is exceeding the deck level. As a result of this green water loading, damage to superstructures on the deck is still a common occurrence. The Maritime Research Institute Netherlands (MARIN) has done extensive model test research to this phenomenon during the last few years. The simulation of this is a complex problem, since the water will behave wildly when it flows on the deck, causing effects like air bubble entrapment. The tests also show complex high velocity flow patterns on the deck.

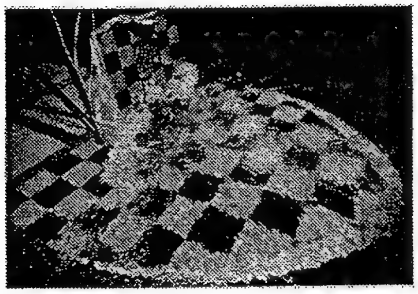

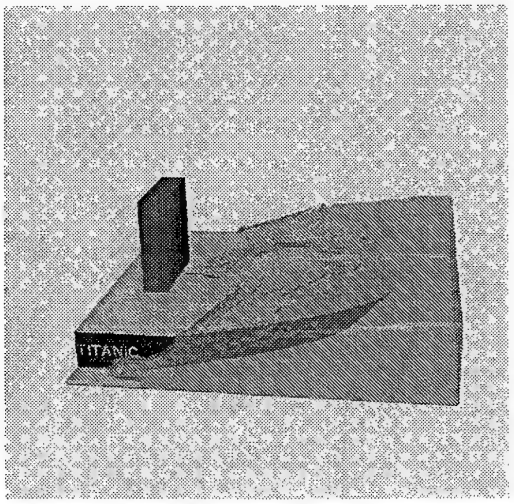

Photo of model test (left) and snapshot of numerical simulation (right)

The problem of green water loading on the foredeck of a ship is discussed and a comparison is made with experimental results of MARIN. Waterheights, pressures and water contours are produced and compared with model tests. Also forces on different structures placed on the deck are compared and analyzed.

Free-surface thin film flows over topography

S. Kalliadasis, Department of Chemical Engineering, University of Leeds, UK
G.M. Homsy, Department of Chemical Engineering, University of Stanford, USA
Email: chesk@sun.leeds.ac.uk

Keywords - Free-surface flows, thin films, coating flows

Abstract - We consider the slow motion of a thin viscous film flowing over a topographical feature (trench or mound) under the action of an external body force. Using the lubrication approximation, the equations of motion simplify to a single nonlinear partial differential equation for the evolution of the free surface in time and space. It is shown that the problem is governed by three dimensionless parameters corresponding to the feature depth, feature width and feature steepness. Quasi-steady solutions for the free-surface are reported for a wide range of these parameters. Our computations reveal that the free-surface develops a ridge right before the entrance to the trench or exit from a mound and that this ridge can become large for steep substrate features of significant depth. Such capillary ridges have also been observed in the contact line motion over a planar substrate where the build-up of pressure near the contact line is responsible for the ridge. For flow over topography, the ridge formation is a manifestation of the effect of capillary pressure gradient induced by the substrate curvature. In addition, the minimum film thickness is always found near the concave corner of the feature. Both the height of the ridge and the minimum film thickness are found to be strongly dependent on both the profile depth and steepness. Finally, it is found that either finite feature width or a significant vertical component of gravity can suppress these effects in a way that is made quantitative and which allows the operative physical mechanism to be explained.

A pore-scale numerical model for flow and heat transfer in fibrous porous media

Jan A. Kolodziej
Institute of Applied Mechanics
Poznan University of Technology PL-60-965 Poznan, Poland
e-mail: Jan.Kolodziej@put.poznan.pl

Keywords - fibrous porous media, Trefftz method, permeability tensor, heat transfer

Abstract - A pore-scale numerical model based on Trefftz method is described for modelling fluid flow and heat transfer in rigid porous media. The performance of the model is demonstrated for two- dimensional flow through idealised porous media composed of spatially regular arrays of parallel fibers. The purpose of paper is determination of permeability tensor and heat transfer coefficients on the base of micro-flow with heat transfer. For solution of micro-fields the Trefftz method is used. In frame of this method the special purpose T-functions are derived and applied. These functions fulfil exactly not only governing equations of creeping flow and temperature field but also some boundary conditions; namely conditions on fibers boundary and some symmetry. The longitudinal and transverse flows relative to fibers are considered. Considerations of heat transfer are given to the fully developed heat-transfer characteristics for creeping flow between fibers. The influence of the geometric parameters (volume fraction of fibers and case of fiber arrays) on non-dimensional components of permeability tensor and Nusselt numbers is discussed. Results of these investigations can be used for developing a proper computational model of the resin transfer moulding process.

A rarefied gas flow caused by a discontinuous wall temperature

Kazuo Aoki, Shigeru Takata, and Hidefumi Aikawa
Department of Aeronautics and Astronautics,
Graduate School of Engineering, Kyoto University, Japan
Email: aoki@kur3.kuaero.kyoto-u.ac.jp

Keywords - Rarefied Gases - Kinetic Theory - Thermal Creep Flow

Abstract - A flow of a rarefied gas caused by a discontinuous wall temperature is investigated on the basis of kinetic theory in the following situation. As shown in the figure (left), the gas is confined in a two-dimensional square container $-L/2 < x_1 < L/2$, $-L/2 < x_2 < L/2$, where x_i is the rectangular coordinate system. The left and right halves of the wall of the container are kept at different uniform temperatures T_1 and T_2, respectively, so that the temperatures of the top and bottom walls are discontinuous at their respective middle points ($x_1 = 0$, $x_2 = \pm L/2$). External forces are assumed to be absent. The steady flow of the gas induced in the container by the effect of the discontinuities of the wall temperature is analyzed numerically by a finite-difference method on the basis of the BGK model of the Boltzmann equation and the diffuse reflection boundary condition. The features of the flow are clarified for a wide range of the Knudsen number. Examples of the flow field are shown in the figure (right), where Kn$= l/L$ is the Knudsen number and l is the mean free path of the gas molecules in the equilibrium state at rest whose temperature is T_1 and density is the average density of the gas in the container. Since the flow is symmetric with respect to x_1-axis, the lower half of the container ($x_2 < 0$) is shown in the figure. A flow is induced from the colder to the hotter part along the bottom wall near the point of discontinuity, and it causes an overall circulating flow. It is shown by detailed computations that, as the Knudsen number becomes small (i.e., as the system approaches the continuum limit), the maximum flow speed tends to approach a finite value, but the region with appreciable flow shrinks to the point of discontinuity; thus, the overall flow in the container vanishes nonuniformly in the continuum limit.

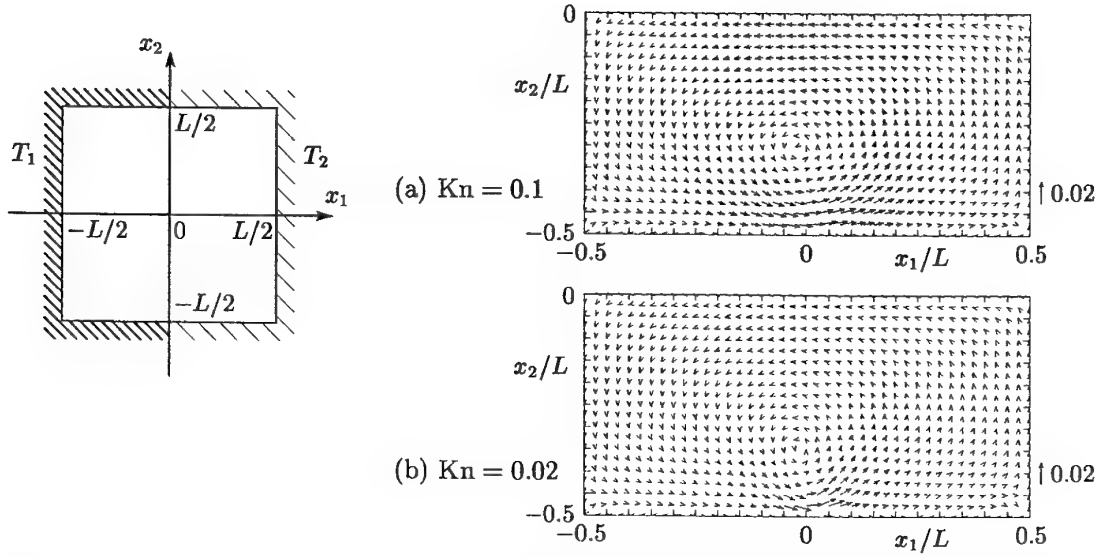

The two-dimensional square container (left) and the flow induced in the lower half of the container for $T_2/T_1 = 2$ (right). (a) Kn $= 0.1$, (b) Kn $= 0.02$. *The arrow indicates the dimensionless flow velocity vector $(v_1, v_2)(2RT_1)^{-1/2}$ (R: specific gas constant) at its starting point, and its length corresponding to the magnitude of* 0.02 *is shown in the figure.*

Parallel Contour Dynamics for 2D Vortex Flow Simulations

R.M. Schoemaker[†,‡], P.C.A. de Haas[†], H.J.H. Clercx[‡], and R.M.M. Mattheij[†]
[†]Dept. of Mathematics and Computing Science and [‡]Dept. of Physics
Eindhoven University of Technology, The Netherlands
e-mail: r.m.schoemaker@tue.nl

Keywords — Contour Dynamics - Parallelization - Background Rotation - Advection

Abstract — In this work it is shown that an acceleration of contour dynamics simulations by means of parallelization is of great importance for simulating complex vortex flows.

Contour dynamics is a numerical method for simulating two-dimensional incompressible inviscid vortex flows, and is based on the observation that the evolution of a patch of uniform vorticity is fully determined by the evolution of its bounding contour. The contours are discretized into nodes and interpolating linear elements. A continuous vorticity distribution can be approximated by nested patches of uniform vorticity. During a numerical experiment the vorticity distribution in the flow becomes more and more complex. The number of nodes on the contours has to increase with this complexity in order to keep the simulation accurate. The contour dynamics method is of order $\mathcal{O}(n^2)$, where n is the number of nodes in the numerical domain. It is clear that this method has computational limitations for complex flow problems.

An example of a complex 2D vortex flow concerns the dynamics of one or more vortices in a background rotation. This is interesting for geophysical flows, where quasi 2D vortices play an important role. Another example is advection of passive tracers in a vortex flow (with or without background rotation).

In order to accomplish the parallelization of contour dynamics, the contour dynamics method has been accelerated first by means of a hierarchical element method. This hierarchical element method (HEM) is of order $\mathcal{O}(n)$. The algorithmic structure of the HEM is very suitable for parallelization. It is this parallelization that accelerates the HEM even further and provides us with a tool for simulating very complex 2D vortex flows in acceptable time.

Examples of complex vortex flows (background rotation, advection) are used to investigate the properties of the parallelized HEM for contour dynamics. Comparisons are made with single-processor computations. The complexity of the algorithmic structure together with some parallelization parameters are used to investigate the parallel efficiency.

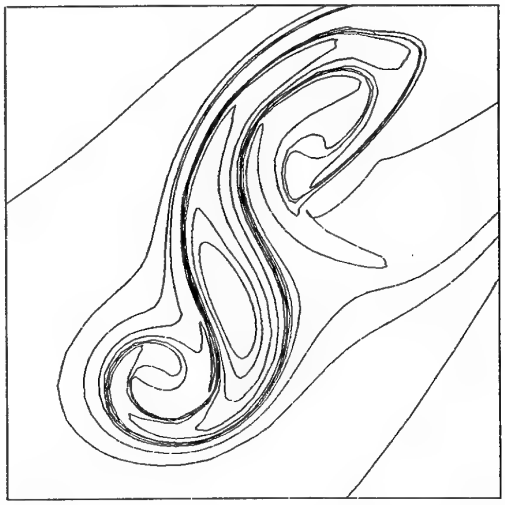

A deformed monopole in a background rotation.

FREE-SURFACE FLOW OF A FLUID BODY WITH AN ECCENTRIC CYLINDER IN IMPULSIVE MOTION

Elin M. Bøhler[1], *Maurizio Landrini*[2] and *Peder A. Tyvand*[1]

1 Dept. Agricultural Engineering, Agricultural University of Norway, Box 5065, N-1432 Aas Norway
2 INSEAN, The Italian Ship Model Basin, Via di Vallerano 139, 00128 Roma. Italy
e-mail corresponding author: peder.tyvand@itf.nlh.no
Keywords: impulsive, free surface, gravitational, potential flow.

A fluid body is released from rest in the gravity field. The flow is assumed incompressible, inviscid, irrotational and two-dimensional. A solid cylinder inside the fluid body is put impulsively into forced motion just as the gravitational flow starts. The fluid body has initially a circular contour with radius $R_{\mathcal{F}}$. The solid cylinder is circular, radius $R_{\mathcal{C}}$, and is initially eccentric with respect to the fluid body. Tyvand and Landrini [1] have recently investigated the corresponding problem with an initially concentric solid cylinder inside the fluid body. The dimensionless physical parameter is the Froude number Fr = forced velocity × (gravity × outer radius)$^{-1/2}$.

In Figures 1-2 we show some numerical results for the exact nonlinear problem, for Fr = 1. Snapshots of inner and outer cylinder contours are shown for non-dimensional time interval 0·25. The inner cylinder has a radius $\epsilon = R_{\mathcal{C}}/R_{\mathcal{F}} = 0{\cdot}5$ and the initial displacement of its center is 0·25 away from the fluid body center.

The nonlinear initial-boundary-value problem is also investigated analytically by a small-time expansion. A bipolar coordinate system is applied, and the boundary-value problem to each order is solved in terms of Fourier series. In Table 1 below, we show some results for the added mass at the initial instant, for different values of the inner cylinder radius ϵ and increasing displacement Δ of the centers, made dimensionless by $R_{\mathcal{F}}$. Added mass coefficients are made dimensionless by $\rho R_{\mathcal{F}}^2$, where ρ is the fluid density. It can be shown that the impulsive force always points in the opposite direction of the forced motion, and its size is independent of the direction of motion. Therefore, the added mass tensor is isotropic and can be represented by a scalar.

	Δ=0·05	Δ=0·25	Δ=0·45	Δ=0·85
ϵ=0·1	0·03080	0·03071	0·03044	0·02441
ϵ=0·5	0·47005	0·44011	0·35986	–

Table 1: Dimensionless added mass for the impulsive motion.

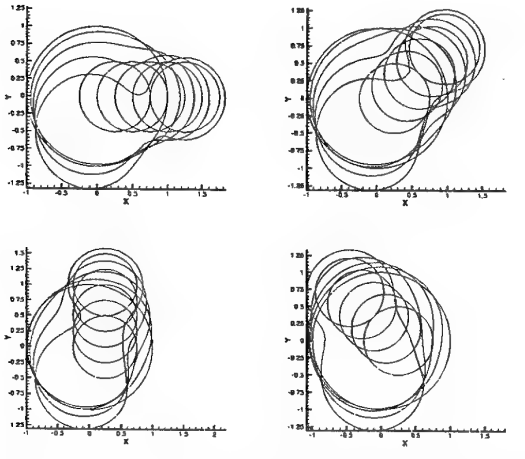

Figure 1: $R_{\mathcal{F}} = 1$, $R_{\mathcal{C}} = 0.5$, $x_{\mathcal{C}}(t=0) = 0.25$, $y_{\mathcal{C}}(t=0) = 0$, $Fr = 1$. The angle θ of the cylinder velocity with respect to the x-axis is 0 (top-left), $\pi/4$ (top-right), $\pi/2$ (bottom-left), $3\pi/4$ (bottom-right).

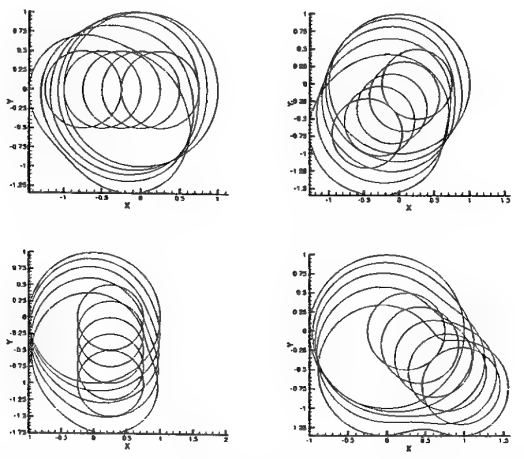

Figure 2: $R_{\mathcal{F}} = 1$, $R_{\mathcal{C}} = 0.5$, $x_{\mathcal{C}}(t=0) = 0.25$, $y_{\mathcal{C}}(t=0) = 0$, $Fr = 1$. The angle θ of the cylinder velocity with respect to the x-axis is (following plots in counter-clockwise direction): π (top-left), $5\pi/4$ (top-right), $3\pi/2$ (bottom-left), $7\pi/4$ (bottom-right).

[1] Tyvand. P.A., Landrini, M. (2000) Free-surface flow of a fluid body with an inner circular cylinder in impulsive motion. *J. Engng. Math.* In press.

DIRECT NUMERICAL SIMULATION OF A COMPRESSIBLE VISCOUS FLOW OVER A PLAN DIHEDRAL

E. CREUSE[†,‡] and I. MORTAZAVI[†]

[†] Université Bordeaux I. 351, Cours de la Libération, 33405 Talence Cedex, FRANCE
[‡] Université Valenciennes. Le Mont Houy, 59313 Valenciennes Cedex 9, FRANCE

KEY WORDS: Vortex dynamics, direct numerical simulation, compressible viscous flow, laminar flow.

In this work, the evolution of a two-dimensional compressible viscous flow over a plan dihedral is studied using direct numerical simulation tcehniques. The aim of the paper is to describe the behaviour of such a flow, especially the swirling dynamics produced downstream of the discontinuity point of the dihedral. New exit boundary conditions are implemented to avoid the return of noisy acoustic waves. Several Reynolds numbers up to highest bounds of laminar evolution are studied.

the main part of this work is devoted to a qualitative and quantitative study of vortex dynamics in this kind of flow. The process used to identify vortices evolving in the flow is first carefully explained and justified. The Weiss criterion, used initially to analyse the incompressible Euler equations [1] [2], is validated to be used in low compressible flows. It reveals a good complementarity with a more classical vorticity threshold criterion, and a high efficiency to isolate the vortices. The evolution of the global enstrophy, energy and circulation as well as the number and the size of the vortices display prominently a more and more heterostrophic behaviour of the concentrated structures with the Reynolds number increase.

Then, an analysis of several time-averaged quantities as a function of the Reynolds number is performed. The straight relationship between these quatities and global flow charachteristics in function of the Reynolds number is observed.

Finally, the instantaneous visualisation of eddy interactions as well as the time evolution of the primitive variables at several monitoring points in the flow allows an accurate diagnostics of the swirling dynamics, both qualitatively and quantitatively. In this case, the relationship between transport properties and the charactheristic evolution of concentrated vortex structures is distinguished as a fact.

References

[1] J. Weiss, 'The dynamics of enstrophy transfer in two-dimensional hydrodynamics', *Physica D*, 48, 273-294 (1991).

[2] C. Basdevant and T. Philipovitch, 'On the "Weiss criterion" in two-dimensional turbulence', *Physica D*, **73**, 17–30 (1994).

Numerical simulation of a viscous swirling flow in pipes with varying radius

J. Ortega-Casanova and R. Fernández-Feria
E.T.S. Ingenieros Industriales
Universidad de Málaga, Spain
Email: jortega@uma.es

Keywords - Swirling Flow - Vortex Breakdown

Abstract - Under the assumptions of an incompressible and axisymmetric flow, the unsteady Navier-Stokes equations are solved numerically in a pipe of varying radius with a central body located inside, see figure.

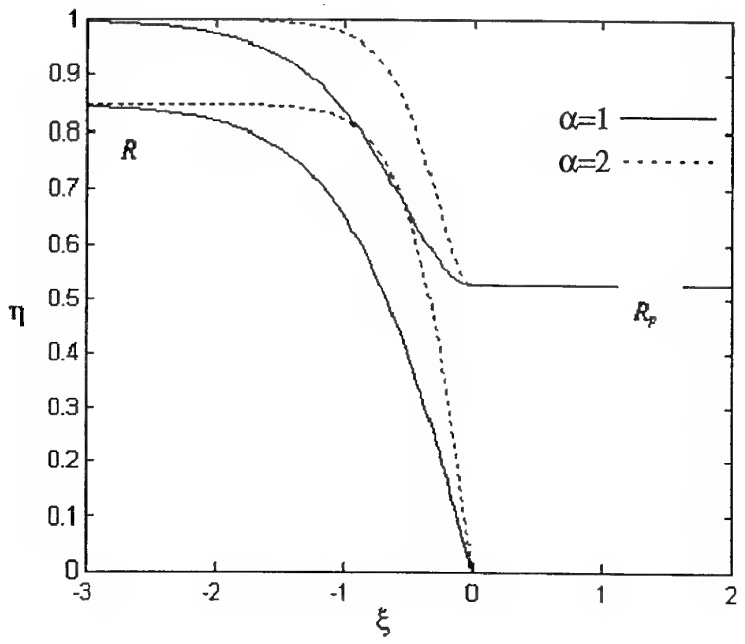

Sketch of the pipe

The Navier-Stokes equations are written using the streamfunction-circulation-vorticity formulation. The presence of the central body adds difficult to the numeric treatment of the equations due to the singularity associated to its base located at the axis. Different numerical techniques have been implemented to deal with this singularity. The flow is governed by five non-dimensional parameters: the upstream radius of the central body R, the downstream radius of the pipe R_p, the characteristic axial length of the central body α, the Reynolds number Re, and a swirl parameter L (ratio between the characteristic azimuthal and axial velocities at the inlet). The swirl of the flow may be generated by the rotation of the outer wall, by rotation of the central body, or by both walls rotating. Given the geometry (R, R_p y α), for each Re there exists a maximum value of the swirl parameter L above which a bubble of flow recirculation appears at the axis of symmetry (the vortex breaks down). Configurations with multiple bubbles may appear for larger L. These different regions are presented in a $Re - L$ plane, and compared with results obtained in the inviscid limit.

Hybrid Navier-Stokes Flow Simulation for Turbine Cascade Flows on structured-unstructured Meshes

H. Sbresny
Institute of Aeronautical Propulsion, University of Stuttgart, Germany
Email: sbresny@ila.uni-stuttgart.de

Keywords - Hybrid Navier-Stokes Method - Structured-Unstructured Meshes - Turbines - Film-Cooling

Abstract - In this study, a hybrid finite volume Navier-Stokes method is presented. This method combines different mesh element types using both, structured data handling on structured meshes (quadrilateral elements), and unstructured data handling on unstructured meshes (triangular elements). It is important to distinguish between mesh element shape and element distribution on the one hand, and data handling on the other. In the present study, it is referred to as structured data handling if mesh and fluid data are stored in a matrix orientated way. In doing so, the neighbouring points of a mesh point, e.g. (i, j), are implicitly known, by $(i-1, j)$, $(i+1, j)$, and so on. The listing orientated data handling, where data and connectivities are treated via arrays and pointers, is referred to as unstructured data handling. As it is already known, both methods of data handling and both mesh structures have pros and cons concerning calculation time, mesh generation and solution accuracy.

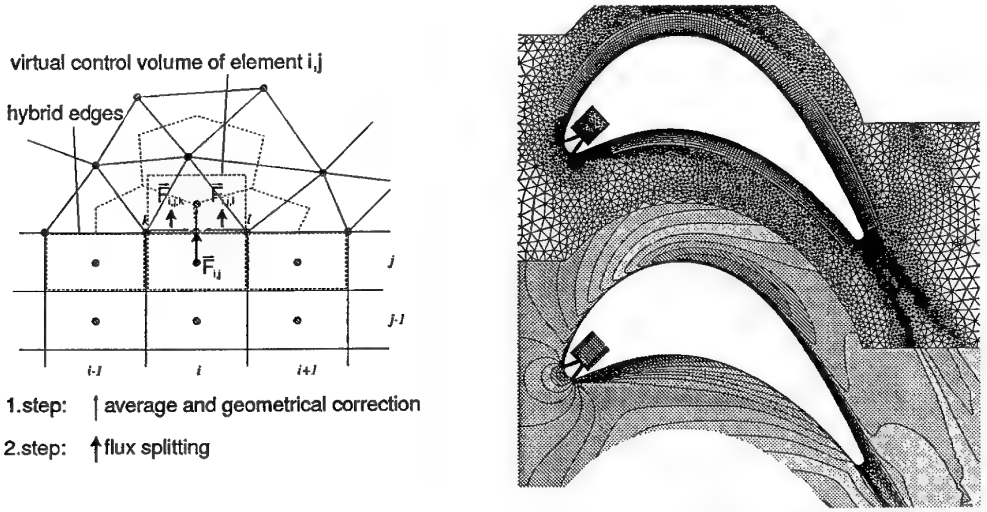

Hybrid data exchange (left) and the ATBS test case with the adapted hybrid mesh and Mach number isolines (right).

Such a hybrid method offers the possibility to decide for each flow case which areas of the flow region are simulated using a structured mesh and data handling and which are simulated using unstructured mesh and data handling. Concluding, the advantages of the different methods can be exploited depending on the individual flow case and aspects of the investigation considered (calculation time, adaptivity, simulation quality, complex geometries). The method is created by combining two flow solvers using different data handling. Therefore, a data interface, organising the exchange between the different flow and solver regions has to be established, also preserving conservativity of the flow quantities. After a short description of the solvers applied here, the basic philosophy of the programme combination and the data interface is described. A short outlook on a similar treatment for other fluid simulation programmes is given. Results of inviscid, viscous and turbulent flow simulations and the comparison of calculated and measured data are presented.

Self-sustained pulsations in pipe systems with closed side branches: Euler simulations

S. Dequand, S. Hulshoff & A. Hirschberg
Eindhoven University of Technology,
Postbus 513, 5600 MB Eindhoven, The Netherlands
Email: s.m.n.dequand@tue.nl

Abstract - A 2-D Euler code has been developed within the framework of the European project Flodac ('Flow Duct Acoustics'). Calculations have been performed in order to validate the code. The pipe configuration considered consists out of two closed side branches placed opposite to each other along a main pipe. We call this a cross-junction. Such a cross-junction displays a strong acoustical resonance for a frequency corresponding to a wavelength equal to four times the side branch length. The radiation along the main pipe is negligible at the resonance frequency. The numerical results are compared to acoustical measurements and flow visualization. We limit ourselves to pipes with square cross-sections and sharp-edged junctions. The flow separation at sharp edges is induced by numerical viscosity. The coupling between acoustic standing waves and instabilities of the shear layers (separating the main flow from the stagnant gas in the closed side branches) induces self-sustained pulsations. The Euler code predicts the pulsation amplitude within ten percent.

Asymptotic Dynamics of Thin Viscous Sheets

N. M. Ribe
Institut de Physique du Globe
4 Place Jussieu, 75252 Paris cedex 05, France
Email: ribe@ipgp.jussieu.fr

Keywords - Viscous Sheets - Polymer Processing - Shell Theory

Abstract - Thin viscous sheets are important in situations as diverse as polymer processing and geophysics. I present a theory for the deformation of general three-dimensional viscous sheets subject to arbitrary distributed loading. The goal is to reduce the three-dimensional equations of viscous flow to two-dimensional equations for the motion of the sheet's "middle surface". Accordingly, the fundamental quantities are six kinematic parameters that describe the deformation of the middle surface (rates of extension, shear, bending, and torsion), and six stress resultants and bending moments, obtained by weighted integration of the local stress distribution across the sheet. Analytical solution of a set of approximate "shallow-sheet" equations reveals the scales for the velocity components and the pressure as functions of the sheet's slenderness $\epsilon \ll 1$, its two principal curvatures k_1 and k_2, and the characteristic wavenumbers q_1 and q_2 of the applied load in the directions of principal curvature. These scales are then used as the basis for systematic asymptotic expansions which yield global constitutive relations for the stress resultants and bending moments in terms of the six kinematic quantities. From the results of separate asymptotic expansions in different regions of the curvature/wavenumber space, I determine composite global constitutive relations that are valid for arbitrary k_1, k_2, q_1, and q_2. The set of equations is completed by kinematic equations that describe the evolution of the sheet's geometry. I will show a variety of numerical solutions of the equations, with particular attention to how the deformation is partitioned between stretching and bending modes.

Boundary Layers

Structure of small amplitude hydraulic jumps in laminar high Reynolds number flow

A. Kluwick, A. Exner and E.A. Cox‡
Institute of Fluid Dynamics and Heat Transfer
Vienna University of Technology, Austria
‡: Math. Phys. Dept., University College Dublin, Ireland
Email: Alfred.Kluwick@tuwien.ac.at

Keywords - Hydraulic jump - Triple deck theory

Abstract - Near critical single layer and two layer fluid flow over bottom topography has received considerable interest in the past twenty years. In the most simple case the flow is contained in a two-dimensional channel with an isolated obstacle on what is otherwise a flat bottom and the fluid is taken to be inviscid and incompressible. By adopting the assumption that the pressure distribution is hydrostatic it is found that small amplitude disturbances of a uniform steady state are governed by a kinematic wave equation. Owing to its nonlinearity solutions constructed by means of the methods of characteristics in general contain regions of multivaluedness which have to be obviated by the insertion of jump discontinuities representing hydraulic jumps. Unfortunately, however, the appropriate form of the jump relationships is still controversial. This is due to the fact that these are not determined uniquely by the simplified form of the governing equation but require additional (ad hoc) assumptions which lead to different formulations as for example the CWBS and YG theories. It is the aim of the present paper to show how this difficulty can be overcome for laminar flows in the limit of large Reynolds number by taking into account the displacement effects of thin shear layers adjacent to the wall and centred at the interface between the two fluid layers. In the limit of large Reynolds number this leads to a structure problem formed by the classical triple deck equations supplemented with a novel nonlinear coupling condition which allows for the passage through the critical state. In the case of positive hydraulic jumps this passage is achieved by the local thickening of the wall boundary layer which acts as a viscous hump. Conversely, the pressure drop at the wall associated with a negative hydraulic jump causes the boundary layer thickness to decrease locally thereby forming a viscous indentation required for the Froude number to pass through one in this case.

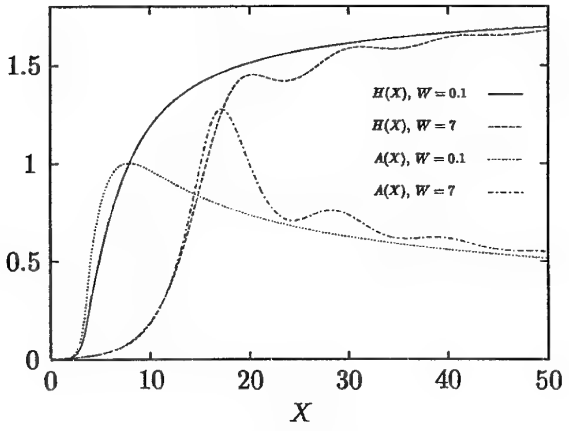

Representative results for a steady positive hydraulic jump in a single layer fluid are depicted in the above figure. The (scaled) quantities H, A and X denote, respectively, the displacement of the free surface, the perturbation displacement thickness of the wall boundary layer and the distance in the streamwise direction. Furthermore, the nondimensional parameter W characterizes the effect of surface tension.

The Klebanoff-Transition in Experiment and DNS

S. Bake[1], H.H. Fernholz[1], D.G.W. Meyer[2] and U. Rist[2]
[1)]Hermann-Föttinger-Institut, Technische Universität Berlin, Germany
Email: bake@pi.tu-berlin.de
[2)]Institut für Aerodynamik & Gasdynamik, Universität Stuttgart, Germany
Email: Daniel.Meyer@iag.uni-stuttgart.de

Keywords – Boundary-Layer Transition – Klebanoff-regime – Experiment vs. DNS

Abstract - The nonlinear stage of laminar-turbulent transition of a boundary layer without pressure gradient was investigated in an experimental study and simultaneously in a Direct Numerical Simulation. The boundary layer was excited by means of a time-harmonic signal introduced through a spanwise disturbance source at the wall. The disturbance source spectrum was adjusted in order to generate the well known Klebanoff-type transition regime (K-regime). By means of hot-wire anemometry the time-mean and fluctuation velocities were measured. Using phase-locked ensemble-averaged time series triggered by the reference signal the transitional flow field was reconstructed. The DNS used the complete Navier-Stokes equations for incompressible flow and was based on the so-called spatial model. High order compact finite differences and Fourier modes were used for discretization in order to get reliable results even at the very late stages of the transition process.

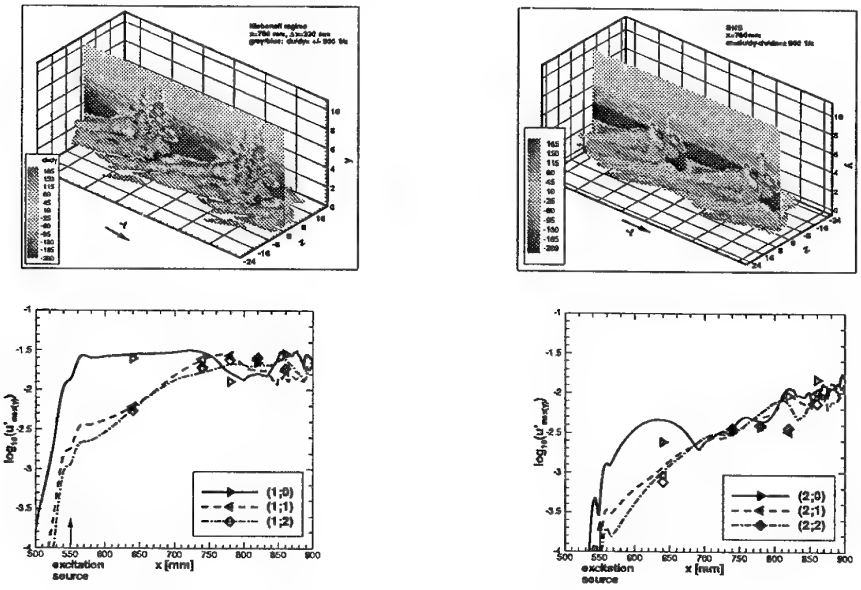

Figure 1: *Top: Iso-surfaces of two values of the spanwise vorticity fluctuation and a contour-plane at $z = 0$ mm at a 'two-spike-stage'; comparison between experiment [left] and DNS [right]. Bottom: Development of the wavenumber spectra; fundamental [left] and 2nd harmonic frequency [right]; experiment (symbols) and DNS (lines)*

In figure 1 the development of the K-regime is shown in a comparison between the experiment in Berlin and the DNS performed in Stuttgart. Good agreement exists when the development of the normal oblique modes and at the topological evolution of the vortex structures is considered. The comparison of the two methods includes time-traces, velocity profiles, wall-skin friction and boundary-layer parameters and gave the researchers the possibility to confirm their results, to check their data processing procedure and to see the limits of their approaches, respectively.

Nonlinear boundary layer transition

H.C. de Lange and R.J.M. Bastiaans
Section Energy Technology, Department of Mechanical Engineering
Eindhoven University of Technology, The Netherlands
Email: h.c.d.lange@wtb.tue.nl

Keywords - Transition - Bypass - Boundary layer

Abstract - Bypass transition of a boundary layer takes place at high main stream turbulence levels. It is governed by the intrusion of non-linear disturbances into the viscous sublayer, where they initiate so-called turbulent spots. These spots grow and merge untill the boundary layer is fully turbulent. In the spot-formation process both the length scale and the initial strength of the disturbance are important.

There are two theories known to describe the bypass transition process. In both theories the actual formation of turbulent spots has to be introduced through a presumed criterion. In the present study fully compressible direct numerical simulation is used to study this formation process. To circumvent the time step restriction of acoustic wave propagation acoustic sub-time stepping is used.

In this paper a numerical study is presented in which a spatially developing laminar boundary layer (Re_δ equal to 400) is subdued to non-linear harmonic disturbances. The three velocity components are isotropically perturbed with varying length scales.

The onset of three-dimensional boundary-layer separation in an impulsively started flow

Federico Domenichini
Dept. Civil Engineering, University of Firenze, Italy
Email: federico@ingfi1.ing.unifi.it

Keywords: Vorticity dynamics - Boundary layer separation.

Abstract: The boundary-layer separation at moderate-to-high values of the Reynolds number is a widely investigate phenomenon. The ejection from the wall-layer of macroscopic vortex structures, which represents the terminal phase of the separation process, has been carefully described by several experimental works (see Doligalski et al., 1994). On the opposite, the early stage of the separation is associated with small time and spatial scales and, despite its relevance for the flow-body interaction and control, it is hardly detectable experimentally and is also difficult to be numerically resolved.
The three-dimensional separation is here studied in simple case of a plane wall in correspondence of an impulsively started uniform stream with a suction imposed at a given distance from the wall. The equations of motion in the asymptotic Prandtl formulation are solved numerically; such an approximation, which does not represent the actual long-time dynamics, is able to describe the initial evolution, up to the appearance of singular points in the flow field (Domenichini & Pedrizzetti, 1998), which can be considered as an indication of the separation.

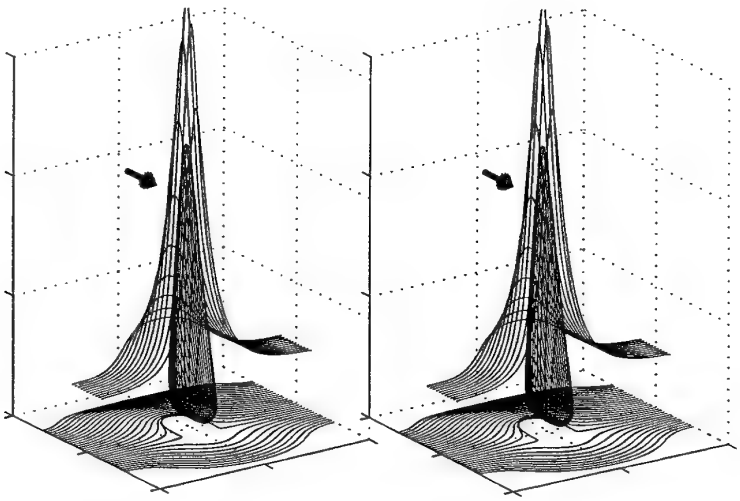

Stereoscopic view of the instantaneous vorticity field; vorticity lines.

The boundary-layer dynamics is initially driven by the external forcing; it shows the birth of singular points of the velocity field, whose topological properties change during the evolution. The separation influences a portion of the flow domain, which can not be easily recognised by analysing the velocity field (Hsieh & Wang, 1996). On the other side, the separated region shows a well defined compact vorticity structure with closed vorticity lines. The dynamics of the compact vorticity structure is presented, and the associated changing topology is identified starting from its birth and during its development inside the boundary-layer up to its injection into the external stream.

Doligalski T. L., Smith C. R. & Walker J. D. A. 1994, Vortex interactions with wall. *Ann. Rev. Fluid Mech.* **26**, 573-616.

Domenichini F. & Pedrizzetti G. 1998, Impulsively started flow separation in wavy-walled tubes, *J. Fluid Mech.* **359**, 1-22.

Hsieh T. & Wang K. C. 1996, Three-dimensional separated flow structure over a cylinder with a hemispherical cap. *J. Fluid Mech.* **324**, 83-108.

Large-Eddy Simulation of oscillatory boundary layers

G. Vittori and V. Armenio
Dipartimento di Ingegneria Ambientale, Universitá degli Studi di Genova.
via Montallegro 1, 16145 Genova-Italy.
Dipartimento di Ingegneria Civile , Universitá degli Studi di Trieste
Piazzale Europa 1, 34127, Trieste-Italy

Keywords -Large Eddy Simulation - Boundary layer - Sea waves

Abstract - The boundary layer generated by harmonic oscillations of a fluid parallel to an infinite fixed plate can be viewed as a prototype of unsteady boundary layers. Moreover Stokes boundary layer is relevant to a variety of applications ranging from offshore and coastal engineering to biomedical sciences.

Experimental investigations have shown that turbulence appears for values of the Reynolds number R_δ larger than 500 ($R_\delta = U_0\delta/\nu$, where U_0 is the amplitude of the velocity oscillations, δ is the boundary layer thickness and ν is the kinematic viscosity of the fluid). It has been observed that turbulence starts to appear in the late stage of the accelerating phase when the flow is characterized by the sudden, explosive appearence of turbulence bursts. Then turbulence is sustained throughout the decelerating phase and is damped during the early stage of the accelerating phase.

Turbulence becomes stronger and spreads over a larger part of the cycle as the Reynolds number is increased. Eventually for $R_\delta > 3500$ turbulence is observed throughout the whole cycle.

Despite the importance of the problem, few numerical simulations have been performed in the past. Recently, Vittori and Verzicco (1998, J.Fluid Mech., 207) performed a Direct Numerica Simulation (DNS) of the flow for values of R_δ smaller than 1200 and showed that turbulence can be triggered and sustained in Stokes boundary layers by the presence of a resonance phenomenon induced by wall imperfections. The results of the simulations were in good agreement with experimental data. Unfortunately, DNS of the flow at larger values of R_δ, where the flow is expected to be turbulent throughout the cycle, are beyond the capabilities of present computers; thus the use of recent techniques for modeling turbulence could be helpful.

Over the last few years Large-Eddy simulation (LES) has proved to be a powerful technique when used for the analysis of both equilibrium and non-equilibrium flows. Recent investigations have shown that dynamic mixed models behave fairly well in non-equilibrium flows.

Recently Armenio *et al.* (1999, in Direct and Large-Eddy Simulation III, Kluwer Academic Publishers) have re-formulated dynamic models in a new contravariant form and incorporated such model into an algorithm which solves the generalized-coordinate formulation of the filtered Navier Stokes equations in order to deal with complex non-orthogonal geometries. In the present contribution the behaviour of eddy-viscosity and scale similar dynamic models in a oscillatory boundary layer is evaluated and the results compared with DNS results by Vittori & Verzicco (1998) at $R_\delta = 800$. The turbulent characteristics of the Stokes boundary layer for large values of the Reynolds number are investigated. In particular it is found that the dynamic models appear to describe well the intermittently turbulent regime where turbulent fluctuations are observed only during part of the cycle.

Three-dimensional vortex/boundary element method for the numerical study of near-wall boundary-layer flow structure

Z. Khatir and P.W. Carpenter
Fluid Dynamics Research Centre, School of Engineering
University of Warwick, United Kingdom
Email: es2184@eng.warwick.ac.uk

Keywords - Discrete Vortex Method - Turbulent Boundary Layer - Hairpin Vortices

Abstract - In the present study a vortex method to investigate the structure in near-wall boundary-layer flow is presented. A novel discrete vortex method is coupled with a boundary element procedure to study the evolution of flow structures within the boundary layer. The simulation is carried out using a three-dimensional discrete vortex method, whereas the impermeability boundary condition is satisfied by means of an integral equation technique. The core of the hybrid method consists of decomposing the velocity fields into a known unperturbed contribution and perturbation vorticity as follows:

$$\mathbf{u} = \underbrace{U(z)\vec{i}}_{mean\,flow} + \underbrace{\mathbf{u}_\omega{}'}_{Rotational\,disturbance} + \underbrace{\mathbf{u}_p{}'}_{Irrot.\,disturbance} .$$

The vortex elements, with the appropriate boundary condition, are tracked using a Lagrangian representation. The vortical velocity computation is done by Biot-Savart integration and the potential velocity field for imposing the normal boundary condition is calculated by an indirect boundary element formulation.

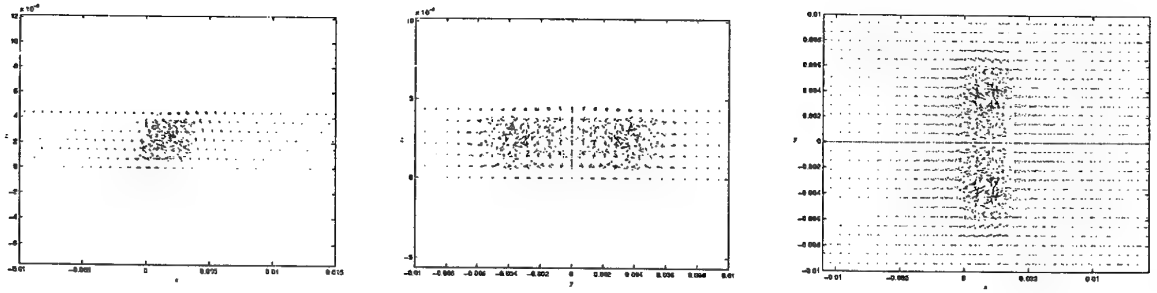

a) *b)* *c)*

Figure 1: *Perturbation velocity field: a) Side view; b) End view and c) Top view.*

Results are presented in the above Figure showing the evolution of hairpin vortices in the near-wall region. Previous studies of this kind, e.g. [1], neglected the interaction between the hairpin vortices and the background vorticity. In fact, as shown in Figures 1*a–c*, this interaction is very strong. Our method fully accounts for this interaction and shows good agreement with experimental observations [2].

References

[1] T.-L. Hon and J. D. A. Walker, Evolution of hairpin vortices in a shear flow, *Computers and Fluids* **20**(3), pp. 343–358, 1991.

[2] M. S. Acalar and C. R. Smith, A study of hairpin vortices in a laminar boundary layer. Part 1 & 2, *J. Fluid Mech.*, **175**, pp. 1–83, 1987.

Compressibility and Heat Transfer Effects on Boundary Layer Receptivity

K. Neemann
Hermann-Föttinger-Institute of Fluid Mechanics
Technical University Berlin, Germany
Email: neemann@hobo.pi.tu-berlin.de

Keywords - Instability - Receptivity - Boundary Layers - Compressible Flow

Abstract - The process by which instability waves in convectively unstable flows like wall boundary layers are excited by external disturbances is usually referred to as receptivity. Receptivity problems can be studied theoretically with asymptotic methods (e.g. triple-deck theory), concentrating on nonlinear developments and nonparallel flows, or on the basis of the parallel flow assumption of linearized stability theory, which is better suited to account for finite Reynolds number effects. In the latter case, however, previous investigations were mainly restricted to incompressible, isothermal flows.

In the present study it is shown that the basic ideas of the linearized, parallel flow theory can be extended to compressible boundary layers with heat transfer. In a Green's function approach the external disturbances are modelled by various kinds of Dirac functions, which can be interpreted in some cases as idealized blowing or suction at the wall, heat sources or vibrating ribbons in the boundary layer. In particular the Green's functions allow a detailed study of parametric influences and excitation mechanisms without the need to single out a special disturbance environment.

Receptivity results are presented in terms of the initial amplitudes of the instability waves at the source positions. The presentation includes the influence of compressibility in subsonic and low supersonic boundary layers (see figure below) as well as the effect of wall temperature and pressure gradient. The excitation by a heat source at the wall is compared to blowing or suction, and the influence of a vibrating ribbon at different positions in the boundary layer is considered.

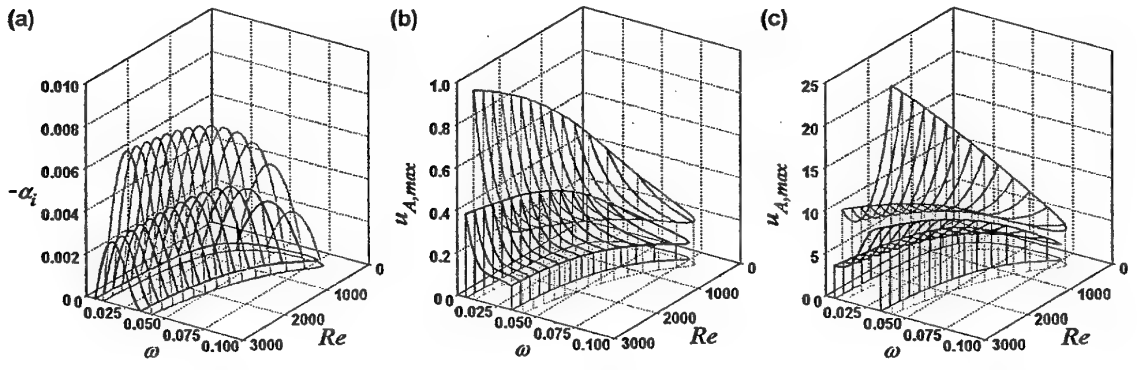

Effect of compressibility in a flate-plate boundary layer with adiabatic wall as function of exciting frequency ω and Reynolds number Re: (a) spatial growth rates $-\alpha_i$, (b) initial amplitudes $u_{A,max}$: blowing/suction at the wall, (c) initial amplitudes $u_{A,max}$: vibrating ribbon in the critical layer. Mach number: black lines $M = 1.2$, grey lines $M = 0.0$.

Experimental study of flat-plate boundary layer receptivity to vorticity normal to leading edge

M.N. Kogan, V.G. Shumilkin, M.V. Ustinov, S.V. Zhigulev
Central Aero-hydrodynamics Institute, Russia
Email: mkogan@aerocentr.msk.su

Keywords - Receptivity - Boundary layer - Vortical disturbances

Abstract - Longitudinal streaky structure usually appears in the boundary layer subjected to free-stream turbulence [1]. It is thought,that the streaks originate through outer flow vortical disturbances penetration into the boundary layer and subsequent amplification of these disturbances. However, there is no generally accepted theory of this process. Some of authors suppose that oncoming vorticity field remains unchanging outside the boundary layer and the growth of vortical disturbances occur only within this layer. In alternative theory of Goldstein [2], the vortex lines stretching by the flow around the leading edge is considered as a predominant mechanism of vortical disturbances amplification.

To reveal the mechanism of vortical disturbances penetration into boundary layer the reported experiment was made. The wake behind vertically stretched wire was used as a source of vortical disturbances and it's interaction with a boundary layer at the horizontally mounted plate was studied. Plates of different leading edge shapes were used to estimate the role of flow around leading edge in wake/boundary layer interaction. Velocity and vorticity fields were found to be substantially deformed by flow around leading edge, but main amplification of disturbances by factor of 10-20 takes place within the boundary layer. Nevertheless, response of boundary layer to wake really depends from the shape of leading edge, with boundary layer distortion at the blunt nose plate was approximately two times grater then this at the sharp leading edge plate.

The streamwise evolution of boundary layer distortion was found to be crucially dependent from the width of oncoming wake. The distortion from wide wake grows monotonically with distance from leading edge, whereas distortion from narrow wake reaches maximum at the vicinity of leading edge and then decay.

When narrow high velocity deficit symmetric wake interacted with boundary layer, the spanwise profile of velocity in boundary layer unexpectedly becomes antisymmetric with respect to the wake center. The nondimensional parameter defining different flow regimes is proposed.

References

[1] Westin K.J.A., Boyko A.V., Klingmann B.G.B., Kozlov V.V., Alfredsson P.H., J. Fluid Mech., **281,** 193 (1994)

[2] Goldstein M.E., Leib S.I., Couley S.J., J.Fluid Mech., **237,** 231 (1992)

Receptivity approach in description of instability wave propagation over flexible section of a channel

Sergei V. Manuilovich
Central Aero-Hydrodynamics Institute (TsAGI), Russia
Email: manu@recp.aerocentr.msk.su

Keywords - Stability - Receptivity - Compliant Wall

Abstract - Two main types of methods for laminar-turbulent transition delay exist. The first type contains methods based on stabilization of boundary-layer mean flow (passive control). The compliant wall used to reduce the growth rate of instability waves is the classical example of such a method (Kramer, 1957). The second type of methods applies the principle of Tollmien-Schlichting (TS) wave cancellation by means of formation of artificial wave with the same frequency and amplitude but opposite phase (active control). The possibility of TS wave cancellation on the basis of the above-mentioned superposition principle was first demonstrated by Milling (1981).

Common feature of these two mechanisms of unstable wave suppression was pointed out by Manuilovich (1992) for the problem of TS wave passage through a channel with a small 2D surface irregularity. The results obtained admit equivalent physical interpretations within the framework of methods of both the above-mentioned types: quantitative TS wave attenuation characteristics can be obtained both by studying the stabilizing effect of the wall roughness and by analyzing the formation of the secondary TS wave via scattering of the incoming TS wave from the flow inhomogeneity over the roughness.

In this paper we investigate the suppression of unstable oscillations based on the interaction between TS wave and a 2D compliant strip of channel wall. This problem was studied by Davies & Carpenter (1997) using direct numerical simulation. Here we investigate this problem analytically using Fourier transformation with respect to streamwise direction. The problem is reduced to solution of integral equation for unknown form of wall oscillations. The quantitative TS wave modification characteristics (complex passage coefficient and complex transformation coefficient) are introduced and calculated. The results obtained show close connection between stability and receptivity phenomena in inhomogeneous flow.

References

DAVIES, C. & CARPERTER, P.W. 1997 Numerical simulation of the evolution of Tollmien-Schlichting waves over finite compliant panels. *J. Fluid Mech.*, **335**, 361-392.

KRAMER, M.O. 1957 Boundary layer stabilization by distributed damping. *J. Aeron. Sci.*, **24**, 459-460.

MANUILOVICH, S.V. 1992 Passage of an instability wave through a channel section of variable width. *Fluid Dynamics*, **27**, 177-182.

MILLING, R.W. 1981 Tollmien-Schlichting wave cancellation. *Phys.Fluids*, **24**, No. 5, 979-981.

Influence of the Prandtl number on the impulsive flow around a thick flat plate

A. Pozzi and R. Tognaccini
Dipartimento di Progettazione Aeronautica
Università di Napoli Federico II, Italy
Email: pozzi@unina.it, rtogna@unina.it

Keywords - Conjugated heat transfer - Boundary layer - Compressible flows

Abstract - We consider the laminar thermo-fluid dynamic boundary layer arising on a thick and thermal conductive semi-infinite flat plate impulsively accelerated at high speed in a fluid characterized by a Prandtl number (Pr) different from one. This problem is generally studied by assigning the temperature or the heat flux at the wall. These conditions are not realistic because either the temperature and the heat flux are unknown: we can only impose the continuity of these two functions across the solid-fluid interface; this problem is named conjugated heat transfer. The main interest in the present problem is driven by the aerospace industry, especially for the study of high-speed aircrafts and rockets, but applications can also be found in other fields such as in the food-freezing industry.

Few works have been written for unsteady conjugated heat transfer problems. The case of a semi-infinite flat plate for $Pr = 1$ was studied in [1] and [2]. The unwetted side of the plate was assumed at a constant temperature in [1] while in [2] the adiabatic case was studied. The latter is more complex because the problem reduces to a second order hyperbolic equation instead of a first order one. For solving these problems we used an approach based on an integral formulation of the equations in the fluid. We neglected the term related to the axial conduction in the energy equation of the solid; moreover the thermal fields in the solid and in the fluid are coupled by imposing the continuity of the temperature and of the heat flux at the solid-fluid interface.

When Pr is equal to one the problem is simpler because we can assume the same thickness for the the enthalpic and dynamic boundary layers; on the contrary when $Pr \neq 1$, the thicknesses are sensibly different and their ratio is a new unknown to be considered for the solution of the problem.

The effects of Pr are studied in this work. The cases of constant temperature and zero heat flux on the unwetted side of the semi-infinite flat plate have been solved by also considering the integral balance of the "moment" of the energy. This equation allows to express the ratio of the dynamic and enthalpic boundary layers only in terms of Pr in the case of plate with infinitely small thickness. These relations allow to extend the methods proposed in [1] and [2] to the case $Pr \neq 1$. The obtained results are compared with the exact solutions available in the limiting conditions of unsteady flow on an infinite plate and steady flow on a semi-infinite plate revealing a good agreement.

References

[1] A. Pozzi, R. Tognaccini, "Coupling of conduction and convection past an impulsively started semi-infinite flat plate", Int. J. of Heat and Mass Transfer, Vol.43, pp. 1121-1131, 2000.

[2] A. Pozzi, R. Tognaccini, "Symmetrical impulsive thermo-fluid dynamic field along a thick plate", Atti del XIV Congresso nazionale dell'Associazione italiana di Meccanica teorica ed applicata (on CD-rom), Como, Italy, 6-9 Oct. 1999.

Conditional analysis for smooth- and rough- turbulent boundary layer

L. Keirsbulck, L. Labraga, A. Mazouz and C. Tournier
Laboratoire de Mécanique et d'Energétique
University of Valenciennes, France
Email : laurent.keirsbulck@univ-valenciennes.fr

Keywords Boundary layer - turbulence - hot wire - coherent structures

Abstract - In the present study the behaviour of coherent events in a smooth- and rough-turbulent boundary layer is investigated using both lagrangien and eulerien approaches. Particle Image Velocimetry (P.I.V.) is now efficient for turbulent flow measurements. PIV permits to reach fluctuating velocity field and spatial information of coherent motions. In the same way, Hot Wire Anemometry complets the previous approach. The effects of surface roughness on a turbulent boundary layer are investigated by comparing measurements over k-type rough-wall with measurements on a smooth wall boundary layer using P.I.V. and Hot Wire Anemometry. In both cases, the roughness effects are clearly visible in the near wall region. A quadrant analysis shows that the distribution of the contribution to the Reynolds shear stress is mainly due to quadrant 2 (ejection) and to quadrant 4 (sweep). The Q2/Q4 ratio indicates that there are differences between the present rough-wall and smooth-wall values in the near wall region. For the smooth-wall, ejection events are greater than sweeps. On the contrary, for the rough wall, an opposite behaviour occurs. This is confirmed by PIV analysis as shown on figure 1.

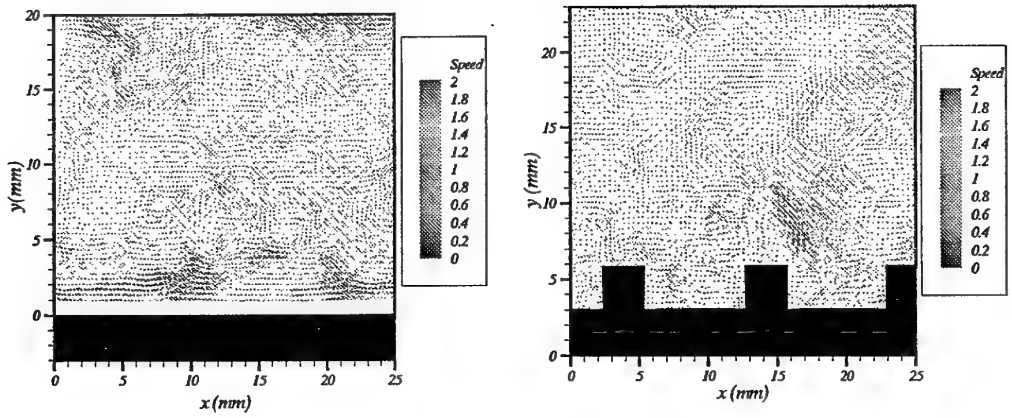

smooth-wall rough-wall

Figure 1: *Fluctuating velocity field*

On a class of unsteady, non-parallel, three-dimensional disturbances to boundary-layer flows

Peter W. Duck
Department of Mathematics
University of Manchester, Manchester, ENGLAND
Email: duck@maths.man.ac.uk

Keywords - Boundary Layers - Instability and Transition

Abstract - Steady, spatial, algebraically-growing eigenfunctions are now known to occur in several important classes of boundary-layer flow, including two-dimensional hypersonic boundary layers (Neiland, 1970, Mikhailov, Neiland & Sychev, 1971, Brown & Stewartson, 1975) and more recently in Blasius boundary layers subject to three-dimensional linearised disturbances - see Luchini (1996, 2000), Andersson, Berggren & Henningson (1999), and in more general three-dimensional boundary layers by Duck, Stow & Dhanak (1999, 2000). These spatial eigensolutions are particularly important and intriguing, given that they exist within the broad limits of the classical steady boundary-layer approximation, and as such are independent of Reynolds number.

In this paper we make the natural extension to these previous (stability) analyses by incorporating the effects of unsteadiness into the model for treating disturbances to a quite general class of similarity-type boundary-layer flows. The flow disturbances are inherently nonparallel, but this effect is properly incorporated into the analysis.

A further motivation for this paper is that Duck, Stow & Dhanak (1999, 2000) have shown that by permitting a spanwise component of flow within a boundary layer of the appropriate form (in particular, growing linearly with the spanwise coordinate), it is found that new families of solutions exist - even the Blasius boundary layer has a three-dimensional 'cousin'. Therefore a further aim of this paper is to assess the stability of the different solution branches, using the ideas introduced in this paper, to give some clues as to which of the solutions may be encountered experimentally.

A number of numerical methods are presented for tackling various aspects of the problem. It is shown that when algebraically growing, steady eigensolutions exist, their effect remains important in the unsteady context. We show how even infinitesimal, unsteady flow perturbations can provoke extremely large-amplitude flow responses, including in some cases, truly unstable flow disturbances which grow algebraically downstream without bound in the linear context. There are some interesting parallels suggested therefore regarding mechanisms perhaps linked to bypass transition in an important class of boundary-layer flows.

References

Andersson, P., Berggren, M. and Henningson, D.S. 1999, Phys. Fluids **11**, 134.
Brown, S.N. and Stewartson, K. 1975, Quart. Jl. Mech. Appl. Math. **28**, 75.
Duck, P.W., Stow, S.R. and Dhanak, M.R. 1999, J. Fluid Mech. **400**, 125.
Duck, P.W., Stow, S.R. and Dhanak, M.R. 2000, to appear in Phil. Trans. Roy. Soc.
Luchini, P. 1996, J. Fluid Mech. **327**, 101.
Luchini, P. 2000, J. Fluid Mech. **404**, 289.
Mikhailov, V.V., Neiland, V.Ya., and Sychev, V.V. 1971, Ann. Rev. Fluid Mech. **3**, 371

Linear Stability of a Gas Boundary Layer Flowing past a Thin Liquid Film over a Flat Plate

D. N. Smirnaios, N. A Pelekasis and J. A. Tsamopoulos
Laboratory of Computational Fluid Dynamics
Department of Chemical Engineering, University of Patras
Patras 26500, GREECE
Email: smyrnaios@chemeng.upatras.gr, pel@chemeng.upatras.gr
tsamo@chemeng.upatras.gr

Keywords- Boundary Layer - Interfacial Waves - Convective/Absolute Instability

Abstract - The flow of a gas stream past a flat plate under the influence of rainfall is investigated. As raindrops sediment on the flat plate, they coalesce to form a water film that flows under the action of shear from the surrounding gas stream. In the limit of (a) large Reynolds number, Re, in the gas phase, (b) small rainfall rate, $\dot{r}$, compared to the free stream velocity, U_∞, and (c) small film thickness compared to the thickness of the boundary layer that surrounds it, a similarity solution is obtained that predicts growth of the liquid film like $x^{3/4}$; x denotes dimensionless distance from the leading edge. The flow in the gas stream closely resembles the Blasius solution, whereas viscous dissipation dominates inside the film. Local linear stability analysis is performed, assuming nearly parallel base flow in the two streams, and operating in the triple-deck regime. Two distinct families of eigenvalues are identified, one corresponding to the well known Tollmien-Schlichting (TS) waves that originate in the gas stream, and the other corresponding to an interfacial instability. It is shown that, for the air-water system, the (TS) waves are convectively unstable whereas the interfacial waves exhibit a pocket of absolute instability, in the streamwise location of the applied disturbance. Moreover, it is found that as the inverse Weber number (We^{-1}) increases, indicating the increasing effect of surface tension compared to inertia, the pocket of absolute instability is translated towards larger distances from the leading edge and the growth rate of unstable waves decreases, until a critical value is reached, $We^{-1} \approx We_c^{-1}$, beyond which the family of interfacial waves becomes convectively unstable. Increasing the inverse Froude number (Fr^{-1}), indicating the increasing effect of gravity compared to inertia, results in shrinking the pocket of absolute instability until a critical value is reached, $Fr^{-1} \approx Fr_c^{-1}$, beyond which the family of interfacial waves becomes convectively unstable. As We^{-1} and Fr^{-1} are further increased, interfacial waves are eventually stabilized, as expected. In this context, increasing the rainfall rate or the free stream velocity results in extending the region of absolute instability over most of the airfoil surface. Owing to this behavior it is conjectured that a global mode may arise at the interface that is responsible for most of the dynamic phenomena associated with the effect of rainfall.

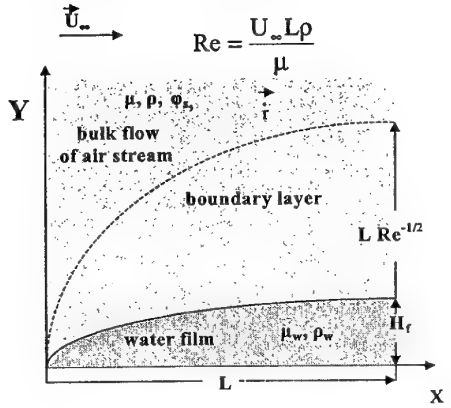

PS: The authors wish to acknowledge support by the EPEAEK (Grant # 51) and EPET II programs.
This work will appear in the Journal of Fluid Mechanics (2000).

Environmental Fluid Mechanics

Mixing and Dissipation in Density Currents

Carlos Härtel, ETH Zürich, Institute of Fluid Dynamics
e-mail: Carlos.Haertel@ifd.mavt.ethz.ch

Key words: Density currents, direct numerical simulation

Density currents of heavy fluid propagating in lighter fluid typically feature a highly unsteady flow pattern at the density interface, which goes along with substantial mixing of ambient fluid into the current. Moreover, the turbulent motion at the interface is associated with energy losses due to viscous dissipation. In numerical models of density currents the flow structure usually cannot be resolved down to the smallest eddies, and some parameterization of mixing and dissipation must be provided. For example, in shallow-layer models one usually assumes that dissipative losses only occur at the head of the front where gravity waves break (see Simpson, 1997; Klemp *at al.*, 1994). However, the validity of the assumptions involved in the parameterization could hardly be assessed in the past due to lack of sufficiently accurate measurements or numerical simulations.

In an ongoing research project we are performing direct numerical simulations (DNS) of plane density currents (see Härtel *at al.*, 2000) where all relevant flow phenomena are resolved in space and time. As an example, the figure below gives a DNS result of a front in a two-dimensional lock-exchange flow at a Reynolds number of about $Re = 3300$ (based on height and speed of the front). The intense mixing at the interface between the two fluids is clearly seen. Also given is the energy dissipation at the interface integrated over the channel height. In contrast to what is commonly assumed, the dissipation is seen to be rather evenly distributed along the interface rather than occurring localized near the head. In the talk we will present results from two- and three-dimensional simulations of lock-release flows and deeply submerged density currents, and we will address in detail their mixing and dissipation properties.

HÄRTEL, C., MEIBURG, E. & NECKER, F. 2000 The flow structure at the head of a gravity current: Direct numerical simulation results. *J. Fluid Mech.* (to appear).

KLEMP, J. B., ROTUNNO, R. & SKAMAROCK, W. C. 1994 On the dynamics of gravity currents in a channel. *J. Fluid Mech.* **269**, 169-198.

SIMPSON, J. E. 1997 *Gravity Currents: in the Environment and the Laboratory.* 2nd. edition, Cambridge University Press, Cambridge.

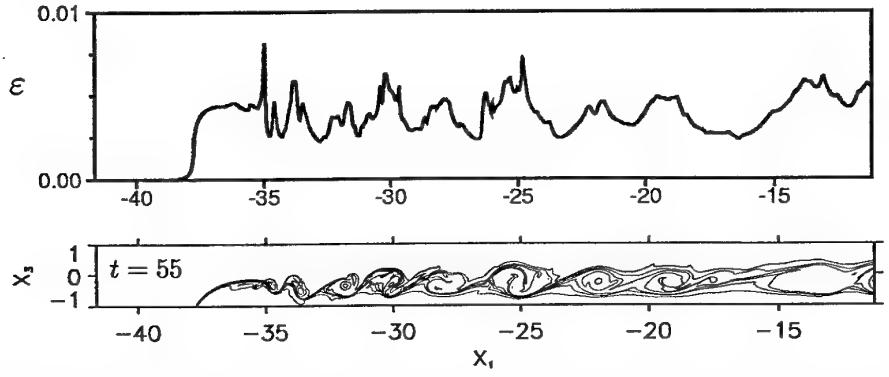

Viscous dissipation ε at the interface (integrated over channel height) obtained from a DNS of a two-dimensional lock-exchange flow at $Re = 3300$. Results for time $t = 55$ (only part of the flow domain is displayed). Bottom: Visualization of the instantaneous flow structure by isocontours of density

Rayleigh-Taylor Instability at a Tilted Interface

Joanne M. Holford and Stuart B. Dalziel
Department of Applied Mathematics and Theoretical Physics
University of Cambridge, UK
Email: j.m.holford@damtp.cam.ac.uk

Keywords - Rayleigh-Taylor instability - Mixing - Baroclinic vorticity generation

Abstract - Many environmental fluids are stratified by variations in either temperature or dissolved solutes. The stratification allows an exchange of mechanical energy between potential and kinetic forms, and introduces anisotropy about the vertical in the fluid motion. The flow is no longer barotropic, so that the vorticity of any fluid parcel can be altered baroclinically. There is also an additional sink for available mechanical energy, through increases in the background potential energy due to irreversible mixing at small scales. Over long times, this energy sink and the associated changes in the mean stratification affect the flow at large scales.

A possible mechanism for mixing in environmental flows is Rayleigh-Taylor (RT) instability, the instability that occurs at an interface with dense fluid above lighter fluid. Local regions of static instability can occur in many time-dependent flows, including stratified shear flow and gravity wave breaking. RT instability is unusual in that the mixing efficiency η, defined as the ratio of the change in background potential energy to the change in available energy (kinetic and potential), is relatively large, typically 0.35. In stably stratified flows, η is generally less than 0.25, and varies with the overall strength and detailed structure of the stratification, and with the nature of the perturbing flow. However, many features of RT instability are sensitive to details of the initial conditions, and it is unclear whether the high mixing efficiency occurs in environmental examples.

Here we present the results of ensembles of laboratory experiments designed to study the evolution of a two-layer unstably stratified fluid, in which the interface is initially tilted at some angle to the horizontal. If the interface is horizontal, we have classical RT instability, whereas if it is vertical, we have a lock exchange flow. Any tilt to the interface encourages the evolving flow to organise into an overturning motion, with a significant baroclinic generation of vorticity, while the added shear at the interface modifies the growth of the RT instability.

Light-induced fluorescence is used to measure the stratification in a vertical plane, from which the total potential energy is estimated. The motion of neutrally-buoyant tracer particles is followed to measure the velocity field in various planes, giving an estimate of the kinetic energy. Variations in the character of the flow, the generation of vorticity and the amount of mixing that occurs are examined, over a range of Atwood numbers (dimensionless density differences) and interface slopes.

A magma dike, a repository with air, and their explosive interactions

Onno Bokhove and Andrew W. Woods
Faculty of Mathematical Sciences, P.O. Box 217, 7500 AE, Enschede, The Netherlands, and
BP Institute for Multiphase Flow, Madingley Rise, Madingley Road, University of Cambridge,
CB3 OEZ, Cambridge, U.K. Email: o.bokhove@math.utwente.nl

Keywords - Volcanism - multiphase magma, compressible fluids, shocks, man-made waste repository, magma dike.

Abstract - We study the ascent of relatively wet basaltic magma through a vertical dike which intersects a horizontal tunnel or drift of comparable cross-sectional area to the dike and located about $300-400\,m$ below the surface. This process is a simplified representation of some aspects of the interaction of a basaltic fissure eruption either with a sub-surface, man-made waste-repository, or with a natural sub-surface cavern, such as the limestone Karts in China. In the model, we assume that prior to breakthrough of the dike, the tunnel is maintained at atmospheric pressure. We examine the decompression and flow which develops following breakthrough into the tunnel. The model provides an averaged one-dimensional picture of the flow, averaging over the prescribed dike and tunnel geometry. It is based on the assumption that the basaltic magma remains in chemical equilibrium with the dissolved volatile phase. This volatile phase is mainly water and is exsolved from the melt as the mixture decompresses. The model predicts that for 2 weight percent water, the magma-gas mixture decompresses extremely rapidly into the tunnel, and as it expands it generates a shock wave in the air displaced down the tunnel. This wave travels at a speed of order $500\,m/s$, reaching the end of a $200\,m$ tunnel in a fraction of a second. If the tunnel end is closed, the shock wave is reflected between the tunnel end and magma-air interface and may be amplified by a factor of $15-50$, with a high pressure region developing at the end of the tunnel. Owing to the difference in density and speed of sound in the air and the magma-gas mixture, then following the reflection, a complex series of interacting shock waves develops near the end of the tunnel. However, a dominant magmatic shock which propagates backwards towards the dike eventually develops. The results indicate that owing to the explosive expansion of magma down the tunnel, then following breakthrough, a region of maximum pressure in the tunnel may develop far from the dike.

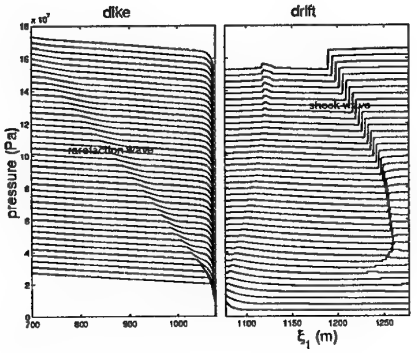

Pressure profiles are shown for magma-air interactions in a dike-drift system as function of a curvilinear coordinate ξ_1 following the vertical dike and the horizontal drift. The simulation encompasses 2.734 s and each of the 41 profiles is spaced 0.0683 s apart. Profiles in dike and drift have been separated to emphasize the different scaling in dike and drift.

Modelling dense gas dispersion in the atmospheric boundary layer

T.J. Taylor and A.G. Robins
Environmental Flow Research Centre
School of Mechanical and Materials Engineering
University of Surrey, United Kingdom
Email: T.Taylor@surrey.ac.uk

Keywords - atmospheric boundary layer - wind tunnel simulation - dense gas dispersion

Abstract - As part of a co-operative program of measurements of vertical diffusion in continuous, two-dimensional (line source) dense gas plumes, the Environmental Flow Research Centre (EnFlo) at the University of Surrey, U.K., undertook experiments in model neutral and stably stratified boundary layer flows. Somewhat surprisingly, for plume Richardson numbers, *Ri**, greater than 3, higher non-dimensional entrainment speeds, *We/u**, were observed in the model stably stratified flow than in the neutral boundary layer flow. The emission velocity ratios, *Wo/u**, (where *Wo* is the source emission speed) were higher in the stable flow experiments, which suggests that the differences in entrainment speed behaviour could be linked to source momentum effects.

A NERC funded project currently in progress at EnFlo seeks to describe the mechanisms through which the dispersion of two-dimensional dense gas plumes differ in neutral and stably stratified atmospheric boundary layers. The work involves a careful parametric study of the effect of Reynolds number on the turbulence characteristics of near-surface flows involving density gradients. The internal characteristics of dense gas clouds are explored over a range of Richardson numbers in neutral and non-neutral boundary layers. Turbulence statistics for velocity (LDA), temperature (cold wire) and mean (16 coil simultaneous storage and FID analysis system) and fluctuating (Fast FID) concentrations are used to examine the extent to which surface roughness characteristics and the nature of the upstream near surface boundary layer flow affect the turbulence structure within the plume and the entrainment process.

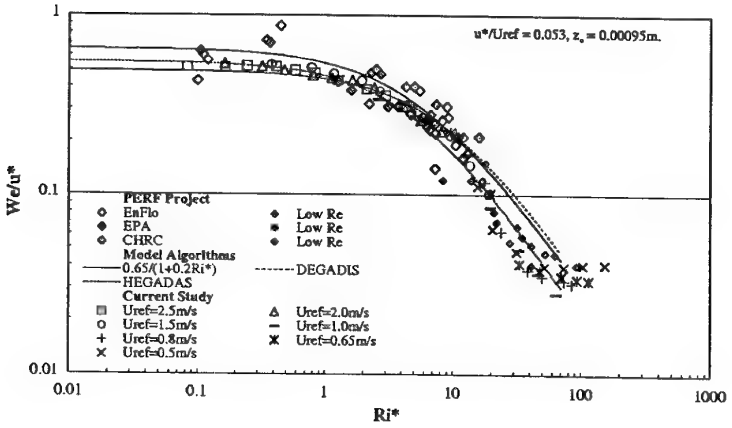

Non-dimensional entrainment velocity verses Richardson number in neutral boundary layer flows.

The work seeks to improve the understanding of the influence of source momentum and the roughness Reynolds number, *Re**, on the entrainment process, and investigate the maximum plume Richardson number that can be achieved whilst maintaining fully turbulent flow conditions within the laboratory model. The influence of boundary layer stability is also investigated. The results of this study will help determine the limits of laboratory scale models for simulating problems of this nature.

Grid-generated turbulence, drag, internal waves and mixing in stratified fluids

Stuart B. Dalziel & Roland C. Higginson

Department of Applied Mathematics and Theoretical Physics
University of Cambridge, Silver Street, Cambridge CB3 9EW, ENGLAND

E-mail: s.dalziel@damtp.cam.ac.uk

Keywords – Turbulence – Stratification – Mixing – Drag

Abstract – Recent studies have demonstrated that the manner in which energy is put in to a stratified system has a profound effect on the partitioning between mixing, dissipation and internal waves. In some cases, the flux Richardson number decreases at higher gradient Richardson numbers, leading to the formation of layers from an initially smooth density stratification, while in other cases the flux Richardson number increases monotonically, preventing the formation of such layers.

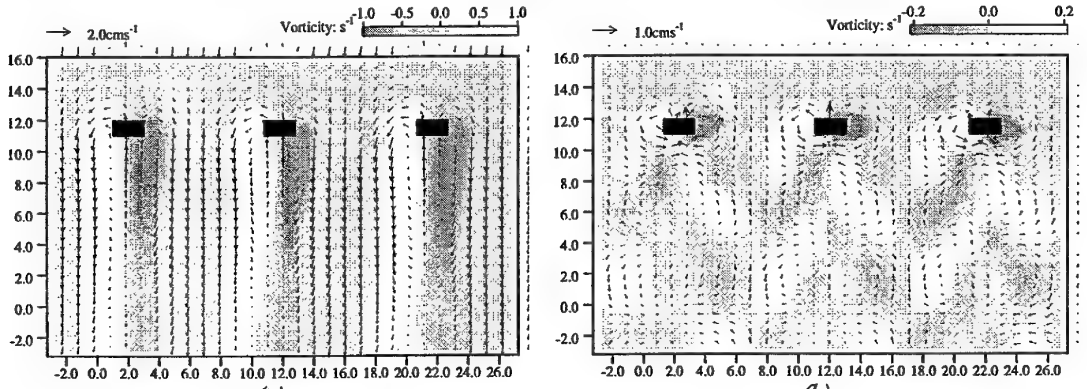

Experiments showing the temporal mean velocity and vorticity behind bi-planar grid. (a) Homogeneous fluid. (b) Stratified fluid.

This paper presents new experimental results that explore the behaviour when the source of energy is a bi-planar grid traversed vertically through a density stratification. At high grid Richardson numbers (low Froude numbers) the wake behind the grid differs fundamentally from that behind a grid in a homogeneous fluid due to the phase-locked excitation of internal wave modes. In order to analyse the mixing that ensues, it is important to understand these wave modes and the additional drag they exert upon the passage of the grid. Measurements of this additional drag are presented and explained, along with details of the internal wave field and the resultant mixing.

Intermittency and non local approach for MHD turbulence

T. Gomez[1], H. Politano[2] and A. Pouquet[2]
[1] Laboratoire de Modélisation en Mécanique, Université Pierre et Marie Curie, France
[2] Observatoire de la Côte d'Azur, France
Email: gomez@obs-nice.fr

Keywords - Turbulence - Magnetohydrodynamic - Intermittency

Abstract - Many physical plasmas, as for example the solar wind or the interstellar medium, are observed in a turbulent state with velocities substantially smaller than the speed of light. In the magnetohydrodynamic (MHD) approximation, two different phenomenologies could be considered; the first proposed by Kraichnan (*Phys. Fluids* **8**, *1965*), which takes into account the specificity of MHD interactions due to the propagation of the Alfvén waves, or the second proposed by Kolmogorov (*Dokl. Akad. Nauk. SSSR* **30**, *1941*), for nonconducting fluids.

We numerically determine the intermittency exponents of the scaling laws of various structure functions, up to order $p = 8$, from the data obtained by direct numerical simulations of a stationnary MHD turbulent flow maintained by a random force at large scale and using resolutions up to 1024^2 grid points (*Phys. Fluids* **11**, *1999*).

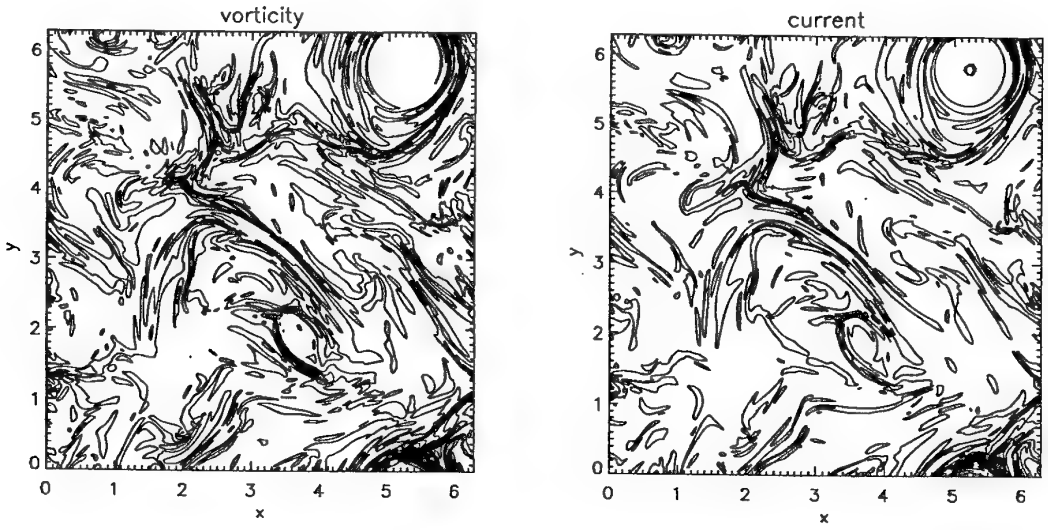

Contours of vorticity (left) and current (right) at $t = 39.43$.

We show that the behavior of the structure functions indicates that the physical fields – the velocity $\mathbf{v}$, the magnetic field $\mathbf{b}$ and the Elsässer variables ($\mathbf{z}^{\pm} = \mathbf{v} \pm \mathbf{b}$) – are more intermittent than in the neutral fluid case, thus favoring the nonlocal approach of the MHD turbulence. However, the intermittency exponents of the fluxes of the increments of $\mathbf{z}^+$ and $\mathbf{z}^-$ indicate a scaling similar to that of neutral fluids. This could be understood as the existence of an universality of the intermittency phenomenon, when appropriate variables are considered.

These results will be compared with recent results we obtained from a simulation of a stationnary conducting flow, with a time dependent large scale forcing and a resolution of 2048^2 grid points.

THE EFFECTS OF SUB-SURFACE THERMAL FIELDS ON EDDY MOTION IN THE SHEAR-FREE CONVECTIVE BOUNDARY LAYER

J.C.R. Hunt[†ɣ], A.J.Vrieling[ɣ], M.E. Roos[ɣ],F.T.M. Nieuwstadt[ɣ]

[†] Department of Space and Climate Physics and Geological Sciences, University College, London
[ɣ]J.M. Burgers Centre, Laboratory for Aero- and Hydrodynamics, Delft University of Technology

Email: a.j.vrieling@wbmt.tudelft.nl

Keywords - convective turbulence, eddy motion

Abstract - Convective turbulence occurs in a wide variety of flows. Many of these flows can be approximated by horizontally homogeneous free convection in a horizontal layer bounded on the lower side by a rigid wall. At this lower surface a constant temperature or a constant heat flux is often assumed as boundary condition. The resulting flow pattern consists of relatively thin regions of updrafts (or plumes) and broader regions of downdrafts (Figure 1).

However, in many cases the boundary condition of a constant temperature or constant heat flux at the lower surface is not correct. In general one should take into account the existence of a conductive layer below the layer of free convection. The inhomogeneity of the fluid motion in combination with the heat-transfer through this conductive layer determines the conditions on the interface between both layers. These may have a significant influence on the flow stucture.

To explore this influence, theoretical calculations and numerical simulations have been performed on the thermal diffusion in the solid (with thermal diffusivity k_g and thickness h_g) below a fluid layer with thermal diffusivity k and thickness z_i in which the flow is driven by free convection. The free convection can be characterized by the velocity scale w_*. It is shown that if a uniform heat flux is supplied at the base of the solid layer and if $h_g > l_g$ where $l_g = \sqrt{k_g z_i / w_*}$, the heat removed by the thermal plumes from the surface of the solid is not being replaced fast enough by diffusion through the solid layer. Then the plumes break off and the convection of heat in the fluid occurs through the motion of unsteady puffs. This transition is confirmed by laboratory studies and by observations of bird flight. There are several geophysical, engineering and culinary applications.

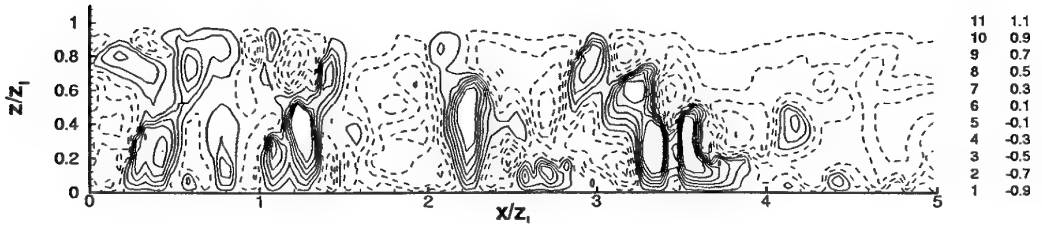

Figure 1: Contourlines of normalised vertical velocity (w/w_*) in a DNS simulation in a wide box (5x5x1) at $Ra = 10^5$. A constant heat flux is supplied at the base of the fluid.

The flow in rotating annular flumes

Robert Booij
Section Hydromechanics, Sub-faculty of Civil Engineering
Delft University of Technology, The Netherlands
Email: R.Booij@ct.tudelft.nl

Keywords - Annular flume - Secondary flow - Erosion

Abstract - Annular flumes , in which a rotation of the lid creates the flow, are used for the study of erosion and/or deposition of fine sediments. Such flumes have important advantages over straight flumes: the large flume length required because of the small fall velocity of fine sediment, the avoidance of inflow and outflow effects, and the absence of pumps. However the curvature of the flow in annular flumes leads to secondary flows, which limits the use for the direct study of deposition of fine sediment in free surface flow. Secondary flow circulations can be counteracted but not completely annihilated by rotating the flume itself in opposite direction to the lid. Much effort is generally devoted to the determination of the optimum value for the ratio ω_t/ω_b of the rotational speeds of the lid, ω_t, and the flume, ω_b, of a rotating annular flume with respect to the secondary flow.

Extensive clear water measurements were executed with a laser-Doppler velocimeter (LDV) in the rotating annular flume of Delft University of Technology. The measurements showed that near optimum the exact pattern of the secondary flow depends strongly on the exact ratio of the rotational speeds ω_t/ω_b. The high cost of experimental investigation of the different flume geometries, the changes in bed shape and the opacity of sediment-laden fluid all necessitate the computation of the flow in annular flumes. Measured flow patterns can be used for the validation of the computational model to be used. Computations with different turbulence models were executed. A correct prediction of the optimum ratio requires a sufficiently exact computation of the flow, which proves more difficult than is suggested by the simple geometry of the flume. The figure below shows a comparison of the measured optimum flow situation and a computation. The vector fields show the secondary velocity field in a cross-section of the flume, the contour lines give the distribution of the tangential velocity component.

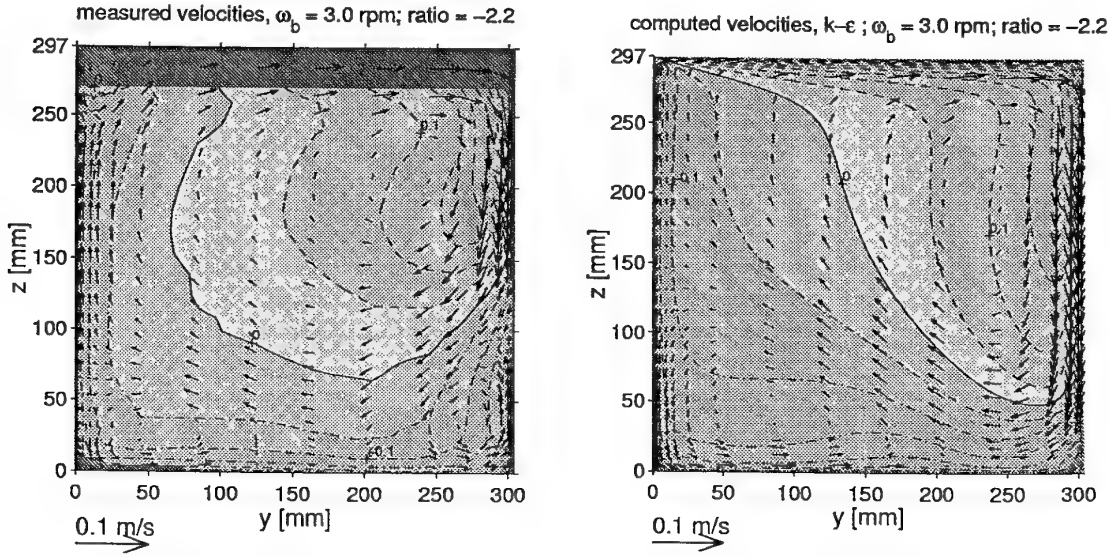

On the Coherent Structure Behaviour in the Jet – Cross Flow Interaction

V. Uruba, P. Jonas, O. Mazur
Institute of Thermomechanics ASCR
Prague, Czech Republic
E-mail: uruba@it.cas.cz

Keywords – Jet – Turbulence – Coherent structures

Abstract – In the jet – cross-flow mixing zone there are several vortex systems due to the interaction of both stationary and non-stationary nature and of highly 3D structure. The steady formations are the dominant rolled-up longitudinal vortex pair and the horseshoe vortex around the jet exit, while the unsteady formations are the unsteady wake vortex street shedding immediately downstream of the jet exit and the free jet ring vortices. All those vortex structures strongly affect the passive scalar exchange between the flows. As the unsteady structures have not been explored in details till now, we have concentrated on this point. The main goal of the presented study is the contribution to the physical merit of the unsteadiness.

Forasmuch as the environmental applications are of our interest, the jet – cross-flow velocity ratio of 4 has been chosen, although the study is of basic research nature. The jet emanates to perpendicular cross-stream from the nozzle of circular cross-section situated on the wall.

The influence of cross-flow structure on coherent structure behaviour in the mixing zone has been examined. The two cases of turbulent (intensity of turbulence of about 6%) and laminar cross-flow are considered, while the jet is of laminar structure and top hat velocity profile.

The middle distance mixing zone (from 5 to 30 nozzle diameters downstream from the jet orifice) has been investigated. To explore the 3D unsteady flow-field we have chosen the multisensor hot element CTA method. The digitised signal is treated using pattern recognition technique to examine the coherent structure behaviour.

The action of wind stresses on convective structures

A.B. Ezersky, A.V. Nazarovsky, and V.V. Chernov
Institute of Applied Physics RAS, 46 Uljanov Str., 603600 Nizhny Novgorod, Russia
Email: ezer@appl.sci-nnov.ru

Keywords - Hydrodynamic instabilities - Thermoconvection - Wind stress

Abstract - The convection in a liquid layer heated uniformly from below, with an air flow above a free surface, is investigated experimentally. Experiments were performed in a low-turbulent wind tunnel in the IAP RAS. We used a cell 30 cm long and 15 cm wide embedded into a flat plate at a distance of 50 cm from the front edge. Silicon oils having different viscosities were used as operating liquids. The structures in liquid were visualized with the aid of aluminium powder, the image was photographed and video recorded for further processing. The air flow characteristics were measured by a hot-wire anemometer.

Visualization of the convective structures shows that cellular convection is realised in the layer in the absence of wind stresses (Fig. 1 a). Shear stresses lead to a drift of convective cells and to an increase of their size in the longitudinal direction (Fig. 1 b). It is revealed that, for the shear stresses above the critical value, bifurcation occurs and convective rolls with the axes oriented along the flow are formed instead of cellular convection (see Fig. 1 c). On the basis of a modified Swift-Hohenberg equation, a theoretical model predicting bifurcations occurring with increasing of wind and leading to stretched convective cells and to rolls convection is developed.

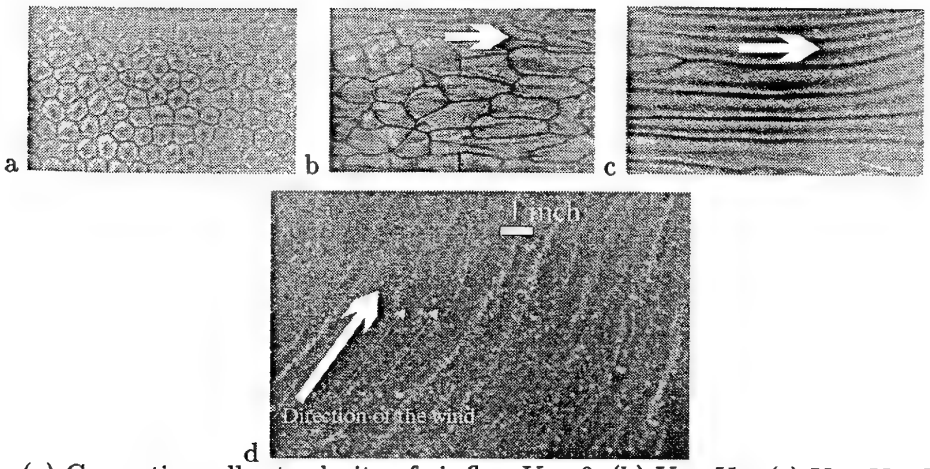

Figure 1: (a) Convective cells at velocity of air flow $V = 0$; (b) $V < V_{cr}$; (c) $V > V_{cr}$, V_{cr} is the bifurcation value of velocity; (d) rolls in natural conditions, visualization is due to the presence of phytoplankton. Arrows show the direction of air flow.

Such a phenomenon – appearance of roll structure on the surface of water in the presence of low wind during sunny weather was observed by one of the authors (V.V.C.) in the Nizhny Novgorod Artificial Sea (Fig. 1 d)). Due to evaporation of water the temperature on the surface was less than under it. A so-called "cold film" was formed and conditions for thermoconvection were satisfied. Appearance of stripes arranged downwind with spatial period of about two centimeters was observed. We believe that these stripes may be interpreted as roll convection in a temperature boundary layer of free surface.

Effects of a canopy on flow over a hill

S.E. Belcher and J.F. Finnigan
Department of Meteorology, University of Reading, United Kingdom

Models for atmospheric boundary layer flow over hills have treated the surface vegetation using a simple roughness parameterisation. Whilst this may be a good approximation when the vegetation is short, many hills are covered with deeper vegetation such as a canopy of trees. We have developed a model for flow over hills when the hill surface has a deep dense canopy to investigate the flow generated within the canopy and the effects a canopy has on the flow over the hill.

The vegetation canopy is represented as a distributed drag on the flow, and turbulent stresses within the canopy are parameterised using the mixing length model with a constant mixing length. The flow over the hill follows the linear theory originally developed by Jackson and Hunt (1975) and more recently by Hunt, Leibovich and Richards (1988) and Belcher, Newley and Hunt (1993).

We find that the perturbation flow in the canopy separates naturally into two layers. Close to the top of the canopy, within a distance of order the mixing length, the perturbed flow is described by a balance between the perturbation stress gradient, the pressure gradient that develops over the hill and the linearised drag in the canopy. Deeper within the canopy the balance is between the pressure gradient and the nonlinear drag. Hence the presence of the hill generates winds deep within the canopy that are in phase with the slope of the hill, whereas the flow above the canopy is in phase with the elevation of the hill. This finding is supported by observations. This phase shift between the different elements of the flow has important implications for the drag on the hill, which is important for parameterisation in numerical weather prediction models, and also for separation of the flow.

In the limit that the time for an air parcel to adjust to the canopy is comparable or large compared to the time for an air parcel at the top of the inner region to be advected over the hill, the canopy changes considerably the flow over the hill when compared with results of previous models that use a roughness parameterisation.

Parameterisation of the roughness sublayer over urban-like roughnesses

H. Cheng and I. P. Castro*

EnFlo, SMME, University of Surrey, Guildford, GU2 7XH, Great Britain. Email: h.cheng@surrey.ac.uk

*School of Engineering Sciences, University of Southampton, Highfield, Southampton SO17 1BJ, Great Britain. Email: i.castro@soton.ac.uk

Key words: wind tunnel, urban surface, roughness sublayer, spatial average.

Abstract:

The dominant features of urban surfaces are the high roughness elements (buildings, trees and other larger structures) which are extremely rough, in aerodynamic terms, irregular and heterogeneous. Boundary layers over urban surfaces in general are not fully understood due to their complex nature and the experimental difficulties that arise in probing them. Currently, numerical weather prediction models represent an urban area (in neutral flow) simply by a roughness length (z_o) and, perhaps, a zero-plane displacement (d), accurate determination of which is important for validation purposes. Because of (typically) height limitations of the measurement tower, meteorological data used to derive u_*, z_0 and d are often obtained in the roughness sublayer - that part of the flow just above the roughness elements which is spatially inhomogeneous - and can thus be inappropriate for overall parameterisation. Also, because sources of pollutant are often situated within or close to the roughness sublayer in urban environments, knowledge of the structure of the turbulence in this layer is essential for improving urban dispersion models, which strongly depend on the meteorological condition. Unfortunately, there is little information available on characterisation of the flow within the roughness sublayer.

In this study, comprehensive measurements over urban-type surfaces have been performed in a wind tunnel. The results have confirmed the strong three-dimensionality of the turbulent flow in the roughness sublayer and the depths of the inertial sublayer (log-law region) and roughness sublayer have been determined. Spatial averaging, never previously attempted in a laboratory simulation, has been used to remove the variability of the flow due to the individual obstacles, and it is shown that the spatially averaged mean velocity in the inertial sublayer and roughness sublayer can (together) be described by a single log-law with a mean zero-plane displacement and roughness length for the surface, provided that the real surface stress is known. The spatially averaged shear stresses in the inertial sublayer and roughness sublayer are compared with the shear stress deduced from form drag measurements on the roughness elements themselves. It is believed that these results will provide fundamental information for modelling urban air quality and forecasting urban wind climates.

Atmospheric measurements and data analysis of wind dynamics in an alpine valley

M. de Franceschi[1], G. Rampanelli[1], M. Tagliazucca[2], F. Tampieri[2] and D. Zardi[1]
[1] Department of Civil and Environmental Engineering, University of Trento, Italy
[2]Institute for Atmospheric and Oceanic Sciences, National Research Council, Bologna, Italy
Email: Massimiliano.deFranceschi@ing.unitn.it

Keywords - Atmospheric boundary layer - Ultrasonic anemometer - Complex terrain -Turbulence

Abstract - Considerable attention has been devoted in recent years to atmospheric dynamics over complex terrain. In particular typical processes of mountain valleys have been the subject of several field campaigns and theoretical work (cf. Whiteman, 1990). In the present work we show some preliminary results of a research project which focused on the case of the Adige Valley near Bolzano (Northern Italy). The project aimed at identifying specific atmospheric processes in the area in connection with the application of pollutant transport models. Various campaigns have been performed in different seasons including both ground based measurements (with conventional weather stations and advanced sensors, namely an ultrasonic anemometer and a doppler sodar) and airborne measurements for the evaluation of thermal structures. Typical local circulations which take place in the valley display weak winds along the valley during the day and quite strong kata-/ana-batic winds in the early morning and at sunset respectively. The eddy correlation technique applied to data collected by the sonic anemometer exhibits specific features of the investigated area. In particular standard deviations of longitudinal and transverse wind components display stronger values, amenable to complex terrain effects.

Reference

Whiteman, C. D., 1990, Observations of Thermally Developed Wind Sytems in Mountainous Terrain, *Atmospheric Processes over Complex Terrain*, Amer. Meteor. Soc. Monogr., **23**, 5-42.

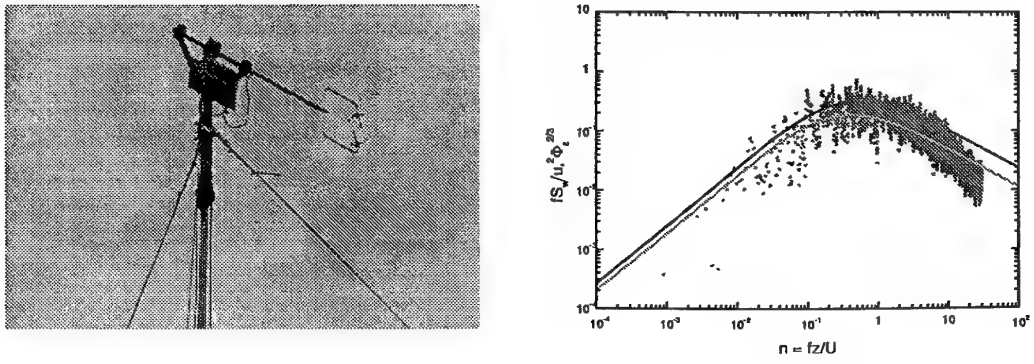

Part of the experimental set-up (left) and a typical spectrum (right)

Structure and dynamics of time-dependent vortices in a rotating barotropic shear layer

W.-G. Früh[1] and P.L. Read[2]
[1]Department of Mechanical and Chemical Engineering, Heriot-Watt University, Edinburgh, UK
[2]Department of Atmospheric, Oceanic and Planetary Physics, University of Oxford, UK
Email: w.g.fruh@hw.ac.uk

Keywords - Barotropic flow - Internal shear layer - Instability - Vortices

Abstract

Rapid background rotation around a vertical axis of a body of fluid concentrates a horizontal velocity shear in relatively narrow shear layers, often referred to as Stewartson layers. While the shear region may be an intricately linked sequence of boundary layers, the velocity is adjusted over a length, δ, which scales with the Ekman number, $E = \nu/(H^2\Omega)$, as $\delta \simeq (E/4)^{1/4}H$ with the kinematic viscosity ν and the fluid depth H. The scaling permits to define an internal Reynolds number based on the shear layer thickness in addition to the standard (external) definition based on the tank geometry. In our study, such a shear layer was generated in a cylindrical tank with horizontal lower and upper boundaries, rotating with a background rotation, Ω. The shear flow was generated by a differential rotation, ω, of disks in the base and lid with a radius, R, half that of the tank radius, as shown in figure 1(a). The horizontal velocity was recorded using both Laser Doppler Anemometry (LDA) at a fixed point in the centre of the shear region (figure 1.b and c) and Particle Tracking using video images recorded from above the tank of tracer particles illuminated by a horizontal light sheet at mid-height in the tank (figure 1.d). At an internal Reynolds number of 24 ± 2, an initial instability leads to a string of steady vortices along the shear layer. The instability and steady vortices have been described previously[1].

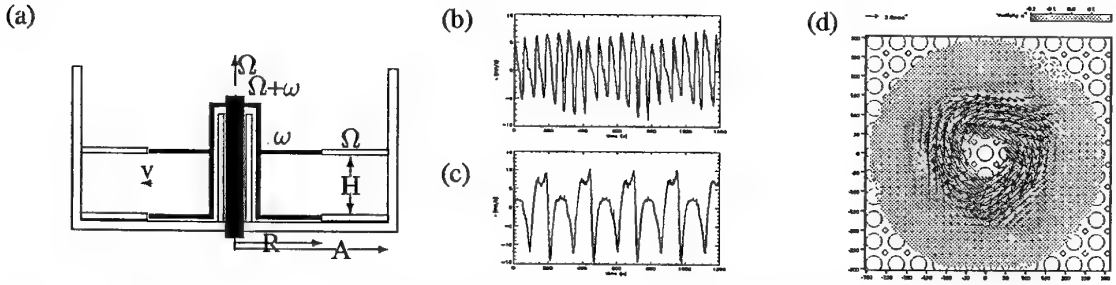

Figure 1. (a) Cross-sectional view of the experimental set-up, (b) and (c) typical LDA signals, and (d) a typical horizontal velocity field (arrows) and vertical vorticity field (contours).

The phenomena presented and discussed here are temporal modulations of the basic vortex flows. Two types of modulation were observed in the experiments using the LDA measurements. One of these was a slow modulation of the vortex amplitude, which would be consistent with a nonlinear interference of two vortex states drifting through the apparatus at different speeds (Figure 1.b). The other suggested a period-doubling of the time series (Figure 1.c) leading eventually to aperiodic fluctuations. Particle tracking experiments were used to investigate these flow types further and to determine the underlying dynamics. The 'period-doubling' was found to be a spatial one to one main vortex and one much weaker secondary vortex. In the 'period-2' state, the two vortices translated at the same, constant speed along the shear layer thus keeping a fixed relative position. Temporal variation developing from this flow could be associated with a vacillation of the position of the secondary vortex relative to the main vortex. It was found that the main relative motion was in the radial position. This lateral motion had a time scale associated with it which was typically around twice the travel time of the vortices through the tank. A nonlinear interaction between the azimuthal drift through the tank and the radial vacillation is evident in the fact that, instead of a quasi-periodic signal, a frequency-locked period-2 or 4 flow was found in the majority of the cases, or flow on a Roessler-type attractor with a non-integer correlation dimension between one and two.

[1]W.-G. Früh and P. L. Read. Experiments in a barotropic rotating shear layer. I: Instability and steady vortices. *J. Fluid Mech.*, 383:143–173, 1999.

Large turbulence structures in a shallow mixing layer

B.C. van Prooijen and W.S.J. Uijttewaal
Section Hydromechanics, Department of Civil Engineering
Delft University of Technology, The Netherlands
Email: b.c.vanprooijen@ct.tudelft.nl

Keywords mixing layer - shallow flow - large eddies

Abstract - Most large scale flows encountered in the practice of civil engineering are shallow free-surface flows, i.e. the width of the flow is much larger than the water depth. This shallowness enables turbulence structures to develop to sizes many times the water depth. These large turbulence structures govern the horizontal transport of mass and momentum. Due to the no-slip boundary at the bottom and the high Reynolds number a turbulent bottom boundary layer develops, which affects the development of the large horizontal turbulence structures.
In order to obtain a clear view on the interaction between bottom shear stress and the large turbulence structures, experiments are carried out in a flume of 20m long, 3m wide and a water depth of 64mm. Two streams of different velocities separated by a splitter plate generate a shallow mixing layer in the horizontal plane downstream the splitter plate (figure 1). Particle

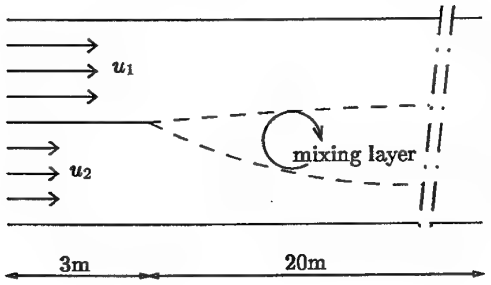

figure 1: Top view of the experimental set-up in which a shallow mixing layer is generated.

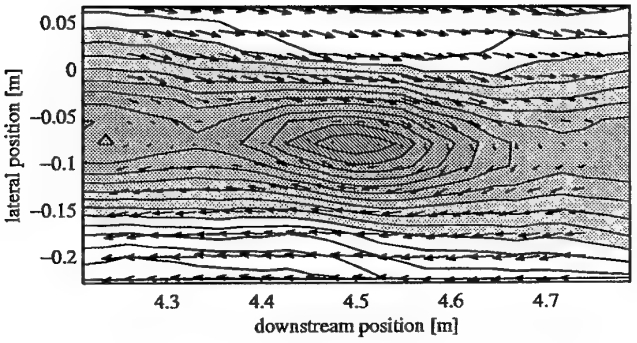

figure 2: Vorticity and relative velocity field of a conditionally averaged eddy. Positions are given with respect to the tip of the splitter plate.

Tracking Velocimetry (PTV) is used with particles floating on the water surface. Velocity fields are determined at different positions downstream the splitter plate. Averaged quantities like mean velocities, turbulence intensities and Reynolds stress were determined, which were in good agreement with previous LDA-measurements. The mixing layer develops initially as a deep-water mixing layer, but is further downstream influenced by the bottom shear stress.
In addition to single point measurement techniques like LDA, PTV offers also spatial information. Time series of velocity fields show the presence and the development of the large turbulence structures. By means of conditionally averaging the representative large scale eddy could be obtained for each downstream position (figure 2). Subsequently, characteristic properties like eddy dimensions, vorticity distribution and propagation velocities could be determined.
Particle Tracking Velocimetry proved to be a powerful tool to detect the large turbulence structures. The evolution of the large turbulence structures subjected to bottom shear stress can be quantified. These measurements offer a dataset to validate and improve numerical models for simulation of shallow water flows.

Free surface flow instability in inclined open channel

A.L. Le Fessant, D. Dartus, J. Chorda
E-mail : fessant@imft.fr

The aim of this study is the diagnostic, through an experimental and numerical approach, of instability's phenomenon for steep slope.

Experiments on water tank have revealed the occurrence of free surface undulations above a smooth ground. These undulations have periodical and stable characteristics, so called roll waves. Equidistant barriers have been placed to increase the roughness. Several configurations have been studied (spacing roughness, slope, flow rate) and have allowed the observation of several types of flows. We have hence verify a control of wave train due to spacing between barriers, but also apparition of other instabilities essentially bidimensional.

In order to understand these phenomena, we propose a linear stability analysis to display criteria of formation of these instabilities. To reach this goal we use the two dimensional shallow water equations, where the friction terms are closed by the Strickler formula.

We carry out validations by developing a numerical code. For a non-linear system like shallow water equations, as physical waves typically are shock induced by the various encountered regimes (quick variation of Froude's number), we use a total variation diminishing (TVD) scheme capable of exactly solve discontinuities.

Boundary conditions are specified with the Thomson's method, which works with the method of characteristics and analysis of the different waves crossing the boundary.

This work's finality is to gain a code that will be able to describe observed two-dimensional instabilities development. So we will be capable to compare it to experimental results and theoretical criteria for various configurations and identify instability's triggers.

Impurity transport and large–scale flows induced by topological defects of the field of parametrically excited capillary ripples

A.B.Ezersky, A.V.Nazarovsky, and S.V.Kiyashko
Institute of Applied Physics, Russian Academy of Science
46 Uljanov Str., 603600 Nizhny Novgorod, Russia
Email: ezer@appl.sci-nnov.ru

Keywords - Defects - Induced flows - Impuriy transport

Abstract - Besides perfect crystals, spatially modulated lattices, and quasicrystalls, spatially periodic structures with topological defects may occur in parametrically excited capillary waves (Faraday ripples). Such defects (edge dislocations) appear in parametrically generated ripples in very viscous liquids or in liquids with small depths. We showed experimentally that topological defects in spatially periodic structures appearing at parametric excitation of waves on the surface of a silicon oil (viscosity approximately 100 times viscosity of water) produce large-scale mean flows.

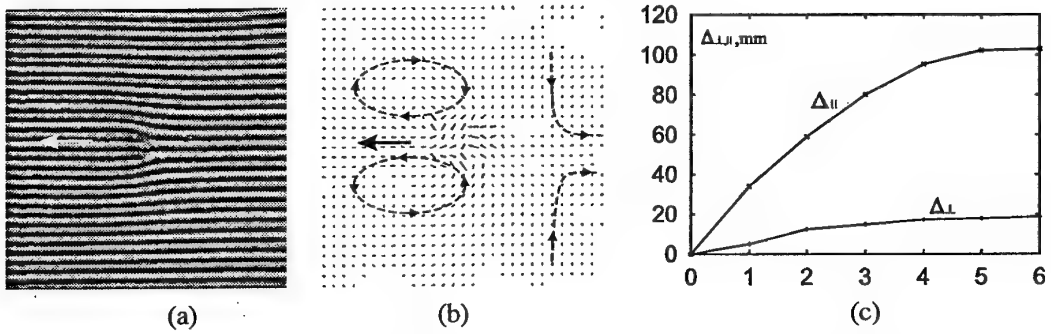

Figure 1: (a) Image of defect occurring in parametrically excited ripples. The arrow shows the direction of motion. (b) Field of velocity induced by the defect. Two vortices and return flow are marked by dashed lines. (c) The increase of cloud size in longitudinal ($\Delta_{\parallel}$) and transverse ($\Delta_{\perp}$) directions versus the number of topological defects passing through the cloud.

Computer processing of images (PIV technique) allows for determination of the structure of the velocity field of these flows. It was found that the topological defect induced two vortices of opposite circulations moving together with it (see Fig. 1 a,b). The vortices appeared when the topological defect arose near the lateral wall, they were rigidly connected with the defect during its clime and broke down when the defect disappeared near the wall. Behind the defect, there exists a return flow which is evidently caused by mass transport. It was found that the defect can entrap and transport passive impurity. The diffusion of a cloud of particles transported by moving topological defects has been investigated. It was found that diffusion of impurity is strongly anisotropic. Along the direction of defect motion, the diffusion is an order of magnitude higher than that in the transverse direction (see Fig. 1 c, where results on impurity motion caused by defects clime are presented).

We believe that such transport of impurity represents a mixing mechanism in the systems where the spatio-temporal chaos is an ensemble of interacting defects.

This work was supported by the Russian Foundation for Basic Research, grant N 99-02-16493.

Exchange processes in a model river with groyne fields

W.S.J. Uijttewaal
Section Hydromechanics, Sub-faculty of Civil Engineering
Delft University of Technology, The Netherlands
Email: W.Uijttewaal@ct.tudelft.nl

Keywords - Mass exchange - Groyne fields - Shallow flows

Abstract - Many rivers in Europe are equipped with groynes, spur dikes that are constructed at both side banks of a river perpendicular to the flow direction. Their purpose is to fix the course of a river and to maintain a proper depth for navigation. The water motion in the shallow cavity enclosed by the river bank and the groynes (called groyne field), is driven by the exchange of mass and momentum. The circulation induced by the momentum exchange has the capability of retaining solutes and sediment particles that are transported in the main stream of the river.

In view of the development of forecasting models for the transport of pollutants and sediment in rivers this groyne field circulation flow is studied experimentally by two means. The retention or exchange time of a passive tracer is determined together with the velocity field of the large scale circulation. To this end a schematised river reach was build as shown in the figure below. The characteristic retention time was determined from the decay time of the mean groyne field dye concentration after distribution of a certain amount of dye in the whole groyne field. The concentration was determined using a calibrated video-system viewing from above. The same system was used to record the motion of floating particles. Particle tracking velocimetry was used as a post-processing tool to determine the surface velocities. The influence of various parameters like aspect ratio, water depth, flow velocity and geometry shape was studied.

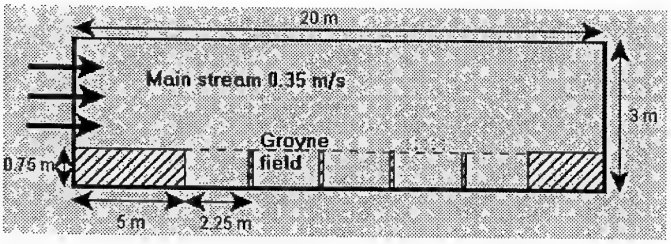

Top view of the experimental set-up showing the main stream with five adjacent groyne fields, depth=10cm.

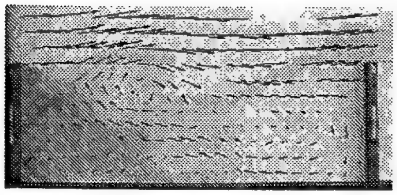

Example of instantaneous distribution of dye and velocity field.

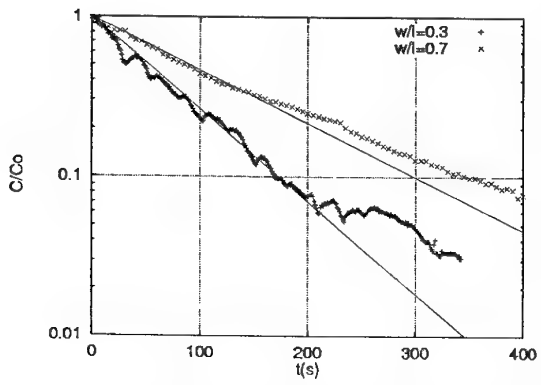

Mean dye concentration in a groyne field vs. time for two aspect ratios.

The experiments revealed a rather dynamic flow field where, in addition to the interfacial mixing layer, large eddies, shed from the upstream groyne accounted for a significant part of the exchange. Despite the dynamics of the large eddies the exchange process appeared to be governed by a single time constant in most cases. In cases were a second time constant could be distinguished the circulation in the groyne field was significantly influenced by a second gyre that exchanged mass with the main stream via the primary gyre. The obtained dimensionless exchange coefficients agreed with those obtained in harbour-like geometries.

Free-forced interactions in braided channels

R. Repetto[1] and M. Tubino[2]
[1]Dipartimento di Ingegneria delle Strutture, delle Acque e del Terreno
Università dell'Aquila, Italy
Email: rodolfo@ing.univaq.it
[2]Dipartimento di Ingegneria Civile e Ambientale
Università di Trento, Italy
Email: tubino@ing.unitn.it

Keywords - Braiding - Fluvial bars

Abstract - The morphological development of erodible bed rivers is essentially governed by the interaction between free bedforms, which spontaneously develop in the channel as the result of an instability process, and bedforms forced by physical constraints such as curvature, width variations, backwater effects ....

With regards to meandering rivers Kinoshita & Miwa (1974) experimentally showed that channel sinuosity induces a damping effect on bar formation and migration. They observed both the coexistence of free bars with the forced topography driven by curvature, at low sinuosity, and the suppression of migrating bars for larger values of channel sinuosity. The above mechanism has been successively theoretically interpreted by Tubino & Seminara (1990) with reference to a regular sequence of small-amplitude meanders. Their results show that it is possible to suppress migrating alternate bars giving the channel a sufficient sinuosity.

Ashmore (1991) experimentally studied the generation of a braided pattern from a straight laterally unconstrained, choesionless channel. Typically the generation of migrating alternate bars is initially observed, which induces a weak curvature of the stream. As a response to this planform width variations are generated, displaying a wavelength equal to half the wavelength of curvature distribution. Under such conditions alternate bars are transformed into a central bar pattern which in turn lead to the generation of a bifurcation. In the present contribution the interaction between migrating alternate bars and periodic width variations is theoretically investigated through a perturbative approach, based on the assumption of small-amplitude width variations. The work is conceptually similar to that proposed by Tubino & Seminara for the case of meandering rivers: in both cases nonlinear interactions between free and forced forms have to be studied. It is noted however that, unlike in the case of meandering channels, in the presence of width variations the forced bed response displays a spatial structure which differs from that of free alternate bars, the former being symmetrical and the latter anti-symmetrical. Results suggest that periodic changes of channel width are likely to suppress migrating alternate bars, promoting the formation of steady central bars, provided the amplitude of width variations is large enough. The suppression is reached for values of the amplitude of width changes sufficiently small to justify the perturbative approach. A further theoretical work is in progress which couples the forcing effects due to width variations and channel curvature.

Bibliography

Ashmore, P. E. (1991). How do gravel-bed rivers braid? *Can. J. Sci,*, 28, 326-341.

Kinoshita, R. & Miwa, H. (1974). River channel formation which prevents downstream translation of transverse bars, *Shinsabo*, 94, 12-17. (In Japanese).

Tubino, M. & Seminara, G. (1990). Free-forced interactions in developing meanders and suppression of free bars. *J. Fluid Mech.*, 214, 131-159.

Some aspects of the physics of river plumes

J.D. Pietrzak[1] and A. Visser[2]
[1]Section Hydromechanics, Sub-faculty of Civil Engineering
Delft University of Technology, The Netherlands
[2]Danish Institute for Fisheries Research,
Charlottenlund, Denmark
Email: J.Pietrzak@ct.tudelft.nl

Keywords - environmental fluid mechanics - computational hydrodynamics - coastal oceanography.

Abstract - Freshwater discharging into coastal seas such as the North Sea results in the formation of river plumes. The out flowing estuarine waters tend to turn to the right on leaving the river mouth (in the Northern Hemisphere) forming narrow coastal currents, which act as conduits for the transport of fresh water and land derived material such as sediment, nutrients and pollutants. River plumes can maintain their cross-shelf structure for hundreds of kilometres and as such are extremely important in determining the transfer of matter and the fate of pollutants in coastal seas. However the mechanisms controlling how far offshore they spread, how far along shore they maintain their structure and when they become unstable are poorly known. Yet these are important considerations for the determination of transport routes and in furthering our understanding of cross-shelf processes.

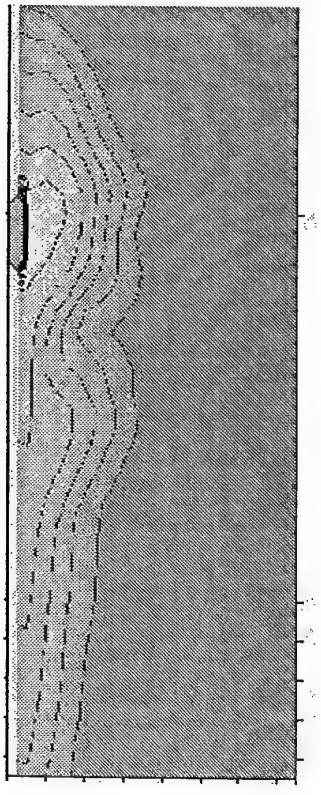

Type-I plume; 2 PSU isolines of salinity.

It is therefore of some interest to understand how large these regions of freshwater influence (ROFIs) are expected to become. In this paper we present a simple analysis, resulting in the definition of a plume number which can be useful in addressing this question.

The physics associated with river plume formation and evolution is complex, while typically dominated by geostrophic adjustment, the interaction between friction, mixing, topographic effects and ambient forcing is also important. Therefore a detailed numerical analysis has also been carried out and the results are presented. Non the less, river plumes can be loosely classified into three categories: I: Coastal buoyancy plumes II: Basin wide regions of freshwater influence and III: Coastally detached plumes. These types of plumes are examined in this paper, paying attention to the plume number classification and the supporting numerical experiments. Particular attention is paid to type I and II plumes typically found in the North Sea and adjacent regions. Shown is an example of a type I plume. The domain is 20 km wide and 80 km in length and the river discharge enters the sea on the upper left side of the domain. The isolines of salinity show a coastal buoyancy plume resulting from the discharge of fresh river water into a coastal sea with constant background salinity of 35 PSU. Due to geostrophy the plume turns to the right, forming the region of lower salinity against the coast.

Waves

The amphidromic structure of inertial waves in a rectangular container

Leo Maas, Netherlands Institute for Sea Research
PO Box 59, 1790 AB Den Burg, The Netherlands, maas@nioz.nl

Enclosed rotating fluids support waves, restored by Coriolis forces and propagating obliquely through the fluid. The angle under which these waves propagate with respect to the rotation axis, is fixed and is set by the ratio of the frequency of the wave and the inertial frequency (twice the angular velocity of the tank). Sloping boundaries therefore generally lead to focusing of these waves upon wave attractors, as observed in experiments and predicted for 2D (infinitely long) containers. This explains the spatial structure of these waves in a vertical plane, though it does not tell much about their horizontal structure. Only in the particular case that boundaries are either parallel, or perpendicular to the rotation axis, focusing will be absent and eigenmodes may be expected. However, the spatial structure of these waves, still quite complicated, can now be completely determined when the plan view of the tank is circular or rectangular. This will be shown here by, first, making the ansatz that a container possesses rigid horizontal surface and bottom surfaces (allowing for modal expansion in the vertical), second, by discussing the 'inertial' analogs of surface Poincaré and Kelvin waves, and, third, by observing how these can be combined to find the amphidromic structure of inertial waves (analogous to the Taylor problem for reflecting Kelvin waves).

Numerical approach of self-sustained tones in flows

A. Coiret, A. Sakout, S. Guérin, R. Henry
Laboratoire L.E.P.T.A.B.
Université de La Rochelle, Avenue M.Crépeau, 17042 La Rochelle
Email : acoiret@univ-lr.fr

Keywords - Self-sustained tones - noise reduction - L.E.S. Models

Abstract - In the present study, stationary and instationary models are used in order to verify conditions which lead to self-sustained tones in air flows. The experimental set-up contains two diaphragms in a duct, spaced by a variable section L. Intense self-sustained tones are encountered when they are sufficiently close to each other, as a result of a feedback loop between vortex shedding in the jet of the upstream diaphragm and the acoustical field in the duct. This feedback loop results from the transfer of energy from the vortices to the acoustical field, according to phase and direction conditions. When the mean velocity U_0 is varied, self-sustained tones are generated for fixed frequencies, because the acoustical field is able to drive the instabilities of the confined jet at the resonance modes.

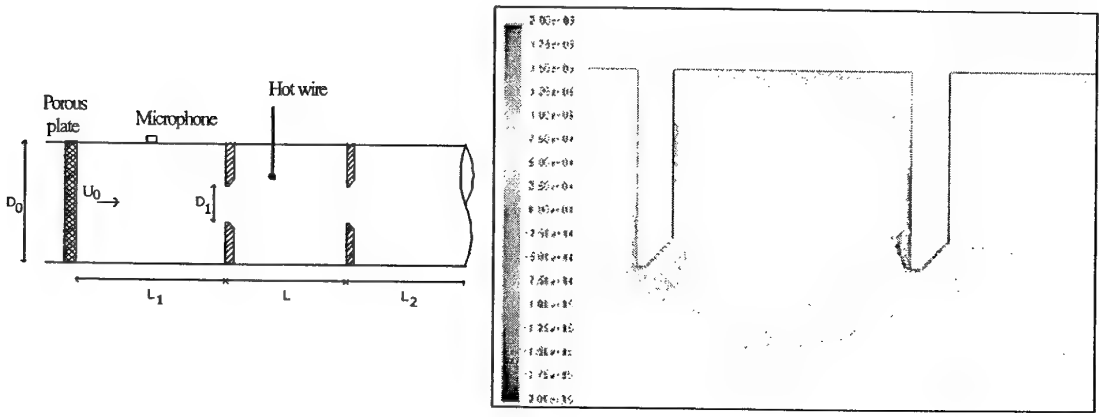

Experimental setup (left) and vorticity contours link to the feedback loop process (right)

A first k-ε stationary, incompressible and two dimensional model allows to corroborate the experimental spacing length condition $L<3*D_1$ for strong self-sustained tones generation. A high transfer of energy in the utterance zone is needed to lead to a strong feedback loop. This transfer is estimated by calculating the gradient of vorticity in the utterance zone, following Howe's theory of sound. An instationary, incompressible L.E.S. model leads to the same result on the spacing criteria and gives the vortex shedding frequencies, which are very close to the experimental tones frequencies for the same inlet conditions. These simple models are focused on the conditions needed by the feedback loop and allow to predict the development of self-sustained tones in a given flow. Furthermore, a modified model with a thin slot added on the upstream diaphragm validates the decreasing of the feedback efficiency measured for the corresponding experimental set-up. These models explain the mechanisms of self-sustained tones generation and will allow the determination of noise reduction method for varied industrial set-ups, by a new way of adding slight suitable geometrical modifications.

Whistling of a Helmholtz resonator: simple analytical model

A. Hirschberg and S. Dequand
Eindhoven University of Technology,
Postbus 513, 5600 MB Eindhoven, The Netherlands
Email: a.hirschberg@tue.nl

Abstract - Coupling of vortex shedding with acoustical resonance of a Helmholtz resonator is responsible for whistling tones produced by blowing through lips (human whistling) or along an empty (Bordeaux) bottle. Figure 1 presents a simple sketch of the phenomenon: self-sustained oscillations are induced by a grazing flow along the narrow opening of the neck of the resonator. At the right-hand side of fig. 1, the vorticity magnitude predicted by Euler simulations is shown. The phenomenon is most efficiently described in terms of Vortex Sound theory. A simple caricature of the flow in terms of line vortices provides already a prediction of critical flow speeds for whistling. We propose modifications of the original model from literature. This yields prediction of the oscillation amplitude within a factor two. We discuss the effect of the influence of shape of the edges and compare theory with experiments. In fig. 2, theoretical and experimental results are compared for two different neck geometries.

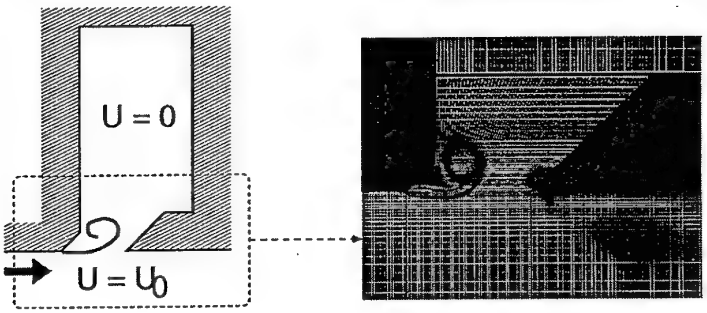

Figure 1: Phenomenon description: sketch of the resonator and Euler simulation of the vortex shedding in the neck of the resonator

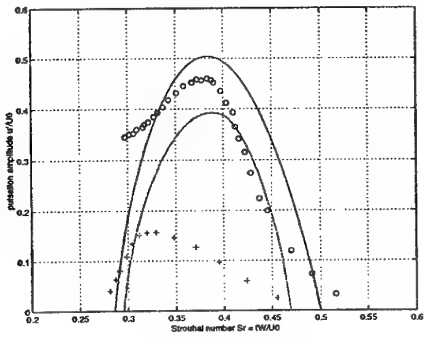

Figure 2: Predicted and measured pulsation amplitudes in terms of the Strouhal number for a neck with rounded edges (o) and a neck with sharp edges (+)

Evolution of nonlinear planar moderately long gravitational waves in a viscous incompressible liquid with a slowly varying bottom

G.A. Khabakhpashev and A.A. Litvinenko
Department of Physical Hydrodynamics, Institute of Thermophysics
Siberian Branch of the Russian Academy of Sciences, Novosibirsk, Russia
Email: geshev@otani.thermo.nsk.su

Keywords - Nonlinear Surface Waves - Numerical Simulation - Topography

Abstract - This paper deals with the development of the weakly nonlinear long-wave theory describing the transformation of the three-dimensional free boundary perturbations of a viscous incompressible fluid [1]. Using the previous assumptions [1], the integration with respect to the vertical coordinate, the ordinary kinematical and dynamic boundary conditions, and if nonlinear perturbations are propagated mainly in one (though arbitrary) direction, the initial system of hydrodynamic equations (the equations of continuity and motion) were reduced to the one evolution equation for three-dimensional disturbances of the liquid free surface over a gently sloping topography. It is emphasized that waves of very small amplitude can travel simultaneously in different (including the opposite) directions.
Some solutions of the new model equation were found numerically. Firstly, our results were compared with the experimental data obtained at U.S. Army Engineer Waterways Experimental Station [2] in the run up problem of a plane solitary wave on a gentle slope. It is shown that calculations describe adequately such processes. In the context of another experiment reported in [2], the problem of the interaction between nonlinear solitary wave and vertical conical-cylindrical structure in the center of the basin was investigated numerically (Fig. 1*a*). It was considered also the evolution of nonlinear solitary wave over the submarine mountain (Fig. 1*b*).

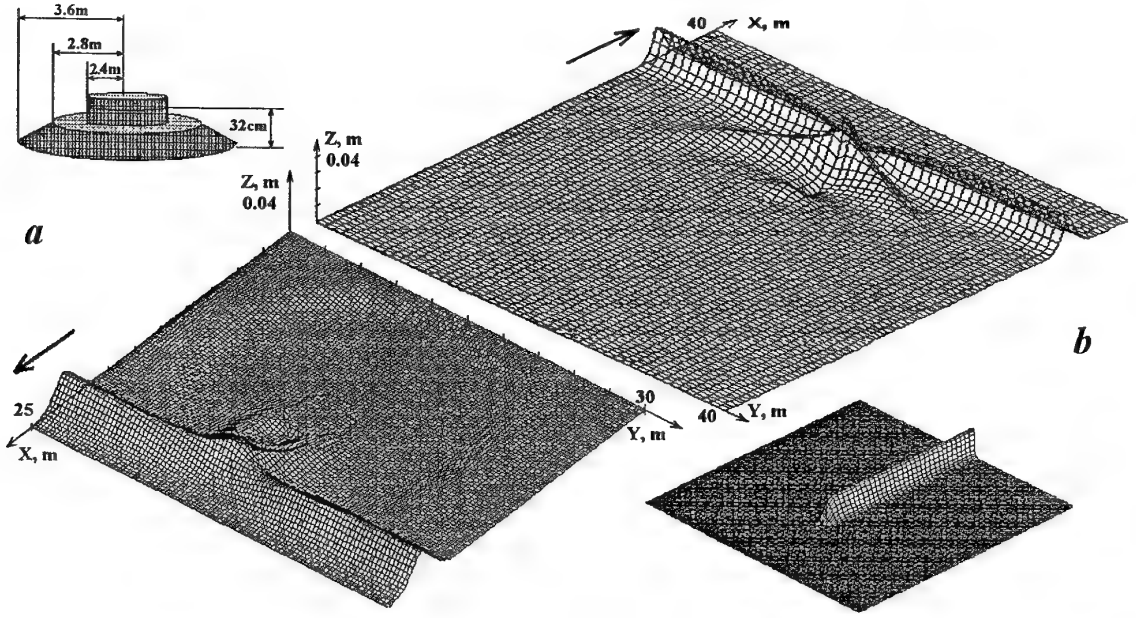

Figure 1: The interaction of plane solitary waves with the vertical conical-cylindrical structure in the center of the basin (*a*) and submarine mountain which is parallel to the wave vector (*b*)

This work was supported by RFBR (grant 00-01-00849) and SB RAS (integrational program).

References - 1. Khabakhpashev G.A., Tsvelodub O.Yu., 3rd EFMC, Göttingen, 1997, P. 176.
2. Proceedings of the International Workshop on Long-Wave Run up Models, WA, USA, 1995.

UNFAMILIAR RESONANT SURFACE WAVES

[1]Sh.U.Galiev and [2]T. Sh.Galiyev
[1]Department of Mechanical Engineering, The University of Auckland, Auckland 1, New Zealand;
[2]New Zealand Funds Management Limited, Private Bag 92163, Auckland, New Zealand;
Email: s.galiyev@auckland.ac.nz

Keywords- Equations of Continuum-2D Waves-Analytic Solutions

Abstract - Anomalous surface waves were recently observed (see, for example *Nature*: 382 (1996) 763 and 793, 402 (1999) 794, 403 (2000) 401 and *J. Fluid Mech.*: 369 (1998) 273). 1D theory of these waves was developed (*Phys.Lett. A* : 246 (1998) 299, 266(2000) 41; *J. Phys. A: Math. Gen.*: 32(1999) 6963). Here we present some results of 2D theory. For some surface weakly nonlinear waves in porous, solid (liquid) layers we obtained that $\varphi_{tt} - a_0^2\nabla^2\varphi = \alpha^{-1}g^{-1}\{\psi - g_d(h - \frac{1}{2}h_0) + \frac{1}{3}h_0[1 - \frac{4}{3}\nu\rho_0^{-1}a_0^{-2}(1-\alpha_s\phi_0)][1-\nu\rho_0^{-1}a_0^{-2}(1-\alpha_s\phi_0)](g^{-1}a_0^2\nabla^2\varphi)_{tt}\} + \mu\nabla^2\varphi_t + \beta(\nabla^2\varphi)^2 + \beta_1(\nabla^2\varphi)^3$. Here φ is the displacement potential. Velocity a_0 and the coefficients can depend on the vertical acceleration and thickness h. If $h \to \infty$ we have the velocity of longitudinal body waves $a_0 = [\lambda^{-1}\rho_0^{-1} + \frac{4}{3}\nu\rho_0^{-1}(1 - \alpha_s\phi_0)]^{0.5}$. If $h \to 0$ then $a_0^2 = gh + \frac{4}{3}\nu\rho_0^{-1}(1-\alpha_s\phi_0)$. If $\lambda \to 0$, $\phi_0 \to 0$ and $\nu \to 0$, then $a_0^2 = gh$. The equation contains the extraneous force, the topographic, dispersive, dissipative and nonlinear terms. The topographic, dissipative and dispersive effects were considered as the second order values. The Airy equation (H. Lamb, *Hydrodynamics*, p.260) rewritten for weakly nonlinear waves and equation (4.3) from *Proc. R.. Soc. Lond. A* (453 (1997) 319) follow from the equation. We obtained a lot of analytical resonant solutions of this equation which describe free, forced, parametric, forced-parametric and parametric-topographic waves. Some results of the theory are presented in Figures. Fig.1 shows the resonant jet-like waves on water calculated for rectangular (*A, B,* see also *Phys. Rev. Lett.*: 76 (1996) 1824) and circular (*C,* see also *Nature* 403 (2000) 401) basins. Fig. 2 show the transition of sawtooth waves into stable breaking-like (see also *Phys. Rev. Lett.*: 76 (1996) 3959, 83 (1999) 3190), jet- and drop-like (see also *J. Fluid Mech.*: 127 (1983) 103; *Phys. Rev. E* 56 (1997) 472) waves when trans-resonant parameter R changes near critical value –1. The harmonic curve in Fig.2 A is an acoustic solution. Fig. 3 show the transition of stripe-like waves (see also *Nature* 402 (1999) 394) into drop-like waves and then the formation of surface foam (see also *Phys. Rev. Lett.*: 76 (1996) 1824). One can see that Figures, calculated according to the analytical solutions, describe qualitatively the observed waves. We have shown the most simple harmonically excited waves which may be in the trans-resonant bands if cubic nonlinearity is important. In general case chaotic oscillations of surface may be generated. Motion of the waves on the plane may be very complex if parametric effect is important.

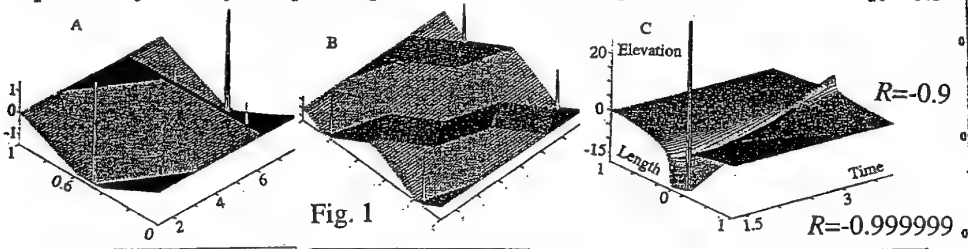

Fig. 1

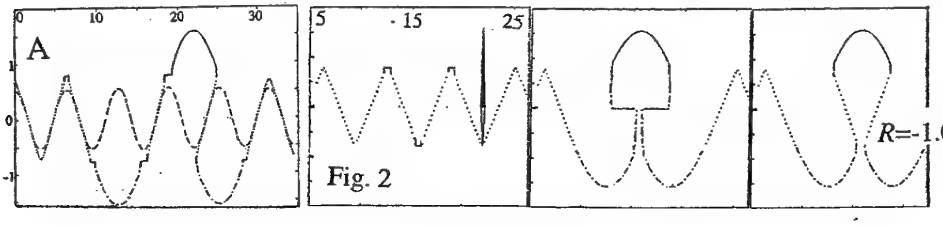

Fig. 2

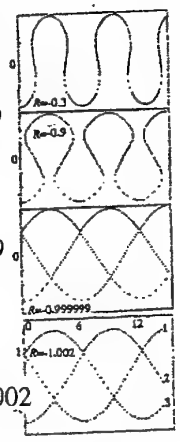

Fig.3

Mass transport induced by sea waves propagating on a constant sloping beach

P. Blondeaux, M. Brocchini and G. Vittori
Department of Environmental Engineering - University of Genova, Italy
Email: blx@diam.unige.it

Keywords - Wave - Steady currents - Boundary layers

Abstract - Although the main water motion induced by propagating sea waves is to and fro, steady streamings and a net flux of water are generated by nonlinear effects. The existence of a steady drift associated with the propagation of a sea wave was first pointed out by Stokes (1887) who treated the problem by using the classical second-order potential wave theory. Then, Longuet-Higgins (1953) tackled the problem with due consideration of fluid viscosity and vorticity within the surface and bottom boundary layers. However, these analyses, as well as most of the subsequent investigations of the problem, were carried out considering constant water depths. A general formula to evaluate steady streamings induced by nonlinear effects within the bottom boundary layer of a three dimensional wave of small amplitude was provided by Hunt & Johns (1963) who, however, did not consider the flow far from the bottom. Carter et al. (1973) and Lau & Travis (1973) applied these results to compute the velocity field at the bottom of a sea wave which approaches the coastline and is partially reflected at the beach. In particular Lau & Travis (1973) considered beaches characterized by gentle slopes such that the wavefield could be locally described in terms of a linear Stokes wave over a constant depth. The perturbation approach used by Lau & Travis (1973) is strictly valid when the ratio $\beta L^*/h_0^*$ is much smaller than one. Herein β denotes the beach slope, h_0^* is a characteristic value of the water depth and L^* is the length of the incoming waves. Hence, close to the beach, where the water depth turns out to be much smaller than the wavelength of the wavefield, it is necessary to consider very small values of β ($\beta \ll h_0^*/L^* \ll 1$). The present contribution is aimed at predicting the shoaling process of a wave propagating on a sloping bottom. Since we consider the region close to the coast, the water depth is assumed to be much smaller than the length of the waves and the shallow water approximation is used. For the consistency of the analysis, the beach slope β is assumed to be of $O(h_0^*/L^*)$. Moreover, waves of small amplitudes with respect to the local depth are considered. The Reynolds number is assumed to be large and the flow regime in the bottom boundary layer to be laminar. Attention is focussed on the steady velocity components. Close to the bottom the results by Longuet-Higgins (1953) and Hunt & Johns (1963) are recovered. Far from the bottom, in the so-called 'core' region, our approach allows to predict the local wave amplitude and the steady velocity components. To compute them, an advection-diffusion equation for the vorticity field is solved. The solution depends on the ratio a^*/δ^* between the wave amplitude and the thickness of the bottom boundary layer. When this ratio is much smaller than one, the creeping flow approximation can be used and the solution can be easily worked out by analytical means. For values of a^*/δ^* of order one or much larger than one, a numerical approach is used. Present theoretical predictions of the steady currents are supported by a comparison with the experimental results of Hwung & Lin (1990).

References

Carter, T.G., Liu, P.F.L. & Mei, C.C. (1973). J. Waterway, Harbours and Coastal Eng. Div., ASCE, 99, 165-184. **Hunt, J.N. & Johns, B.** (1963). Tellus, 15, 343-351. **Hwung, H.H. & Lin, C.** (1990). Proc. 22nd Int. Conf. Coastal Eng., ASCE, 544-556. **Longuet-Higgins, M.S.** (1953). Phil. Trans. Roy. Soc., 345, 535-581. **Lau, J. & Travis, B.** (1973). J. Geophys. Res., 78, 21, 4489-4497. **Stokes, G.G.** (1847). Trans. Cambridge Phil. Soc., 8, 441-455.

Wave turbulence in the Faraday experiment

M.T. Westra and W. van de Water
Section Fluid dynamics, Physics Department
Eindhoven University of Technology, The Netherlands
Email: m.t.westra@tue.nl

Keywords - Wave turbulence - Faraday experiment - Wave interaction - Nonlinear systems

Abstract - A vertically oscillated fluid layer develops waves on the free surface. At high amplitude forcing, many waves are present which all interact through nonlinearities in the equations of motion. The waves show a cascade in energy, where longer waves pass their energy to smaller waves. In analogy with 3D turbulence, this state is called "wave turbulence". In our research, we characterize the turbulent state of the free surface by the experimental setup shown below.

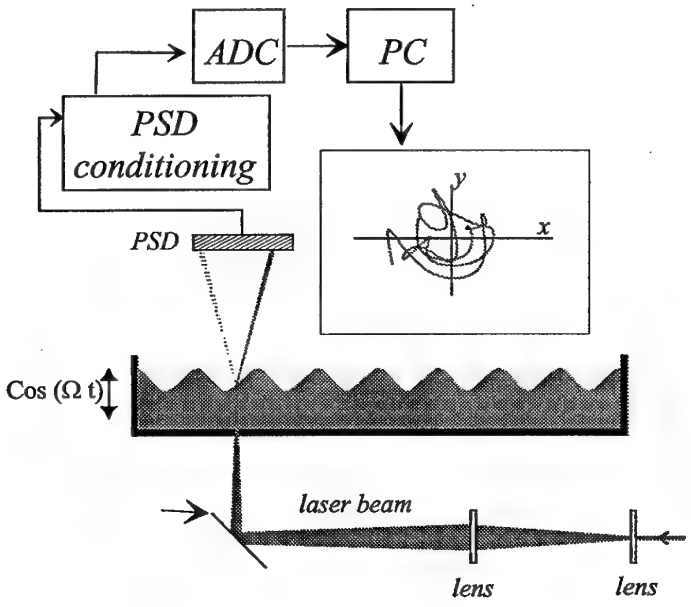

The experimental set-up. The position of a refracted laserbeam is recorded with a Position Sensing Device (PSD). In this way, we obtain a measurement of the local slope of the surface.

We show that the system shows a clear inertial region over a large range of frequencies. We also discuss the location of the damping region, and the input of energy.

Stability of rivulets sheared by turbulent gas flow

S. Alekseenko, V. Antipin, A. Bobylev, D. Markovich
Institute of Thermophysics, Siberian Branch of RAS, Novosibirsk, Russia
E-mail: dmark@itp.nsc.ru

Keywords - rivulet - waves - turbulent gas flow

Abstract - In the present work the experimental study of wave formation on the surface of rivulet flowing down on the lower side of incline cylinder has been performed for the conditions of co- and countercurrent turbulent gas (air) flow. Such types of flow exist in recently developed condensers and heat exchangers with inclined tubes. Similar to the case of falling liquid films, the waves affect essentially the hydrodynamics of the rivulet and should apparently have a strong action on the heat and mass transfer. The scheme of the experiment is shown in Fig. 1. As a test section the stainless steel tube and rough glass tube (outer diameters D of 20 mm and 19 mm) are used. The length of tubes is 1 m. Liquid is supplied to the test section in the form of a jet issuing from a convergent nozzle. The incline of cylinder, α, changed from 2 to 15°. The ethanol and two kinds of fluorocarbons whose peculiarities are high density and low surface tension were used as working fluids. The flow of air was organised by using the rectangular channel with inner dimensions of 40x40 mm^2, where the working section - inclined tube - is placed. The local film thickness and phase velocity of waves were determined with the aid of shadow method. The distributions of the rivulet thickness along the test section, the length of a smooth zone, and the liquid ejection were measured in relation to the liquid flow rate, inclination angle and Reynolds number of gas flow. It was found that some intermediate range of gas flow velocities exists for each tube incline and liquid flow rate when gas provides the most instability of rivulet flow and as a result the ejection of the liquid from the cylinder takes place. Both natural and excited wave regimes were investigated during experiments. The characteristics of natural waves are in satisfactory agreement with the maximum growth waves model. The example of the transition of rivulet motion from the stable wave flow to the turbulent film is presented in Fig. 2 as a consequence of wave profiles with increasing gas Reynolds number. The film becomes fully turbulent at some value of $Re_{gas} = Re_t$. For given in Fig. 2 conditions $Re_t = 3000$. It is found that in number of flow regimes rivulet and plane film wave profiles are very similar and the regularities of wave propagation are qualitatively the same. This similarity is not obvious because of principal distinctions between two kinds of flow. The film waves are strictly two-dimensional and the film is uniform in transversal direction. Contrary, the rivulet waves are significantly three-dimensional and the cross-section of a rivulet is nonuniform and represents a hanging droplet. At the same time the new regularities are found in comparison with plane films. For example, the stationary waves of triangular profile and multi-hump solitary waves were observed.

This work was supported by INTAS grant N 99-1107.

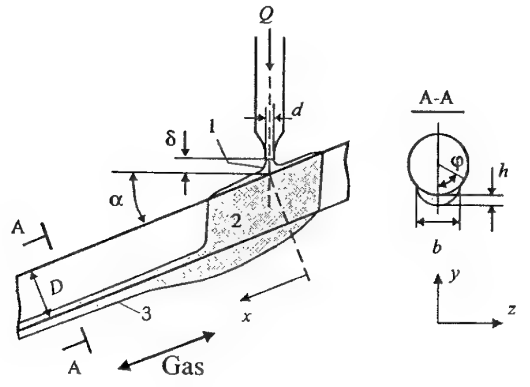

Fig. 1. Scheme of rivulet flow. 1- irrigation zone, 2 - continuous film, 3 - rivulet

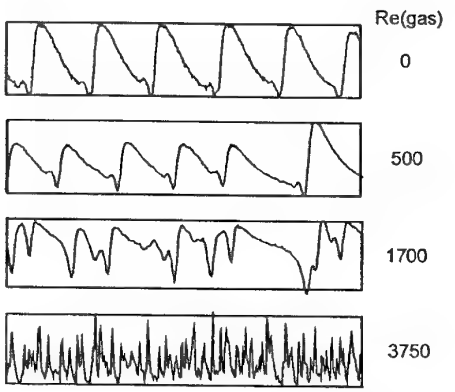

Fig. 2. Wave patterns versus Reynolds number of gas flow. Ethanol - air, $Q_{liq} = 0.67$ ml/s, $\alpha = 5°$.

Zero gravity sloshing

J.Billingham and E.O. Tuck
School of Mathematics and Statistics, The University of Birmingham, U.K.
Department of Applied Mathematics, The University of Adelaide, Australia
Email: J.Billingham@bham.ac.uk, etuck@maths.adelaide.edu.au

Keywords - Moving Contact Line - Surface Tension - Microgravity

Abstract - We study the effect of a time-periodic, lateral acceleration on the two-dimensional flow of a Newtonian fluid with a free surface subject to surface tension. The fluid is confined between two plane, parallel walls under conditions of zero gravity. We assume that the velocity of each contact line is a linear function of the dynamic contact angle between fluid and solid at the wall alone. This problem is relevant to the study of fluids processing in a microgravity environment, but is also of more general interest as a flow in which the dynamics of the moving contact lines completely determines the behaviour of the fluid.

We begin by obtaining analytical solutions for the small-amplitude standing waves that evolve when the fluid is inviscid and the lateral acceleration is sufficiently small. This leads to damping of the motion, unless either the contact angles are constant or the contact lines are fixed. In these cases, we include the effect of the boundary layers on the lateral walls, which are the other major source of damping. From this, we can estimate under what circumstances viscosity is negligible.

Finally, we compute numerical solutions of the nonlinear, inviscid problem. We use a desingularized integral equation technique combined with adaptive time-stepping, and artificially modify the advection of the collocation points to keep their spacing fairly even. After checking the accuracy of our method using the analytical solutions for small-amplitude standing waves, we study solutions for large-amplitude lateral accelerations. A typical solution, showing the free surface meeting the wall under the action of a lateral acceleration of large-amplitude, is shown below.

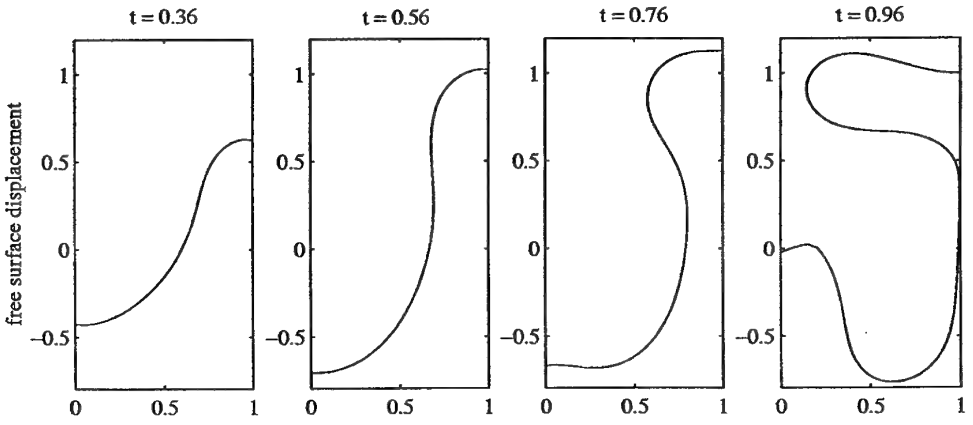

A numerically-calculated solution for large-amplitude forcing, showing the free surface in collision with one side wall of the container.

Structure of surface waves parametrically excited by noise

V.O. Afenchenko, A.B. Ezersky and S.V. Kiyashko
Institute of Applied Physics, Russian Academy of Science
46 Uljanov Str., 603600 Nizhny Novgorod, Russia
Email: ezer@apll.sci-nnov.ru

Keywords - Faraday ripples - Noise excitation

Abstract - We report results of laboratory investigation of waves on the liquid surface oscillating homogeneously in space by a random time law. Experiments were performed in round and square cells with horizontal dimensions much larger than the characteristic scale of surface waves. We investigated various cases of spatially homogeneous oscillations – harmonic oscillations with randomly modulated frequency and solitary envelope impulses of oscillations with randomly modulated frequency.

It has been found that wave excitation has a threshold character. Namely, waves are not excited by external force directly on the liquid surface in the case of spatially homogeneous excitation of the layer and only parametric generation is possible. The dependence of the threshold of parametric excitation on the pump spectrum width is determined. It is revealed that for harmonic oscillations with randomly modulated frequency, an irregular wave field appears even at small supercriticalities. Pulsations of capillary wave amplitudes have been observed in a square cell, with the structure of the wave field being unchanged. It is shown that, at small supercriticality, surface waves are generated with a large temporal gap. As the supercriticality is increased, the repetition rate of surface wave impulses increases and the surface wave amplitude becomes modulated in time at large enough external force. The characteristic frequency of modulation calculated by the sequence of images of capillary ripples recorded in experiment is increased with increasing supercriticality.

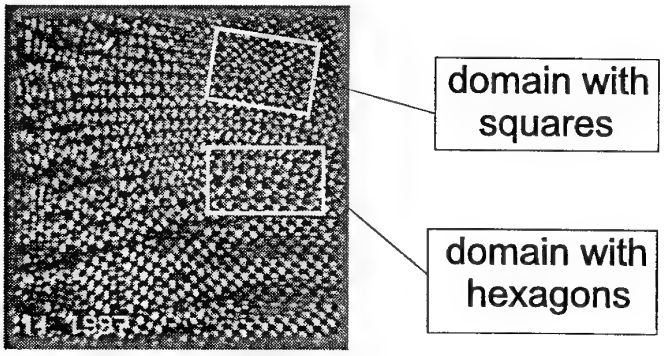

Figure 1: Image of the field of capillary ripples excited by noise. It is possible to find domains with different textures.

It was found that when the waves are excited by envelope impulses of oscillations with random modulation of frequency, the capillary ripples are an ensemble of interacting domains inside which mutually orthogonal pairs of standing waves have different orientations. When the waves are excited in a round cell, part of domains have irregular wave field. The area occupied by the chaotic phase does not depend on the value of the index of frequency modulation provided, it is small enough.

Application of obtained results for physical modeling of seaquakes with epicenter in the ocean are discussed.

Experiments in solitary wave dynamics of film flow

M. Vlachogiannis and V. Bontozoglou
Department of Mechanical & Industrial Engineering
University of Thessaly, Pedion Areos, GR-38334 Volos, Greece
Email: bont@mie.uth.gr

Keywords - Solitary waves - Nonlinear interactions - Fluorescence imaging

Abstract - Recent progress in the theory of nonlinear dynamics of free surface flows has centered on the existence and properties of coherent structures, or dissipative solitary waves. A series of simplified equations have revealed families of stationary solutions bifurcating from the primary instability of the flat film (Trifonov & Tsvelodub 1991, Chang 1994). Experimental studies have relatively recently become detailed enough to test predictions of nonlinear evolution (Alekseenko et al. 1985, Liu et al. 1993, Liu & Gollub 1994).

The main two-dimensional interaction between solitary waves systematically documented so far is coalescence, the merging of a preceding hump with a larger and faster one, which follows (Liu & Gollub 1994). However, a host of theoretically predicted nonlinear phenomena, related to the evolution and interaction of solitary waves (Chang et al. 1995), appear not to have been yet experimentally confirmed or rejected.

In the present work, we report on experimentally observed two-dimensional interactions of solitary waves in water and water-28% glycerol film flow over a flat inclined wall. Non-linear disturbances are introduced at the entrance section of a linearly unstable film; thus, a rich solitary wave structure is observed over a short fetch. A fluorescence imaging technique -combined with frame grabbing and image-analysis software- is used to record every 1/10s the instantaneous film thickness in a view window of 10cm x 8cm.

Numerous coalescence events are systematically recorded. The time duration of the merging process is examined for a range of viscosities and inclination angles, and is found to depend to first order only on the difference in height between the two solitary waves. Based on the characteristic time of the coalescence events, we argue that waves of similar height may resist coalescence and instead form a double-hump pulse.

Coalescence is accompanied by interesting transient phenomena. The front-running bow waves temporarily recede, and reappear only when the hump regains the skewed, solitary shape. This observation confirms the physical mechanism, according to which bow waves arrest further steepening of the solitary hump due to the pull of gravity by creating a negative capillary pressure and sucking liquid out of the crest.

In the water-glycerol runs, the exited hump resulting from a coalescence event presents a stable, elevated back substrate, which scales with the wave height in agreement with theoretical predictions (Chang et al. 1995). However, in the experiments with water, the elevated back-substrate is observed rarely, and then it is highly unstable and yields to a tail modulation with wavelength similar to that of the front-running bow waves. The tail modulation decays when the exited hump is isolated, but when another solitary wave follows, the tail instability may trigger nucleation of a new solitary wave between the two.

References

Alekseenko S. V., Nakoryakov v. Ye. and Pokusaev B. G., *AIChE J.*, **31**, 1446-1460 (1985).
Chang H.-C., *Annu. Rev. Fluid Mech.*, **26**, 103-136 (1994).
Chang H.-C., Demekhin E. and Kalaidin E.,*J. Fluid Mech.*, **294**, 123-154 (1995).
Liu J., Paul J. D. and Gollub J. P., *J. Fluid Mech.*, **250**, 69-101 (1993).
Liu J. and Gollub J. P., *Phys. Fluids*, **6**, 1702-1711 (1994).
Trifonov Yu. Ya. and Tsvelodub O. Yu., *J. Fluid Mech.*, **229**, 531-554 (1991).

Experiments in laminar film flow over a corrugated wall

M. Vlachogiannis and V. Bontozoglou
Department of Mechanical & Industrial Engineering
University of Thessaly, Pedion Areos, GR-38334 Volos, Greece
Email: bont@mie.uth.gr

Keywords - Stationary waves - Solitary waves - Three-dimensional instability

Abstract - Film flow over a corrugated wall appears to have attracted relatively little attention, despite extensive engineering applications in process equipment aimed at enhancement of heat/mass transfer rates. Recent asymptotic and numerical studies beyond the limit of creeping flow (Bontozoglou & Papapolymerou 1997, Trifonov 1998, Malamataris & Bontozoglou 1999, Bontozoglou 2000) indicate that significant free-surface/wall interaction occurs for corrugations with length in the order of millimeters. However,available theoretical results are presently limited to stationary flow (the equivalent of Nusselt solution for flow over a flat wall) and experimental data appear to be very scarse (Zhao & Cerro 1992).

The present work reports visual observations of film flow over a periodic wall recorded by a fast (up to 2000 frames per second)digital video camera. Pure water and 28% glycerol solution were used as the liquid, and the range of Re numbers considered is $10 \leq Re \leq 400$. The wall corrugations have the form of orthogonal grooves at right angles to the flow direction, with height 0.8 mm and wavelength 12 mm (6 mm elevated and 6 mm depressed).

The free surface over the first few periods of the periodic wall is found to be stationary and its shape compares favorably with theoretical predictions. In particular, a stationary modulation with the same wavelength as the wall appears. As the Re number increases, the amplitude of the modulation goes through a maximum and higher harmonics become visible.

However, the stationary flow is usually unstable (a stability map, in terms of inclination and Re number is presented), and two distinct instability modes are identified. One is streamwise and leads through a nonlinear amplification mechanism to the formation of solitary waves. With increasing Re, the two-dimensional solitary waves disintegrate into a staggered pattern of horseshoe solitary waves with highly curved fronts. The development of this instability mode seems to parallel the sequence of events over a flat wall, with the corrugations drastically accelerating the evolution with fetch.

The second mode of instability is transverse and is isolated more easily at high Re and very low inclination angles, where it developes earlier than the streamwise mode. The transverse mode results in a series of depression troughs along each groove, with wavelength of 1-2 cm and nonzero phase speed towards one or the other side-wall. The random sequence of directions gives the free surface a herring-bone appearance. With increasing Re, period-doubling bifurcations are observed and the free surface attains a small-scale chaotic appearance.

References

Bontozoglou, V. and Papapolymerou, G. *Int. J. Multiphase Flow*, **23**, 69-79 (1997).
Bontozoglou, V. *Computer Modeling Engng. & Science*, **1**, 129-138 (2000).
Malamataris, N. A. and Bontozoglou, V. *J. Comp. Phys.*, **154**, 372-392 (1999).
Trifonov, Yu. Ya. *Int. J. Multiphase Flow*, **24**, 1139-1161 (1998).
Zhao, L. and Cerro, R. L. *Int. J. Multiphase Flow*, **18**, 495-516 (1992).

VISCOUS LIQUID LAYER FLOWS OVER A CORRUGATED SURFACE. ANALYSIS OF WAVES FORMATION ON THE FILM FREE SURFACE

Trifonov Yu.Ya.

Institute of Thermophysics, Academician Lavrentyev St., 1, Siberian Branch of Russian Academy of Sciences, Novosibirsk, Russia, 630090, e-mail: trifonov@itp.nsc.ru

Theoretical studies of film flows began with the classical work of Nusselt where he obtained exact solutions for Navier-Stokes equations for a thin layer of viscous liquid free falling down a smooth vertical wall. Further theoretical and experimental investigations have demonstrated that the Nusselt solution is not achieved in practice and, as a rule, the film surface is covered with waves. The problem of nonlinear waves in the film falling down a smooth plate has much in common with that of a steady-state viscous layer flow along a corrugated surface. In both cases the equations are significantly non-linear, the free surface is previously unknown, the surface tension forces play great role and there exists a spatial period. In our recent paper [1] the hydrodynamics of the flow down corrugated surfaces was studied on base of both Navier-Stokes equations and integral model. Viscosity, inertia and surface tension were taken into account. The purpose of the present paper is to study hydrodynamics of the film flow down over both one-dimensional and two-dimensional corrugated surfaces and to analyze linear and nonlinear stability of the film free surface. Different shape of corrugations was considered and their amplitude was comparable with the Nusselt's film thickness. In the case of two-dimensional vertical corrugated surface the inclination angle of ribs is additional parameter and at zero value of the parameter we have one-dimensional flow. As a result it has been obtained that, for example, in the case of two-dimensional surface the critical inclination angle was obtained when the steady-state film flow solution with completely wetted wall surface existed.

It is well known that the viscous liquid film falling down a vertical smooth plate is unstable at any value of Reynolds number. Both in theory and experiment there are long-wavy disturbances of the film free surface which are increasing in time and lead to the formation of nonlinear structures [2]. In the present paper both the linear and nonlinear stability of the film flow down the vertical corrugated surface with respect to the free surface disturbances is investigated. Amplitude and period of the corrugation were comparable with the Nusselt's film thickness and the capillary constant, respectively. Stability of Nusselt's smooth solution is the limit of our problem when amplitude of corrugation was zero. As a result the range of the parameters of corrugations where we have no unstable disturbances has been obtained. Neutral curves are found and the most amplified disturbances are evaluated. As a result of unstable disturbances evolution the new regimes of flow over corrugated surface are formed. It is shown in the paper that the new regimes are represented by the double Fourier series and ones are calculated numerically..

REFERENCES

1. Trifonov, Yu.Ya. Viscous liquid film flows over a periodic surface. *Int. J. Multiphase Flow*, **24(6)**, pp. 1139-1161, 1998.
2. Trifonov, Yu.Ya., Tsvelodub, O.Yu. Non-linear waves on the surface of a falling liquid film. P.1. Waves of the first family and their stability. *J. Fluid Mech.*, **229**, pp. 531-554, 1991.

Long two-dimensional waves on an inclined nonisothermal film: effects of non-uniform heating and evaporation

S. Miladinova[1], S. Slavtchev[1], G. Lebon[2] and J. C. Legros[3]
[1]Institute of mechanics, Bulgarian Academy of Sciences, Sofia, Bulgaria
[2]Institute of Physics, University of Liege, Belgium
[3]Microgravity Research Center, Universite Libre de Bruxelles, Belgium
E-mail: svetla@imbm.bas.bg

Keywords - Falling films - Thermocapillarity - Evaporation

Abstract - The heat and mass transfer processes employing falling liquid films are widely spread in chemical and food technology, power engineering, etc. Owing to the long-wave instability of a film flow, the film surface is covered by waves which can increase the transfer rates. However, for falling films on a heated surface, it is a common experience that dry spots are formed. A natural question arising is whether the tendency to the surface rupture can be suppressed. The experimental observations show that non-uniform heating produces a large steady-state deformation of the free surface without dry spots. The mechanism suppressing a liquid-flow breakdown has not been discussed.

In the present report, long two-dimensional waves on a thin film of a Newtonian fluid falling down an inclined plate are studied. A non-uniform heating is imposed along the plate in the downstream direction and the liquid film is volatile. The physical properties of the fluid are assumed constant except the surface tension which decreases linearly with the temperature. A linear kinetic relation between the mass flux from the free surface and the interface temperature is also used. The flow and the heat transfer in the film are governed by the Navier-Stokes and energy equations with appropriate boundary conditions including the normal and tangential force balance, the kinematic condition and the energy balance at the interface. In the long-wave approximation the free surface development is described by an evolution equation of Benny type. This nonlinear partial differential equation incorporates viscosity, gravity, surface tension, thermocapillarity and evaporation effects. Our aim is to distinguish different physical effects and examine their interactions.

The evolution equation is solved by a finite difference method. It is integrated numerically in conservative form in a periodic domain. The second-order-accurate Crank-Nicholson scheme is used in time and the spatial derivatives are approximated using central differences. The relevant nonlinear difference equations are solved by Newton-Ralphson's iteration. Numerical solution shows the nonlinear development of the film flow and describes the finite-amplitude behaviour that determines the propensity for dryout of the film. When thermocapillarity and vapour recoil are important, there occurs a significant local thinning of the layer, resulting in decrease in the rupture time. The rupture time is found to increase when the non-uniform heating is present.

Mixing & Dispersion

Stirring properties of point vortex interactions

V.V. Meleshko and G.J.F. van Heijst
Department of Vortex Motion, Institute of Hydromechanics
National Academy of Sciences, Ukraine
and
Fluid Dynamics Laboratory, Department of Technical Physics
Eindhoven University of Technology, The Netherlands
Email: v.v.meleshko@tue.nl

Keywords - Point vortices - Interaction with Sharp Edge - Stirring by Vortices

Abstract - The talk addresses the analysis of some typical two-dimensional flows of an incompressible inviscid fluid with several point vortices. The main issue consists in considering processes of stirring of the surrounding fluid (the 'atmosphere' of vortex pair, in particular) under vortex interactions. The contour kinematics method for tracing the interface line has been developed. Comparisons with our experimental results and with more complicated contour dynamics simulations of Chaplygin – Lamb dipoles interactions show a good correspondence. Although an extreme idealization, the model of point vortices appears to shed considerable light on what to expect in the laboratory experiments. The fascinating old experimental phenomena connected with the vortex ring, namely, its attraction by a solid body (Thomson, 1869) and impossibility of cutting it with a sharp knife, since "it would wriggle away from the knife" (Tait, 1876), are explained by means of studying two-dimensional interaction of a vortex pair and its atmosphere with a cylinder and a wedge. For the latter case, the importance of imposing the Kutta (1902) – Joukowski (1906) condition is elucidated. The discussion of stirring of surrounding fluid by point vortices for the von Kármán vortex street is based upon the general invariants of the Lagrangian topology. The coherent structures formed by stable and unstable manifolds are identified. Construction of Poincaré mapping allows to distinguish other coherent structures related to elliptic periodic points that remain unstirred under periodic regimes. The results obtained by the contour kinematics method are in agreement with von Kármán's (1911) opinion that "many peculiarities of real flow can be understood based on the notion of existence of separated vortices in the flow and the laws of motion of such vortices in an ideal fluid".

Dynamics of advected impurities in two-dimensional turbulence

L. Montabone[1], A. Provenzale[1] and A. Babiano[2]
[1]*Istituto di Cosmogeofisica del CNR - Torino, Italy*
and [2]*Laboratoire de Météorologie Dynamique, CNRS,*
Ecole Normale Supérieure - Paris, France

Email: shear@icg.to.infn.it

Keywords - Impurities - Coherent vortices - Two-dimensional turbulence

Abstract - We numerically study the dynamics of passively advected spherical impurities with small but finite size and density which may be different from that of the fluid in which they are embedded. The advective flow is provided by two-dimensional turbulence with fully-developed coherent vortices. The effects of the Stokes drag term, the added mass term and the Coriolis term in the equation of motion for impurities in a rotating fluid are taken into account both for light and heavy particles and for neutrally buoyant ones. We use different values for the non-dimensional parameters related to the length and velocity scales of the turbulent flow, the particle size (Stokes parameter) and the rotation of the system (Rossby number). Without rotational effects, light impurities concentrate in the cores of the vortices whereas heavy impurities are ejected from coherent structures and move in the background turbulence. Neutrally buoyant particles with finite size tend to concentrate in the vortex cores, depending on their initial relative velocity with respect to the fluid, possibly providing biassed estimates of the Lagrangian statistics. The introduction of the Coriolis term leads to an asymmetry between impurity dynamics in cyclones and anticyclones, allowing heavy particles to enter the anticyclonic vortices and light particles to be ejected from them.

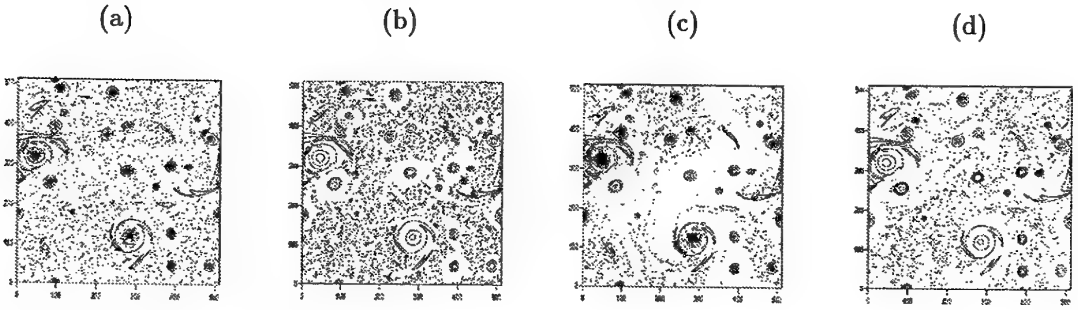

Typical distributions of impurities in the 2D flow; panel (a)-(b) represent light and heavy particles without Coriolis effects, panel (c)-(d) are for light and heavy particles in the presence of rotation.

Turbulent dispersion in flows not exhibiting inertial-subrange scaling

A.M. Reynolds and J. E. Cohen

Silsoe Research Institute,
Silsoe, Bedford, MK45 4HS, United Kingdom
Email: andy.reynolds@bbsrc.ac.uk

Keywords - Turbulent dispersion - Kolmogorov's constant - Stochastic models

Abstract - The effects of departures from inertial-subrange scaling on turbulent dispersion are investigated in numerical simulations using the stochastic model of Cohen and Reynolds (1999). This model is based on the fractional Langevin equation, the analogue of the Langevin equation where fractional Gaussian noise rather then Gaussian noise is the source of randomness. The model satisfies a natural generalization of the well-mixed condition and has a structure function proportional to dt^{2H}, where dt is the time increment and $0<H<1$. In accord with an exact analytical calculation for isotropic stationary turbulence, turbulent dispersion in grid turbulence, a surface-layer with neutral-stability and a laboratory-scale fully convective boundary-layer is shown to be strongly sensitive to small departures, $|\delta H|=0.1$, from inertia-subrange scaling (H=0.5). It is suggested that this sensitivity accounts for some of the variation in the estimates for the value of Kolmogorov's constant (C_0) reported in the literature, obtained by optimizing the agreement between experimental dispersion data and predictions obtained using standard Lagrangian stochastic models appropriate for H=0.5. It is found that the effects of departures on inertial-subrange scaling on turbulent dispersion can be accounted for within these standard Lagrangian stochastic models by an appropriate adjustment to the value of C_0. This adjustment is, of course, flow specific.

Cohen, J. E. and Reynolds, A.M. 1999: A modified Fokker-Planck equation corresponding to the fractional Langevin equation. *Physica D* (Submitted).

A nibbling and engulfing circular shear layer

Joseph Mathew and Amit J Basu
Department of Aerospace Engineering, Indian Institute of Science, Bangalore 560 012, INDIA
Email: joseph@aero.iisc.ernet.in

Keywords - Entrainment - Round jet DNS

Abstract - Nibbling describes the classical model of the entrainment of ambient fluid into a turbulent region. The process occurs on Kolmogorov scales within a 'laminar superlayer' at the turbulent flow boundaries. The more recent view suggested by visualization of plane mixing layers is that large eddies 'engulf' large packets of irrotational fluid which then break down well within the turbulent region. Here we present some results on entrainment processes revealed by a Direct Numerical Simulation of a circular shear layer—a model for round jet flow.

With a Fourier spectral method, the Navier-Stokes and passive scalar transport equations for incompressible flow were integrated. The initial, thin, cylindrical vortex sheet (a model for the flow in round jets near nozzles) rolls-up into vortex rings which pair, undergo azimuthal instabilities and break down to turbulence. The Reynolds number based on the initial jet diameter and velocity difference was 1600 and $128 \times 128 \times 128$ grid points were used. The trajectories of 1852 particles located within a quadrant of a plane across the jet were simultaneously computed and local levels of vorticity magnitude and scalar levels were stored.

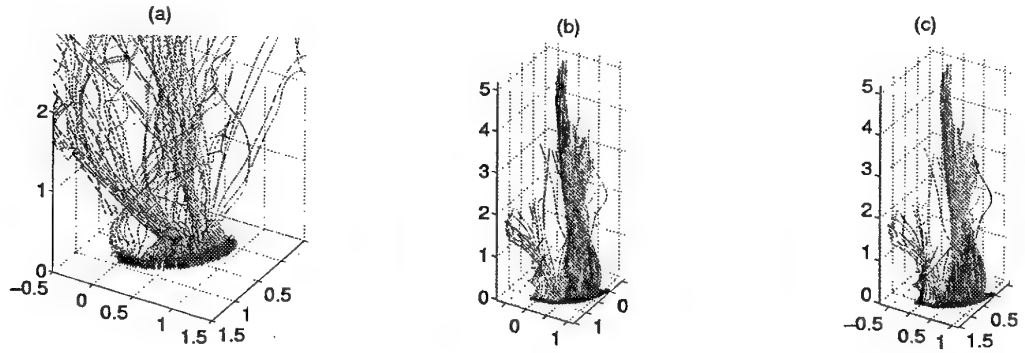

Pathlines colored by vorticity (a and b), and scalar (c).

Two ways of defining entrainment are: 1) the process of growth of vorticity in ambient irrotational fluid, and 2) the process of growth of scalar levels to those characteristic of the turbulent part of the flow. Figures (a) and (b) show pathlines which begin from approx. twice the radius of the initial vortex sheet. Segments are coloured by local vorticity magnitude Ω. Blue indicates essentially irrotational fluid ($\Omega < 0.5$), red is rotational ($\Omega < 1.0$), and green is for intermediate (transitional) levels. Pathlines begin in a circular band (blue, indicating that these were in the irrotational region outside), and then travel upward and into the jet. Most strikingly, the change from blue to red occurs very quickly and close to the shaer layer periphery. This is *nibbling*. Pathlines in Figure (b) begin from a slightly greater radius than those in (a). Note that a packet of fluid travels deep within the turbulent flow, being carried far downstream, without acquiring vorticity (remains blue). Figure (c) shows these same pathlines coloured by scalar levels. The same central packet has acquired turbulent region scalar levels (central portion colored red). This is engulfment when entrainment is defined on the basis of growth of vorticity. Statistics of time to entrainment and mean radial locations have been obtained. It would appear from this simulation that nibbling is by far the more frequent process of entrainment.

Fluid exchange between recirculation regions and the externally perturbed flow

R. Arina, C. Cancelli and M. Falossi
Department of Aerospace Engineering
Politecnico di Torino, Italy
Email: arina@polito.it

Keywords - Perturbed Flows - Backward-Facing Step - Cavity Flows - Incompressible Flows

Abstract - In this work we investigate the role of large-scale structures in separated flows. In particular, their contribution to transport of fluid in such flows is the aim of the present work. To this end, a simplified flow model is used, namely a two-dimensional laminar flow of an incompressible fluid over a backward-facing step and inside cavities, at moderate Reynolds numbers. The motivation for focusing on these laminar flows lies in the fact that, in these situations, fluid evolves in a more regular fashion than in complicated turbulent flows and the attendant computational problems are vastly reduced. However, the separating streamline acts as a transport barrier, and the recirculating fluid region is isolated. This inconsistency is avoided by adding a time-varying perturbation of small amplitude upstream of the step; unsteady motion then results, and the transport barrier presumably opens. This provides a controlled way of introducing relatively simple time dependent motion into the separated flow, much as is done in experiments. The flow is numerically simulated, solving the incompressible Navier-

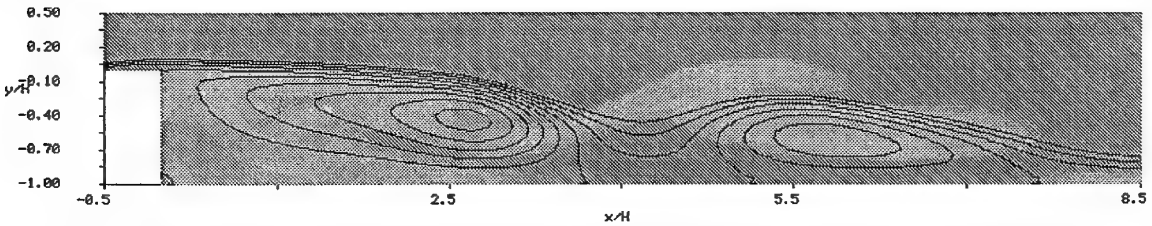

Figure 1: *Backward facing step: Passive scalar distribution and instantaneous streamlines*

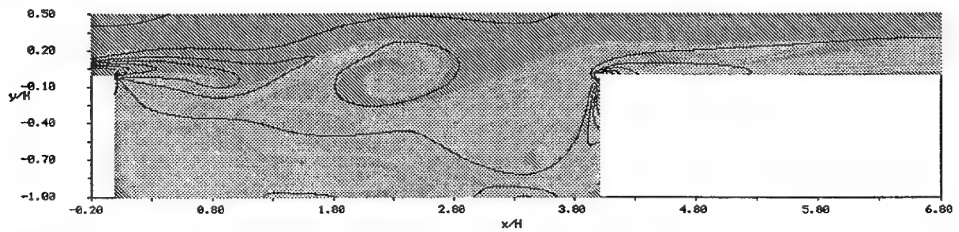

Figure 2: *Cavity flow (L/H=4): Passive scalar distribution and isovorticity lines*

Stokes equations. The forcing used here is a vortical perturbation of the upstream flow. The unsteady disturbances that are introduced into the flow by this forcing are advected downstream and interact with the separated flow in the region behind the step or in the cavity. Different flow regimes then develop for different forcing frequencies. The recirculation region undergoes various deformations, and, in particular, splits into different vortical structures when the forcing frequency lies within a suitable range. This effect arises from a sort of *blunt* resonance between the wavelength of the perturbation and the length of the recirculation region. In this case, large-scale vortices form in the flow and are shed downstream carrying a large portion of fluid. Several numerical experiments have been conducted in the case of the flow past a backward-facing step (Fig.1) and inside cavities (Fig.2). The mass exchange mechanisms is individuated, also with the aid of Lagrangian tracers, for different forcing frequencies and Reynolds numbers (125-400).

Can effective diffusion coefficients be extracted from symmetry measures?

G.P. King[1], M. Rudman[2], A. N. Yannacopoulos[3], G. Rowlands[4], and I. Mezić[5]
Email: greg.king@warwick.ac.uk

[1] Fluid Dynamics Research Centre, School of Engineering, University of Warwick, Coventry CV4 7AL, UK;
[2] CSIRO Building, Construction and Engineering, PO Box 56, Highett, Victoria 3190, Australia;
[3] School of Mathematics and Statistics, University of Birmingham, Birmingham B15 2TT, UK;
[4] Department of Physics, University of Warwick, Coventry CV4 7AL, UK;
[5] Departments of Mathematics and Mechanical and Environmental Engineering, University of California, Santa Barbara, CA 93106-5070, USA

Keywords - Transport - Mixing - Chaos - Taylor-Couette Flow

Abstract - As is well known, the presence of a continuous symmetry implies the existence of conserved quantities, and this in turn reduces the effective dimension (increases the integrability) of the flow field. This fact is the basis of an Eulerian diagnostic approach that we developed in Ref [1]. In this contribution we apply the Eulerian diagnostic methodology to investigate the transport of particles that behave as passive tracers in velocity fields obtained from numerical solutions of the incompressible Navier-Stokes equations for wavy Taylor vortex flow, a nonaxisymmetric flow occurring in the flow between concentric rotating cylinders [2]. The waviness of the flow field breaks the invariant surface separating adjacent Taylor vortices, thus creating a complicated pathway enabling particles to wander from vortex to vortex. This gives rise to inter-vortex mixing (axial dispersion) which can be quantified by an effective axial diffusion coefficient, D_{eff}.

The Reynolds number dependence of D_{eff} for a radius ratio of $\eta = 0.875$ was measured in numerical experiments by Rudman over the Reynolds number range $155 \leq \mathrm{Re} \leq 756$ [2]. We plot his results in Fig. 1 in terms of $D_z = D_{eff}/\nu\mathrm{Re}$ for a flow with six azimuthal waves. Also shown in the figure is a plot of the product of the volume averaged symmetry measures

$$\phi_\theta \phi_\nu = \left[\frac{1}{V}\int \left|\frac{\partial \mathbf{u}(\mathbf{x})}{\partial \theta}\right| dV\right]\left[\frac{1}{V}\int \left|\nabla^2 \mathbf{u}(\mathbf{x})/\mathrm{Re}\right| dV\right],$$

where ϕ_θ measures the extent to which $\mathbf{u}$ departs from rotational symmetry, and ϕ_ν measures the departure from Euler flow (dynamical symmetry). Both quantities have been normalized with their values at $\mathrm{Re} = 324$. The remarkable agreement between the two curves shows that the effective diffusion coefficient is proportional to symmetry measures averaged over the velocity field. Thus we provide evidence for a connection between Eulerian and Lagrangian pictures of transport - a problem of fundamental and wide-spread interest.

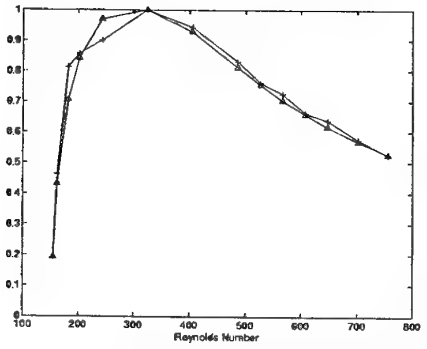

Figure 1: D_z (+) and $\phi_\theta \phi_\nu$ (Δ).

References -

[1] A.N. Yannacopoulos, I. Mezić, G. Rowlands, and G.P. King, *Phys. Rev. E* **57** (1998) 482–490.

[2] M. Rudman. *AIChE J.* **44** (1998) 1015–1026.

MIXING AND SCALING PROPERTIES OF VARIABLE DENSITY JETS IN STRONGLY PULSED COFLOW

Bury,Y. ; Saudreau, M. ; Borée, J. ; Charnay, G.
I.M.F.T. ; UMR CNRS/INPT-UPS 5502 Av. Camille Soula ; 31400 TOULOUSE - France

Key Words : Mixing , Variable density , turbulence

Complex internal turbulent flows, strong density variations and high unsteadyness are key words for the physics associated with mixture preparation in internal combustion engines (Borée 2000). The academic situation studied here (Bury 2000) corresponds to a variable density turbulent jet exhausting at a constant ejection velocity in a strongly pulsed coflow (fig. 1). The coflow velocity $U_\infty(t)$ is quasi-uniform and varies from $5m/s$ to $30m/s$ with time at a frequency of $75Hz$. $\dot{U}_\infty(t)$ rises up to $+400g$ and $-700g$. This experiment is designed for the test of RANS or LES models (Saudreau et al. 2000). In particular, boundary conditions are precisely controlled and measured. The phase averaged statistics of velocity field are measured by two-components LDV and mean phase averaged concentration field by Mie-Scattering measurements.

Three main results are intended to be presented :

(i) Comparison of relevant time scales permit to propose a longitudinal partition of the jet which separates quasi-steady from unsteady and acceleration dominated regions. Memory effects and phase-lag can be understood by using simple hyperbolic model equations that mimic the response of the jet structure. In particular, a convergence zone of starting jet type develops during the acceleration phase and have a strong effect on the turbulence field.

(ii) For light - $(\rho_{mix}/\rho_{air}=0.55)$ - or heavy - $(\rho_{co_2}/\rho_{air}=1.6)$ - jets, buoyancy effects due to the acceleration field imply a new dynamical behaviour. The role of the baroclinic torque will be analysed (Hunt 1987; Lundgren et al. 1992). Relevant non dimensional numbers are introduced in this unsteady situation. Typical contributions to the evolution of mean excess velocity and second order moments will be presented and analysed.

(iii) Finally, the influence of coflow pulsation on mixing will be discussed. The global rate of entrainment of external air in the jet structure during one period is derived from velocity and concentration measurements and will be compared with quasi-steady evolutions. First results show that mixing is severely reduced in the present situation. A physical analysis is proposed.

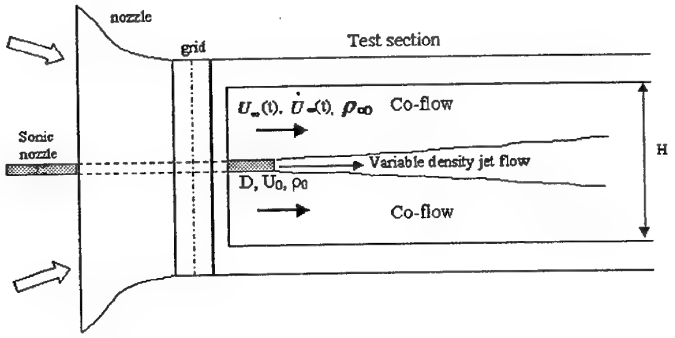

figure 1. Sketch of the test section

Borée, J. (2000). Invited Lecture at International Conference VDTF, Banyuls, France - June 22-23.
Bury, Y. (2000). Thèse de l'I.N.P. Toulouse.
Hunt, J. C. R. (1987). Trans. of the CSME **Vol. 11, n°1**: 21-35.
Lundgren, T. S., J. Yao and N. N. Mansour (1992). J. Fluid Mech. **239**: 461-488.
Saudreau, M., Y. Bury, J. Borée, O. Simonin and G. Charnay (2000) VDTF, France - June 22-23.

Mixing in frozen and time-periodic two-dimensional vortical flows

A.H.P. Wonhas and J.C. Vassilicos
Department of Applied Mathematics and Theoretical Physics, University of Cambridge, United Kingdom
Email: a.wonhas@damtp.cam.ac.uk

Keywords: Vortices - Advection–Diffusion Equation - Streamlines - Geometrical Measures

Abstract

In the present study we investigate how passive scalar or tracer is advected and diffused in frozen closed 2-dimensional streamline geometries, by decomposing the underlying flow into nested streamline geometries. We develop an asymptotic description of the scalar field in a time range $1 \ll \frac{t}{T} < Pe^{1/3}$, where T is the formation time of the spiral in a nested streamline geometry and Pe is a Péclet number, assumed much larger than 1. Using this description we derive the leading order in the decay of the scalar variance $\bar{E}(t)$ for a singular non circular streamline geometry,

$$\bar{E}(0) - \bar{E}(t) \propto \left(\frac{t^3}{T^3\, Pe}\right)^{\frac{2+\mu}{2}\frac{\beta}{1+\beta}} .$$

The variance decay is solely determined by a geometrical parameter μ and the exponent β describing the behaviour of the closed streamlines' periods. We develop methods to predict the variance decay from snapshots of the advected scalar field. In the case of slightly non circular streamlines, we can relate the decay exponent to the Kolmogorov capacity D_K, i.e. box counting dimension, of the advected scalar, and recover the result of Flohr and Vassilicos[1]. For arbitrary non circular streamline geometries we develop a method to reconstruct the streamlines and their period from just two snapshots of the advected scalar field, which then enables us in principle to predict the decay exponent.

Furthermore, we investigate variance decay in a periodically moving singular vortex. We identify three different regions (core, chaotic and KAM-tori). We find fast mixing in the chaotic region and make a conjecture about mixing in the KAM-tori region. The conjecture enables us to use the results for the frozen case and therefore relates the Kolmogorov capacity of the advected scalar to the decay of the scalar's variance. We check our theoretical predictions against a numerical simulation of advection-diffusion of scalar in such a flow

[1] P. Flohr and J.C. Vassilicos, *Accelerated scalar dissipation in a vortex*, J. Fluid Mech. **348**, 295 (1997)

Mixture morphology evolution in chaotic laminar mixing flows

P.D. Anderson, O.S. Galaktionov, P.G.M. Kruijt, G.W.M. Peters and H.E.H. Meijer
Section Materials Technology, Department of Mechanical Engineering
Eindhoven University of Technology, The Netherlands, Email: patricka@wfw.wtb.tue.nl

C.L. Tucker III
Department of Mechanical and Industrial Engineering, University of Illinois at Urbana-Champaign, USA

Keywords Chaotic mixing - Area tensor - Microstructural mixing - Mapping Method

Abstract - A global, multi-scale model of fluid mixing in laminar flows is presented, which describes the evolution of the spatial distribution of the microstructure in the mixture, for two fluids of identical viscosity with no interfacial tension. Composition fluctuations smaller than the cell size are represented by cell values of the area tensor (Wetzel and Tucker, 1999), which quantifies the size, shape, and orientation of the microstructure within each cell. The method is validated by comparison to an explicit interface tracking calculation. We show examples for two-dimensional, time-periodic flows in a lid-driven rectangular cavity and the journal-bearing flow. The spatial distribution of interfacial area is found to be highly non-uniform, with cell-to-cell differences of three orders of magnitude or more. If the flow is globally chaotic then the microstructural pattern becomes self similar, and interfacial area increases exponentially with time.

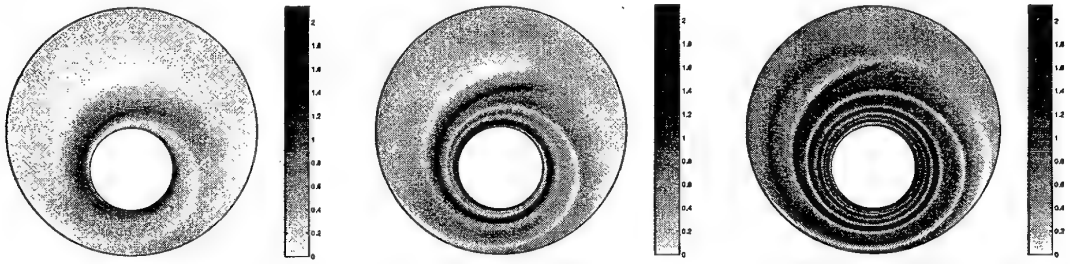

(a) **(b)** **(c)**

Figure 1: Stretching of initially isotropically oriented interfaces during one period of flow: **a)** $\theta = \pi/2$, **b)** $\theta = \pi$, **c)** $\theta = 2\pi$. Gray scale represent the decimal logarithm $log_{10}\lambda$ of the stretching values.

Figure 1 shows the stretching distribution after one period of flow in the journal bearing mixer with rotation angle θ equal to $\pi/2$, π and 2π respectively. Even after a single period of flow, the stretching distribution is highly non-uniform with zones of high stretching closely interleaved with zones of weak stretching. In all three plots the same logarithmic scale and dark areas correspond to higher stretching. The results show the stretching during a single period starting from an isotropic initial distribution.

The strength of the current extended mapping method is that it models mixing directly. One can specify the initial configuration of the two fluids, subject them to a prescribed amount of mixing, and predict the concentration and microstructure distributions at every point in the resulting mixture. Thus, there is no need to resort to any correlation between properties of the flow and properties of the mixture. The present calculations are two-dimensional, but the method can readily be applied in three-dimensional problems.

References

Wetzel, E. D. and Tucker, C. L. (1999). Area tensors for modeling microstructure during laminar liquid-liquid mixing. *Int. J. Multiphase Flow*, **25**, 35–61.

Three-Dimensional Chaotic Advection in a Cylindrical Cavity

M.F.M. Speetjens, H.J.H Clercx and G.J.F. van Heijst
Dept. Fluid Dynamics, Faculty of Applied Physics
Eindhoven University of Technology, The Netherlands
Email: m.f.m.speetjens@tue.nl

Keywords - $3D$ Chaotic Advection - Flow Topology - Nonlinearity

Abstract - The work to be presented concerns theoretical, numerical and experimental investigations on chaotic advection of passive particles in a three-dimensional ($3D$) cylindrical domain, serving as an archetypal case study of the fundamentals underlying mixing and particle dispersion in nature and industry. The research is motivated by the poor understanding of this phenomenon, despite the omnipresence of $3D$ mixing in the world around us.
Confining the scope of interest to the laminar flow regime allows for a dynamical systems approach to the outlined research objective by studying the behaviour of passive particles following release in an *a priori* known deterministic velocity field. Subsequent flow analysis takes place through the isolation of coherent structures in the web of trajectories weaved by the released tracers. In a periodically agitated flow, the sought after objects encompasses two prinicipal categories, namely i) level surfaces and lines associated with constants of motion and ii) periodic structures, that collectively compose the flow topology. The relevance in this *modus operandi* exists in that the coherent structures impose geometrical constraints on the particle paths and in that capacity dominate the dispersion of tracers in the domain of interest.
The presentation centers around the physical aspects of chaotic advection, as highlighted above, and involves a comparative analysis on the flow topology found by several tools of investigation. The ground level is formed by the families of coherent structures that emerge in the flow field defined by an exact solution to the linear Stokes equations and subject to either stationary or periodic forcing conditions. The isolated entities seal off subregions in the flow domain and consequentially act as transport barriers to global diffusion. Upon introduction of inertial effects, enabled through numerical resolution of the Navier-Stokes equations by means of the spectral method, these obstructions prove to gradually disintegrate under increasing degree of nonlinearity, parametrized by the Reynolds number Re, in consequence paving the way to unlimited dispersion of released particles. Flow visualization in an experimental apparatus via tracking of advected dye and $3D$ PTV provides a complementary point of view on the aforementioned phenomena.

Biological Fluid Mechanics

Haemodynamic aspects of the umbilical circulation

C. Guiot and S. L. Waters
Neuroscience Dept., University of Turin, Italy
Email: guiot@medfarm.unito.it
Department of Applied Mathematics and Theoretical Physics, University of Cambridge, UK
Email: slw1001@damtp.cam.ac.uk

Keywords - Haemodynamics - Peristalsis

Abstract - Deoxygenated blood travels from the fetus to the placenta via the two umbilical arteries and, after the blood has been oxygenated within the placenta, the blood returns to the fetus along the umbilical vein. The umbilical arteries are coiled or twisted in spirals about the umbilical vein. The umbilical vessels are enclosed within the umbilical cord and there is a high degree of contact between the arteries and the vein. Blood flow in the elastic arteries is highly pulsatile and the arteries distend with each pressure pulse, thus imposing an external pressure on the umbilical vein which they surround. In 1951 Reynolds [1] hypothesised that this *massaging* of the vein by the arteries may enhance venous blood flow.

We develop a mathematical model in order to investigate this hypothesis. The blood is modelled as a homogeneous, incompressible, Newtonian fluid and the vein as an isotropic, thin-walled, elastic tube. The arterial pressure pulse is reflected at the placental wall and hence we assume the external pressure on the tube to be the superposition of a forward and a reflected travelling wave. The coupling of the fluid and wall motions is a complex problem. However, by assuming that the tube wall is elastic and that the longitudinal wall motion is negligible, the equations describing the wall motion can be simplified and we can solve the nonlinear problem for the fluid flow. Our results are also applicable to the related problem of peristaltic pumping, where fluid is transported by the progression of contraction waves along a distensible tube [2], [3].

The results indicate that the effect of the *massaging* is to generate a mean venous flow, the details of which depend on the elastic wall properties, the vessel geometry and the external pressure. The physiological implications of this work are discussed.

References

[1] Reynolds, S. R. M. 1978 Mechanisms of placentofetal blood flow. *Obstet. Gynecol.* **52**(2), 245–249.

[2] Shapiro, A. H., Jaffrin, M. Y. & Weinberg, S. L. 1969 Peristaltic pumping with long wavelengths at low Reynolds number. *J. Fluid Mech.* **37**, 799–825.

[3] Yih, F. & Fung, Y. C. 1969 Peristaltic waves in circular cylindrical tubes. *J. Appl. Mech.* **36**, 579–587.

Pulsatile flow in quasi-rigid vessels

Gianni Pedrizzetti
Dept. Civil Engineering, University of Trieste, Italy
Email: gianni@dic.univ.trieste.it

Keywords: Artery flow - Elastic walls - Wall shear stress - Boundary layer separation.

Abstract: The calculation of the simultaneous fluid-structure evolution for a fluid flowing inside an elastic vessel reserves many difficulties (see Davies & Carpenter 1997; Luo & Pedley 1998; Pedrizzetti 1998 as recent examples); the development of a method able to evaluate the influence of wall elasticity in large artery flow motivated this work. *In vivo* measurements reveal that the wall motion in large arteries is of relatively small entity (generally it is below ten percent of the *lumen* size) also in response to significant pressure variations. It is therefore natural to seek a solution of the fluid-wall system with a perturbative approach where the zeroth order solution is given by the flow in a rigid vessel, the first order correction gives the wall deformation and the induced flow modification without the need to solve the difficult coupled problem. Such an approach essentially assumes a locally infinite celerity, therefore it represents a good approximation for the fluid-wall interaction in sites of limited extent (branches, stenosis, aneurism etc.), which include typical situations associated with vascular diseases.

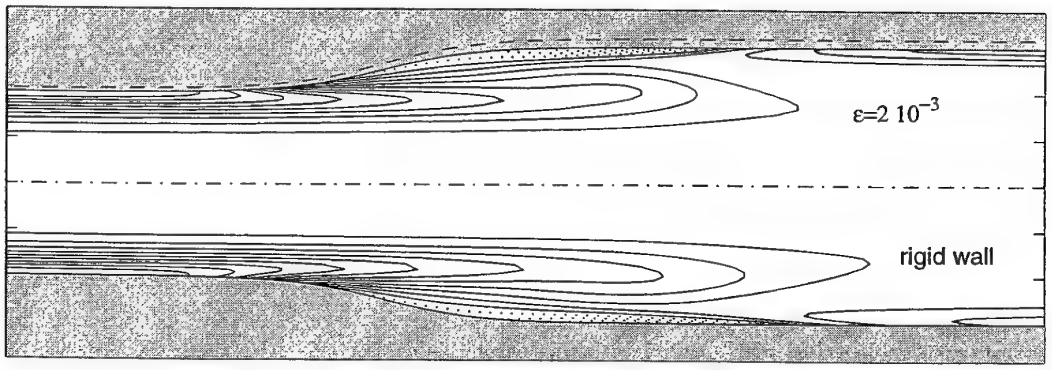

Instantaneous vorticity contours at systole in the case of rigid (lower half) and elastic (upper half) wall for synchronous pressure pulse.

The approach is here applied to the case of pulsatile flow inside a circular tube with a smooth expansion. All variables are expanded in series of $\varepsilon = \rho U^2 R/Eh$, where E is the Young modulus and h is the vessel thickness (ρ is the fluid density, U is the velocity scale, R is the tube radius). The problem is studied numerically in the axisymmetric approximation following the lines previously developed for rigid ducts (Pedrizzetti 1996): the Navier-Stokes equations, in the vorticity-streamfunction formulation, and the wall equations are solved for the zeroth and first order terms. The influence of wall elasticity on the flow and on the unsteady wall shear stress is studied in correspondence of parameters taken from the carotid artery, attention is also posed to the role of phase difference between the incoming pressure and flow pulses, an example flow is reported in the figure.

Pedrizzetti G. 1996, Unsteady tube flow over an expansion, *J. Fluid Mech.* **310**, 89-111.

Davies C. & Carpenter P.W. 1997, Instabilities in a plane channel flow between compliant walls, *J. Fluid Mech.* **352**, 205-243.

Luo X.Y. & Pedley T.J. 1998, The effects of wall inertia on flow in a two-dimensional collapsible channel, *J. Fluid Mech.* **363**, 253-280.

Pedrizzetti G. 1998, Fluid flow in a tube with an elastic membrane insertion, *J. Fluid Mech.* **375**, 39-64.

Pulsatile flow in compliant tubes with stenoses

K.W. Lee and X.Y. Xu
Department of Chemical Engineering and Chemical Technology
Imperial College, London, UK
Email: k.lee1@ic.ac.uk

Keywords – stenosis, coupled fluid–wall interaction, computational analysis

Abstract – Atherosclerosis is a disease of arteries in which fatty streaks develop on their inner walls at young age, with eventual obstruction of blood flow. For severe cases, it limits the oxygen supply to the brain and heart. Furthermore, disruption of these atherosclerotic plaques can lead to thrombosis, where blood clots at sites of tissue fissure. It is well known that geometry of the flow domain, pulsatiliy of the cardiovascular system, non–Newtonian properties of blood and the wall compliance of vessels are the main factors affecting the blood flow behaviour, while for the case of wall movement, vessel structure, material composition and properties are major determinants. The objective of this study is to quantitatively analyse the regional flow patterns and wall behaviour of a vessel with mild stenosis.

The models for such purpose were built using the combination of a CFD and structural analysis code. The geometry of a 45% axisymmetrically stenosed (by area) cylindrical vessel was adopted for both the decoupled flow and structural models. The fluid used was assumed to be Newtonian, and the pulsatility was simulated by a sinusoidal inflow waveform. The flow model was constructed based on, and later validated with, the experiment performed by Ojha et al [1]. The wall was assumed to be a multi–layered thick–walled composite material having a Young's modulus of 500 kPa for the normal vessel wall and 1000 kPa for the plaque. Typical results for the circumferential stress distribution are shown in Fig.1.

Fig.1. Circumferential stress distribution of the wall in model 1 (left) in which the elastic properties of the wall and plaque are the same, but different in model 2 (right). Red colour corresponds to high tensile stress and blue indicates high compressile stress.

The effect of wall compliance on wall shear stress will be investigated by comparison between the compliant and rigid models. Similar study were performed by Tang et al [2,3], who calculated the wall stress and strain distributions in a stenosed vessel under a steady flow condition. The present study differs from their work in that: (a) the flow is unsteady so that the wall is subject to a time–dependent loading due to the pulsation of flow; and (b) the effects of different elastic properties of the wall and plaque on stress concentration and wall shear stress are investigated.

References

1. Matadial Ojha, Richard S.C. Cobbold, K. Wayne Johnston and Richard L. Hummel, Pulsatile flow through constricted tubes: an experimental investigation using photochromic tracer methods. J. Fluid Mech., 1989; vol 203: 173–197
2. Dalin Tang, Chun Yang, Yan Huang and David N. Ku, Wall stress and strain analysis using a three–dimensional thick–wall model with fluid–structure interactions for blood flow in carotid arteries with stenoses. Computers and Structures, 72 (1999): 341–356
3. Dalin Tang, Chun Yang, Yan Huang and David N. Ku, A 3–D thin–wall model with fluid–structure interactions for blood flow in carotid arteries with symmetric and asymmetric stenoses. Computers and Structures, 72 (1999): 357–377

Fluid-structure interaction in elastic vessels

G.E. Loots, H.W. Hoogstraten and A.E.P. Veldman
University of Groningen, Department of Mathematics
P.O. Box 800, 9700 AV Groningen, The Netherlands
Email: g.e.loots@math.rug.nl

Keywords - Cartesian grid - Fluid Structure Interaction - Wall Shear Stress

Abstract - Many CFD codes have in common that they use body-fitted coordinates. Although this has advantages in the field of boundary treatment, the construction of new grids for each separate problem is often more costly than the simulation itself. Our approach is to use finite-volume discretization of the Navier-Stokes equations on a simple, rectilinear (Cartesian) grid, thus enabling applications with arbitrary complex (3D) geometries. The drawback of this are the measures that have to be made at the non-gridaligned boundaries; here we make use of the so-called cut-cell approach.

While the code was originally intended for free-surface computations (using Eulerian VOF-functions and local level set methods), modelling of elastic walls has recently been implemented. The wall is considered as an elastic membrane, modelled by 3D spring marker particles which form a large mass-spring system. Although 3D markers are awkward in describing arbitrarily moving free surfaces, they suffice for the kind of applications that range from slightly perturbed walls up to partly collapsed tubes.

Fluid-structure interaction (FSI) is simulated by a weak coupling of the membrane equations (which use pressure differences as boundary conditions) and the flow equations (which need the deformation and velocity of the wall), respectively. This involves the use of efficient means of geometry reconstruction, for each time step, from the surface markers towards grid cells.

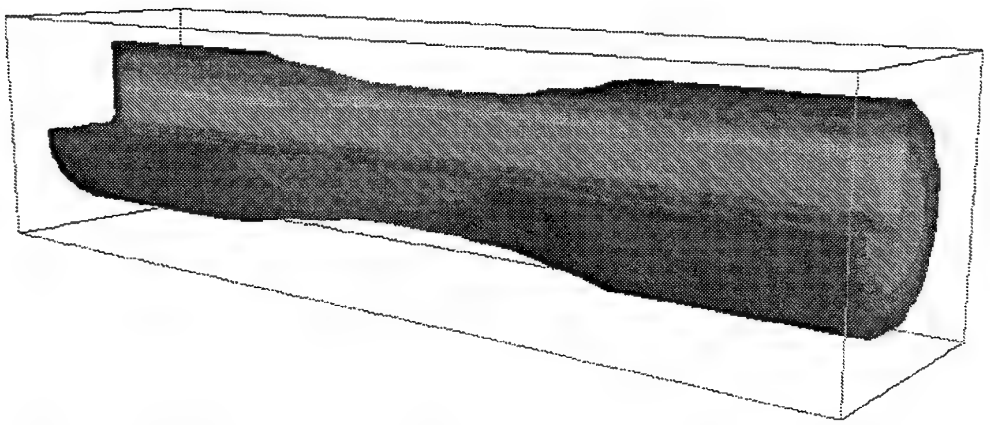

Moderately deformed tube due to negative pressure difference; coloured by velocity

A hemodynamical application of the described model is the change of the wall shear stress (WSS) in pulsating tubes like blood veins. Comparisons of the computed WSS of rigid tubes, steadily deformed tubes and pulsating (unsteadily deformed) tubes are being made. The simulations provide useful information of the changes in WSS in tubes of different configurations, giving insight in the occurence of several medical phenomena like atherosclerosis.

Computation of flow in collapsible tubes

H. Bijl and S. Kalse
Section Aerodynamics, Department of Aerospace Engineering
Delft University of Technology, The Netherlands
Email: h.bijl@lr.tudelft.nl

Keywords - Flow in collapsible tubes - Boundary layer model - Computational Fluid Dynamics

Abstract - With the present one-dimensional boundary layer model for the computation of flow in collapsible tubes separated flow can be computed. Since separation is of major importance for the birth and character of oscillations in collapsible tubes, this is an important advantage over existing one-dimensional models which only model separation in a crude way. A particular application of flow in collapsible tubes is biol ogical fluid dynamics, i.e. air flow through lungs and blood flow through veins . In these flows Reynolds numbers will be typically medium to low, which raises the question what the lowest Reynolds number is for which our boundary layer model can be applied. This is currently being investigated.

Background and existing one-dimensional models- It has long been observed that in flow in collapsible tubes even under steady external conditions, the strong non-linear coupling between fluid mechanic and elastic forces can give rise to strong oscillations of the flow and the tube wall. These phenomena are of particular interest for physiological applications. Two examples are the limit cycle oscillations due to coupling between the venae cavae and blood flow during heart surgery, and the Korotkoff sounds listened for during blood pressure measurement.
Eventhough flow separation is essential for the onset of oscillations, existing one-dimensional models of collapsible tubes do not accurately model this phenomenon. In literature two classes of models can be found. The first approximates the energy loss after the separation point by a constant times the convection term in the momentum equation. The second constructs a better approximation of the separation region using Karman-Pohlhausen similarity solutions and empirical formulas. However, the gap with experimental values is still such that we think there is room for improvement. Therefore, we present a new one-dimensional model for flow through collapsible tubes which can compute through separation regions.

Present one-dimensional model-Our one-dimensional model is based on a boundary layer approximation with strong viscous-inviscid interaction a.o. developed by Veldman. Through use of this interaction method the Goldstein singularity in the classical boundary layer equations for separated flow is removed, so that we can compute through separation regions. The crucial feature is that the displacement thickness and outer velocity are not prescribed, but follow from interaction between the inner viscous region and the outer inviscid region.
Results will be shown for two types of problems. Flow through rigid tubes, and flow through collapsible tubes. The rigid tube test case is used to validate our boundary layer method with experimental and computational results reported in the literature. With this test case we will show the crudeness of the energy loss model discussed in the previous paragrapgh. Furthermore, it will become clear for which Reynolds number range our boundary layer method can be applied. With the collapsible tube test case we will show the arise of oscillations of the tube walls.

Unsteady bubble propagation in convergent and flexible channels: modelling the reopening of collapsed lung airways

O.E. Jensen[1], M.K. Horsburgh[2] and D. Halpern[3]
[1,2]DAMTP, University of Cambridge, Silver Street Cambridge CB3 9EW, UK
[3]Dept. Mathematics, University of Alabama, Tuscaloosa, AL 35487, USA
[1]Email: o.e.jensen@damtp.cam.ac.uk

Keywords - airway mechanics - surface tension - viscous flow

Abstract - At the end of each breath, it is usual for some of the small airways at the base of the lung to experience airway closure. Mechanisms leading to airway closure include capillary instabilities of the airway liquid lining, leading to the formation of occlusive liquid plugs, and subsequent buckling and collapse of the airway wall resulting from low capillary pressures in these plugs. To reopen a flooded and collapsed airway, a bubble of air must be driven along the airway, peeling apart the airway walls and restoring gas exchange. While not normally serious, airway closure is a major problem for severely premature infants suffering the effects of elevated surface tension due to surfactant deficiency. Understanding the mechanics of the reopening process is therefore important in the development of ventilation strategies for these infants.

As a simple physical model of airway reopening, we consider a planar fluid-filled channel, the walls of which are membranes held under longitudinal tension and supported by external springs. A semi-infinite bubble of air is blown into the channel at a pressure p_b sufficiently large to peel apart the airway walls and subsequently to hold the channel open. The motion is two-dimensional, and the flow is viscous. Experiments [1] and numerical simulations [2] have shown how p_b must exceed a critical value for steady reopening to occur, and that thereafter the speed of steady, stable bubble motion, measured by a capillary number Ca, rises with increasing p_b. An important experimental observation [1], having direct clinical implications, is that during the initiation of reopening, as a bubble starts to move, p_b can transiently rise to a level significantly in excess of its final steady value.

This simple model can be well characterised using an asymptotic analysis based on the assumption that the membrane tension is large, so that that the channel walls have uniformly small slopes. The flow then divides naturally into three regions: (I) a long inflated region behind the advancing bubble tip; (II) a long fluid-filled region ahead of the bubble tip, well described with lubrication theory; and (III) a short region near the bubble tip where the local Stokes flow is inherently two-dimensional. At leading order the flow in region III is equivalent to the well-studied problem of a semi-infinite bubble advancing along a planar parallel-sided channel. At large Ca, however, the slope of the channel walls in region III becomes significant. Using a boundary element method, we therefore computed the creeping motion of a semi-infinite bubble advancing into a uniformly tapered convergent channel, determining the thickness of the film deposited on the channel walls behind the bubble tip. Computations show that while this film thickness rises with channel angle at low Ca, it can fall with angle as Ca increases. This unexpected effect contributes to elevated reopening pressures at large Ca, and partly accounts for discrepancies between asymptotic predictions and experimental results for fast-moving bubbles.

The asymptotic model also provides a convenient framework with which to investigate transient motions; simulations exhibiting transient peaks in reopening pressures will be presented.

[1] M.L. Perun & D.P. Gaver III (1995) *J. Appl. Physiol.* **79**, 1717; *J. Biomech. Eng.* **117**, 245
[2] D.P. Gaver III, D. Halpern, O.E. Jensen & J.B. Grotberg (1996) *J. Fluid Mech.* **319**, 25

Acknowledgements - *This work was supported by EPSRC Grant GR/M84572.*

Experimental study of the airflow through in-vitro models of the vocal folds

C. Vilain *, A.Hirschberg**, X. Pelorson*, J.F.H. Willems**
*Institut de la Communication Parlee, Institut National Polytechnique de Grenoble, France
**Fluid Dynamics Laboratory, Eindhoven University of Technology, The Netherlands
Email: cvilain@icp.inpg.fr

Keywords - Sound production by humans - Speech - Unsteady flows.

Abstract - In this study, we present experimental results concerning the air flow through the glottis during the production of voiced sounds. The measurements are carried out on in-vitro upscaled replicas of the vocal folds. They aim at validating theoretical models for speech analysis and synthesis. Different mechanical models and flow configurations of increasing complexity are successively presented.

First, we present steady flow measurements through rigid vocal-folds replicas. It is shown that a spurious phenomenon: the Coanda effect (asymetry of the flow in a symmetric channel), can occur and thus strongly affect the relevance of this kind of measurements.

More realistic, unsteady flow measurements through rigid vocal fold replicas are presented. Unsteady flow conditions are obtained in three ways: impulsively started flow (by valve opening), pulsated flow (using a collapsible tube device) or oscillating flow (using a siren).

These conditions correspond to Strouhal numbers ranging from 10^{-2} (typical values for speech) up to 1.

The experimental results are then compared to different theoretical predictions (based on increasingly complex methods: Bernoulli equation, quasi-steady Boundary Layer methods...).

Lastly, a further more realistic setup is presented. It allows unsteady flow measurements through self-oscillating vocal-fold replicas. Each replica consists of a thin-walled latex tube filled with pressurised water. The main control parameters for the oscillation are the wall tension of the tube, the water pressure, the pressure drop across the replicas and the distance between the two replicas.

Applications of this work in the field of voiced sounds synthesis and pathological voice analysis will be presented and illustrated.

Numerical simulation of the flow through a human nose model

I. Hörschler, M. Meinke and W. Schröder
Aerodynamisches Institut Aachen, RWTH Aachen, Germany
Email: ingolf@aia.rwth-aachen.de

Keywords - human nose model - nasal cavity flow field

Abstract - The flow field through a model of the human nasal cavity is numerically simulated by solving the Navier-Stokes equations and the results are compared to experimental studies.

The human nose covers - besides respiration - a variety of functions such as moistening, smell and taste. All these functions are strongly influenced by the internal flow conditions. Therefore a detailed investigation of the flow field is essential to enable successful surgery in cases of impaired respiration due to accidents or unnaturally shaped nasal cavities. The numerically simulated flow field is supposed to indicate where the surgeon has to correct the nasal cavity to improve e.g. the respiration of the patient.
To generate the computational grid, the model of the human nasal cavity (Fig. 1 left) used for experiments is scanned by a computer tomograph. The density distribution from this scan is the data base for the unstructured surface defining the geometry of the flow problem. This surface is used to generate a structured multiblock grid (Fig. 1 right). The grid consists of 30 blocks and between 300.000 and 2.000.000 nodes (coarse and fine grid).

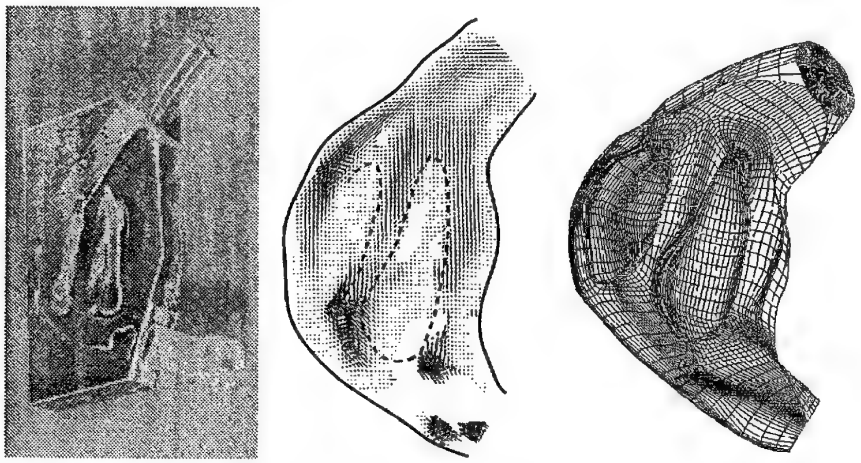

Figure 1: Nasal cavity model (left), DPIV of inspiration (middle), Multiblock grid (right)

For three dimensional compressible flows the Navier-Stokes equations are solved using an AUSM scheme for the inviscid terms and central differences for the viscous expressions such that a spatially second-order accurate discretization results. To compute the highly unsteady flow due to the human respiration cycle a Runge-Kutta method second-order accurate in time is used to do the time stepping. Experimental data for comparison covers respiration at rest with a frequency of f=15min^{-1} and Re=1240 for inspiration and Re=970 for expiration and forced respiration with a frequency of f=25min^{-1} and Re=2090 for inspiration and Re=1635 for expiration. That is, the flow can be considered laminar. The digital particle image velocimetry (DPIV) was employed to measure the flow in 18 different layers parallel to the septum (e.g. Fig. 1 middle). Experiments were conducted to validate the numerical solution. Besides comparison of CFD data with experiments, a detailed analysis of the flow field will be presented and we want to analyze the susceptibility of the overall flow field on small modifications of the turbinates.

Flow in a tube with helical internal channelling

C.G. Caro[1], N. Watkins[1], D.J. Doorly[2], S.J. Sherwin[2], J. Peiró[2], P.T. Franke[2],
[1]*Biological and Medical Systems and* [2]*Aeronautics, Imperial College, London SW7.* c.caro@ic.ac.uk
Key words: helically channelled tube, swirling flow, atherosclerosis

Among observations that encourage study of the flow in a tube with helical internal channelling are: the influence of the local flow field (including wall shear stress and fluid/particle residence times) on vascular biology and pathology (eg Davies, 1995; Dull et al, 1992; Tardy et al, 1997); the non-planar curvature and branching of arteries and associated swirling flow (Caro et al, 1996); and the helical distribution of atherosclerotic lesions in arteries (Fox et al, 1982).

We have visualised the flow associated with a coiled spring (wire diameter 0.85 mm, length 5 cm, pitch in different studies 3 or 6 mm) fitted closely into the downstream end of a 40 cm straight length of 8 mm id PVC tubing. Experiments were performed at steady rates of flow of water of 0.5, 1.0 and 6 ml/sec, representing tube Reynolds numbers (Re_{tube}) of 80, 160 and 960, respectively. A needle (od 0.5 mm) was passed through the tube wall and indicator was injected at the lowest velocity compatible with visualisation of the flow. The injection was made first into the core and then into the channel formed by adjoining turns of the spring,

Core flow was laminar in all studies and non-swirling. Channel flow was laminar in all studies. At lower values of Re_{tube} the indicator followed the helical channel. At higher values of Re_{tube} channel flow was swirling. With the ratio of channel depth to tube diameter fixed, Re_{tube} and channel pitch determined whether channel flow swirled and the swirl pitch. The swirl results from separation of the flow about the channel sides (where the sides correspond to adjoining turns of the spring) combined with a pressure gradient directed along the channel. Swirling can be expected to enhance mixing and increase the uniformity of channel wall shear stress (Doorly et al, 1997).

In some studies, the channelling was made annular (wire rings 3 mm apart arranged normal to the tube axis). Wire diameter and tube id were as before 0.85 mm and 8 mm respectively and studies were performed over the same range of Re_{tube} as in the helical channel work. At higher values of Re_{tube} the indicator revealed closed recirculation zones within the channels. At the same Re_{tube} indicator injected as a bolus upstream into the bulk flow cleared considerably faster from the helical than the annular channelling, particularly at higher values of Re_{tube}. A preliminary computational study has been made of steady flow in a straight tube with helical channelling (Re_{tube} 250) with proprietary software using an unstructured mesh finite volume solver. Cross flow velocity had near zero magnitude in the core, but there was an appreciable swirl component in the periphery.

Caro, C.G., Doorly, D.J., Tarnawski, M., Scott, K.T., Long, Q. & Dumoulin, C.L. (1996). Proc. Roy. Soc. A. **452**, 185-197.
Davies, P.F. (1995). Physiol. Rev. **75**, 519-560.
Doorly, D.J., Peiró, J., Sherwin, S.J., Shah, O., Caro, C.G., Tarnawski, M., McLean, M., Dumoulin, C.L. and Axel, L. (1997). ASME FED SM '97 (Bio-medical Fluids Engineering II), 1-8.
Dull, R.O., Tarbell, J.M. and Davies, P.F. (1992). Mechanisms of flow-mediated signal transduction in endothelial cells: Kinetics of ATP surface concentrations. J.Vasc. Res. **29**, 410-419.
Fox, B., James, K., Morgan, B. & Seed, W.A. (1982). Atherosclerosis **41**, 337-347.
Tardy, Y., Resnick, N., Nagel, T., Gimbrone, M.A. & Dewey, C.F. (1997). Arterioscler. Thromb. Vasc. Biol. **17**, 3102-3106.

Reduced Navier Stokes in axisymmetrical stenoses

Pierre-Yves Lagrée and Sylvie Lorthois
L. M. M., Univ. PARIS VI, FRANCE ; I. M. F. T., TOULOUSE, FRANCE
Email: pyl@ccr.jussieu.fr, lorthois@imft.fr

Keywords - Reduced Navier-Stokes (RNS) - Stenosis - Biomechanics -

Abstract - The high values of the wall shear stresses (WSS) in advanced occlusive lesions are likely to play a role in the mechanism of thrombo-embolism and artherosclerotic plaque rupture. Navier-Stokes solvers are now very efficient in computing WSS. However, asymptotic methods provide a better understanding of the structure of the flow and of the relevant scalings. For example, the use of an interactive boundary-layer (IBL) method leads to a simple scaling law between maximal WSS, Reynolds number and geometrical parameters of the stenosis, for a steady, newtonian, axisymetrical flow [1]. This was not achieved previously using Navier-Stokes solvers [2]. However, due to the underlying assumption of existence of a potential core of perfect fluid, the IBL theory breaks down if the boundary-layer fills out the whole vessel's cross-section. Therefore, it is not suited to study transitions from boundary-layer/perfect fluid to fully viscous flow regions (entry flows) and vice versa. For this kind of flow, the relevant non-dimensional quantities are $x = \frac{x^\star}{r_0^\star Re}$, $r = \frac{r^\star}{r_0^\star}$, $u = \frac{u^\star}{\overline{u_0}^\star}$ and $v = \frac{v^\star Re}{\overline{u_0}^\star}$, where $x^\star$, $r^\star$, $u^\star$ and $v^\star$ are respectively the axial and radial coordinates and velocity components, and Re is the Reynolds number based on the entry radius ($r_0^\star$) and mean velocity ($\overline{u_0}^\star$). This holds if Re is large. At first order, Navier-Stokes equations are then written as :

$$\frac{\partial u}{\partial x} + \frac{1}{r}\frac{\partial (rv)}{\partial r} = 0, \quad u\frac{\partial u}{\partial x} + v\frac{\partial u}{\partial r} = -\frac{\partial p}{\partial x} + \frac{1}{r}\frac{\partial}{\partial r}\left(r\frac{\partial u}{\partial r}\right), \quad \frac{\partial p}{\partial r} = 0, \tag{1}$$

This set of RNS equations is solved by a marching finite-differences scheme. The left figure displays the evolution of the velocity profile along the convergent part of a 70% stenosis, for two different imposed entry profiles: a flat profile (fully potential entry) and a Poiseuille profile (fully viscous entry). When the

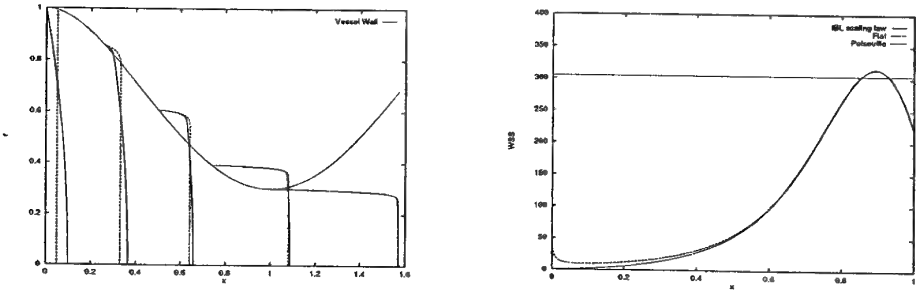

Evolution of the velocity profile (left) and WSS distribution (right) along the convergent part of a 70% stenosis ($Re = 500$) ; solid line: Poiseuille entry profile ; broken line: flat entry profile.

entry flow is fully viscous, the strong acceleration causes the velocity profile to flatten. At the stenosis throat, the flow is thus independant of the entry. This is interesting because the *in vivo* entry profile is unknown but not parabolic as assumed in most studies [2]. In particular, the maximal WSS, independant of the entry, is in good agreement (7% discrepancy) with maximal WSS obtained by our IBL scaling law [1] (see right figure). In conclusion, the described set of RNS equations is "fully interactive" without any matching step and well suited for studying stenotic flow fields. Extension to unsteady and non-axisymetrical flows is currently in progress.

References

[1] S. Lorthois and P.-Y. Lagrée, *CRAS IIb* **328** (2000), 33–40.

[2] J.M. Siegel et al, *ASME J. Biomech. Egng.* **116** (1994), 446–451.

The development and decay of idealised haemodynamic flows

M.G. Blyth and A.J. Mestel
Department of Mathematics, Imperial College, London SW7 2BZ, UK

Email: mgblyth@ic.ac.uk

Keywords - Haemodynamics, pipe flows

Abstract - Many factors influence the flow of blood in the larger vessels of the body. The arterial geometry is complex, with many bends and bifurcations, which are frequently non-planar. Furthermore, the driving pressure gradient, though essentially periodic, has a non-trivial time-dependence.

Idealised models can investigate the effects of pulsatility and arterial curvature, but these usually require a flow which is fully developed. For example, steady Dean flow has been used to model motion at some distance from the heart, while flow in helical pipes has been studied with reference to the aortic arch. However, real flows may have insufficient space to adjust to the asymptotic state. While some flows require an entry length of order the Reynolds number, the rapidly oscillating Womersley-like flows require a much shorter distance.

In this paper the scales on which flows in idealised geometries develop and decay are examined. Eigenfunctions with exponential down-pipe behaviour are found for both the Womersley potential flows, and those with a rotational entry profile. The effects of two-dimensional and three-dimensional pipe curvature are quantified.

SHEAR STRESS CALCULATIONS IN CAROTID ARTERIES MODELS CALCULATED FROM EXPERIMENTAL LDA-MEASUREMENTS

D.Liepsch,* T. Matsuo, B. Lesniak, C. Weigand. University of Applied Sciences and Technical University of Munich, Germany, Liepsch@fh.rz.muenchen.de

Abstract

It is believed that low and high shear stress regions are responsible for chemical reactions forming arterial plaques. Previous shear stress studies have measured the axial velocity component. To calculate the exact shear stresses, however, all three velocity components must be measured. The viscosity must also be considered at the local points. We used an elastic silicon rubber model of a carotid artery in a physiologically accurate circulatory system. The model compliance was similar to that of the human arterial vessel wall. The model was immersed in a Glycerin water solution with the same refraction index as the model wall. The fluid was a Dimethylsulfoxide-polyacrylamide solution with the same viscoelastic behavior as blood. This fluid is transparent and has the same refraction index as the model wall. At each measuring point, 8 pulse cycles were measured. Sixty-nine measured points were measured in each plane. Measurements of all 3 velocity components were done with a 3D-LDA fiber optic system simultaneously. Shear stresses were calculated from these measurements. In areas with high secondary flow, values were twice as high values as those reported previously. The highest values were about 20 Pa. Calculated shear stresses were quite different in areas of flow separation regions with high secondary flow, compared to calculations done with only one velocity component. Therefore, it is important that all three velocity components be measured to calculate velocity vectors accurately. One-component measurements are helpful to get a quick overview of the flow conditions and may be useful for physicians, however for fundamental studies, time consuming 3D-LDA measurements or PIV measurements are necessary.

KEYWORDS **Laser-Doppler-anemometer, carotid artery models, shear stress, velocity distribution,**

REFERENCES

1. Liepsch, D, Moravec, Baumgart, R: Some flow visualization and laser-Doppler- velocity measurements in a true-to-scale elastic model of a human aortic arch-A new model technique. Biorheology 29: 563-580, 1992

2. Liepsch, D: Strömungsuntersuchungen an Modellen menschlicher Blutgefäss-Systeme. VDI Fortschrittberichte Reihe 7: Strömungstechnik.

3. Liepsch, D., Pflugbeil, G., Matsuo, T., Lesniak B.: Flow visualization and 1- and 3-D Laser-Doppler-Anemometer measurements in model of human carotid arteries.(1998) Clinical Hemorheology, 18 (1): 1-30. 1998.

4. Karner VG, Perktold K. Hofer, M, Liepsch, D,: Flow Characteristics in an anatomically realistic compliant caroatid artery bifurcation model. Computer Methods in Biomechanics and Biomedical Engineering. 2 (1999) 171-185

THE EFFECTS OF GEOMETRY ON THE FLOW PATTERNS OF FEMORAL GRAFT-ARTERY ANASTOMOSES

C.Lally and T.McGloughlin

Department of Mechanical and Aeronautical Engineering &
University of Limerick Biomedical Institute (ULBMI)
Unviversity of Limerick, Ireland

Email: tim.mcgloughlin@ul.ie

Local haemodynamic factors are believed to play a significant role in the development of atherosclerosis and intimal hyperplasia in arterial bifurcations and graft-artery bypass anastomoses. The localised formation of atherosclerotic plaque and intimal thickening, predominantly at the heel and toe and on the artery bed of anastomoses, has led to a number of theories on the mechanism of intimal thickening. Most theories have postulated that abnormal haemodynamic wall shear stresses (WSS) play a role in the formation of occlusive intimal hyperplasia. It has been found that the sites subjected to abnormal WSS magnitudes, associated with areas of flow separation, recirculation and flow stagnation in distal femoral end-to-side anastomoses, are also the areas predisposed to intimal hyperplasia formation *in vivo*. These characteristic flow patterns in distal femoral end-to-side anastomoses have been found be largely dependant on the geometrical shape of the bypass configuration. The main objective of the current study was to determine the influence of specific geometrical features, of distal femoral end-to-side anastomoses, on the haemodynamics and hence the WSS distributions at anastomoses with a view to establishing an optimum geometrical configuration.

Computational fluid dynamics (CFD) was used to simulate the haemodynamics in various graft-artery anastomosis configurations, under steady and pulsing flow conditions. The criterion for determining the optimum geometrical configurations was based on a critical wall shear stress theory, whereby an upper and lower WSS threshold limit were specified.

A variety of numerical studies have been carried out, to investigate the effects of the anastomosis angle, the interposition of a Miller cuff between the graft and the artery and the graft-to-artery diameter ratio, on the haemodynamics at femoral end-to-side distal anastomoses. The effect of the geometrical configuration of the anastomosis is also analysed by comparing idealised anastomoses to more realistic anastomoses designs, whereby the graft tapers in at the graft-artery interface. An alternative graft design, where there is a smooth transition from an essentially S-shaped graft into the artery, is also compared to the more conventional graft-artery anastomosis configuration to determine its influence on the haemodynamics at the anastomosis.

The flow patterns in the numerical models under steady flow conditions were validated experimentally using Laser Doppler Anemometry (LDA), to determine the velocity profiles in a typical end-to-side anastomosis. In order to validate the models under pulsing flow conditions, the flow patterns observed during the pulse cycle were compared to documented physiological pulsing flow patterns in similar numerical models of end-to-side anastomoses.

The study illustrates that the geometry of the distal end-to-side anastomosis is a key factor influencing the haemodynamics at graft-artery bypasses and that improvements in the design of the anastomosis may significantly increase the patency of femoral distal graft-artery bypass procedures.

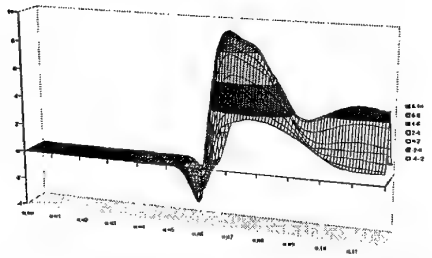

Normalised Wall Shear Stress(WSS) Magnitudes along the Artery Bed of an idealised anastomosis with 45° graft angle at time t_3

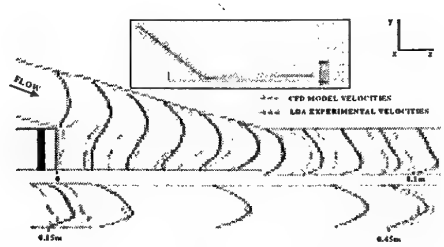

Comparison between the LDA and CFD Results in the anastomosis model for a Reynolds No. = 170

1- Anayiotos, A.S., S.A. Jones, D.P. Giddens, S. Glagov and C.K. Zarins. 1994. "Shear Stress at a Compliant Model of the Human Carotid Bifurcation" ASME Journal of Biomechanical Engineering, 116, 98-106.

2- Archie, J.P., 1994. "Femoropopliteal Bypass With Either Adequate Ipsilateral Reversed Saphenous Vein or Obligatory Polytetrafluoroethylene" Annals of Vascular Surgery, 8(5), 475-484.

The influence of geometric modification on the haemodynamics within a distal bypass graft

S.J.Sherwin, D.J. Doorly, J. Peiro and C.Caro
Department of Aeronautics, Imperial College of Science, Technology & Medicine, Prince Consort Road, London, SW7 2BY
Email: s.sherwin@ic.ac.uk

Keywords - Computational Haemodynamics, Arterial bypass grafting

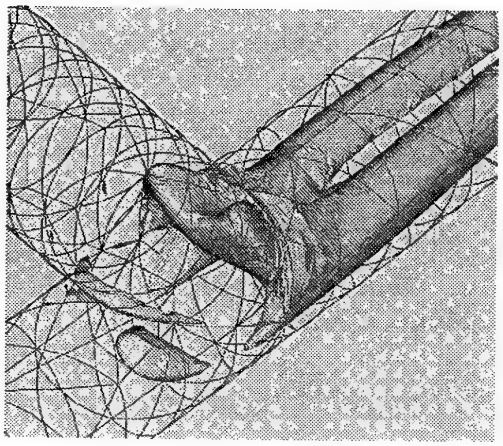

(a)

(b)

Figure 1:Computational modelling of distal bypass grafts (a) Coherent structure in model bypass graft, (b) wall shear stress distribution in reconstruction of a porcine bypass junction

Abstract - The downstream or distal end of a bypass graft is generally considered as a preferential site for the occurrence of myo-intimal hyperplasia leading to the graft failure. For this reason this junction has been a favoured configuration for many computational and experimental investigations. Predominantly these investigations have focused on model configurations similar to the problem shown in figure 1(a). Typically these studies have considered the role of pulsatility and graft angle on the flow pattern or in the case of peripheral bypass grafting the effect of geometric modifications such as the Taylor hood and Miller cuff.

Current investigations, in collaboration with coronary vascular surgeons at Hammersmith hospital, London have been focused on reconstructing physiologically correct porcine coronary bypass grafts as shown in figure 1(b). These reconstructions recover the inner lumen of the bypass graft not directly visible to the surgeon. An interesting characteristic of this study has been the regular occurrence of narrowing or stenosis in the vicinity of the junction between the host and bypass vessel as evident in figure 1(b). The increase in wall shear stress at the junction, as depicted in figure 1(b), is a natural consequence of the reduction of the lumen cross section however the extent of separation and possible influence on residence times has currently not been determined. In this paper we will numerically address this issue by considering the influence of stenotic modifications on the flow within a distal junction in both model and physiologically relevant geometries in comparison with non-stenosed configuration.

Numerical analysis of coronary artery flow

F.N. van de Vosse, B.J.B.M. Wolters, J.J. Wentzel*, R. Krams* and C.J. Slager*
Section Materials Technology, Faculty of Mechanical Engineering
Eindhoven University of Technology, The Netherlands
* Section Hemodynamics, Thoraxcenter
Erasmus University Rotterdam, The Netherlands
Email: vosse@wfw.wtb.tue.nl

Keywords - Coronary flow - Numerical analysis - Atherosclerosis

Abstract - Local wall shear stress induced by coronary artery flow and local wall stress (or strain) induced by wall deformation are known to be important factors in wall adaptation and the development of atherosclerosis in coronary arteries.
The wall shear stress, induced by local flow phenomena, depends on: i) the *vessel geometry*, which is three-dimensional, non-planar and time-dependent due to wall motion induced by the pressure pulse and the movement of the heart (figure 1a), ii) the *flow* that is time-dependent pulsatile and iii) the *rheological properties* of blood, that is shear thinning (figure 1b).
The wall stress, induced by the wall deformation, in general depends on: i) the *geometry*, that is three-dimensional and time-dependent and exhibits a non-uniform wall thickness (figure 1a), ii) the *motion of the heart* (figure 1a), iii) the *pressure wave* and iv) the *material properties* of the arterial wall.

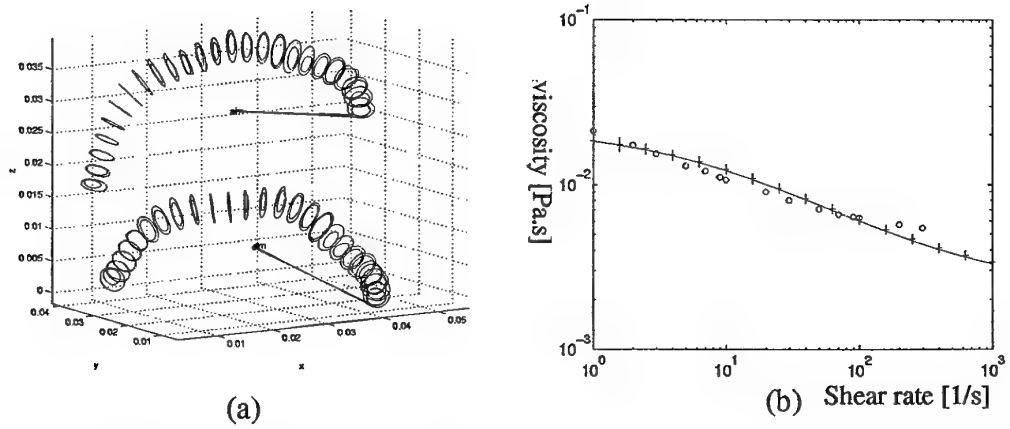

Figure 1: *(a) Typical geometry of a coronary artery in systolic (top) and diastolic (bottom) phase of the cardiac cycle, obtained from intra-vascular ultrasound measurements, showing both inner and outer countours of the artery wall. (b) Viscosity of blood as a function of the shear rate, showing the shear thinning behaviour.*

In this study the importance of time-dependence of the flow pulse, motion of the arterial wall and non-Newtonian properties of blood for the wall shear stress and wall stress distribution is investigated numerically with the aid of an arbitrary Euler-Lagrange fluid-solid interaction finite element method. Although significant influence of the parameters given above are found, studies based on steady flow in rigid geometries still seem to be valuable for clinical studies on coronary artery wall adaptation.

Curvature effect on flow and mass transport in a coronary artery bifurcation model

K. Perktold[1], M. Prosi[1], A. Leuprecht[1], Z. Ding[2] and M.H. Friedman[3]
[1]Institute of Mathematics, Graz Institute of Technology, Austria
Email: perktold@matd.tu-graz.ac.at
[2]Department of Diagnostic Radiology, Yale University, New Haven, CT, USA
Email: ding@boreas.med.yale.edu
[3]Biomedical Engineering Center, The Ohio State University, Columbus, OH, USA
Email: friedman.1@osu.edu

Keywords - Coronary Arteries - Flow Dynamics - Oxygen Transport - Branching Effect - Dynamic Curvature Effect

Abstract - The coronary arteries undergo large dynamic variations during each cardiac cycle due to their position on the beating heart. The local artery curvature varies significantly. The aim of this study is to analyse the effects of dynamic curvature on coronary artery hemodynamics (flow patterns and wall shear stress distribution) and on oxygen transfer into the artery wall in a coronary artery branching model, and to compare these effects with the effects due to the vessel branching. The pulsatile flow field and the oxygen transfer were simulated in an anatomically realistic model of the bifurcation of the left anterior descending coronary artery (LAD) and its first diagonal branch (D1) including time-varying curvature of the arteries.

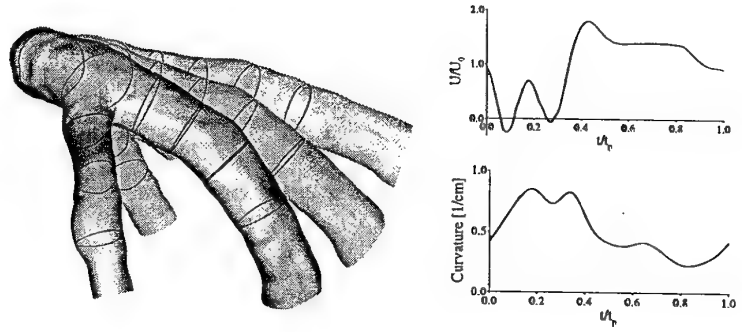

Left: Computational geometric model of the LAD-D1 bifurcation. Top, right: Flow pulse wave form in the LAD. Bottom, right: Heart motion: dynamic curvature during the pulse cycle at the branching site.

The mathematical model applies the ALE-modified Navier-Stokes equations and convection-diffusion equation describing the blood flow and the mass transport in the time-varying geometry with large, externally imposed boundary motion. The numerical approach uses the finite element method. The model allows to consider the effects on the shear field of the bifurcation, the out-of-plane curvature, and of the changing curvature. The simulation demonstrates that the influence of the curvature and the curvature dynamics on bifurcating flow and on mass transport is of minor importance in the bifurcation region, and becomes dominant at sites further downstream from the branch.

Acknowledgements - This study is supported by the Austrian Science Foundation, Project-No. P 11982-TEC, Vienna, Austria, by EUREKA, Project No. E! 2061, and by the NIH Grant No. HL58856.

Viscoelastic flow and mass transport in large artery models

A. Leuprecht and K. Perktold
Institute of Mathematics, Technical University Graz, Austria
Email: leu@matd.tu-graz.ac.at

Keywords - Blood Flow - Mass Transport - Viscoelasticity - Large Arteries - Numerical Study

Abstract - The present study deals with the influence of viscoelastic effects on blood flow in large arteries. In addition to flow related quantities as wall shear stresses the oxygen transport in the artery and into the artery wall is investigated in the computer simulations. The transfer between the blood and the artery wall is an important factor in atherogenesis, and thus, the influence of local flow patterns on the mass transport is of great interest. The mathematical description of the viscoelastic blood flow applies the conservation of mass and momentum and a constitutive relation of Jeffrey's type (Oldroyd-B model). The mass transport process is described by the convection-diffusion equation.

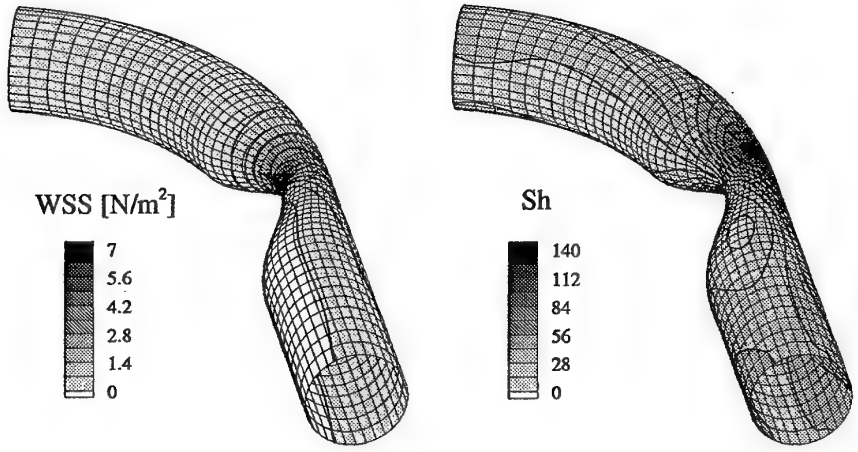

Distribution of wall shear stress (left) and Sherwood number (right) (Oldroyd-B fluid at $Re = 100$ and $We = 0.3$)

The solution of the viscoelastic flow problem applies a decoupling of kinematics and extra-stresses. The governing equations are solved by means of a Galerkin finite element method. Upwind schemes are applied to face the hyperbolic character of the constitutive equation and to achieve stability of the convection dominated transport process. The numerical studies are carried out in 90° curved stenotic tubes under steady flow conditions (Dean number $\kappa = 40.8$). The stenosis is located at the inner wall at the end of the bend. Different degrees of stenosis are considered. The reduction in lumenal cross-sectional area demonstrates an increase of the influence of the viscoelastic properties on local flow behavior. In configurations with moderate stenotic constrictions viscoelasticity hardly affects local flow patterns. Flow through the 75% stenosis, however, shows larger elongational components. At increased Weissenberg numbers the velocity patterns differ significantly from Newtonian flow. Wall shear stresses and mass wall flux increase in the stenotic region. The maximum flux occurs at the outer wall opposite the stenotic throat.

Acknowledgments - This study is supported by the Austrian Science Foundation, Project-No. P 11 982-TEC, Vienna, Austria, and by EUREKA Project No. E! 2061.

Blood Flow and Atherosclerosis

N.A. Hill and M.K. Spendiff
Department of Applied Mathematics
University of Leeds, U.K.
Email: N.A.Hill@Leeds.ac.uk

Keywords - Blood Flow - Atherosclerosis - Arterial Disease

Abstract - The interaction between blood flow and the transport of cholesterol through the arterial wall is critical in the formation of atherosclerosis. We have developed a mathematical model of a large artery which describes the early stages of the disease, i.e. intimal hyperplasia and the evolution of fatty streaks which are the precursors to the formation of atherosclerotic plaques. The arterial wall is modelled by two layers, the innermost layer (the intima) and the media, through which cholesterol both diffuses and is advected with the slow flow of water through the wall. Within the intima, cholesterol is converted to oxidised cholesterol and is then consumed in situ by macrophages which bind to the substrate and turn in to fatty foam cells. These processes are described by

$$\frac{\partial c_L}{\partial t} = -\nabla \cdot j_I - k_1 c_L \quad \text{and} \quad \frac{\partial c_{LO}}{\partial t} = k_1 c_L - \gamma\, c_{LO},$$

where c_L and c_{LO} are the concentrations in the intima of native cholesterol (L) and oxidised cholesterol (LO) respectively. k_1 is the rate of conversion to LO and γ is the constant background decay rate for LO. j_I is the flux of in the intima and is given by

$$j_I = -D_I \cdot \nabla c_L - c_L U\, \chi_I\, \hat{\mathbf{z}},$$

where D_I is a diffusion tensor, χ_I is the slip coefficient (the mean velocity of the molecule relative to that of the fluid), $-U\hat{\mathbf{z}}$ is the mean fluid velocity through the vessel wall, which is taken to be constant. No conversion takes place in the media which has relatively low diffsion and advection coefficients and thus acts a barrier to the transport of cholesterol so that the governing equation is

$$\frac{\partial c_M}{\partial t} = -\nabla \cdot j_M, \quad \text{where} \quad j_M = -D_M \cdot \nabla c_M - c_M U\, \chi_M\, \hat{\mathbf{z}},$$

where c_M is the concentration of L in the media, D_M is a diffusion tensor and χ_M is the slip coefficient. The key concepts are that the permeability to cholesterol in the blood of the endothelial layer (which lines the inside of the artery) depends on the local wall shear stress due to the flow of blood, and that the presence of LO in foam cells leads to swelling of the arterial wall changes the flow producing a feedback mechanism. Specific functional forms are specified for these two processes.

For simplicity a two-dimensional channel geometry has been used. Both steady and pulsatile flows are simulated using standard asymptotic results for high Reynolds number flows. The results confirm that changes in the structure of the wall with age increase the likelihood of incidence of atherosclerosis, and also suggest an unexpected connection with the early stages of the formation of another important arterial disease — abdominal aortic aneurysms.

Activation and Extinction Models for Platelet Adhesion

by T.David and P. Walker, School of Mechanical Engineering, University of Leeds, U.K.
t.david@leeds.ac.uk

Keywords: Platelet adhesion, Fluid Dynamics

Background and Theory

Fluid dynamic studies of blood flow, in models of arteries, suggests a set of fluid dynamic conditions which appear to predispose thrombus formation, principally at arterial bifurcations, T-junctions and curved sections. The formation of platelet aggregates can be initiated by means the eruption of an atherosclerotic plaque providing a diffusive cloud of activation factors which can initiate the activation of platelets causing them to adhere. A mathematical model is presented which simulates the activation of flowing platelets in the bulk fluid by these activating chemicals. The activation flux is produced by the adhesion of platelets at the surface. Under the condition of low diffusion coefficients for platelets a similarity variable, utilising the fluid shear stress at the vessel wall (WSS), furnishes a set of coupled o.d.e.'s parametrised by a Damkohler number (Dm, a ratio of chemical time to fluid passage time). These are solved for varying surface reaction (platelet adhesion) rate, the bulk reaction (platelet activation) rate and the WSS. A fully analytic asymptotic solution in the form of incomplete gamma functions is also presented for the case of $Dm \to \infty$.

Results

For high Dm, activated platelets are concentrated in an inner layer, which is separated from the 'outer' layer, consisting of unactivated platelets, by a 'diffusive' zone. However the activation process may be eliminated altogether for low enough Dm with the result of an area devoid of activated platelets and thus adhesion may be extinguished altogether. The value of Dm may be reduced by an increase in the outer fluid flow velocity, that is areas of high WSS.

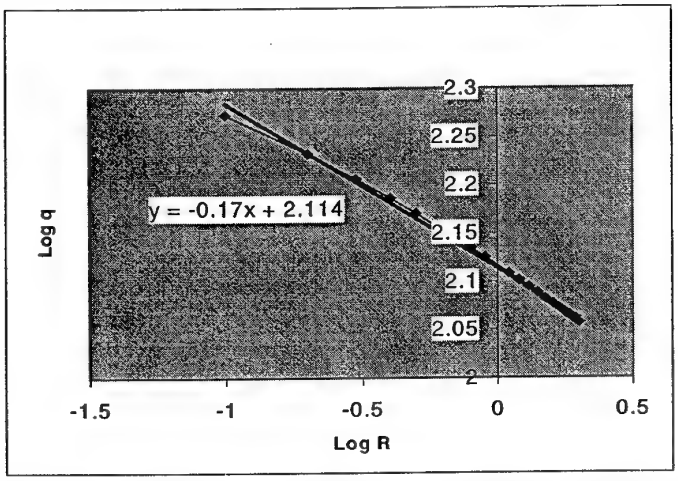

Figure 1 Log of Platelet Flux vs Log R

(♦: numerical , —: experiment)

In addition experimental evidence suggests a gradient of -0.17 for a log-log plot of platelet flux, q versus downstream distance, R, whereas conventional theory predicts -1/3. Figure 1 shows a simple linear regression fit to the numerical solution for a specific value of the surface adhesion rate hence providing the required gradient of -0.17. This indicates that experimental results can be modelled directly by a simple reduction of the platelet adhesion rate. The model can be used to simulate adhesion (and other clotting factor reaction processes) for a variety of fluid flow regimes, such as stagnation points and general flows where the WSS is a known function.

Aquatic vertebrate locomotion: Wakes from body waves

J.J. Videler, U.K. Müller and E.J. Stamhuis
Department of Marine Biology, Groningen University
The Netherlands

Vertebrates swimming with undulations of the body and tail have inflection points where the curvature of the body changes from concave to convex or vice versa. These inflection points travel down the body at the speed of the running wave of bending. In movements with increasing amplitudes, the body rotates around the inflection points, inducing semicircular flows in the adjacent water on both sides of the body that together form proto-vortices. Like the inflection points, the proto-vortices travel towards the end of the tail. In the experiments described here, the phase relationship between the tailbeat cycle and the inflection point cycle can be used as a first approximation of the phase between the proto-vortex and the tailbeat cycle. Proto-vortices are shed at the tail as body vortices at roughly the same time as the inflection points reach the tail tip. Thus, the phase between proto-vortex shedding and tailbeat cycle determines the interaction between body and tail vortices, which are shed when the tail changes direction. The shape of the body wave is under the control of the fish and determines the position of vortex shedding relative to the mean path of motion. This, in turn, determines whether and how the body vortex interacts with the tail vortex. The shape of the wake and the contribution of the body to thrust depend on this interaction between body vortex and tail vortex. So far, we have been able to describe two types of wake. One has two vortices per tailbeat where each vortex consists of a tail vortex enhanced by a body vortex. A second, more variable, type of wake has four vortices per tailbeat: two tail vortices and two body vortices shed from the tail tip while it is moving from one extreme position to the next. The function of the second type is still enigmatic.

On the sound of snapping shrimp: the collapse of a cavitation bubble

Michel Versluis[1], Barbara Schmitz[2], Anna von der Heydt[1,3], and Detlef Lohse[1]

[1]*Fluid Mechanics and Heat Transfer, University of Twente, P.O. Box 217, 7500 AE Enschede, The Netherlands*
[2]*Institut für Zoologie, TU München, Lichtenbergstr. 4, 85747 Garching, Germany*
[3]*Department of Physics, Philipps-Universität Marburg, Renthof 6, 35032 Marburg, Germany*

Email - m.versluis@tn.utwente.nl

Keywords - Snapping shrimp - Cavitation

Abstract - The snapping shrimp, *Alpheus heterochaelis*, (figure to the right; actual size) produces a snapping sound by an extremely rapid closure of its large snapper claw. It generates sound so loud that it disturbs submarine communication. Hydrophone measurements in a large artificial seawater pond indicate intensities of up to 180 dB re 1 μPa at a distance of 1 m. It was commonly believed that the sound is generated when the two claw surfaces hit each other.
In this work we show that the sound originates, in fact, from the collapse of a cavitation bubble. When rapidly closing its snapper claw (figure to the left; angular speed exceeding 3000 rad/s !), a high-velocity water jet (25 m/s) is emitted from the claw which exceeds cavitation conditions. Hydrophone measurements, in conjunction with time-controlled ultra high-speed imaging of the claw closure, demonstrate that the sound is emitted at the cavitation bubble collapse, i.e. at the time where the bubble size is at minimum. The ultra high-speed images were recorded with digital monochrome video cameras at a frame rate of up to 40500 frames per second (fps).

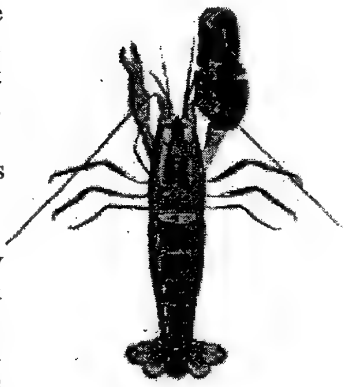

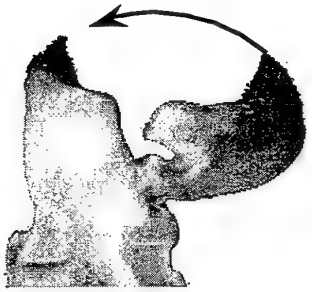

Below a sound pressure recording of the snap is displayed. The dots indicate when a high-speed image is captured. The first dot to the left corresponds to the time when the claw is fully closed. To the bottom, five high-speed side-view images of the tip of the snapper claw are shown. From the time correlation with the sound pressure signal one can see that none of the sound is associated with the mechanical claw contact, while a very prominent signal is observed during the collapse of the cavitation bubble.

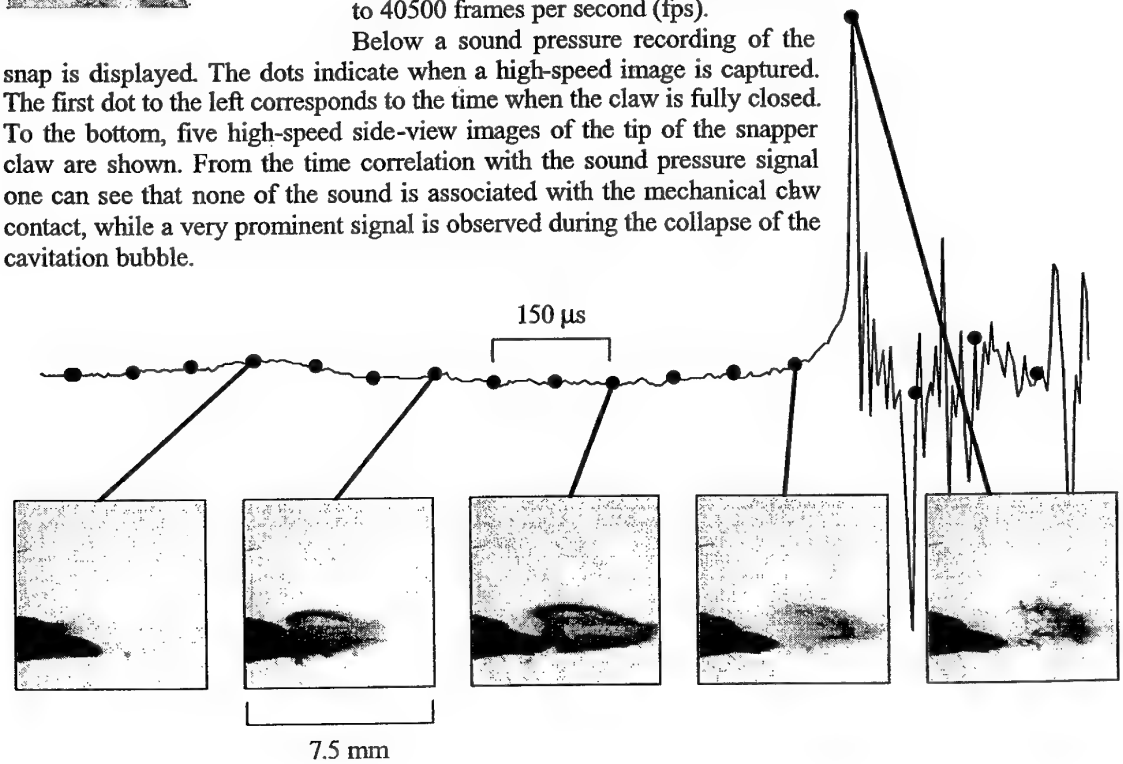

ENTRANCE OF A CELL INTO A FILTRATION PORE

A. Diaz, D. Barthès-Biesel,
UMR CNRS 6600, University of Technology of Compiègne, France.
Email : Anna.Diaz@utc.fr

Keywords : Capsule, filtration model, viscous effect, numerical study.

Abstract : Over the years, many experimental devices have been proposed to evaluate cell or capsule mechanical properties (geometry at rest, membrane constitutive properties and internal viscosity). Among these, filtration through a small pore is particularly attractive because of its simplicity[1]. Theoretical work has been dedicated to the analysis of filtration experiments[2,3] but there is little information about the influence of the viscosity ratio λ between internal and external liquid during the entrance flow of a capsule in a pore. The aim of this work is thus to investigate the influence of this parameter on the entrance process. The proposed model will allow to evaluate approximately the variation of electrical resistance of the pore and thus will provide some comparison basis with experimental results. The pore is an axisymmetic channel consisting of a cylindrical tube with symmetrical coaxial hyperboloidal entrance and exit sections[3]. It is filled with a Newtonian incompressible liquid which flows with a constant flow rate. The capsule reference geometry is a spheroid. It is filled with a Newtonian incompressible liquid and is enclosed by a infinitely thin membrane. The membrane constitutive law is described by Skalak equation. The configuration is axisymmetric. The tube is supposed to be sufficiently long to allow the capsule to reach a steady motion in the cylindrical part. Non dimensional variables are used. The dimensionless parameters governing the capsule dynamics are : the capsule initial aspect ratio, the viscosity ratio λ and the capillary number ε (ratio of external viscous forces to elastic forces). The motion of the inner and outer fluids is described by the Stokes equations, recast in axisymmetric boundary integral form.

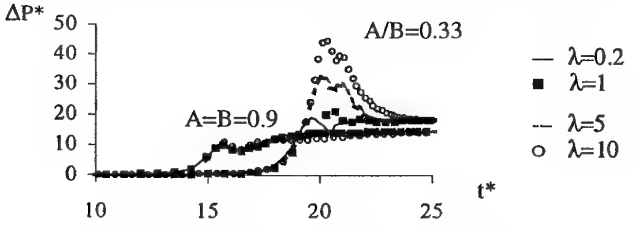

Figure 1 : Evolution of non dimensional additional pressure drop versus non dimensional time t* for different λ and for ε=0.01, A=B=0.9 and A/B=0.33.

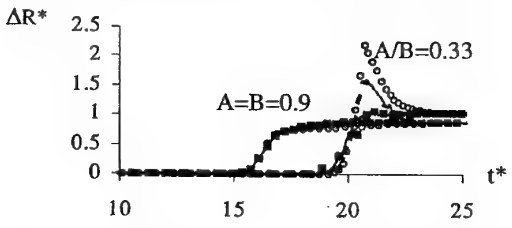

Figure 2 : Variation of non dimensional electric resistance with non dimensional time t* for different λ and for ε=0.01, A=B=0.9 and A/B=0.33.

As an example, the entrance process of two isovolumic capsules with a Skalak membrane (with a surface dilatation modulus equal to zero) is presented. The entrance process is very dependent on the capsule initial shape (Figure 1). For spherical capsules, the local maximum in viscous dissipation, as measured by ΔP^*, is small and the additional pressure drop depends only slightly on λ. For discoidal capsules, the effect of λ is enhanced due to the situation of pore quasi-plugging as the capsule enters the pore. The electric resistance of the pore is computed by assuming the pore walls and the cell to be non conducting and by using the long cylindrical conductor approximation. It is quite insensitive to the viscosity ratio for spherical small capsule (Figure 2), whereas it is very sensitive for discoidal capsules. Its maximum, as well as the local maximum in ΔP, are found to be linear with λ. Complementary results show that the electric resistance is very sensitive to capsule size. It follows that the entrance time is very sensitive to cell size, as was found for cells swollen by osmotic pressure[1]. As a conclusion the present model allows to study the influence of a cell intrinsic properties on its entrance into a pore. In particular, the respective roles of bulk internal viscosity and of membrane viscosity can be assessed.

References :

1. Fisher T.C., Wenby R.B. & Meiselman H.J. (1992) Biorheology, **29**, 185-201.
2. Secomb T.W. & Hsu R (1996), Biophys. J., **71**, 1095-1101.
3. Quéguiner & Barthès-Biesel (1997), J. Fluid Mech. **348**, 349-376, 199

Plumes in bacterial bioconvection

T.J. Pedley and A.M. Metcalfe[1]
Department of Applied Mathematics & Theoretical Physics
University of Cambridge, U.K.
Email: T.J.Pedley@damtp.cam.ac.uk

[1] Leeds University

Keywords - Bioconvection - Micro-organisms - Plumes

Abstract - Experiments by Kessler (see [1]) on bioconvection in laboratory suspensions of bacteria (*Bacillus subtilis*), contained in a deep chamber, reveal the development of a thin upper boundary layer of cell rich fluid which becomes unstable, leading to the formation of falling plumes. We use the continuum description of such a suspension developed by Hillesdon et al [2] as the basis for a theoretical model of the boundary layer and an axisymmetric plume. If the boundary layer has dimensionless thickness $\lambda \ll 1$, the plume has width $\lambda^{1/2}$, A similarity solution is found for the plume in which the cell flux and volume flux can be matched to those in the boundary layer and in the bulk of the suspension outside both regions. The corresponding model for a two-dimensional plume fails to give a self-consistent solution.

References

[1] Pedley, T.J. & Kessler, J.O. 1992 Hydrodynamics phenomena in suspensions of swimming micro-organisms. *Ann. Rev. Fluid Mech.* **24**: 313–358

[2] Hillesdon, A.J., Pedley, T.J. & Kessler, J.O. 1995 The development of concentration gradients in a suspension of chemotactic bacteria. *Bull. Math. Biol.* **57**: 299–344

Stability

EXPERIMENTAL STUDY OF PERIODIC WAKES : FROM LOW ASPECT RATIO CYLINDERS TO SPHERE

Lionel SCHOUVEILER , Caroline MICHALSKI and Michel PROVANSAL

Institut de Recherche sur les Phénomènes Hors Équilibre UMR 6594 CNRS
Faculté de Saint Jérôme, S 252 ,F-13397 Marseille Cedex 20, France,
lionel.schouveiler@lrc.univ-mrs.fr

Abstract

We present an experimental investigation of the periodic vortex shedding in the wake of circular cylinders with free hemispherical ends. The two control parameters of this problem are the Reynolds number $Re = UD/\nu$, built upon the upstream velocity U, the diameter of the circular cylinder D and the kinematic viscosity ν , and the aspect ratio L/D where L is the spanwise length. For a given aspect ratio, the flow becomes periodic when the Reynolds number is above a critical value Re_c. At constant supercritical Reynolds number, the transition from the cylinder wake, i.e. the Bénard-Von Karman vortex street, to the sphere wake is observed when the aspect ratio is reduced from five to one.

Experiments have been carried out in an open wind-tunnel of square test section (0.25 m × 0.25 m). Five circular cylinders, of same diameter $D = 10$ mm and of aspect ratio respectively equal to 5, 4, 3, 2 and 1, are used. They are held at the center of the working section, with axis perpendicular to the free stream U, by a bent rigid rod in order to control the orientation of the wake. For the sphere wake, the transition to instationarity is preceded by a regular axisymmetry breaking bifurcation, at a critical Re_1 measured to be in the range 180-210.

First, thresholds for the transition to instationarity Re_c have been estimated by extrapolating to zero the linear evolution, with Re, of the square amplitude of the streamwise velocity fluctuations. As for cylinders confined between two end plates, the stability of the wake of free end cylinders is strongly affected by the variation of the aspect ratio. In fact, the critical Reynolds number Re_c increases when the aspect ratio is reduced. The vortex shedding frequency is obtained through a standard spectrum analyzer. The two non dimensionalized frequencies, Strouhal number $St = fD/U$ and Roshko number, $Ro = fD^2/\nu$, are functions of the Reynolds number. Their evolutions appear continuous for the cylinders ($L/D = 5$ to 2) and for the case of the sphere ($L/D = 1$). In contrast with the well-known alternate vortex street behind a cylinder, visualizations of the sphere wake reveal a non alternate (one sided) vortex loops shedding.

Spanwise investigation of the periodic vortex shedding modes have also been realized. It is known that, due to finite size effects, vortex shedding exhibits three dimensional features. The measurements of the amplitude of the vortex shedding modes show that the vortex shedding is suppressed near the free ends and thus, the effective mode length L' is lower than the cylinder length L. No spanwise variation of the frequency is detected in this single mode regime.

Numerical simulation of long-wavelength instabilities in aircraft wake vortex pairs

R. Steijl and H.W.M. Hoeijmakers
Section Engineering Fluid Mechanics, Department of Mechanical Engineering
University of Twente, Enschede, The Netherlands
Email: r.steijl@wb.utwente.nl

Keywords - Wake vortices - Navier-Stokes simulations - High-resolution methods

Abstract - In the present study the development of long-wavelength instabilities in wake vortex pairs is investigated. Aircraft shed two initially rectilinear counter-rotating vortices. The mutually induced velocity makes the vortices susceptible to instabilities that are commonly called *cooperative instabilities*. The most-studied instability is the Crow instability, which for aircraft cruise conditions has a wavelength of $\pm$ 8 times the initial separation distance of the vortices. The present study investigates the mechanisms of this type of instabilities. For this purpose a high-resolution Navier-Stokes solution method is developed that simulates time-dependent three-dimensional flows of an incompressible medium using a uniform Cartesian mesh. High-order accuracy (4th/6th order) is achieved for the spatial discretization. Parallelization makes large-scale simulations possible within acceptable computing times.

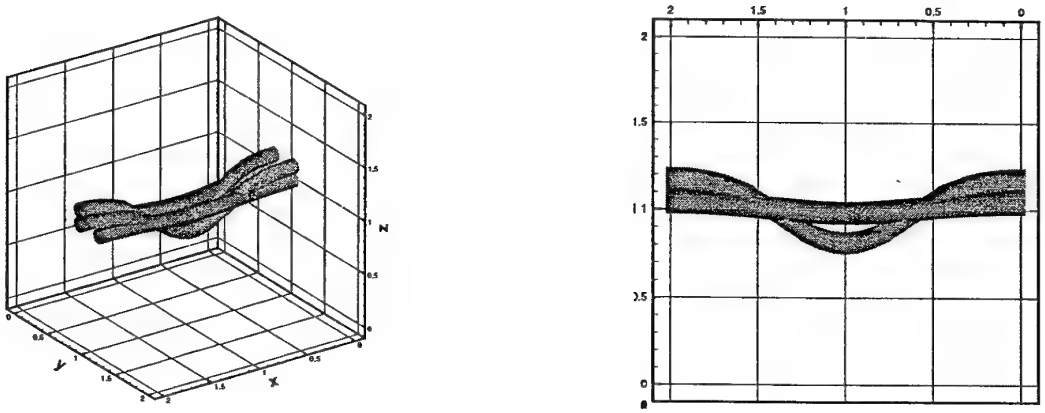

Iso-pressure contours at two different times in a time-dependent simulation of a evolving long-wavelength instability. 3D view (left) and side view (right)

The figures show results of a recent simulation of the growth of a long-wavelength instability in a computational domain periodic in x-direction. The initial solution is a counter-rotating vortex pair perturbed by the most unstable mode according to linear stability theory. This mode determines the length of the computational domain in the periodic direction. The influence of various parameters on the long-time behaviour is the subject of the proposed paper, as is a discussion on numerical aspects of the simulations.

Jet visualization at the mouth of a recorder : Influence of length and chamfering

Claire Ségoufin (1) Benoît fabre (1) Avraham Hirschberg (2)
(1) LAM Paris 6 (Fr) (2) Université Technique de Eindhoven (NL)
Email: segoufin@ccr.jussieu.fr

Keywords - Visualization - jet - flue channel - chamfers - musical instrument

Abstract - Visualization of the jet at the mouth of a recorder (where the sound is produced and entertained) can help understand the influence of given parameters on the sound production and on the instrument stability. The jet is formed at the end of a flue channel by flow separation. It then interacts with the transverse acoustical field and with the labium, and the whole system auto-oscillates.

Two parameters - said to be of crucial importance by recorder makers - were investigated on an experimental setup reproducing the geometry typical of a Dutch street organ pipe : the length of the flue channel, and its chamfering (i.e the cutting of the sharp 90° edges at the end of the flue channel to a 45° one over 1mm).

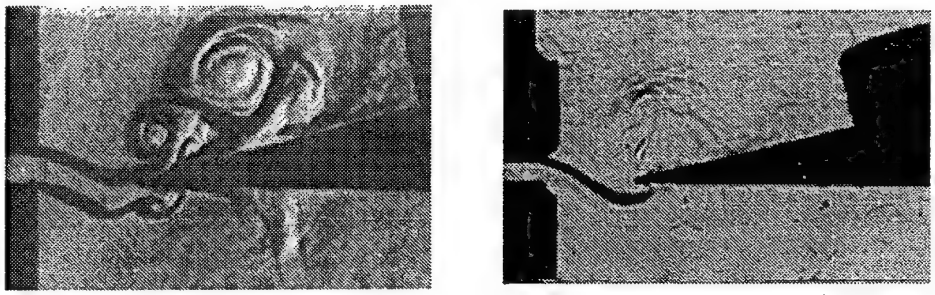

Fig1 : Visualization of the flow at the recorder mouth during steady-state oscillations. Left: short channel (3mm). Right: long channel (15mm) with chamfers at its exit.

In Fig1 we show two visualizations of the stationary jet for a short channel and a long channel with chamfers during steady-state oscillations. Visualizations were made also during attack transients for 3 configurations (long channel, short channel, long channel with chamfers). Pressure measurements at different spots in the instrument and frequency measurements were done simultaneously.

The flow looks very different when the channel is shortened compared to the long channel with chamfers : we can see more developped vortices and turbulence. This is also the case during attack transients. Varicose modes of the jet motion seem enhanced.

These features are then correlated to pressure and frequency measurements obtained. Correlations are done.

One of the main conclusion is that shortening the windway makes the system dramatically unstable. On the contrary, chamfering the sharp edges of a long channel greatly enhances the stability.

Non-linear modes of primary and secondary instabilities and flow patterns in the wake of a sphere

J. Dušek and B. Ghidersa
Institut de Mécanique des Fluides
2, rue Boussingault, 67000 Strasbourg, France
Email: dusek@imf.u-strasbg.fr

Keywords - sphere-wake, instabilities, flow visualizations

Abstract - The relation between experimental flow visualizations and the the non-linear instability theory is analysed for the primary (axisymmetry breaking) and secondary (onset of unsteadiness) instabilities of the wake of a sphere on the basis of numerical simulations and of the non-linear instability theory. The linear and weakly non-linear theory of the primary instability setting in at $Re = 212$ explains the mechanism of axisymmetry breaking and the selection of a symmetry plane. The non-linear modes coincide with azimuthal Fourier modes with the fundamental wave-number equal to one. It is shown that the corresponding expansion converges very rapidly. As a result, the instability can very well be described in terms of just two azimuthal modes: the axisymmetric one and the fundamental one. In particular, it is possible to describe both qualitatively and quantitatively the origin and evolution with the Reynolds number of the so called bifid wake intriguing experimentators for many years (see fig.).

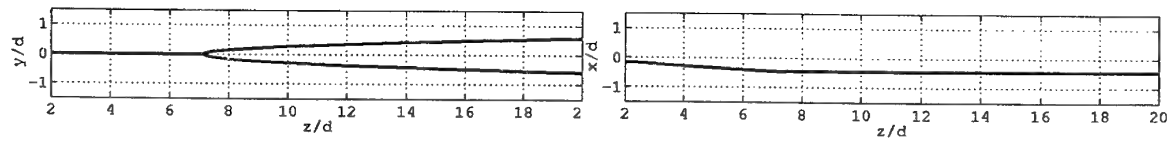

Dye trace in the sphere wake close to the instability threshold predicted by the theory showing the fork-like structure with a single thread close to the sphere and two threads farther streamwise. Left figure: view normal to the symmetry plane, right figure: view parallel to the symmetry plane.

Similarly, at the secondary instability, which sets in an $Re \approx 275$, the relation between the vortical structures evidenced in numerical simulations and flow visualization patterns resulting from dye injection and characterized by hairpin vortices is not yet fully clarified. In this regime, the non-linear modes are identified as time Fourier modes and their spatial structure is shown to be that of propagating waves. The onset hairpin vortices is shown to be basically due to the superposition of the mean flow and the fundamental mode of the secondary instability expressed in terms of just two lowest azimuthal modes.

Transient effects on the stability of heterogeneous jets

L. de Luca, Michela Costa, Ciro Caramiello
Dipartimento di Energetica, Termofluidodinamica Applicata e Condizionamenti Ambientali
Università di Napoli "Federico II"
DETEC, P.le Tecchio,80 - 80125, Napoli-ITALIA
Email:deluca@unina.it

Keywords - Transient growth - Jets instability

Abstract - Inadequacy of eigenvalues analysis has been recently recognised in assessing stability or instability of many shear dominated flows. In the case the governing operator is non-normal, in fact, even in subcritical ranges of the involved parameters, the potential of a substantial growth in the energy of small amplitude perturbations over short time or space scales exists, which is not amenable to be highlighted by the sole study of eigenvalues.
Physical mechanisms involved in transient growth have been generally linked to the presence of a crosswise gradient in the basic flow velocity profile due to shear. On the other hand, in analysing the behaviour of homogeneous and heterogeneous plane jets, present authors highlighted the occurrence of energy transient growth although a uniform velocity, exhibiting a discontinuity at the free surface according to the so-called *top hat* profile, was considered. Such a velocity discontinuity (the tangential stress being on the contrary continuous), would thus constitute a further mechanism leading to transient growth which adds to the aforementioned continuous crosswise nonuniformity due to shear. The present work is aimed to weight importance of the two different mechanisms by evaluating their relative contribution to energy growth for a family of basic flow velocity profiles which are not uniform in the crosswise direction, all preserving the discontinuity at the free interface.
Computation bases on eigenfunctions expansion determined by means of a spectral discretisation of the governing equations, which are written in vector form in terms of the normal velocity and normal vorticity. While for the top hat profile dependent variables are no forced by each others, a coupling operator arises in the other cases when the spanwise wavenumber is different from zero, implying vorticity to be forced by velocity. Conditions for no energy growth, the time dependence of the growth and the way it is affected by the streamwise and spanwise wavenumbers and flow parameters, namely Weber and Reynolds numbers as well as the external to internal fluid density ratio, are taken under consideration.
Iso-level curves of the maximum energy growth function are used to individuate the possible most dangerous disturbances and to make a tentative comparison with available experimental data concerning the conditions for which jet break-up occurs.

Influence of a three-dimensional instability on vortex merging

P. Meunier and T. Leweke
Institut de Recherche sur les Phénomènes Hors Equilibre
CNRS / Universités Aix-Marseille
12 avenue du Général Leclerc, F-13003 Marseille, France.
Email: meunier@marius.univ-mrs.fr

Keywords - Vortex Dynamics - Elliptic Instability - Vortex Merging

Abstract - We investigate experimentally the 3D dynamics of a pair of co-rotating laminar vortices. A well-known feature of such a flow is the merging of the two vortices into a single one. It has been established by numerous studies, mostly of 2D inviscid flows, that merging occurs whenever the size of the vortex cores, scaled on their separation distance, exceeds a certain limit. However, such a criterion does not take into account the effect of viscosity as well as the possibility of 3D instabilities, which may significantly change this picture.

The vortices are generated in water at the sharpened edges of two flat plates impulsively started from rest, and visualised using fluorescent dyes. The left figure shows a cross-cut view of the vortices during the normal 2D merging process at a Reynolds number (based on the circulation of one vortex) of about 2000. The well-separated cores initially rotate around each other until their characteristic radius has increased, through viscous diffusion, to a limit of roughly 25% of the vortex separation. The vorticity distributions then deform rapidly and merge into a single laminar vortex which is still two-dimensional.

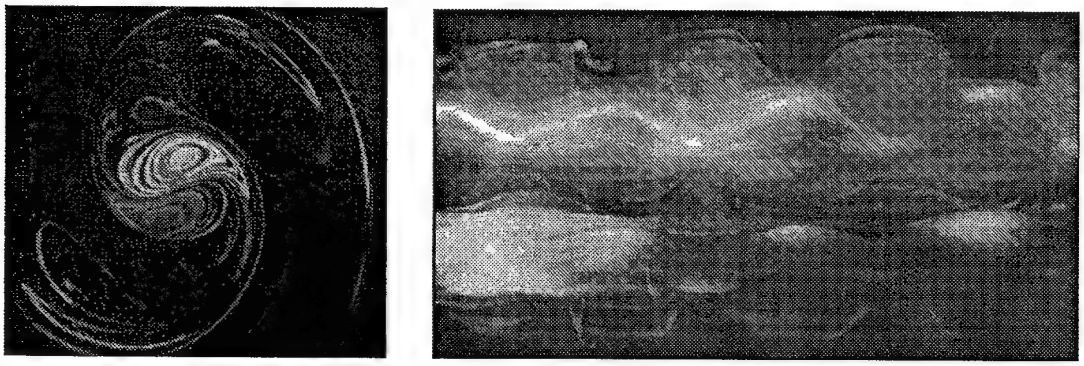

2D merging (left) and 3D instability (right) of two corotating vortices

When increasing the Reynolds number to 4000, the initial phase of viscous core growth is longer, long enough for the pair to undergo a three-dimensional instability, shown on the right figure. The pair is seen from the side, and the initially straight vortex center lines, marked by bright dye filaments, are subject to wavy perturbations. This distinct spatial structure is a characteristic sign of an elliptic instability, which is here observed for the first time in a corotating vortex pair. The visualisation also shows that the perturbations of the vortices are in phase, *i.e.* that the instability develops in a cooperative way. This 3D instability has consequences for the merging process. After saturation, perpendicular secondary vortices are generated, which lead to a rapid breakdown of the primary vortices and to the formation of a single *turbulent* vortex. Besides the fact that real (viscous) co-rotating vortices always merge, our study shows that merging can be significantly altered and accelerated in the presence of a 3D elliptic instability of the vortices.

Double-diffusive instabilities at heated vertical boundaries for weaker salinity gradients

Oliver S. Kerr
Department of Mathematics, City University,
Northampton Square, London EC1V 0HB, U.K.
Email: o.s.kerr@city.ac.uk

Keywords - Double-diffusive convection - Stability

Abstract - A recent linear stability analysis of double-diffusive convection in a laterally heated vertical slot containing salt-stratified water identified four different modes of steady instability, and one where the onset of instability is oscillatory. The asymptotic natures of three of the steady modes of instability were identified, the other having been found previously. The asymptotic natures of the oscillatory instability was not found.

Here we will show how the oscillatory instability is connected with the oscillatory instability found in the lateral heating of an unstratified fluid in a vertical slot where the fluid has a higher a higher Prandtl number. We find the asymptotic nature of this oscillatory portion of the boundary.

The relationship between the instabilities of a laterally heated fluid with a strong salinity gradient in a vertical slot and those found when a strong salinity gradient is heated from a single vertical wall has been shown before. Here we will look at how the other modes of instability in a vertical slot corresponding to weaker salinity gradients correspond to instabilities at an isolated vertical boundary when the strong salinity gradient approximation does not hold.

First Hopf bifurcation in the singular driven cavity flow

N. Parolini and F. Auteri
Dipartimento di Ingegneria Aerospaziale, Politecnico di Milano, Italia
Email: auteri@aero.polimi.it

Keywords - Navier–Stokes equations - Lid-driven cavity flow - Hopf bifurcation

Abstract - In the field of the Navier–Stokes equations, it is of great interest to study the instability scenarios leading to transition to turbulence. In this respect, problems in confined domains represent the most favourable situation for investigations of this kind, the prototypes being the classical Rayleigh–Benard and Taylor–Couette flows, see e.g. [1, 2].

In recent years, the driven cavity flow has also been considered, both in two dimensions, where the investigation is necessarily numerical [3, 4], and in three dimensions, where the numerical and experimental techniques complement each other [5]. A serious difficulty in the numerical solution of the Navier–Stokes equations in rectangular regions is the singular behaviour of the solution in the two corners adjacent to the moving wall. As a consequence, the attention by several investigators was directed to solve a modified problem with the singularity in the velocity boundary condition smoothed appropriately [6].

The aim of the present work is to takle the singular driven cavity problem, without any smoothing, to provide an accurate characterization of first Hopf bifurcation of the flow in a square domain. This goal is achieved by numerical simulation using a second-order-in-time spectral method [7] which represents the Galerkin–Legendre counterpart of the incremental projection method of Guermond and Quartapelle [8]. To allow for the problem singularity within the context of a spectral weak approximation, the singularity subtraction technique adopted by Botella and Peyret [9] has been used.

The spectral projection technique localizes the critical Reynolds number of the first Hopf bifurcation in the range $[8017.6, 8018.8)$. An analysis of the temporal series for the kinetic energy of the impulsively started flow is provided which allows us to formulate hypotheses on the nature of the dynamical portrait in the state space. We also describe the development of other oscillatory modes active beyond the first instability threshold. In the final presentation, results on the system dynamics for 2D flows at higher Reynolds numbers $\leq 10\,000$ will be given.

References

[1] E. Bodenschatz, W. Pesch, and G. Ahlers, Recent developments in Rayleigh–Bénard convection, *Annu. Rev. Fluid Mech.*, **32** (2000) 709–778.

[2] P. Chossat and G. Iooss, *The Couette–Taylor Problem*, Springer-Verlag, New York, 1994.

[3] A. Fortin, M. Jardak, J. Gervais, and R. Pierre, Localization of Hopf bifurcation in fluid flow problems, *I. J. Numer. Meths. Fluids*, **24** (1997) 1185–1210.

[4] J. W. Goodrich, K. Gustafson and K. Halasi, Hopf bifurcation in the driven cavity, *J. Comput. Phys.*, **90** (1990) 219–261.

[5] N. Ramanan and G. M. Homsy, Linear stability of the lid-driven cavity flow, *Phys. Fluids*, **6** (1994) 2690–2701.

[6] J. Shen, Hopf bifurcation of the unsteady regularized driven cavity, *J. Comput. Phys.*, **95** (1991) 228–245.

[7] F. Auteri and N. Parolini, A mixed basis spectral projection method, *in preparation*, 2000.

[8] J.-L. Guermond and L. Quartapelle, Calculation of incompressible viscous flows by an unconditionally stable projection FEM, *J. Comput. Phys.*, **132** (1997) 12–33.

[9] O. Botella and R. Peyret, Benchmark spectral results on the lid-driven cavity flow, *Computers and Fluids*, **27** (1998) 421–433.

Electrohydrodynamic flow of a dielectric liquid around a blade electrode

F. J. Higuera

E.T.S. Ingenieros Aeronáuticos
Pza. Cardenal Cisneros 3, 28040 Madrid, Spain

Injection of charge into a dielectric liquid, and a Coulomb force that sets the liquid into motion, may be obtained by applying a dc voltage to a blade-shaped, metallic electrode immersed in the liquid. An analysis of this motion and its influence on the transport of electric charge is carried out for a simple charge injection law. It is shown that the liquid motion, the electric field, and the charge distribution in a region around the electrode tip of size of the order of the electrode curvature radius determine the injected current as a function of the far electric potential seen by this region. The current increases exponentially with the potential when the contribution of the space charge to the electric field is negligible and algebraically when it is dominant, and presents a range of multiplicity in between. When the inertia of the liquid matters, the region around the electrode tip is also the origin of an electrohydrodynamic plume. An oscillatory current regime is found in which the space charge in the interelectrode space rearranges into many discrete lumps that, under constant voltage bias and small current, induce oscillations of the electric field at the injecting electrode and thus fire new lumps. An order of magnitude analysis and numerical computations for this regime give results in line with known experimental data. In conjunction with the hydrodynamic instability of the plume, this pulse firing mechanism is seen to lead to more complex, non periodic oscillations.

Critical velocities in open capillary flow

M.E. Dreyer, U. Rosendahl and H.J. Rath
Center of Applied Space Technology and Microgravity
University of Bremen, Germany
Email: dreyer@zarm.uni-bremen.de

Keywords - Capillary dominated flow - Choking - Microgravity experiment

Abstract - In this study the forced flow of a liquid through an open capillary channel is investigated. The capillary channel consists of two parallel plates and free surfaces at the sides. The pressure along the channel changes due to convective and molecular momentum transport and the free surfaces at the sides adjust by changing the curvature. The hydrostatic pressure is neglected since the experiments are performed under microgravity conditions. This allows larger gap distances than the Laplace length.

The aim of the investigation is to determine the critical flow velocity which leads to the collapse of the free surface and gas ingestion at the outlet (see Figure 1). The flow is then choked and the flow rate cannot be increased. This instability occurs at a certain Weber number which relates the flow velocity in the channel to the capillary wave speed.

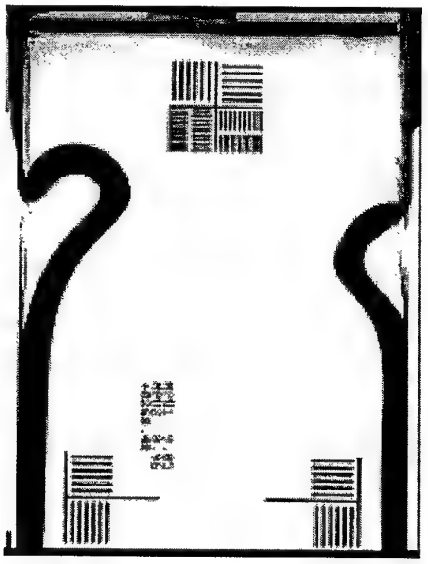

Figure 1: Video image of the upper part of the capillary channel. The flow direction is from the bottom to the top. The instability grows and the becomes unsymmetric. The free surface appears dark, the liquid region in the middle white.

The results of this work are important for the design of liquid acquisition devices (LAD) for propellant management systems in space. LADs are use to position and transport the propellant such that the engines of the space craft can be supplied with gas free propellant for any residual acceleration. The flow in these systems is capillary dominated and requires microgravity condition for the experiments.

Model Control of the Unsteady Separated Flow Past a Flat Plate

Angelo Iollo and Luca Zannetti
Dip. Ing. Aeronautica e Spaziale, Politecnico di Torino, 10129 Torino, Italy

Key words: flow control, low order model

Several authors have envisioned and studied the use of trapped vortices to enhance airfoil lift or to reduce flow unsteadiness. The flow past a flat plate can be considered the archetype of such problems, for a trapped vortex adequately placed would increase lift and stabilize the massive separation at the leading edge. We resort to a low-order model to study the essential features of such flow, and moreover to design control laws that can be subsequently tested on more sophisticated models.

It is seen that a flat plate at incidence admits equilibrium configurations for an external point vortex if a source/sink singularity is present on the flat plate contour, see fig. 1. However, such equilibrium points are unstable and therefore a control should be implemented so to stabilize the vortex in the equilibrium position. In our presentation, we will discuss a control technique based on wall suction and blowing for the *unstable* vortex equilibrium point present in the case of a flat plate at incidence. By formulating the problem as an optimal control problem the control law is designed so that a given functional $\mathcal{L}$ measuring the merit or the cost of a certain solution has a maximum or a minimum respectively. The method to find the actuator control law $g(t)$ so that for any arbitrary $\delta g(t)$ we have $\delta\mathcal{L}(g) = 0$, is based on the Lagrange multipliers technique.

This framework is amenable to be used for on-line control based on feed-back information about the actual flow conditions. Indeed, as mentioned above, the model we use gives only a very coarse description of the actual dynamics. The vorticity of the true flow is distributed over a finite flow region corresponding to the recirculation bubble and in its relative shear layer, so that the parameters of the simplified model used for synthesizing the control law must be constantly updated.

In the perspective presentation we intend to give an overview of previous work, formulate the problem, derive the control, and finally discuss the robustness of control laws thus obtained.

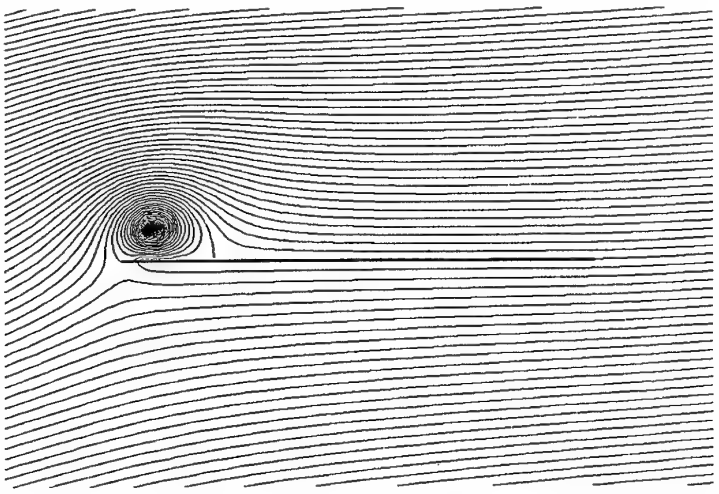

Figure 1: Streamlines corresponding to the equilibrium position of a point vortex satisfying the Kutta condition on both the leading and the trailing edges. A source and a sink of equal intensity are present in corresponding locations of the plate upper and lower surfaces.

Global behaviour corresponding to the absolute instability of the rotating-disk boundary layer

P.W. Carpenter and C.Davies
Fluid Dynamics Research Centre
University of Warwick/Coventry University, England
Email: pwc@eng.warwick.ac.uk

Keywords - Global instability, absolute instability, laminar-turbulent transition.

Abstract - The three-dimensional boundary layer over a rotating disk has long been a model flow for studying instability and transition. In 1995 Lingwood [*JFM* **299**] showed theoretically that this flow is absolutely unstable. Moreover, the critical Reynolds number R_a for absolute instability more or less coincides with the experimentally determined transition point. A little later Lingwood (1996) [*JFM* **314**] described an experimental study which appeared to corroborate her theory. Her analysis was based on the usual local stability analysis whereby the so-called parallel-flow approximation is made (i.e. the boundary-layer flow is approximated by a spatially homogeneous flow with a velocity profile equivalent to the local one in the real flow). Indeed the concept of absolute instability itself is purely local. The question addressed in the present paper by means of direct numerical simulation is: How does the real spatially inhomogeneous flow behave globally in the region of absolute instability? For example, is there a linear amplified global mode? The region of absolute instability extends from R_C to a Reynolds number of infinity where the maximum growth rate is found. Many examples of global/absolute instability have been studied by previous authors. See, for example, Huerre and Monkewitz (1990) [*Ann. Rev. Fluid Mech.* **22**]. And, had the rotating-disk boundary layer followed the conventional pattern, we might have expected to find an amplified global mode downstream of the onset of absolute instability. However, after carrying out a painstaking and careful study based on direct numerical simulation of the complete linearized Navier-Stokes equations, we find that the long-term global behaviour for the rotating-disk boundary layer is convective at all Reynolds numbers. Nevertheless our results are in good agreement with Lingwood's experimental investigation. In brief, what appears to happen is that the short-term behaviour of the flow in the vicinity of R_C following impulsive excitation behaves very much like an absolute instability, exhibiting both temporal growth and upstream propagation. But the convective part of the disturbance is always much stronger and temporal growth is not sustained at any spatial location in the long term. Whereas for many flows which are locally absolutely unstable, the region of absolute instability acts like a global oscillator and dominates downstream regions of convective instability, for the rotating-disk flow the region of strong convective instability appears to dominate the absolutely unstable region existing downstream. The absolute instability gives rise to a region of transient temporal growth, somewhat like the transient spatial growth found with so-called algebraic instabilities.

Effect of surfactants on the stability of liquid film flow on a rotating disk

G. Leneweit[1,2], K.G. Roesner[1] & R. Koehler[2]

[1]TU Darmstadt, Institut für Mechanik, Hochschulstr. 1, D-64289 Darmstadt, e-mail: karo@tollmien.mechanik.tu-darmstadt.de;
[2]Carl Gustav Carus-Institut in der Gesellschaft zur Förderung der Krebstherapie, Am Eichhof, D-75223 Niefern-Öschelbronn, Tel: ++49-7233-68-443, Fax:++49-7233-68413, e-mail: physik.carus@t-online.de

The linear stability of thin liquid film flows was already described in the early 1960s. In the following decades, important contributions towards an understanding of the nonlinear evolution of film flows were achieved. Especially in industrial applications surface active agents, abbreviated as ‚surfactants', very often play a key role in modifying the stability characteristics. It is an interesting fact that surfactants are able to either stabilize [1] or destabilize [2] flowing films, depending on the solubility and volatility of the surfactant, and thus yield either plane film surfaces needed for coating or wavy surfaces with increased mass and heat transfer. Although the stabilizing effect of nonvolatile surfactants was sucessfully integrated into linear stability theories [1], there are no experimental results that enable quantitative comparison to existing theories so far. This is perhaps because experimental investigations on the stabilizing effects of surfactants are fraught with two major problems:

1. The monolayers formed by surfactants are usually not in thermodynamic equilibrium which is assumed by linear theories, but only gradually approach the equilibrium state.
2. Former studies mostly used detergents as surfactants which form soluble monolayers whereas stability in the linear concentration range can only be accomplished with unsoluble monolayers according to stability theories.

In this study, the latter problem was solved using a protein that forms unsoluble monolayers. The former problem is inherent to film flows and the thermodynamic properties of surfactants, but it could be minimized by realizing film flow on a rotating disk. The thickness of a rotating film is 100 to 1000 times smaller than that on an inclined plane, yielding much higher dimensionless film lengths.

Our results with artificially induced waves confirm the theoretical predictions on the wave velocities. Studying naturally induced waves, the spatial evolution of film stability allows us to conclude on the gradual approach of the forming monolayer to thermodynamic equilibrium.

This work was funded by the Deutsche Forschungsgemeinschaft (Ro 311/13-1,2).

[1] Whitaker, S. & Jones, L.O. (1966) Stability of falling liquid films. Effect of interface and interfacial mass transport. AIChE J. **12**: 421-431.
[2] Ji, W. & Setterwall, F. (1994) On the instabilities of vertical falling liquid films in the presence of surface-active solute. J. Fluid Mech. **278**: 297 – 323.

Loss of rotational symmetry and breakdown in the similarity equations for the flow between two rotating disks

R.E. Hewitt
Department of Mathematics
University of Manchester, Manchester, England
Email: hewitt@ma.man.ac.uk

Keywords - Symmetry breaking - Finite-time singularities - Stability - Exact Navier–Stokes

Abstract - We consider the flow of a viscous fluid forced by the independent rotation of two infinite parallel planes. We assume that the flow field possesses a radial self-similarity and concentrate on the low to moderate Reynolds number regime. The relevant governing equations are derived with no assumptions of rotational symmetry, and we show that an *exact* solution can exist corresponding to nonlinear, non-axisymmetric states. These steady, non-axisymmetric solutions appear through subcritical symmetry-breaking bifurcations of the classical axisymmetric, steady states. For example, when the disks are in exact counter rotation, a bifurcation point (leading to linear instability) is found at $Re \approx 50$; with the Reynolds number Re based on the gap width and rotation rate of the disks.

To determine the post-critical evolution, a fully nonlinear initial-value problem is considered and we show that unsteady calculations typically break down at a finite time with the development of a singularity in the (exact) system of equations. An asymptotic description is given in the neighbourhood of the singularity. The singular structure has an inviscid core flow to which an infinity of solutions are possible within the framework of the same asymptotic description. Exactly which breakdown structure is realized for the bulk of the flow in the initial-value problem is shown to depend on the initial conditions.

Direct Numerical Simulation of three-dimensional transition in the incompressible flow around a wing

by Y. HOARAU, P. RODES, M. BRAZA, D. ANNE-ARCHARD

Groupe E.M.T.2, Institut de Mécanique des Fluides de Toulouse,
Unité Mixte de Recherche CNRS/INPT UMR N° 5502,
Allée du Prof. Camille Soula, 31400 Toulouse, France
Tel. 33 (0) 5 61 28 58 36, Fax: 33 (0) 5 61 28 58 31, email: hoarau@imft.fr

Keywords – Turbulence – instability – 3D transition – DNS - wing

Abstract - The successive steps of 3D transition to turbulence are examined in the flow around a wing of constant NACA0012 section along the spanwise direction. The wing is placed in uniform flow at 20° incidence, Reynolds number 800. The solution of the complete Navier-Stokes system in velocity-pressure variables is performed by using the ICARE algorithm developed in IMFT, based on finite-volume predictor-corrector schemes. The algorithm is fully parallelised on distributed-memory supercomputers. This study analyses the successive transition steps from the primary (von Karman) instability to the secondary instability along the span. The birth mechanism of streamwise and vertical vorticity filaments is studied and the predominant spanwise wavelength are quantified. These steps of 3D bifurcation are analysed by global oscillator models (e.g. the Landau model), based of amplitude versus period evolutions, provided by the present DNS. The amplification of primary and secondary instability are provided by the spectral amplitude evolution of the fundamental frequencies in the downstream direction of the near wake. A conditional sampling of the DNS data near the wall allows study of the whole Reynolds-stress tensor and of velocity gradients in the context of phase-averaging decomposition. These data enable a critical assessment of different constitutive laws for turbulence, from the linear Boussinesq concept to non-linear ones.

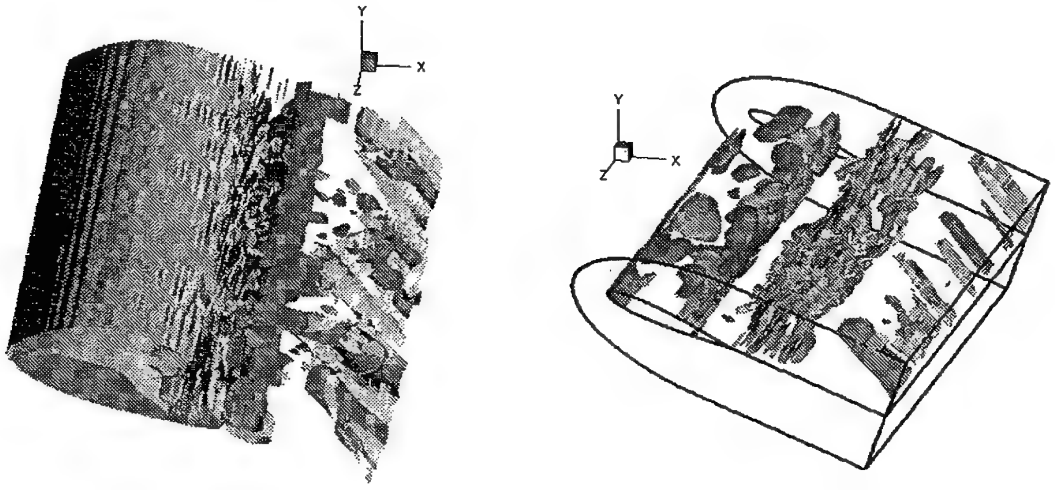

Figure a) Development of streamwise vorticity filaments and distortion of the von Karman vortex rows along the span. ω_z=-8.02 (red); ω_z=0.97 (yellow); ω_x= -1.46 (blue).
b) Vertical vorticity filaments, ω_y=±0.08 (blue and cyan) and ,• ω_y=±1.2 (yellow and purple).

Experiments on Boundary-Layer Transition Over a Rotating Compliant Disc — New Experimental Method

A.J. Colley and P.W. Carpenter
Fluid Dynamics Research Centre
University of Warwick, England.
Email: es2030@eng.warwick.ac.uk

Keywords – laminar-turbulent transition, compliant surfaces, rotating disc

Abstract – In order to investigate the laminar-turbulent transition in the 3D boundary layer in water over both a rigid and compliant rotating disc, experience to date has suggested that an enclosed chamber is necessary in order to detect the development of Type I (cross-flow) and Type II vortices and their subsequent break down to turbulence. This enclosure, in the form of a Perspex 'lid', is not needed in the case of air-based experiments. Colley et al (1999) [*Phys.Fluids* **11**] described such 'enclosed' experimental results for the rigid (and compliant) disc in water and showed the close agreement of these with those obtained theoretically: Malik (1986) [*J.Fluid Mech.***164**], experimentally in air: Lingwood (1996) [*J.Fluid Mech.***314**], and experimentally in water: Jarre et al (1996) [*Phys.Fluids* **8**]. However, although this agreement with the data from 'unconstrained' discs in air is acceptable, it must not be forgotten that the lid enclosure causes turbulent flow from the perimeter of the disc to be recirculated to the centre of the disc. Thus obviously, such an experimental arrangement was not ideal and it was therefore to be hoped that water-based experiments could be achieved without such a constraint.

Results have now been obtained in water without the lid enclosure for both a rigid disc and for a compliant disc. Furthermore, the results for the compliant disc case are obtained using a much more flexible material having a modulus of elasticity an order of magnitude less than previously investigated.

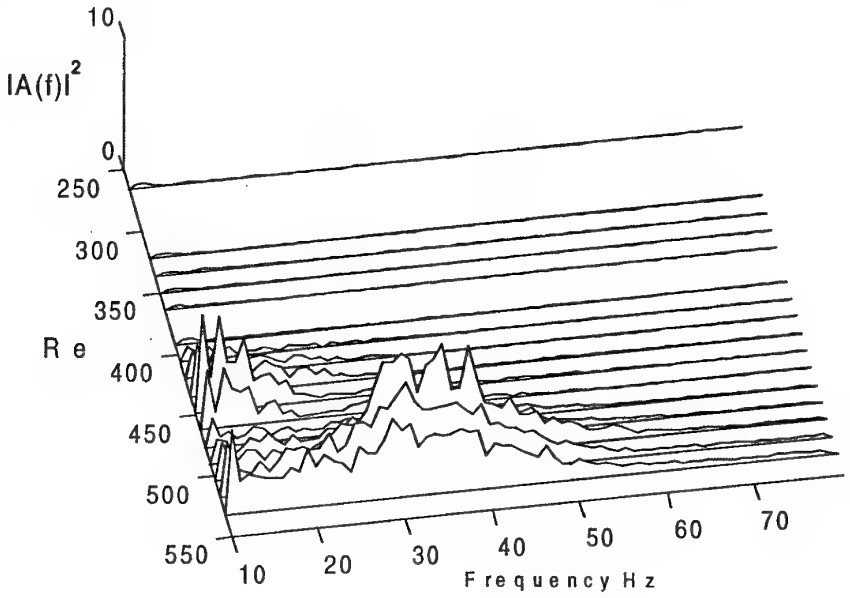

The above shows the ensemble-averaged frequency spectra for a range of values of Reynolds number for the compliant disc rotating in water without the lid. The development of a low frequency (15-20 Hz) can clearly be seen and is suggestive of the Type II instability, which attenuates and a higher frequency suggestive of the Type I instability then predominates with increasing Reynolds number up to the point of transition. Experiments carried out on the rigid disc only show the presence of frequencies suggestive of the Type I instability.
At a higher rate of rotation with the same compliant surface, the frequency spectra suggest that transition has been delayed to a higher value of Reynolds number, this because the effective compliance of the surface is increased due to the higher speed.

Breaking Up Process of Polymer Threads

A.Y. Gunawan, A.A.F. van de Ven and J. Molenaar
Department of Mathematics and Computing Sciences
Eindhoven University of Technology, The Netherlands
Email: a.y.gunawan@TUE.nl

Keywords - Morphology of Polymer Blends - Breaking Up -Stokes' Equations

Abstract Nowadays, the demand for new synthetic materials increases and becomes more specific. These new synthetic materials are produced by blending different types of polymers. The material properties of a polymer blend are strongly related to the morphology of the resulting polymer blend, which at its turn is highly determined by the blending process which takes place in an extruder. Therefore, the eventual material properties can be predicted if a better understanding of this blending process exists. During this process, due to shear stresses, long threads of dispersed phase are formed. Surface stresses cause these threads to break up in spherical droplets ('Rayleigh instability'). In this talk we deal with this breaking up process.

In a blend, interactions between two or more threads are essential. A blend containing two parallel threads in one plane, immersed in a second polymeric fluid (the matrix), is modelled, and the breaking up of the threads is investigated by analytical means. Initially, the threads are cylindrical, but due to thermal fluctuations they may have small initial perturbations. The flow in the blend is only driven by surface stress, and therefore the velocities and the shear rates will be small. Thus it is justified to model both the threads and the matrix as Newtonian fluids and to use the creeping flow approximation, resulting in Stokes' equations. Based on this equation, together with the boundary at the lateral surfaces of the threads, the (in)stability of the initial state is investigated. If the initial state becomes unstable, the threads will break up. It turns out that this breaking up can occur both in-phase as well as in anti-phase. This depends on the viscosity ratio of the two fluids and on the distance between the threads. All this is in correspondence with experimental observations.

The instability problem is solved analytically by means of a separation of variables in two systems of cylindrical coordinates, each connected to one of the two threads. In this, the dependence on the azimuthal directions is written in the form of Fourier series. Substitution of the general solution into the boundary conditions yields an infinite set of linear equations for the unknown coefficients. This set can be solved by using a method of moments; a solution in the first two orders will be presented. If this solution shows an increase in time of the initial perturbations, the initial state is called unstable and breaking up is observed. These results also predict whether the breaking up will be in-phase or in anti-phase.

Mechanism of the instability of a thin fluid layer sheared by a viscous fluid

F. Charru and E.J. Hinch
IMFT, Allée C. Soula, Toulouse, France. Email: charru@imft.fr
DAMTP, Cambridge CB3 9EW, United Kingdom

Keywords - Interfacial Instability - Sheared Viscous Flows

Abstract - The flow of a thin liquid layer sheared by a viscous fluid is encountered in many industrial processes such as coating or molten polymer handling. A well-known stability result is that long waves are stable if the thin layer is less viscous, and unstable if more viscous. One would like to understand why, so that one could exploit the phenomenon. We propose a physical mechanism for this instability for Couette flow, and show how the mechanism differs from the short wave mechanism described by Hinch (1984, J. Fluid Mech., **144**, 463). Consider a sinusoidal disturbance of the interface, with viscosity of the thin layer less than the other (figure). Due to different values of the viscosity, the velocity gradient is discontinuous, and velocity disturbances develop in order to satisfy continuity at the perturbed interface. The sign change of these disturbances with the viscosity ratio is the origin of the difference in the stability. From the shear stress continuity, mass conservation in the thin layer, and continuity of x-velocity at the interface, the leading order velocity disturbances as well as the wave speed can be found.

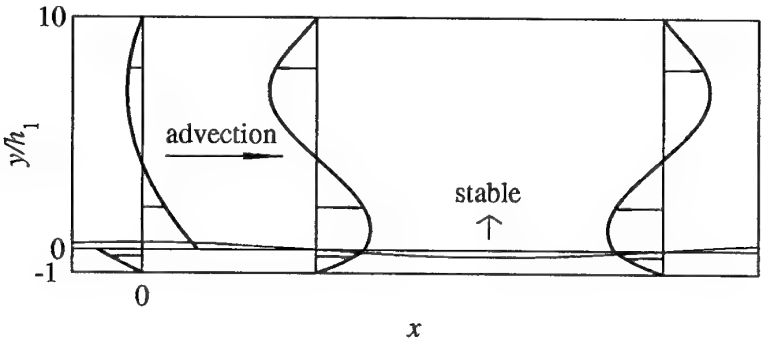

Dominant order x-velocity disturbance and out-of-phase inertial correction (eigenfunctions)

The wall reduces everything in the thin layer. Hence inertia only acts effectively in the thick layer. It turns out that the positive inertially induced couple in the lower 2/3 of the layer dominates, rotating the fluid so that there is a positive flow at the bottom and a negative flow near the top (to ensure no net flux). The inertial correction to the flow in the lower thin layer is not driven by the inertia there, but by the shear stress exerted by the inertial correction flow in the upper thick layer. This then drives a linear flow in the thin layer, and it is the horizontal divergence of this flow which causes decay of the disturbance. Hence the growth depends on the sign of the flow in the thick layer, which depends on whether the thin or thick layer is the less viscous. Estimates of the penetration depth of vorticity disturbances and effective Reynolds number give the right scaling against all parameters. In particular, the growth rate scales as k^2 if the upper fluid is bounded and as $k^{4/3}$ if unbounded.

Three dimensional stability analysis of extruded thin annular films

Kostas Housiadas and John Tsamopoulos[1]

Laboratory of Computational Fluid Mechanics
Department of Chemical Engineering, University of Patras
Patras 26500, GREECE
E-mail: tsamo@chemeng.upatras.gr

Key words: - Annular Film stability – Three dimensional stability

Abstract. The stability analysis of thin annular films is very important in a well-known process for manufacturing thin films of polymeric materials the Film Blowing Process, FBP. In FBP, molten polymer is extruded vertically upwards at a constant flow rate through an annular die and forms a thin tubular film of varying radius and thickness. The polymer freezes and it is collected at the other end. Internally applied pressure, axial drawing and cooling air at the outer free surface of the film affect the final product. Under the assumption of axial symmetry, the shape and the thickness distribution of the film has been studied both theoretically and experimentally at steady state and stability analysis to axisymmetric disturbances has been reported.

Experiments have shown [1,2] that the process may become unstable to both 2-D and 3-D disturbances. However, 3-D stability analysis is lacking and it will be given in this presentation, based on our recently developed alternative methodology [3,4] that allows us to eliminate previous approximations. This methodology consists of two crucial steps: The first one is to introduce new independent variables in order to make the location of the unknown free surfaces of the film known and constant. The second step is the application of a regular perturbation expansion with small parameter the ratio of the film thickness to its inner radius at the exit of the die.

Viscous, gravitational, surface tension and elastic forces have been taken into account in the model. Thermal effects have been included also. The Oldroyd-B constitutive equation has been employed. Our analysis has revealed, for the first time, that indeed non-axisymmetric disturbances become unstable under operating conditions that axisymmetric ones are still stable or exhibit smaller growth rates. This result is valid for both a Newtonian and a viscoelastic (polymeric) fluids. It is shown that the film is stabilized by increasing its elasticity and the cooling rate.

Acknowledgement: This work was supported by GSRT (EKVAN and PENED programs)

References:

[1]. Han, C.D. & Park J.Y., *J. Appl. Pol. Sc.*, 19, 3291-3297, (1975)

[2]. Ghaneh-Fard, A., Carreau, P & Lafleur, P., *AIChE J.*, 42, 1388-1396, (1996).

[3]. Housiadas, K. & Tsamopoulos, J., *J. Non-Newtonian Fluid Mech.*, 88(3), 229-259, (2000).

[4] Housiadas, K. and Tsamopoulos, J., *J. Non-Newtonian Fluid Mech.*, 88(3), 303-325, (2000).

[1] To whom correspondence should be addressed

Multi Phase Flows

Visco-thermal interaction in porous media

A. Cortis and D.M.J. Smeulders
Delft University of Technology, PO Box 5028, 2600 GA Delft, The Netherlands
Email: a.cortis@ta.tudelft.nl
D. Lafarge
LAUM, UMR 6613, Av. O. Messiaen, 72017 Le Mans, France
M. Firdaouss and J.L. Guermond
LIMSI, UPR 3251 (CNRS), BP 133, 91403 Orsay, France

Keywords - Porous Media - Scaling Experiments - Viscous and Thermal Effects - CFD

Abstract - The viscous and thermal interaction between the solid and the fluid in a porous medium as a result from wave propagation is inherently taking place on the microscopic pore scale. On the macroscale, where measurements can be performed and boundary-value problems can be stated and solved, the viscous and thermal interaction can be described in terms of so-called scaling functions. The scaling function for the inertial and viscous interactions between the gas and the pore space was introduced by Johnson et al. (1987) in terms of a dynamic permeability, whereas the dynamic compressibility introduced by Champoux & Allard (1991) describes the heat exchange effects between the two domains. Both scaling functions are described by averaged parameters such as the tortuosity α_∞, the viscous and thermal permeabilities k_0 and k_0', and the viscous and thermal lengthscales Λ and Λ'. These parameters comprise the information on the microgeometry of the porous material, and they can be evaluated by solving the Laplace and Stokes equations for such a microgeometry. For different pore microstructures, we computed these thermal and viscous parameters by means of Finite Element Methods (FEM). Once these parameters have been determined, the scaling functions can be calculated, and directly be compared with FEM computations for oscillating flow. For the case of smooth pore geometries, these FEM computations are in excellent agreement with the proposed scaling functions. However, as it was also previously suggested (Smeulders et al. 1994, Firdaouss et al. 1998), we found that the viscous scaling function fails for sharp-edged pore structures. Nevertheless, the temperature scaling function still remains sufficiently accurate in this case. The findings for the viscous scaling function will experimentally be verified by means of a piston-induced oscillating fluid flow through a scaled porous medium consisting of an ensemble of orifice plates. This will enable a direct comparison between experiments and numerical predictions for a sharp-edged structure.

References

Champoux Y, Allard JF 1991. J Appl Phys 70, 1975–1979.
Firdaouss M, Guermond JL, Lafarge D 1998. Intl J Engng Sci 36, 1035–1046.
Johnson DL, Koplik J, Dashen R 1987. J Fluid Mech 176, 379–402.
Smeulders DMJ, van Hassel RR, van Dongen MEH, Jansen JKM 1994. Intl J Engng Sci 32, 979–990.

Flow and reaction in solid oxide fuel cells

A.C. King, R.J. Cooper and J. Billingham
School of Mathematics and Statistics
University of Birmingham, UK
Email: a.c.king@bham.ac.uk

Keywords - Fuel Cells - Reacting Flow

Abstract - Solid oxide fuel cells (SOFCs) are a clean and efficient alternative to conventional electricity production. They can and will be used on a local scale to provide power for individual homes, schools, hospitals and the like and also on a large scale as auxiliary power generators for whole cities. Using the property of a solid ceramic, zirconia, to be able to conduct oxygen ions when hot (typically between $700°C$ and $1000°C$), we can generate electricity by burning hydrogen (H_2) or methane (CH_4) according to the reaction scheme

$$CH_4 + H_2O \rightleftharpoons CO + 3H_2$$

$$CO + H_2O \rightleftharpoons CO_2 + H_2$$

$$2H_2 + O_2 \rightleftharpoons 2H_2O$$

$$2CO + O_2 \rightleftharpoons 2CO_2.$$

Our study of a new tubular design of SOFC consists of a fluid flow model for the gas mixture and a model of the flow of oxygen ions into the system through the zirconia layer. The reaction scheme above appears in the model as boundary conditions, since all the reactions take place on the anode surface, due to the presence of a nickel catalyst in the anode composition. The model takes advantage of the small aspect ratio of the tube, and the dominance of reaction processes over all others to find an asymptotic solution for the mass fractions of all the chemical species involved, and then proceeds to make predictions about the power and current in the cell.

PIV measurements of an isothermal single burner flow

S Kucukgokoglan, A Aroussi, M Menacer, S.J Pickering

School of Mechanical, Materials, Manufacturing Engineering and Management
University of Nottingham, *Nottingham, NG7 2RD, UK*

Keywords: PIV, swirling flow, coal burners

Abstract

The objective of this paper is to present experimental results of swirling flows from an isothermal single coal burner. Burners used in pulverised coal fired power stations produce a complex multiphase swirling flow including combustion. The motivation of the present investigation is the lack of sufficient knowledge on burner flows and the interaction between burners in power station furnaces. For the purposes of this research the problem has been simplified so that the fundamental mechanisms can be identified.

In this application, Particle Image Velocimetry (PIV) technique has been used to extract velocity measurements. This new approach is a big advantage on the LDA method for a proper comparison of flow patterns with the computational modelling. The local velocity vectors, average velocity, velocity magnitude, and streamlines are presented. These measurements give an insight into the burner flows in a furnace.

The PIV system is based on Nd:Yag twin pulsed lasers giving 150mJ at 15Hz and a Kodak ES 1.0 Megaplus CCD camera. The resolution of the camera is 1008x1018 array pixels, with 256 grey levels. The experimental rig, of a small scale furnace model, consists of a tank made from a stainless steel frame with glass and Perspex walls, where the burner discharges. Swirl is generated by means of vane swirlers where the flow rate is controlled by a variable speed pump.

The results obtained from the PIV measurements are presented as velocity vectors, velocity magnitudes, streamlines and vorticity contours. They were obtained from a distance of 1/2D up to 8D from the burners exit, where D is the burner exit diameter. The flow field has been mapped to the longitudinal and vertical planes at 1/2D, 3/4D, D, 1.5D, 2D, 5D and 8D.

Transition from the perfect core-annular flow to discontinuous core, continuous annular flow in a constricted tube[1]

Ch. Kouris and J. Tsamopoulos
Laboratory of Computational Fluid Dynamics, Department of Chemical Engineering
University of Patras, Greece
Email: tsamo@chemeng.upatras.gr

Keywords: - Flow Transitions in Core-Annular Flow - Constricted Tube - VOF

Abstract – In this study we investigate the time evolution of the axisymmetric Core-Annular Flow (CAF) in a cylindrical tube whose radius varies sinusoidally with the axial distance and for such values of the operating conditions that the interface between the two immiscible fluids loses its integrity. Then, the bi-continuous CAF becomes discontinuous core, continuous annular flow. The goal of this study is to simulate the experimentally observed pulsing flow regime which occurs in trickle bed reactors which is characterized by the continuous flow of the annular fluid and a periodic transition between continuous and discontinuous flow in the core. To our knowledge, this task can be performed optimally by identifying the fluid/fluid interface using the Volume of Fluid (VOF) numerical method of solution. The procedure that we have developed consists of the following steps: (1) The continuity, radial and axial momentum equations are transformed using a body fitted coordinate transformation. This transformation is essential in order to impose accurately the no-slip, no penetration conditions on the wavy solid wall. Although the generated mesh consists of quadrilaterals in the computational domain, in physical space it is neither orthogonal nor conformal. (2) The equations of motion of both fluids are solved in space using central finite differences in a staggered mesh imposing periodicity of all variables in the axial direction. (3) The momentum equations are explicitly advanced in time, while the incompressibility constraint is used to compute the pressure field at the current time step. (4) The interface is tracked by a passively convected scalar quantity, $F(x,y,\tau)$, which is the percentage of the volume occupied by core fluid to the volume of the computational cell. The interface at each cell is approximated by a line whose normal vector is computed using Young's method, which is $O(kh^2)$ where k is the curvature of the interface, and the constant term of the equation of this line is computed by the constraint that the volume of the core fluid inside the computational cell equals F. Particular attention has been given to the interface reconstruction as well as the time integration of the volume of fluid function as the mass of each fluid is indeed conserved with an error $<10^{-6}$ % after 10^5 time steps and although the interface has undergone drastic topological changes. The effect of surface tension has been incorporated as a body force according to Brackbill, Kothe and Zemach (1992). The left figure shows the interface position, at time 2.985, when the annular fluid is 50 times more viscous and 10 times heavier than the core one and when Re=25. Shortly thereafter the interface breaks up forming one and subsequently more bubbles. The right figure shows the time evolution of the volumetric flow rates of both fluids. Different patterns of breaking up arise depending on the operating conditions and the fluid properties.

[1]Research partially supported by the Gen. Secretariat of Res. & Technology of Greece (EPET II, Grant # 550)

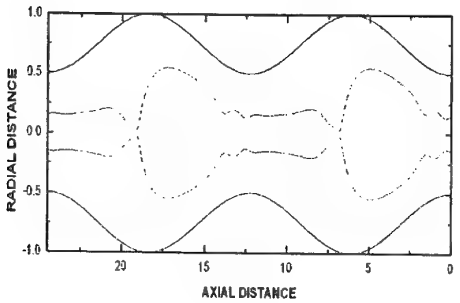

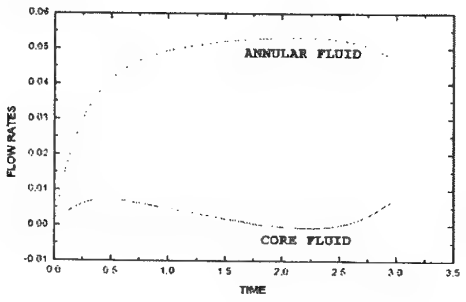

Effect of particle phase on vortex shedding mechanism in two phase planar jet flow

Mutlu Tunç[1], C.Ruhi Kaykayoğlu[2] and Orhan Gökçöl[2]
[1]İstanbul University, Faculty of Engineering
Department of Mechanical Engineering
Avcılar, 34850, İstanbul, Turkey
Email: mtunc@istanbul.edu.tr

[2]Bahçeşehir University, Faculty of Engineering
Bahçeşehir, 34900, İstanbul, Turkey
Email: rkaykay@bahcesehir.edu.tr

Keywords - Two-Phase Jet Flow, Vortex Dynamics

Abstract - In this study the effect of particle size and particle concentrations on the unsteady evolution of a two-phase planar turbulent jet flow is investigated by using a purely Lagrangian computational model. The flow field is modeled by the vortex elements so called Discrete Vortices. The solid sphere particles injected into the upstream jet flow are acted as the second phase. While the viscous effects are mimicked by using a Random Walk Approach, the Rankine Vortex Model is used to simulate the laboratory vortices. Both the passive (One-way Coupling) and active (Two-way Coupling) interaction between the particles and flow are studied. It was shown that the flow field characteristics are a strong function of both the particle diameter and particle concentration in the flow field. The instantaneous vortex distributions are investigated for ranges of different particle diameters. The jet flows are characterized by the side vortices at high Reynolds numbers. It was observed that the particle phase characteristics modify vortex shedding properties causing delays in downstream vortex patterns. Figures below show the cases for the instantaneous view of a two phase jet with the presence 50m, 75m, 100m particles. Figure (a) exhibits the instantaneous vortex distribution for the passive (One way coupling) case where particles are only carried out by the flow. On the other hand, due to complex interaction between the flow and particle, the flow fields are drastically different than the cases (b,c,d) for the active (Two-way Coupling) cases. Particle presence changes the nature of vortex formation along the edges of the jet. In order to understand the nature of the change, line marker is shown in figures. The change of the near field vortex structures are more evident for the cases where particle sizes are 75m and 100m respectively . While the particles seem to flow the basic flow characteristics in the one-way coupling case, this is not the case for two-way coupling simulation.

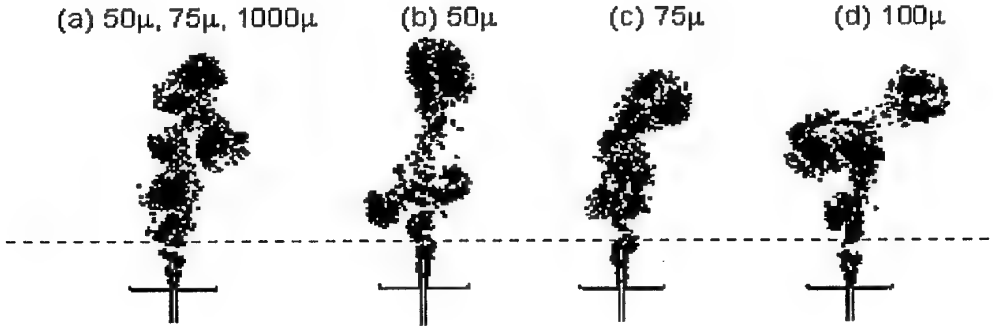

Transonic Two-phase Flows
- Unsteady Nucleating Flows in Wakes and in Turbulent Boundary Layers -

G. Winkler, M. Heiler, G.H. Schnerr
Fachgebiet Strömungsmaschinen
Universität Karlsruhe (TH)
Kaiserstrasse 12
D–76128 Karlsruhe, Germany
e-mail: guenter.schnerr@mach.uni-karlsruhe.de

Keywords: Transonic two-phase flow, nonadiabatic shock/boundary layer interaction, rotor/stator interaction

In order to improve the efficiency of steam turbine cycles in the very last stages low exit static pressures and temperatures are required. Therefore, the vapor starts to condense within the blade passages and creates a complicated unsteady turbulent transonic two-phase flow. The associated wetness loss caused by nonequilibrium condensation reaches values as high as 50% of the stage total loss. The working fluid typically contains natural impurities such as particles and soluble components which have a strong impact on local condensation dynamics. High metastable supersaturation initiates homogeneous nucleation and additional steady or unsteady shocks. Heterogeneous phenomena tend to reduce the shock strength and/or to stabilize moving shocks. Viscous effects like shock/boundary layer interaction and blades wakes, as known from adiabatic cascade flows, are strongly influenced in the two-phase region, especially the boundary layer separation and the frequency of the vortex dynamics in blade wakes. Rotor/stator interaction represents a natural source of unsteadiness of the internal flow with high frequencies. Stator wakes enter and pass through the rotor blade passages. The associated high temperature waves tend to diminish supersaturation and nucleation which can be identified at the rotor exit plane by instantaneously increasing droplet radii.

Our physical modeling includes simultaneous homogeneous and heterogeneous nucleation dynamics coupled to appropriate droplet growth laws, covering the whole Knudsen number range, imperfect gas effects and laminar and turbulent boundary layers. Axial cascade stages are considered with sliding interfaces in between. The numerical method is a cell centered MUSCL-type FVM method of second order accuracy in time and third order in space [1, 2].

We show in detail how nonequilibrium effects diminish in turbulent boundary layers near adiabatic walls. Concerning understanding and control of erosion by droplet impact on blade surfaces, we found that the relative droplet size maximum establishes inside boundary layers, near the edge, with about twice of the mean radii outside the viscous layer. By varying concentration and size of hetereogeneous particles we show that seeding is only effective in a very narrow parameter range and can be used for flow control and effective reduction of losses due to nonequilibrium. Stator inflow conditions of total pressure and temperature are varied to investigate onset of nucleation and droplet growth in the stator and in the rotor, respectively.

[1] Heiler, M., Instationäre Phänomene in homogen/heterogen kondensierenden Düsen- und Turbinenströmungen, Dissertation, Fakultät für Maschinenbau, Universität Karlsruhe (TH), Germany, 1999.

[2] Adam, S., Schnerr, G.H., Instabilities and Bifurcation of Nonequilibrium Two-phase Flows, J. Fluid Mech, Vol. 348, pp. 1–28, 1997.

Modelling of homogeneous condensation in Laval nozzle flows

G. Lamanna and M.E.H. van Dongen
Fluid Dynamics Laboratory, Department of Applied Physics,
Eindhoven University of Technology, The Netherlands.
Email: g.lamanna@tue.nl

Keywords - Nucleation - Droplet growth - Supersonic nozzle flow

Abstract - Numerical and experimental investigations are performed of nonequilibrium condensation processes of humid nitrogen in Laval nozzle flow. Objective of the present study is to validate models for homogeneous nucleation and droplet growth on the basis of an experimental study which includes both density field and droplet size measurements. For two different slender nozzles, a detailed comparative analysis of different condensation models has been performed [1, 2]. It was found that the best agreement was given by the following combination: the (corrected) *Internally Consistent Classical Theory* for the nucleation process and a generalised transitional growth model, with the droplet temperature calculated explicitly via the wet-bulb equation.

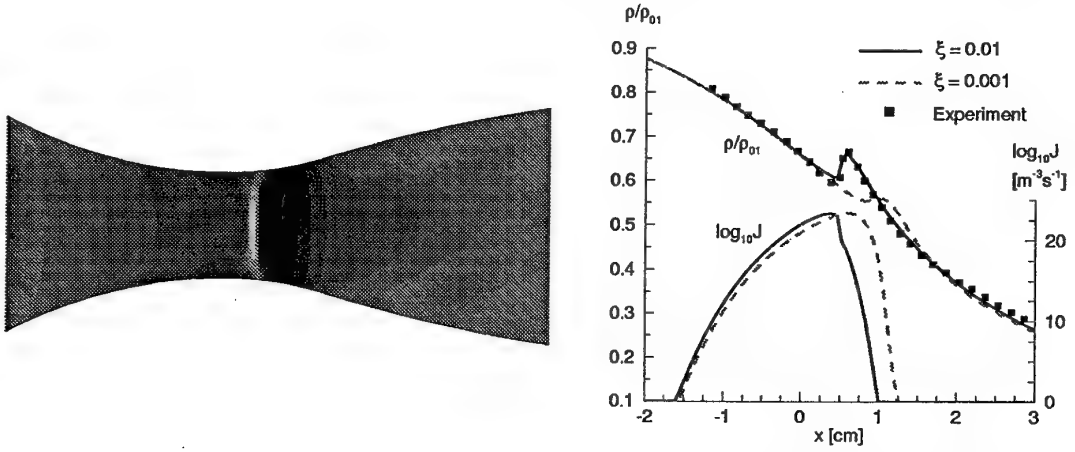

Nozzle G1: Numerical schlieren picture (left); axial distribution of densities and nucleation rates (right)

Here we intend to verify the sensitivity of the nucleation models for Laval nozzles characterised by strong 2D effects. The two-dimensional character of the flow can be distinctively recognised from the picture on the left, where the shock system presents a clear Mach stem close to the nozzle walls. By expressing the nucleation rate as $J = \xi \cdot J_{ICCT}$, four different conditions were considered, where the parameter ξ varies in the range $[0.001 \div 1]$. A result is shown in the figure on the right, together with the experimentally determined axial density distribution. From the picture, it can be inferred immediately that the best agreement is found for values of the parameter ξ close to 0.01, in full agreement with our findings for slender nozzles. From the picture it can also be inferred how crucial it is to predict correctly the nucleation rates, since an axial shift of only 2.5 mm of the nucleation peak causes significant differences in the flow pattern. For values of the parameter $\xi \geq 0.1$ the flow even becomes unsteady. For such unsteady flows a semi-analytical model is proposed, which predicts the frequency of oscillations.

References

1. van Dongen, M.E.H., Lamanna, G., Prast, B., *GAMM Conference Göttingen, 2000.*
2. Lamanna, G., van Dongen, M.E.H., *Nucleation and Atmospheric Aerosols, Rolla, Missouri, 2000.*

Numerical Simulation of Transient Nozzle Flow under Diesel Engine Conditions

M. Konstantinov*, F. Obermeier**

*IAV (Ingenieurgesellschaft Auto und Verkehr) GmbH Chemnitz, Germany
** Technische Universität Bergakademie Freiberg, Germany
E-mail: M_Konstantinov@t-online.de

Keywords – Nozzle – Cavitation – Atomization – Spray

Abstract - The quality of atomisation of liquid fuel in a diesel engine is probably the most essential factor determining the performance of engine and the soot production. The atomisation process depends among other things on the velocity of the fuel exiting the nozzle and on the extent of cavitation within the nozzle.

Under real engine conditions unsteady fluctuations of the injection pressure of up to 100 bars are possible. Experimental investigations with nozzles demonstrate that even at the injection pressure of more than 200 bars cavitation may disappears for short times, provided the pressure increases sufficiently rapidly. Correspondingly, cavitation may be expected when the injection pressure decreases fast enough.

In the present paper a numerical model is presented which simulates the unsteady nozzle flow including the transient behavior of cavitation. For that purpose the two-phase nozzle flow (liquid and cavitation bubbles) is replaced mathematically by a single flow characterized by an artificial barotropic equation of state, where the density varies sharply between the density of vapor, when the total pressure decreases to the vapor pressure, and the density of liquid, when the pressure is slightly above the vapor pressure.

The disappearance and re-occurrence of cavitation zones observed experimentally are nicely reproduced by the numerics. Examples of different cases of steady and transient flow and pressure conditions are discussed. The model presented may be used in different CFD-Codes for the problem of spray formation and liquid atomization.

DPIV in a particle-laden gas flow - The influence of the particle fluctuating velocities on the accuracy of several cross-correlation-based analysis methods

B. Grota and Prof. Dr. K. Strauss
Chair of Energy Process Engineering and Fluid Mechanics
Department of Chemical Engineering, University of Dortmund, Germany
Email: grota@ept.chemietechnik.uni-dortmund.de

Keywords - PIV in gas-solid flows - accuracy of PIV analysis - particle fluctuating velocities -

Abstract - It ist well known that the accuracy of PIV measurements among other things depends on the number of tracer particles contained in the correlation window and on the extent of uniformity of the tracer particle movement. These are two reasons why particle velocity measurements with PIV in highly turbulent, dilute particle-laden gas flows often leed to great errors in the displacement measurement. In this study the effect of particle fluctuating velocities on the accuracy of the mean particle velocities calculated by several PIV analysis methods is investigated. These methods are applied to both measured and simulated PIV-data of gas-solid flows in a vertical channel with a mean particle volume ratio of 10^{-3}. The particle fluctuating velocities are in the range of one third of the mean particle velocity. It was found that in spite of a good performance of PIV-recordings and PIV analysis parameters (concerning the in-plane and out-of-plane loss-of-pairs e.g.) the conventional PIV analysis does not calculate the correct particle displacement. Even if the correct mean displacement is used as a window-offset for the cross-correlation analysis, the calculated displacement is not identical with the given one. To

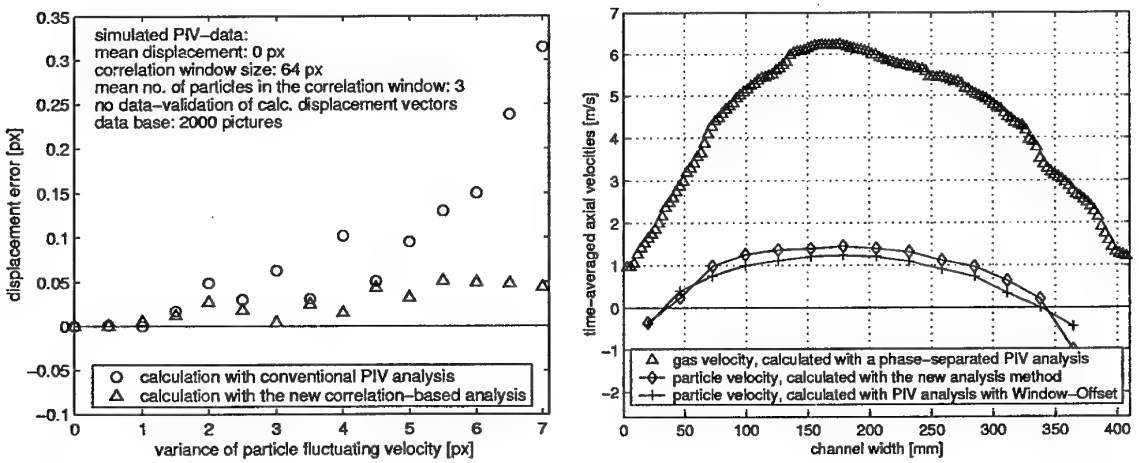

Influence of particle fluctuating velocity on displacement error for simulated PIV data (left), measured velocity profiles in a particle-laden gas flow ($Re > 10^4$)(right)

overcome this problem a new analysis method for estimating the mean particle velocity in the described flows has been developed. The proposed analysis method is mainly based on adding up the cross-correlation functions of several PIV picture pairs. This method is very fast and supplies the best results for the measured and simulated PIV-data. Another significant advantage of the new method is that no further data validation of the calculated displacement vectors is necessary. To demonstrate the efficiency of the developed analysis method some experimental results of the described gas-solid channel flow will be presented.

Effect of the particles' scattering in particle–wall collisions on dilute and dense gas–particle flows over obstacles

Yu.M. Tsirkunov, S.V. Panfilov and A.N. Volkov
Department of Physical Mechanics (M4)
Baltic State Technical University, St.Petersburg, Russia.
E-mail: tsrknv@bstu.spb.su

Keywords - Direct Simulation of Particles' Scattering - Models of Collisionless and Collisional Particle Phase - Flow over a Wedge

Abstract - In actual gas–particle flow over a body or an obstacle, the process of impact particle–wall interaction is, as a rule, random in nature, that results in a nonregular rebound of particles and, hence, their scattering. This phenomenon is caused by two main reasons: surface roughness and nonsphericity of particles. In the case of nonregular reflection of a particle, its parameters just after rebound should be considered as random values, which must be described in terms of the probability density functions. One of the most important performance of a nonregular particle reflection is the scattering indicatrix.

In the present study, the scattering of spherical particles from a rough surface as well as the scattering of nonspherical particles from a smooth surface are analyzed separately. The surface roughness is specified by the two-dimensional stochastic profile taken from the experiments on erosion, or generated with the use of a special algorithm. Every single collision of a particle with a roughness profile was calculated on the basis of the semiempirical model applied for the local wall inclination. When simulating the particle–rough wall impact interaction, we took into account the shadow zones on the roughness profile that occur at small angles of impingement, and also possible multiple particle–wall collisions within one hollow on the profile. The shape of nonspherical particles was taken as an ellipsoid of revolution or a cube. The reflection of nonspherical particles was considered in simplified two-dimensional formulation. In all cases the scattering indicatrixes were obtained by direct simulation method. Numerical results for ellipsoidal and cubical particles are compared with the ones for spherical particles.

Supersonic gas–particle flow over a wedge with the rough surface was investigated, as an example, to establish, in the frame of the one-coupling approach, the role of particles' scattering in the forming of the dispersed phase flow pattern. Particles were assumed to be spherical. Particle volume fraction in the free stream was varied in a wide range, so that the dispersed phase may considered as the collisional medium or the collisionless one, depending on the fact that either particle–particle collisions play an important role in the flow or not. The Crowe approach and the DSMC method were used for computational simulations of particle phase flow fields. In parallel with consideration of flow of mono-sized particles, motion of the dispersed phase with the log-normal particle size distribution in the free stream was simulated. In the latter case the particle radius ranged from 1 μm to 100 μm. In all calculations, the particle diameter was less than a cycle of the roughness. The dispersed phase flow field and the effect of shielding of a body surface from high-speed particles by a layer of colliding particles were studied in details.

This research was supported by the Russian Foundation for Basic Research under grants N 96-01-01467 and N 99-01-00674.

Hydrodynamic interactions in homogeneous bubbly flows

F. Risso and K. Ellingsen
Institut de Mécanique des Fluides de Toulouse,
Allée C. Soula, Toulouse, France
Email: risso@imft.fr

Keywords - Bubbles - Hydrodynamic Interactions - Liquid Induced Velocity

Abstract - Bubbly flows occur in many industrial and geophysical situations. Their complexity comes from the large number of interfaces that separate the gas and the liquid. Here, we focus on situations where the only cause of motion is the buoyancy that acts on bubbles, the liquid being otherwise at rest. The objective is the understanding of the hydrodynamic interactions between bubbles. The strategy consists in comparing experimental results obtained in homogeneous bubbly flows with the reference situation of an isolated rising bubble.
The experimental test section is an open glass tank of 700 mm height and 150 mm width, filled with tap water. A regular array of 14*14 capillary tubes located at the bottom allows the injection of a population of bubbles that all have the same diameter. The arrival times and velocity of the bubbles are detected by means of a double optical probe. The liquid velocity is measured at the same point by a two-component Laser Doppler Anemometer. Measurements over all the test section show that the flow is homogeneous provided the distance from injection is higher than 150 mm.

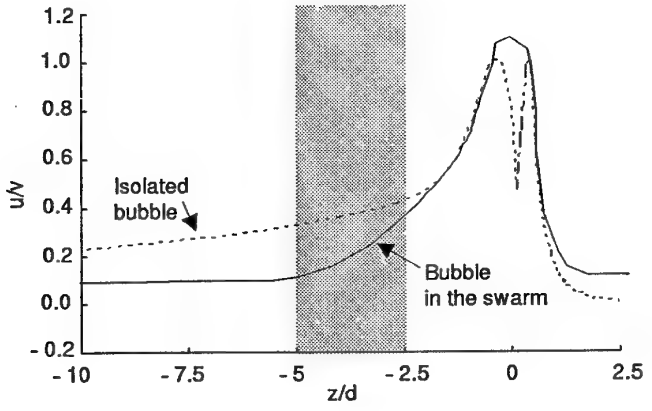

Liquid velocity versus the vertical distance from the bubble (positive z in front of the bubble, negative z behind)

The present results concern bubbles having an equivalent diameter d=2.5 mm and void fractions from 0 to 0.01. On the one hand, the statistics of the time intervals between two successive bubbles suggest the existence of a short-range repelling force acting between bubbles separated by less than 2.5d. However, the velocity measurements show that this interaction has no significant influence on the statistics of bubble motions. On the other hand, the liquid velocities measured behind a test bubble located inside the bubble swarm exhibit the following trends (see figure): up to 2.5d behind the bubble, the liquid velocity is similar to that induced by an isolated bubble; from 2.5d to 5d, the decrease of the liquid velocity is faster than behind an isolated bubble; beyond 5d an asymptotic situation independent of the presence of the test bubble is reached. These results indicate that the intensity of liquid velocity fluctuations depends on the non-linear interactions between the individual bubble wakes.

Modeling of annular-dispersed wet-gas flow through a venturi

M. van Werven, G. Ooms, B.J. Azzopardi and H.R.E. van Maanen
J.M. Burgers Centre, Laboratory for aero- and hydrodynamics,
Delft University of Technology, Delft, The Netherlands
E-mail: m.vanwerve@siep.shell.com

Keywords – Venturi – Annular-dispersed flow – Boundary layer – Deposition and re-entrainment

Abstract - A venturi can, in principle, be used to measure simultaneously the mass flow rates of gas and its condendate through a natural-gas pipeline. It is assumed that we deal with so-called wet gas, for which the mass flow rate of the liquid is not larger than that of the gas. As the liquid density is considerably larger than the gas density (also at the high gas-pressure), the liquid volume fraction is usually not more than a few percent. The gas velocity is assumed to be so high, that the flow pattern in the pipeline and in

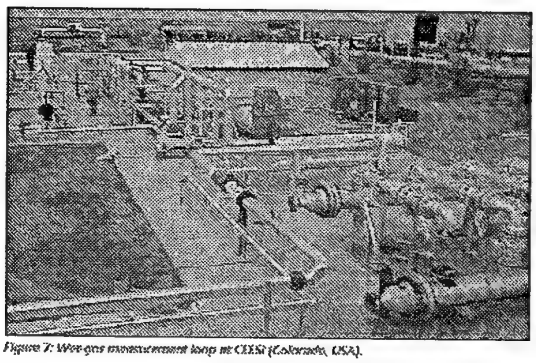

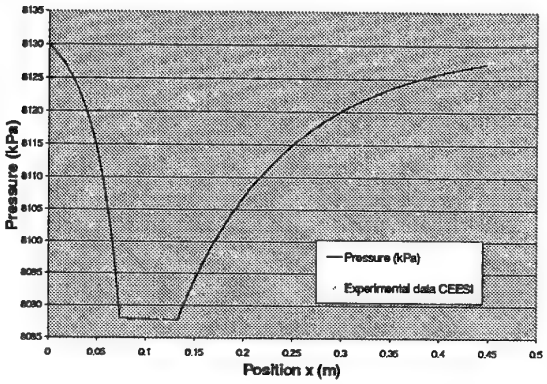

The wet gas experimental test loop at CEESI (left) and a typical calculated pressure profile along the venturi together with the measured data (right).

in the venturi is annular-dispersed flow. The idea is to measure the pressure drop over the throat of the venturi and over the total venturi, and to derive from these two measurements, using a theoretical model in inversion, the mass flow rates of gas and condensate. So it is essential to have a reliable theoretical model for the annular-dispersed flow of a wet gas through a venturi. To that purpose we have further developed an existing theoretical model published in the open literature. The accurate modeling of the boundary layer growth in the divergent part of the venturi (with the opposing pressure gradient) appeared to be crucial. Moreover the modeling of the deposition of droplets onto the venturi wall and their subsequent re-entrainment was essential. Much attention was also paid to the roughness of the liquid film at the venturi wall. The following quantities can be calculated with the model as function of the axial coordinate of the venturi: the velocities of the gas and the liquid droplets, the pressure, the concentration of the droplets in the gas, the thickness and roughness of the liquid film at the venturi wall, the boundary layer thickness of the gas, etc. Moreover, a set of experimental data (for the pressure drop over the venturi-throat and the total venturi) for a wide range of experimental conditions have become available from experiments carried out in the wet-gas test loop at the Colorado Engineers Experiment Station Inc., USA (see the figure on the left). We have compared these data with theoretical predictions made with the model. A good agreement was found. An example is given in the figure on the right. It will now be investigated, whether the mass flow rates of gas and condensate can uniquely be determined from the measured pressure drops over the throat and the total venturi or whether more information is needed.

Large Eddy Simulation of Turbulent Bubbly Flow

M. Milelli[a], B. L. Smith[a] and D. Lakehal[b]
[a]Thermal-Hydraulics Laboratory
Paul Scherrer Institute, Switzerland
Email: massimo.milelli@psi.ch
[b]Nuclear Engineering Laboratory
Swiss Federal Institute of Technology
Zürich, Switzerland

Keywords - Turbulence Modelling - Two-Phase Flow - Bubble Plume

Abstract - Complex, 3D mixing of multi-phase flows occur in a number of situations of interest in energy technology. Industrial applications include gas stirring of liquid metal ladles in metallurgical processes, aeration in water purification plants, venting of vapour mixtures to liquid pools in chemical and nuclear reactors. Environment protection problems involving bubble plumes are the aeration of lakes to avoid eutrophication and, generally, destratification of water reservoirs. For all these applications, the basic need is to determine the currents induced by the ascending gas plume in the surrounding liquid and thereby the consequent mixing and partition of energy, or species concentration, in the body of the liquid.

To predict these situations, it is important to study the large-scale turbulence modifications induced by the bubbles. Many models of a bubble plume have been published, mostly using a single-phase $k-\epsilon$ model with extra source terms in the k and ϵ equations to account for the interaction between the two phases. In addition, in some formulation, extra viscosity terms have been used to account for the bubble effect. These modifications are patch-ups which introduce *ad hoc* empirical coefficients which can be tuned to get good comparison with the data. Further, the hypothesis of turbulence isotropy has been demonstrated to be incorrect in the case of bubble plumes. The Reynolds Stress Models (RSMs), which are in principle appropriate for this kind of flow (since equations are solved for each component of the Reynolds stress tensor), are unstable and not robust enough, and it is difficult to achieve the convergency even for single-phase flows. Therefore, attention is focused here on Large Eddy Simulation (LES) turbulence models.

In LES, all large-scale structures which can be resolved by the numerical method should be separated from the small-scale structures (subgrid scales or SGS) which can not be captured on a given grid; the latter structures are modelled assuming homogeneity and isotropy. The main advantage of LES for this class of flows is that it inherently captures the interactions of the bubbles with the resolved large-scale structures up to those of wave number $K_b \sim 1/L$, where L is the size of the grid (equal to the bubble diameter), whereas the interaction with the subgrid scales can be approximated. In other words, the turbulent dispersion of the bubbles is due only to the largest structures, which are calculated directly with LES. Since this is a new area of study, many open questions will need to be addressed: a universally-accepted, two-phase subgrid model does not exist, and the influence of the grid on the simulation is also not clear since this determines the scales that are going to be resolved. To pursue this approach, the LES model was first implemented in the commercial CFD code CFX-4. First, a single-phase test has been calculated to validate the model against published data. Second, a simple case (a 3D box with homogeneous distribution of bubbles) has been run to study the modifications induced by the bubbles on the turbulence of the system and the effect of the filter (mesh size). The simplicity of the problem, which can represent the core of the bubble plume, permits a parametric study on the effects of the mesh, of the bubble size, on the subgrid model and on the turbulence scales to be carried out. The results have been obtained with the Smagorinsky subgrid model.

DESTRUCTION OF BUBBLE LIQUID, PRESSURE WAVES AND MASS TRANSFER

Nikolai A. Pribaturin

Institute of Thermophysics, Russian Academy of Science, Siberian Branch
630090 Novosibirsk, Russia
E-mail: pribaturin@itp.nsc.ru

Keywords: pressure wave, gas-liquid medium, mass transfer

The influence of pressure perturbation of bubble-liquid media on medium stability and mass transfer on interface is discussed. The results of the analysis is based on experimental data received during experiments on shock tubes. The absorption of gas on the liquid and vapour condensation in the liquid was chosen as mass transfer processes. The intensity of these processes is changed by the change of the gas sort. The specific amplitude of initial pressure wave was changed from 0.02 up to 20. Simultaneously measuring the void fraction and the pressure profile at the same point are used to define the mass flux and the mass transfer coefficient.

It is shown that exists a correlation between the stability of bubble medium to the action of pressure wave, regime of pressure wave propagation in the medium and the rate of mass transfer between phases. It was experimentally shown that the shock wave effecting the bubble system can cause an essential increase of mass transfer coefficient. The thresholds for the influence of a shock wave on mass transfer were established and the values of the reached specific mass flux were analysed. There is an analogy in the regime of pressure perturbation evolution in different medium, also. So, for example, for a liquid-vapour medium and suspension of a liquid with soluble gas exists areas, where an essential transformation of an initial perturbation to high amplitude shock pulse are occurs. Is shown that the effect of such amplification is directly connected with destruction of bubble liquid in a pressure wave.

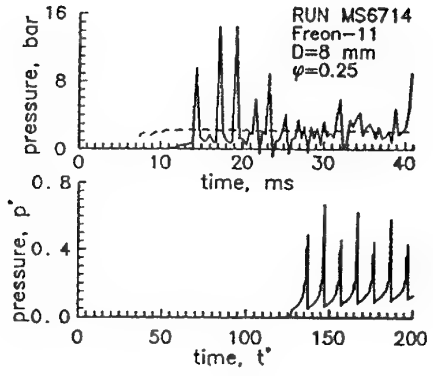

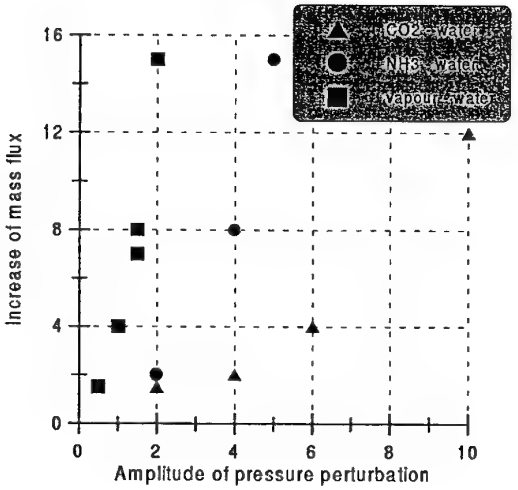

Fig.1. Simple of pressure wave evolution and amplitude amplification in bubble medium. Dash line show the profile and level of initial pressure perturbation.

Fig.2. Influence of pressure wave amplitude on mass flux between gas and liquid.

Flow Patterns in Two-Phase Rimming Flow

P.J. Thomas, G.D. Riddell, S. Kooner, G.P. King
Fluid Dynamics Research Centre, School of Engineering
University of Warwick, United Kingdom
Email: pjt@eng.warwick.ac.uk

Keywords - Rimming Flow - Coating Flows - Two-Phase Flows - Suspensions

Abstract - The flow inside a partially fluid-filled, horizontally rotating cylinder is considered (Fig. 1). This flow geometry is often referred to as a rimming flow. Rimming flows can display a number of fundamentally different flow patterns [1]. The experimental conditions determine which flow state is adopted. Different states are separated from each other by well-defined phase-transition boundaries. Recently we discussed for the first time [2] how the addition of successively increasing amounts of a granular additive affects the location of the transition boundaries in the phase diagram. Our previous data in [2] were obtained for spherical granules with one particular particle size and one particular particle density only. Here we will describe our latest experiments investigating how results depend on the granule properties. We will consider flows modified by spherical granules with different sizes and different densities. We will also briefly consider granule mixtures containing two different size classes and non-spherical granules.

In connection with our results in [2] we reported the observation of a new granular-banding structure appearing inside the cylinder. This structure is characterised by the formation of granular rings developing from granule accumulations at regularly spaced, circumferential locations on the inner cylinder wall (Fig. 2). Any two successive granule rings are separated from each other by a fluid region which is free of granules. Our latest results show that this banding structure can develop a hitherto not observed fine structure for granules with very low densities. Whenever this fine structure is present each of the relatively broad, primary rings has adopted a compound structure consisting of a set of three narrower, secondary rings. When the fine structure develops there are, thus, two different wavelength scales associated with the banding phenomenon.

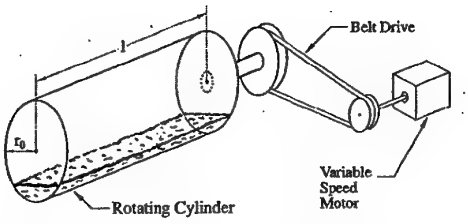

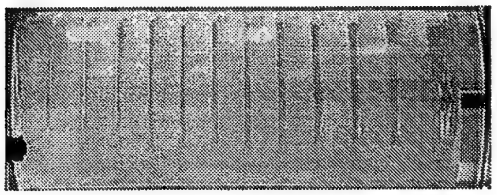

Fig. 1 (left): Experimental set-up. Fig. 2 (right): Photo of primary granular-band structure.

References:

[1] Thoroddsen, S.T., Mahadevan, L. (1997), Experimental study of coating flows in a partially-filled horizontally rotating cylinder. *Exp. in Fluids* **23**, pp. 1-13.

[2] Boote, O.A.M., Thomas, P.J. (1999), Effects of granular additives on transition boundaries between flow states of rimming flows. *Phys. Fluids* **11**, pp. 2020-2029.

Wavelength Scaling of Ripple Patterns in Rotating and Non-Rotating Fluvial Systems

F. Zoueshtiagh and P.J. Thomas
Fluid Dynamics Research Centre, School of Engineering
University of Warwick, Coventry CV4 7AL
United Kingdom
Email: es2201@eng.warwick.ac.uk

Keywords - Patterns - Granular Flow -

Abstract - The scaling of the wavelength of a new type of pattern in a rotating fluvial system is discussed. We compared our data to results for ripples in non-rotating fluvial systems. The particular rotating system we consider consists of a granule layer ($\approx 5mm$) on the bottom of a rotating, fluid-filled tank (diameter 50cm). Initially the granules are uniformly distributed across the bottom of the tank and the fluid above the granule layer is in a state of solid body rotation. The patterns are observed to form when the rotational velocity of the tank is instantaneously increased from one constant rotation rate ω_0 to a higher rotation rate ω_1. The fluid in the tank cannot follow the instantaneous acceleration of the tank. This results in shear forces being established between the granule layer and the fluid above it. If the increment $\Delta\omega = \omega_1 - \omega_0$ is sufficiently large the granules are set in motion and a re-organization process is initiated which results in the formation of spiral patterns such as the one displayed in the left figure below.

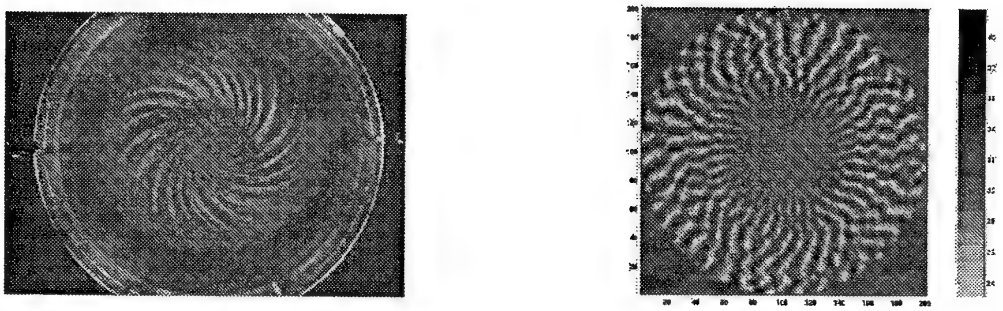

Typical spiral pattern formed by small ($\approx 0.3mm$) grey granules against the red bottom of the tank (left) and a typical computational pattern (right)

A simple cellular-automaton model is introduced which succeeds in producing computational ripple patterns similar in appearance to the spiral patterns observed experimentally (see right figure above). The computed ripple patterns are found to display the same scaling behaviour for the number of arms n and the radius r_0 of the inner patch from which the spiral arms originate. Prompted by the good correspondence between the experimental and the computational results, simple physical arguments are advanced which readily yield the observed scalings as a consequence of critical threshold conditions inherent in the physical system and in the computational model. The results suggest that the spiral patterns might be some type of rotating analogue of sand ripples such as observed on the bottom of the ocean. In order to test this hypothesis we compare our results to experimental data of other authors who studied ripple formation in various types of fluvial systems. The comparison reveals that the ripples formed in the different systems display the same type of scaling behaviour as the spiral patterns observed in the present experiment.

Differences and similarities of fluid and granular flows inside a rotating cylinder

T.S. Krasnopolskaya[1,2], S.A. Trigger[1,3], J.H. Voskamp[1], P.P.J.M. Schram[1] and G.J.F. van Heijst[1]
[1]Fluid Dynamics Laboratory, Department of Applied Physics
Eindhoven University of Technology, The Netherlands
[2]The Environmental and Resources Research Institute of Ukraine
Kiev, Ukraine
[3]Institute for High Temperatures, Russian Academy of Sciences
Moscow, Russia
Email: t.krasnopolskaya@tue.nl

Keywords - Cellular Patterns - Rotating Layer

Abstract -We discuss differences and similarities between patterns observed in fluid and granular flows inside a partially-filled horizontally rotating cylinder. Three kinds of liquid were used in our experiments: ordinary tap water, demi water (distilled water) and a viscous fluid, composed of mixtures of demi water and glycerin in various ratios. The viscosity of the fluid was varied from $\mu = 1cP$ to $\mu = 35cP$. Granular media comprised different mixtures of salt and poppy seeds, with the salt grains being, on average, 7 times lighter than the poppy seeds and 15 times smaller.

Eight classes of similar patterns in fluid and in granular mixtures were found experimentally for various volume fractions and angular velocities of rotation. These classes are: vortex-like structures (1); similar deformations of the rear front (2) and the leading front (3) of the flow pool; shark-teeth or cellular patterns in the azimutal direction (never reported before for granular flow) (4); fish-like patterns (5); creation of half-rotating and half-flowing structures (6); ring or curtain-shaped structures (7) and disk or ridge patterns (8).

In addition to the patterns common to both fluid and granular mixtures, some others are observed only in granular flows. For example, we observed a novel pattern, viz a rotating layer with a gap zone and a kink in the curvature of the layer surface in the azimutal direction (shown in the pictures below). Among patterns typical for granular media are segregated structures and traveling waves. These patterns demonstrate the dual solid-fluid nature of granular materials.

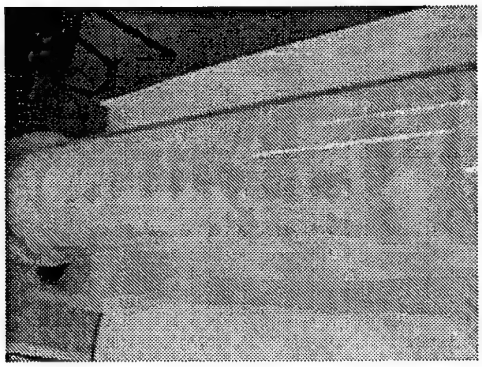

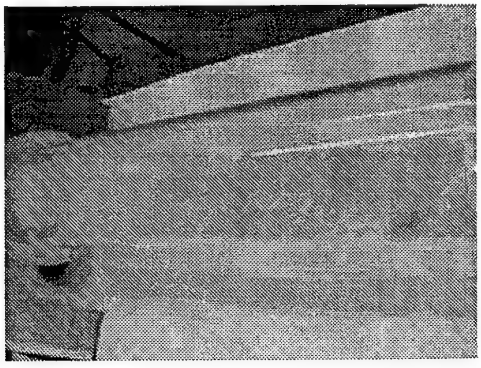

Photographs of a rotating granular layer showing pattern formation

From discrete to continuous models for stress distributions in sandpiles

S.A. Trigger[1,2], T.S. Krasnopolskaya[1,3], G.J.F. van Heijst[1] and P.P.J.M. Schram[1]
[1]Fluid Dynamics Laboratory, Department of Applied Physics
Eindhoven University of Technology, The Netherlands
[2]Institute for High Temperatures, Russian Academy of Sciences
Moscow, Russia
[3]The Environmental and Resources Research Institute of Ukraine
Kiev, Ukraine
Email: strig@gmx.net

Keywords - Dense Granular Systems - Stress Components

Abstract - Dense granular systems (DGS) have similar as well as very different features compared with liquids and with elastic media depending on the state, structure, geometry and type of motion. In contrast with the systems mentioned, the general macroscopic equations describing equilibrium states and motion of DGS have still not been formulated rigorously [1].

In this report we describe the static states for two-dimensional piles of particles (disks) with different structures and derive the distribution of microscopic forces as a function of the discrete coordinates of the particles and the macroscopic parameters, which determine the structure of the pile (grain size and inner contact angle between the grains, for example). On this basis we formulate the transition to the continuous (coarse-grained average) description of stress, which does not require in this case any phenomenological relations between the macroscopic (averaged) components. Then the possibility arises to check the applicability of elasticity theory to the problem of stress distribution in DGS, as well as to establish the relations between the continuous stress components. For the models considered, without inner torsion between the grains, we find rigorous constitutive relations between the macroscopic stress components. These relations depend on the structure of DGS and in general do not correspond with the relations used in the phenomenological consideration of the theory of elasticity. Inclusion of torsion leads to a principal redistribution of forces in sandpiles. We also discuss which kind of equations can be used for the description of equilibrium states in DGS. In parallel we find some useful macroscopic rules for the determination of average stresses, which can be used without detailed calculations of microscopic forces.

The results of this investigation provide an important step forward to a consistent macroscopic dynamic theory of DGS.

[1] P.G.de Gennes, Rev.Mod.Phys. 71 (1999) 374.

Maxwell's Demon in a Granular Gas

Ko van der Weele and Detlef Lohse

Fluid Dynamics and Heat Transfer (TN), University of Twente, P.O. Box 217, 7500 AE Enschede, The Netherlands.
E-mail: j.p.vanderweele@tn.utwente.nl; lohse@tn.utwente.nl
Keywords: granular gas – Maxwell's demon

Abstract – One of the extraordinary features of a granular gas, which can be traced back to the fact that the collisions between the gas particles are not completely elastic, is its tendency to spontaneously separate in dense and rarefied regions [1]. We present new results on this - theoretical, numerical *and* experimental - in the context of the clear-cut system of Fig.1 (top view): a compartmentalized box, mounted on a speaker, with a few hundred beads in each compartment. If the box is shaken vigorously the beads will be distributed uniformly, but as soon as the driving is lowered below a certain critical value, the beads instantly start to cluster. This results in a lot of nearly empty, "hot" compartments (containing a few rapid beads) interspersed with an occasional well filled "cold" compartment (containing many sluggish-moving beads). Thus, Maxwell's demon - so notoriously powerless in any ordinary, molecular gas - rules in granular gases.

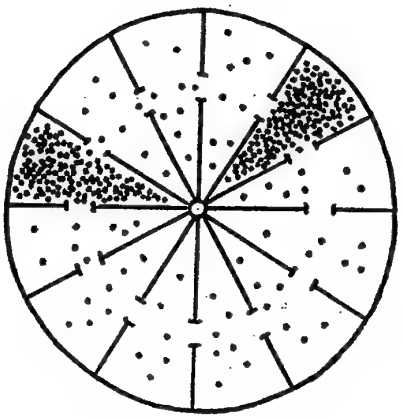

The original Maxwell-demon experiment [2] consists of only two boxes, but in the present work we go beyond this in several ways. First, we take a whole series of compartments, in a row or in a circle, and study the variety of non-trivial patterns (i.e., sequences of well-filled and nearly empty boxes) that arise. An example is shown in Fig. 2, for a circular array of 80 compartments, which originally were filled nearly uniformly. The patterns, wave-like structures and solitary peaks, are found to depend sensitively on the initial conditions.

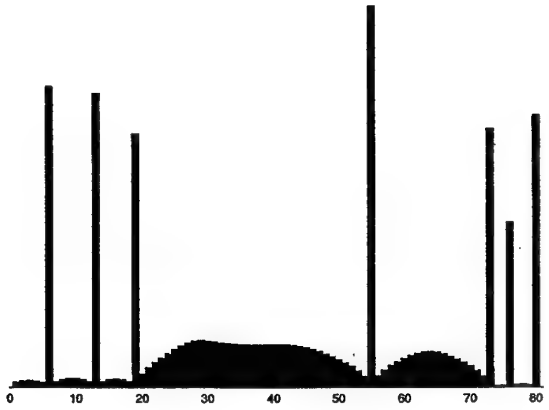

We also consider the continuum limit for an infinite number of very narrow compartments. In this case the dynamics of the system is governed by a convection-diffusion equation of the Burgers type. The phase clustering of the discrete model now corresponds to the transition from diffusion to anti-diffusion.

Second, we make the gas multi-disperse (a mix of particles of different sizes) and discuss the competition between the several segregation mechanisms at work: the well-known size segregation on the one hand, and the segregation brought about by Maxwell's demon on the other.

Finally, we have a brief look on possible applications of this work in the context of gas-fluidized beds.

[1] H.M. Jaeger, S.R. Nagel, R.P. Behringer, *Granular solids, liquids, and gases*, Rev.Mod.Phys. 68 (1996) 1259-1273.
[2] J. Eggers, *Sand as Maxwell's Demon*, Phys. Rev. Lett. 83 (1999) 5322-5325.

Rotating Flows & Vortex Dynamics

Structure of corner vortices in swirl flow in a cavity of square cross-section

P.A. Kuibin and E.A. Varlamova
Institute of Thermophysics, Novosibirsk, Russia
Email: kuibin@itp.nsc.ru

Keywords - Swirl flows in cavity - Corner vortex - Helical symmetry

Abstract - The structure of flow in a closed container of square cross-section subjected to a disk rotation on the top of the container is investigated experimentally as well as a model of the vortex structure of flow based on the integral laws is developed.

The modeling of vortex flows in closed containers is attractive due to (*1*) well-defined flow conditions in experiment (minimization of external actions) and (*2*) possibility to create a data base for development of numerical codes for problems with well-posed boundary conditions. The advantage of square geometry of container cross-section lies in convenience for application of the optical methods of the flow velocity measurements. In the same time such simple geometry is preferable in different branches of the industry. The structure of flow in a model of vortex combustor with square cross-section (Alekseenko et al., JFM, 1999, v. 382, 195-243) was shown to be close to flow in a cylindrical channel due to presence of corner vortices. In the case of disk-driven flow in a closed container of square cross-section we have found a single paper by Chiang et al. (Computers & Fluids, 1999, v. 28, 41-61) where numerical simulations were presented. The main attention was paid to the flow details at the Reynolds number $Re = R^2\omega/\nu = 1000$ (R is the disk radius, ω is its angular velocity and ν is the liquid viscosity). The simulations revealed a complicated structure of flow practically without corner vortices. Our PIV measurements in a transparent cubical container with flow of a water-glycerin mixture confirmed the simulated picture at Re = 1000. At larger Reynolds numbers the flow structure looks simpler and more evident come the corner vortices. As seen from figures *a*, *b* at Re = 2500 the main part of the middle cross-section is occupied by flow with practically circular pseudo-streamlines. Obviously such picture is provided by the corner vortices. The velocity components in the corners in the horizontal plane are small relative to the central area. A thorough analysis of flow in the corner revealed structure shown in figure *c*. One can see a vortex-source-like pattern. Vortex lines in the central part of the cube present parts of practically perfect helices. In the corners vortex tubes are deformed and vortex lines are twisted on them. Based on experimental data a model of central vortex

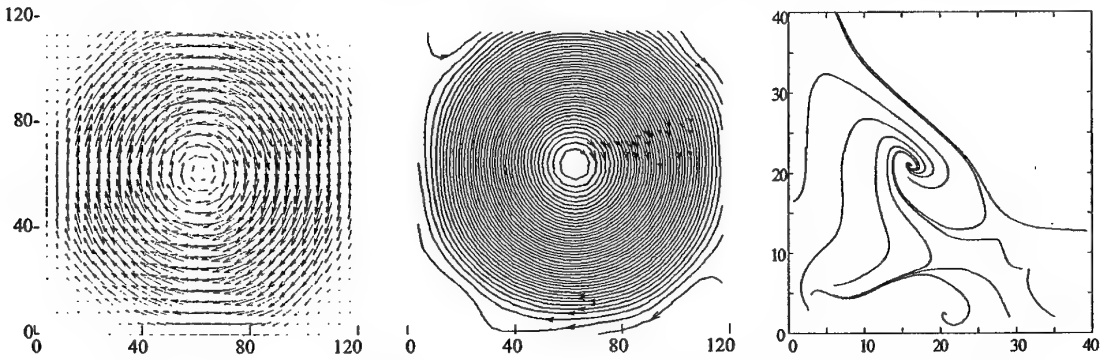

The vector flow map (a), pseudo-streamlines (b) in the middle horizontal cross-section of cubical cavity and pseudo-streamlines in the corner vortex (c)

with four corner vortices is constructed without account of the end-face effects. The model supposes a helical-like structure of vortex lines and uniform vorticity distributions in the vortex cores. The shape of vortex cores has being found from the solution of the problem on matching of regions with vortical and potential flows. All geometrical and hydrodynamical parameters of the model have being determined through the integral laws - flow rate, circulation, fluxes of momentum and moment of momentum in ascending and descending flows. In a perspective the model developed can be used for description of the vortex breakdown phenomenon in a cavity with square cross-section.

Changes in the axial symmetry of the velocity field and in the helical symmetry of the vorticity field downstream of a bend and a diffuser

V.L. Okulov*), O.G. Dahlhaug**) and H.I. Andersson**),
*)Institute of Thermophysics, Novosibirsk, Russia
Email: okulov@itp.nsc.ru
**)Norwegian University of Science and Technology, Trondheim, Norway
Email: ole.g.dahlhaug@tev.ntnu.no and helge.i.andersson@mtf.ntnu.no

Keywords - Swirl flows - Helical vortex

Abstract - Recent analyses of numerous experimental data for swirl flows show that the velocity field may be correctly approximated by axial helical vortices exhibiting either right- or left-handed symmetry or a combination of both [Alekseenko *et al*, JFM (382), 1999]. The existence of the relation $w_z = w_0 - rw_\varphi/l$ (with $w_0 = const$) between the axial (w_z) and tangential (w_φ) velocities for the flow-induced helical vortices with pitch - $2\pi l$ was established [Okulov, RJET (2), 1995]. The behaviour of the axial velocity profile depends on the sign of the pitch. When the vortex consists of right-handed helical filaments with positive pitch, the axial velocity exhibits a maximum on the flow axis. Likewise, if the vortex consists of left-handed helical filaments with negative pitch the axial velocity has a minimum on the axis. The main objective of the present study is to explore experimentally local disturbances and changes in axial and helical symmetry of vortices submitted to simple tube distortions: a diffuser and a bend. Three experimental configurations were examined: a straight tube with a diffuser (fig. *a*); a tube with a bend downstream of a diffuser (fig. *b*); a tube with a diffuser downstream a bend. The Reynolds number was kept constant at 280 000 in all experiments and swirling motion with swirl number (S) in the range from zero to 0.70 were generated upstream of the test sections. Profiles of all three velocity components were measured by means of LDV at three different cross-sections A, B and C; cf figs *a* and *b*.

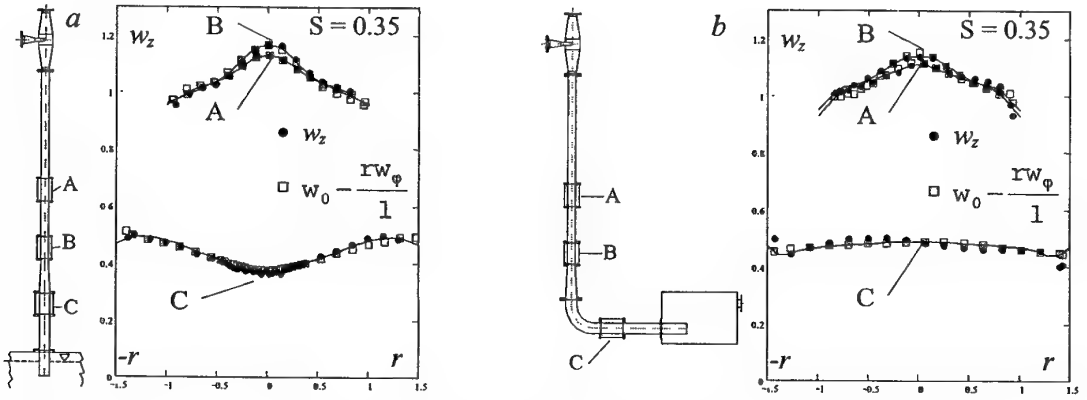

Two interesting examples are shown in the diagrams above. The measured axial velocity (points) is compared with axial velocity (boxes) deduced from the measured tangential velocity. These profiles reveal a close correspondence between the two at all test sections in both installations. This implies that the helical symmetry is conserved after the diffuser and bend. It is noteworthy that the axial velocity at section C is different in the two cases. Downstream of the diffuser in fig. *a* the axial velocity has minimum on the flow axis, which signifies a transition from right- to left-handed helical symmetry. Such transitions in swirl flows through diffusers are known as *vortex breakdown*; see, for example, the axial profiles in [Garg & Leibovich, Phys. Fluids (22), 1979]. If the diffuser is followed by a bend, however, the change of type of helical symmetry disappears in the tube downstream of the bend. Indeed, the axial velocity in fig. *b* exhibits a maximum on the flow axis, which can be explained as an effect of the centrifugal force caused by the bend and the extra amount of vorticity in the flow.

Influence of a vorticity distribution in the vortex core on abrupt alteration of the helical symmetry in swirl flows

T.O. Murakhtina*, ** and V.L. Okulov**
*Novosibirsk State University, Novosibirsk, Russia
**Institute of Thermophysics, Novosibirsk, Russia
Email: okulov@itp.nsc.ru

Keywords - Swirl flows - Helical vortex - Vortex breakdown

Abstract - An adequate modeling of the high swirl flows encounters an existence of abrupt changes in flow regimes. This phenomenon may be explained as spontaneous transitions between right- and left-handed helical vortices (with the pitch - $\pm 2\pi l$) generated under the same integral flow characteristics: the flow rate; the flow velocity circulation; the axial fluxes of angular momentum, momentum and energy (E). This fact was established for an axisymmetrical type of vorticity distributions in a core for swirl flows within the framework of the perfect fluid model [Okulov, Tech. Ph. Lett., 1996, 22(10)]. Any distribution of axial vorticity in the core of the axisymmetrical helical vortex is an exact solution for the Euler equations, hence the unique choice of the vorticity distribution is impossible within the framework of the model itself. The main goal of the present study is to investigate a question of an influence of a vorticity distribution choice on the spontaneous changes in flow regimes. Two widespread types of distributions with gaussian (G) and rational (R) approximations of the vortex core were studied. As the result it was shown that the choice between the approximations should depend on the values of the Reynolds number (Re).

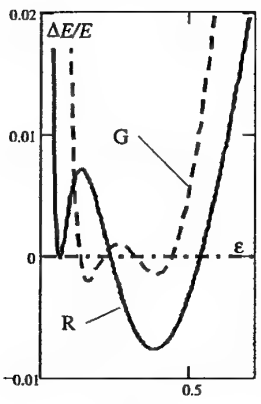

Fig. 1.

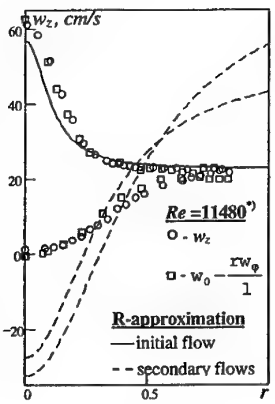

Fig. 2a.

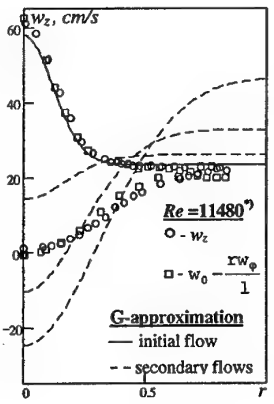

Fig. 2b.

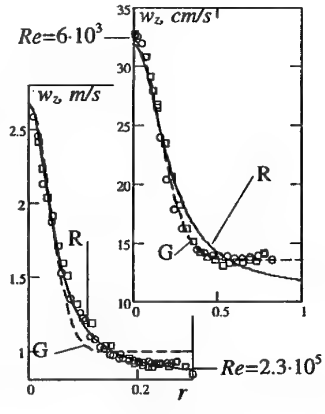

Fig. 3.

The problem was reduced to an investigation of an energy equation with a vortex radius, ε, as a variable. An analysis of the equation has shown that the number of roots (flow regimes) may be various, when the flow is described by different vorticity distributions in the core (*Fig.1*). The differences in secondary regimes of flow, corresponded to the roots in *Fig.1* are shown in *Fig.2a* and *2b*. Here the correlation between the measured axial velocity (circles) and the recalculated one (boxes) through the tangential velocity [Alekseenko *et al.* JFM (382), 1999] was made for the flow regime measured by Garg & Leibovich [Phys.Fluids, 22(11), 1979]*). We have analyzed data obtained in set-ups with the same parameters [Faler & Leibovich, Phys. Fluids 20(9), 1977; Sarpkaya & Novak, AIAA 99-0135] at different Reynolds numbers (from 3 000 to 230 000). The correlation of the G- and R-approximations with velocity profiles was made to choose between them. The results for the two flows with low and large Reynolds numbers are shown in *Fig. 3*. For low *Re*, corresponding to laminar regimes, the flows are more exactly described by G-approximation, while at large *Re*, for the turbulent flows, the R-approximation gives a better result. For this reason, the calculated secondary flows at low *Re*, showed in *Fig. 2b* describe experimental data better then in *Fig. 2a*. The R-approximation has a more smooth character over the tube cross-section and it naturally better describes the turbulent flows, where the vorticity diffusion from the flow core to its periphery is more intensive.

Fluid depth dependent evolution of isolated vortices in a rotating fluid

M.P. Satijn and G.J.F. van Heijst
Dept. of Physics, Fluid Dynamics Laboratory
Eindhoven University of Technology, The Netherlands
Email: m.p.satijn@tue.nl

Keywords - Rotating fluids, vortex dynamics

Abstract - The evolution of cyclonic isolated vortices in a rotating fluid has been studied with respect to their height-to-width aspect-ratio. This was done by carrying out laboratory experiments as well as by performing 3D numerical simulations. Depending on the value of the aspect-ratio several evolution scenarios were observed such as tripole formation, dipole splitting, dipole-monopole splitting and the formation of a triangular vortex (see the pictures below). These different instabilities were observed for subsequent lower aspect-ratios. It is known that for purely 2D flows the steepness of the vorticity profile determines the instability behaviour. Here, indeed an aspect-ratio dependent steepening of the initial vorticity profile was found to be responsible for these different evolutions. The change in the steepness of the vorticity profile is caused by two mechanisms: Ekman effects (not present in 2D modelling of the flow), making the profile steeper and (less important) lateral diffusion, which tends to make the profile less steep. These mechanisms act at different time scales in this problem: the Ekman time scale, which depends on the height H of the fluid column ($T_E = \frac{H}{\sqrt{\nu\Omega}}$), and the diffusive time scale, depending on the horizontal dimension L ($T_d = \frac{L^2}{\nu}$) of the vortex. Thus, for smaller fluid depth Ekman effects become more and more important, leading to the different scenarios in the vortex evolution.

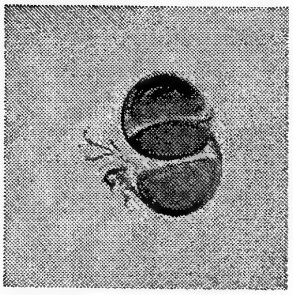
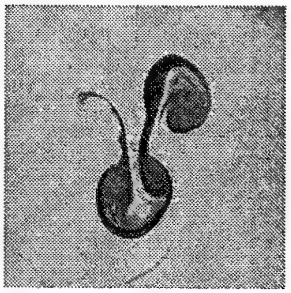
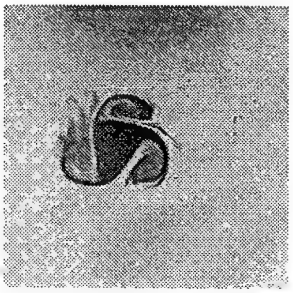

Experimental study of the multipolar instability

Christophe Eloy, Stéphane Le Dizès and Patrice Le Gal
Institut de Recherche sur les Phénomènes Hors Equilibre
CNRS UMR 6594, Universités Aix-Marseille I et II, France
Email: eloy@marius.univ-mrs.fr

Keywords - Vortex Dynamics - Rotating Flows - Elliptic Instability

Abstract - It is known that when a vortex is submitted to an external strain field, its streamlines become elliptic at first order. This deformation leads to the *elliptic instability* which has been recognized as a secondary instability in parallel shear flows and wakes. This instability mechanism has recently been generalized to flows with higher azimuthal symmetry (1) giving rise to the *multipolar instability*. Indeed, it has been shown theoretically that a small dipolar, tripolar or quadripolar deformation of the vortex has an unstable character. The present study is the first experimental evidence of the instability in a tripolar configuration.

We used an experimental set-up similar to the one used by Malkus (2) (see figure). A transparent deformable cylinder filled with water is rotated around its axis at a constant angular velocity. Two or three parallel rolls can be positioned in order to apply a dipolar or a tripolar constrain. Anisotropic particles are added and a laser sheet containing the cylinder axis is formed for visualization.

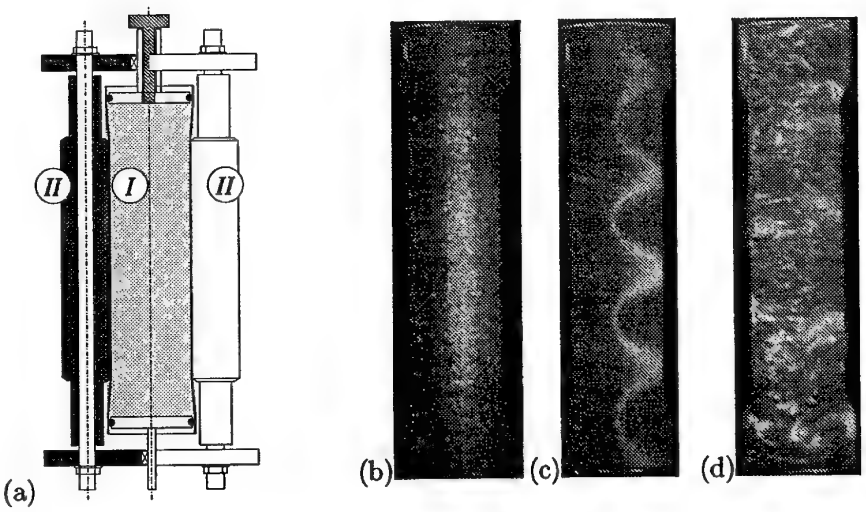

(a): Experimental set-up, deformable cylinder (I), rolls (II). (b,c,d): three successive images of the flow for a vortex submitted to a tripolar constrain

Depending on the aspect ratio and the angular velocity, different modes of the elliptic and triangular instability have been observed. Their wavelength and frequency, measured by image analysis, are in excellent agreement with theoretical prediction. For small angular velocity (above threshold), a single mode of saturated amplitude can be observed. However, for large angular speed, the multipolar instability eventually evolves to a vortex break up (figure d).

References

(1) - Le Dizès, S. & Eloy, C. *Phys. Fluids*, **11**(2), 500–502 (1999).
(2) - Malkus W. V. R. *Geophys. Astrophys. Fluid Dynamics*, **48**, 123–134 (1989).

Asymmetric vortex merging in a rotating fluid

R.R. Trieling, M.A.T. Doorewaard and G.J.F. van Heijst
Fluid Dynamics Laboratory, Department of Physics,
Eindhoven University of Technology, The Netherlands
Email: R.R.Trieling@tue.nl

Keywords - Vortex merging - Vortex dynamics - Rotating fluids

Abstract - The evolution of two-dimensional turbulence towards an organized state is characterized by complicated vortex-interaction processes. One of the important mechanisms is the interaction of two nearby like-signed vortices. Generally, these vortices will merge when their distance of separation is smaller than some critical value. If both vortices are identical this process leads to a single vortex which size is generally larger than that of the original vortices. Previous high-resolution contour dynamics calculations have shown, however, that the merger of unequal vortices with uniform vorticity is not always associated with vortex growth. In fact these asymmetric vortex interactions may lead to smaller vortices than the original ones.

In order to investigate whether these results also hold for vortices with continuous vorticity distributions, laboratory experiments were carried out in a rotating fluid. Cyclonic vortices were generated by locally syphoning fluid through perforated tubes. The initial flow characteristics were controlled by varying the suction rate, the forcing period and the separation distance of the tubes. The subsequent flow evolution was visualized by injecting different colours of dye into the cores of the vortices. High-resolution Particle Velocimetry (HPV) was used to obtain the vorticity field. The laboratory experiments were supported by contour dynamics simulations in which the continuous vorticity distributions were approximated by nested patches of uniform vorticity.

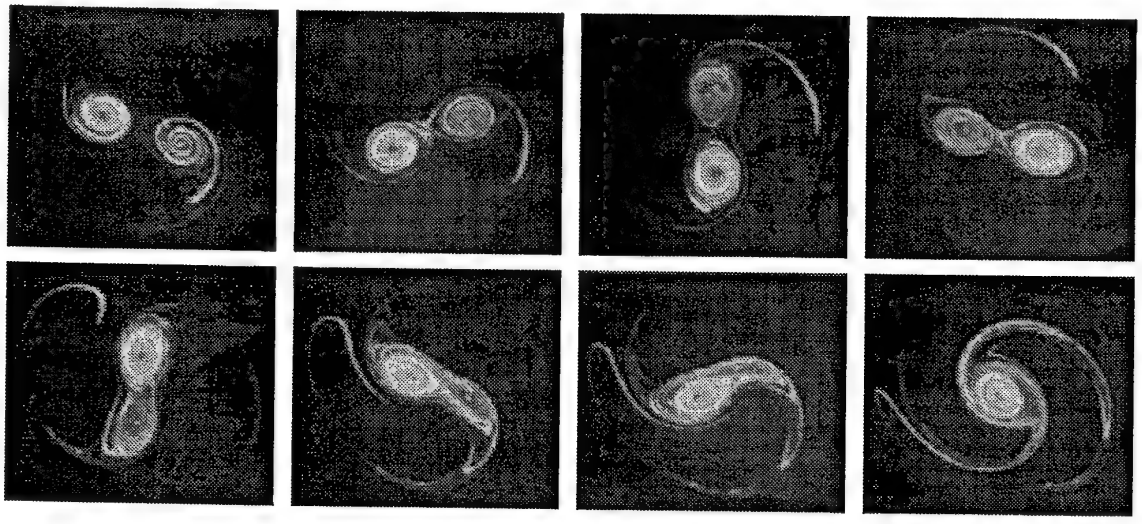

The dynamics of monopolar vortex structures on a topographic beta plane

J.-B. Flór
LEGI, Laboratoires des Ecoulements Geophysiques et Industriels
B.P. 53, 38041 Grenoble Cedex 09
France

I. Eames
Department of Mechanical Engineering
University College London
Torrington Place
London, WC1E 7JE, UK

Abstract

The dynamics of a monopolar vortex on a topographic beta plane is studied experimentally. Detailed measurements of the vortex structure are conducted by using high resolution quantitative velocity measurements. The initial velocity profiles were compared with similarity solutions describing monopolar vortices on the f-plane, and described in terms of a radius R_{vm}, maximum azimuthal velocity $v_{\theta m}$, and a dimensionless parameter α which characterises the steepness of the velocity profile.

The initial direction of motion of the monopolar vortex is critically dependent on α and weakly dependent of the initial strength and size of the vortex: isolated vortices ($\alpha \sim 3$) move North, while vortices characterised by $\alpha \sim 1$ move to the Northwest. When the azimuthal velocity decays weakly with radial distance ($\alpha < 1.4$), Rossby wave generation dominates the vortex dynamics and the translation speed of the vortex correlates with the Rossby wave speed. When the vortex is isolated ($\alpha > 1.4$), the translation speed is much slower than the Rossby wave speed.

To interpret the effect of the vortex structure on the direction of motion, a mechanistic model is developed which includes the Rossby force and a lift force arising from circulation around the vortex. The Rossby force results from the integrated effect of the Coriolis force on the vortex and drives the vortex North; the lift force is determined from the circulation around the vortex and drives the vortex West. The model does not include the effect of Rossby waves. Comparison with the experimental data reveals two regimes: $\alpha < 1.4$, where the vortex dynamics are dominated by Rossby waves and $\alpha > 1.4$ where good agreement is found with the model.

Numerical study of 3D wave structures developing in rotating containers due to baroclinic instability

N.G. Ivanov and E.M. Smirnov
Department of Aerodynamics
St.-Petersburg State Technical University, 195251, Russia
Email: aerofmf@citadel.stu.neva.ru

Keywords – Thermal Convection – Baroclinic Instability – Numerical Simulation

Abstract – The present work deals with oscillatory thermal convection in rotating containers filled with low-Prandtl-number fluid subjected to an imposed radial temperature difference. The appearance of the baroclinic instability is investigated for two flow configurations. The first one is an annular ring of fluid confined between two concentric vertical cylinders and two flat rigid lids. The second configuration is a cylindrical container with an upper central disk placed in contact with the liquid (see Figure).
Computations have been carried out on the base of a 3D multi-block finite-volume code of second order accuracy both in space and in time. Block-structured grids were used, with nodes clustered to the wall and to the free surface.

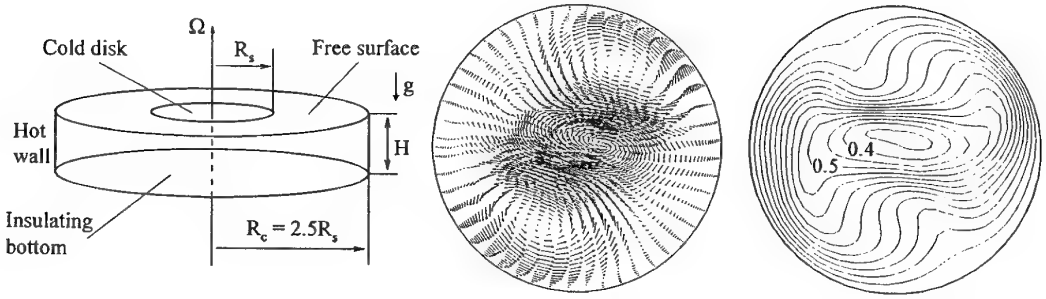

Geometry of a rotating cylindrical container,
instantaneous velocity vectors and temperature contours in the middle horizontal section

The annular configuration corresponds to the classical experiments of Fein and Pfeffer [1]. Numerical simulation, refining our previous computation [2], has shown the appearance of non-geostrophic turbulence superimposed upon baroclinic waves with the wavenumber of 4 – 7. The results are in agreement with the experimental results for mercury.
The convection problem in the cylindrical container is considered for conditions of Lee and Chun's experiment performed for a model Czochralski crystal growing configuration [3]. Regular non-axisymmetric two-folded thermal wave drifting with an angular velocity smaller than the cylinder rotation rate has been obtained. Both the velocity and temperature fields, illustrated in Figure, have got a strong deviation from the rotational symmetry. The computed wave frequency and amplitude agree well with the measurement data.

1. J.S. Fein, R.L. Pfeffer. "An experimental study of the effects of Prandtl number on thermal convection in a rotating, differentially heated cylindrical annulus of fluid", J. Fluid Mech. 75 (1976) 81.
2. V. Goriatchev, N. Ivanov, E. Smirnov. "Postcomputational visualization of baroclinic wave drift", 3rd International Conference on the Interaction of Art and Fluid Mechanics, Zurich, Switzerland (2000) 6p.
3. Y.-S. Lee, Ch.-H. Chun. "Transition from regular to irregular thermal wave by coupling of natural convection with rotating flow in Czochralski crystal growth", J. Crystal Growth 197 (1999) 297.

Experimental investigation of strongly rotating turbulent channel flow

G.E. Mårtensson[1] and J. Gunnarsson[2]
Department of Mechanics, Royal Institute of Technology
S–100 44 Stockholm, Sweden
Email: gustaf@mech.kth.se

Keywords - rotational effects - something else -

Abstract - Studying the effect of system rotation on turbulent flow is a most difficult and important area of turbulence research. This area is of fundamental interest, as well as of considerable industrial importance concerning applications such as centrifugal separators and turbines. In centrifugal separator applications the flow is subjected to extremely high system rotation rates, the Rossby number being typically around or below one. At these low Rossby numbers the flow field in a channel is strongly asymmetric and contains large zones of relaminarized flow on the stable side.

Experimental data on wall-bounded turbulent flows exposed to system rotation are relatively rare. This fact is due to the difficulties associated with obtaining accurate measurements in rotating frames of measurement. In the present study, just such an experimental set-up has been implemented to study the dependence on both the magnitude and the direction of the rotation vector for this type of flow. Experimental data were taken for a set of five different rectangular channel geometries, , which were investigated for different rotational velocities and directions and Reynolds numbers. The range of Reynolds numbers was 5000 to 30000, while the Rossby number lay in the interval 1.0 to ∞.

From the data, suitable scalings for the frictional coefficient, using the Reynolds number and the Rossby number, were extracted for the different trials. It is found that the coefficient of friction grows with a decreasing Rossby number. Evidence is given that the friction coefficient scales with the width of the duct.

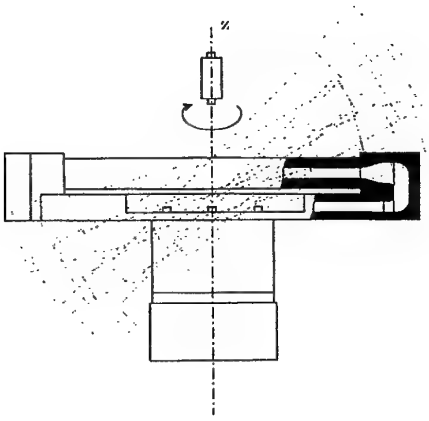

Figure 1: The experimental set-up. The rotation occurs around the z-axis.

[1]even Faxén Laboratory
[2]now Adtranz Sweden, 721 73 Västerås

Similarity profiles of eccentrically dosed spin-coated layers

M.M.J. Decré, R. Buyze and J.H. Lammers
Group Mechanics, Heat and Particle Optics
Philips Research Laboratories Eindhoven, The Netherlands
Email: michel.decre@philips.com

Keywords - Spin-coating - Lubrication theory

Abstract - Spin-coating is a process widely used to apply homogeneous coatings from the liquid phase a.o. on cathode ray tubes, silicon wafers, and optical storage discs. A liquid layer undergoes spreading centrifugal forces by spinning the substrate. This process is known for providing a constant layer thickness solution. That results from the combination of axisymmetric mass balance and centrifugal forces. However, things are different when no liquid is present in the center of the substrate up to a radius r_0; a situation we call *eccentric dosing*. We use the

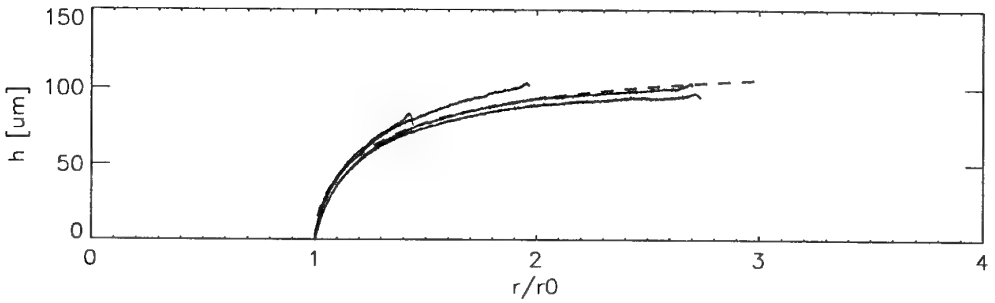

Figure 1: *Five eccentrically dosed profiles, scaled with the dosing radius r_0 to obtain self-similar profiles. Theoretical profile in dashed line, h_{eq}= 120 μm. Peaks in the experimental profiles are scaled substrate edge effects.*

lubrication approximation. A similarity solution for the radially varying thickness distribution is found for the case of the liquid profile starting at a radial distance r_0 from the center of the substrate.

When the thickness h is a function of r, one has to solve equation $\partial_T v + v\partial_\xi v = 0$, with variable separation $v = r^{4/3}h^2$, $\xi = 3/4r^{4/3}$, and $T = \rho\omega^2 t/\mu$ [Acrivos et al., *J. Appl. Phys.* **31** (1960)]. We show that the case of an infinite initial thickness of fluid for $r \geq r_0$ can be solved analytically, providing a similarity solution for the final expression for thickness: $h(r,t) = h_{eq}\sqrt{1-(r/r_0)^{-4/3}}$, with $h_{eq} = \sqrt{\frac{3\mu}{4\rho\omega^2 t}}$ the equivalent thickness for a fully dosed substrate.

In order to verify this formula, we have performed some experiments. Several discs have been spin-coated with eccentric dosing. A ring of liquid resin was dosed at 30 rpm, at a fixed radius r_0 using an injection system fitted with a syringe. The process was tuned to aim for an equivalent final thickness of 120 μm. UV-curing of the liquid was performed while spin-coating was continued, in order to "freeze" the flow and prevent capillary relaxation.

The measured profiles for five different initial eccentric positions r_0 are scaled and compared to the similarity solution with h_{eq}=120 μm (Fig.1). One can conclude from the good agreement that the self-similar form is indeed valid, and describes an intrinsic behaviour of spin-coated flows when eccentrically dosed.

Bathtub Vortices

A. Andersen[1,2], T. Bohr[1], M. Schram Christensen[1], M. Nørgaard Nielsen[1], and J. Richter[1]
[1]Department of Physics, The Technical University of Denmark, DK-2800 Lyngby, Denmark
[2]Risø National Laboratory, Optics and Fluid Dynamics Department, DK-4000 Roskilde, Denmark
Email: aanders@fysik.dtu.dk

Keywords - Free surfaces - Swirling flows - Vortices

Abstract - Bathtub vortices, i.e., swirling flows with a free surface which extends down to the outlet of the fluid container are well known. The properties of such flows are, however, to our knowledge not described in detail neither experimentally nor theoretically. We have constructed an experimental set-up consisting of a cylindrical container with a circular hole at the center of the bottom. The cylinder is rotating about a vertical axis and using a recirculation system we can obtain a steady bathtub vortex flow. We describe the flow field qualitatively and measure the shape of the free surface for different values of the rotational frequency of the container and the flux of the flow in the system. In addition we investigate the transient corkscrew like free surface observed when the rotational frequency is changed.

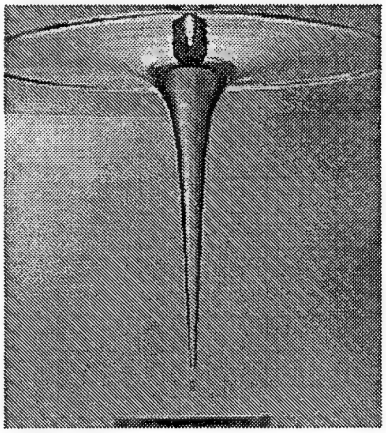

Recorded image of the free surface for a steady bathtub vortex.

The experimental measurements are compared with theoretical results. We model the flow starting from the full Navier-Stokes equations and the free surface boundary conditions. We will describe the transition between solutions with qualitatively different velocity fields and shapes of the free surface. We also intend to calculate the free surface shapes analytically in an approximation including viscous effects but neglecting surface tension.

Non-Newtonian Fluid Mechanics

A New Class of Integro-differential Constitutive Equations for Polymer Melts

M.H. Wagner, H. Bastian*) and P. Rubio*)
Polymertechnik/Polymerphysik, Technische Universität Berlin, Fasanenstr. 90, D-10623 Berlin
*) Institut für Kunststofftechnologie, Universität Stuttgart, Böblinger Str. 70, D-70199 Stuttgart
Email: manfred.wagner@tu-berlin.de

Keywords: Molecular Stress Function Theory - Tube Model - Tube Kinematics

Abstract - By generalizing the Doi-Edwards tube model to the Molecular Stress Function theory of Wagner and Schaeffer, the extensional viscosities of polymer melts in uniaxial, equibiaxial and planar constant strain-rate experiments can be described quantitatively. While the strain-hardening of linear polymer melts (high-density polyethylene, polystyrene, polypropylene) can be accounted for by a tube diameter, which decreases affinely with the average stretch, long-chain-branched polymer melts (low-density polyethylene, long-chain-branched polypropylene) show enhanced strain hardening in extensional flows due to the presence of long-chain branches. This can be quantified by a molecular stress function, the square of which is quadratic in the average stretch and follows from the junction fluctuation theory of Flory. The ultimate magnitude of the strain-hardening effect is governed by a maximum value of the molecular stress, f_{max}, which is specific to the polymer melt considered. As an example, the figures shows damping functions and extensional viscosities (symbols) of a polystyrene melt in uniaxial elongation and biaxial extension. Lines are predictions using the Doi-Edwards (DE) model, the Linear Molecular Stress Function (LMSF) theory, and a one-parameter Molecular Stress Function (MSF) theory with f_{max}=3.6.

A new integro-differential formulation of the Molecular Stress Function Theory for general flows (including shear flow) of polymer melts is presented. It is based on tube kinematics, which is shown to be fundamentally different for rotational versus irrotational flows.

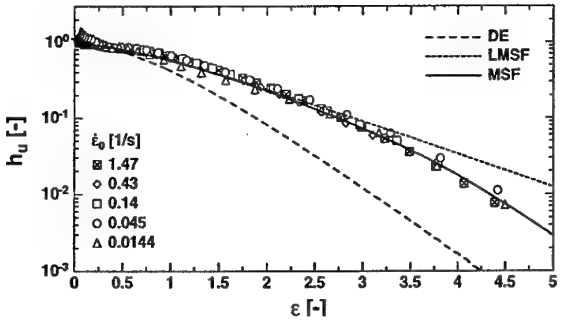

Fig.1a) Damping function h_u of PS

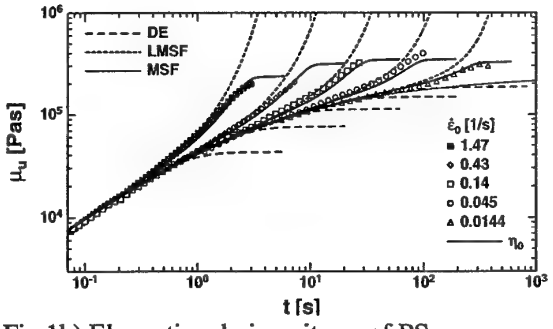

Fig.1b) Elongational viscosity μ_u of PS

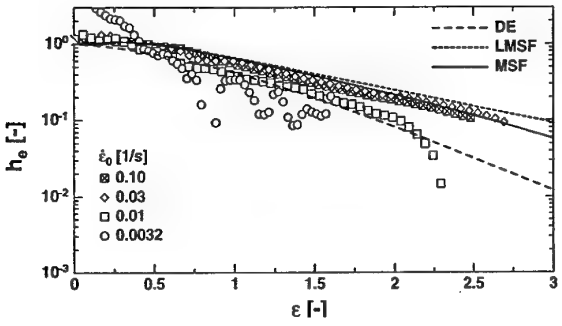

Fig.1c) Damping function h_e of PS

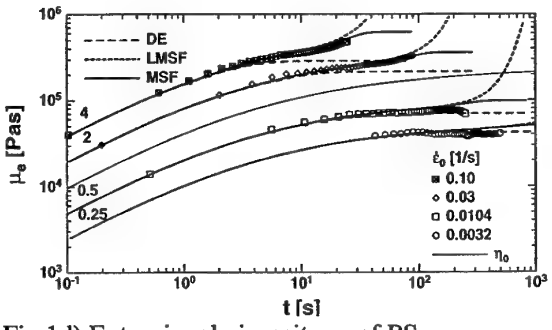

Fig.1d) Extensional viscosity μ_e of PS

The Deformation fields method in viscoelastic flow simulations

M.A.Hulsen, E.A.J.F. Peters, A.P.G. van Heel and B.H.A.A. van den Brule
J.M. Burgerscentre for Fluid Mechanics
Delft University of Technology, The Netherlands
Email: m.a.hulsen@wbmt.tudelft.nl

Keywords - Deformation Fields - Viscoelastic fluids - Numerical simulation

Abstract -

In [1] a new method for solving viscoelastic flows is presented. The method is based on so-called deformation fields. In each deformation field the Finger tensor $\boldsymbol{B}_{t'}(t)$ is stored, representing the deformation from a time t' in the past to the current time t. The Finger tensor satisfies the following convection equation for fixed t'

$$\frac{\partial}{\partial t}\boldsymbol{B}_{t'} + \boldsymbol{u}\cdot\nabla\boldsymbol{B}_{t'} = \nabla\boldsymbol{u}\cdot\boldsymbol{B}_{t'} + \boldsymbol{B}_{t'}\cdot\nabla\boldsymbol{u},$$

where $\boldsymbol{u}$ is the velocity vector. By solving this equation for a sufficient number of fields, it is possible to compute the complete deformation history of particles at any point in space and at any instant in time. The deformation history fully determines the stress tensor, which can subsequently be used to solve the velocity and pressure by the momentum and mass balance.

The deformation fields method is particularly useful for viscoelastic models having no differential model equivalent. The classic example is the Rivlin-Sawyers integral type models, but modern models for polymer melts such as the Mead-Larson-Doi or the pom-pom model also fall into this category and cannot be solved by standard schemes for differential models.

In the presentation we will explore some of the details of the current implementation of the deformation fields method and consider possible improvements. Furthermore, new results will be presented for complex flows using various polymer melt models.

1. E.A.J.F. Peters, M.A. Hulsen, B.H.A.A. van den Brule (2000): "Instationary Eulerian viscoelastic flow simulations using time separable Rivlin-Sawyers constitutive equations", J. Non-Newtonian Fluid Mech., 89 (2000) 209-228.

Numerical Simulation of Viscoelastic Planar and Axisymmetric Contraction Flows

T. N. Phillips* A. J. Williams†

April 7, 2000

This paper is concerned with the numerical simulation of viscoelastic contraction flows. In particular, the differences between planar and axisymmetric flows are studied with respect to vortex enhancement. Two types of non-Newtonian elastic liquids are modelled, namely constant viscosity Boger liquids and shear thinning liquids. Comparisons are made with experimental work which is also being performed at the University of Wales Aberystwyth.

The basis of the numerical simulations is a semi-Lagrangian finite volume method which combines the advantages of fixed grids inherent in Eulerian methods with modifications to treat the convective terms using particle tracking methods. The method alleviates some of the difficulties encountered when discretizing differential constitutive equations which are, invariably, of hyperbolic type. The semi-Lagrangian technique is applied to the convective terms in the momentum and constitutive equations. It is a natural way of treating these terms without resorting to upwinding techniques.

A range of numerical results are presented for viscoelastic contraction flows with particular emphasis given to the convergence and stability of the method and the development of vortex structure with increasing elasticity.

*Department of Mathematics, University of Wales, Aberystwyth SY23 3BZ, United Kingdom.

†School of Computing and Mathematical Sciences, University of Greenwich, Greenwich, London SE10 9LS, United Kingdom.

Viscoelastic contraction flows : comparison of axisymmetric and planar configurations

S. Nigen, K. Walters*
Department of Mathematics, University of Wales, Aberystwyth, UK

Attention is given to experimental flows through contractions, with particular reference to the phenomenon of vortex enhancement. Two types of non-Newtonian elastic liquids are considered, namely constant-viscosity Boger liquids and also shear thinning liquids. A particular issue of interest is the differences observed between flow in an axisymmetric contraction and the corresponding flow in a planar contraction.

Provocatively, it is found that, whereas Boger liquids exhibit vortex enhancement in axisymmetric contractions, it is *absent* for these liquids in planar contractions. In contrasts, shear thinning elastic liquids show vortex enhancement in both axisymmetric and planar contractions.

We attempt to provide a comprehensive portfolio of behaviour in geometries with different contraction ratios and for different flow rates. It is our hope that the data will provide a challenge to the many workers in the field of computational rheology.

Some consideration is also paid to the interpretation of contraction flow data in terms of "extensional viscosity". We raise the obvious question as to whether the provocative differences between the behaviours of constant-viscosity and shear-thinning liquids reflect differences in uniaxial and planar extensional-viscosity levels.

Planar Elongational Flow of Highly Dilute Viscoelastic Polymer Solutions

B. Gampert, C. Wilkes and T. Eich
Universität Essen, Angewandte Mechanik, Schützenbahn 70, 45127 Essen, Germany
Email: bernhard.gampert@uni-essen.de

Keywords - Planar Elongational Flow - Opposed Jets - Viscoelastic Polymers - Highly Dilute Polymer Solutions

Abstract - Experiments on planar elongational flow of highly dilute viscoelastic polymer solutions are reported. The elongational flow experiments undertaken here were carried out using the commercial, anionic polyacrylamide Sedipur AF 701 with a hydrolysis factor of 70% and a molar mass of $\bar{M}_w \approx 14 \cdot 10^6$ g/mol and the self polymerised non-ionic polyacrylamide PAA-T19 with a molar mass of $\bar{M}_w \approx 5.6 \cdot 10^6$ g/mol. The elongational viscosity as a function of the strain rate was measured for this aqueous polymer solutions. In order to assess the orientation of the polymer molecules, flow induced birefringence was measured at the same time.

Two flow regions have been observed in the diagram of the elongational viscosity as a function of the strain rate. A Newtonian region of strain independent of the elongational viscosity and a region with distinctly and continuously increasing elongational viscosity. Calculations applying the FENE dumbbell model were shown to be in good accordance with the experimental results of the non-ionic solution, see figure left.

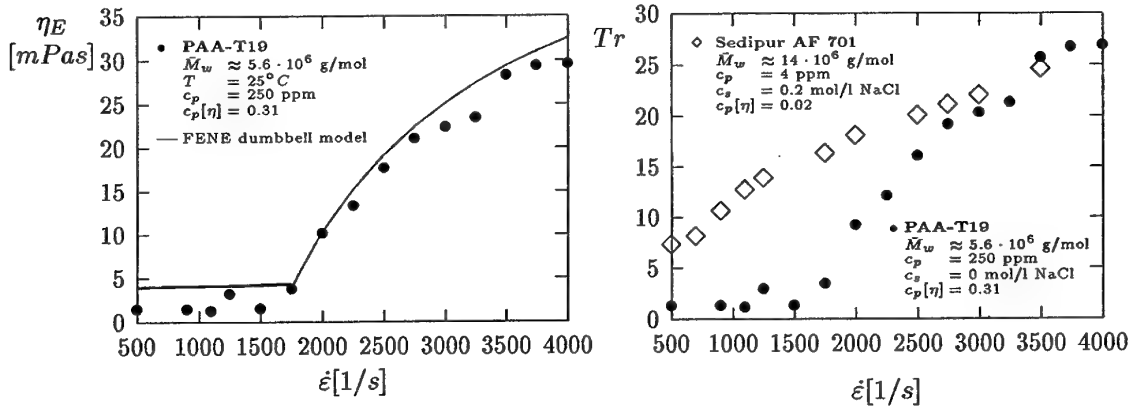

The elongational viscosity of the PAA-T19 solution (left) and the Trouton number Tr as a function of the strain rate for the Sedipur AF 701 and the PAA-T19 solutions (right)

The figure right represents curves of the Trouton number as a function of the strain rate. The Trouton number of the Sedipur AF 701 solution with a polymer concentration of $c_p = 4$ ppm and a salt concentration of $c_s = 0.2$ mol/l NaCl increases between $\dot{\varepsilon} = 500\ s^{-1}$ and $\dot{\varepsilon} = 3500\ s^{-1}$ from Tr = 7 to Tr = 24. The Trouton number of the PAA-T19 solution with a polymer concentration of $c_p = 250$ ppm, lies between Tr = 4 at $\dot{\varepsilon} = 1600\ s^{-1}$ and Tr = 27 at $\dot{\varepsilon} = 4000\ s^{-1}$. This demonstrates that both solutions with an overlapping parameter of $c_p[\eta]_{\text{Sedipur AF 701}} = 0.02$ and $c_p[\eta]_{\text{PAA-T19}} = 0.31$ respectively have distinct elastic properties.

Modelling the flow of linear polymer melts using a modified version of the MGI model

A. Leygue, P. Wapperom, A. Beris, R. Keunings
Université catholique de Louvain
CESAME, Division of Applied Mechanics
Louvain-la-Neuve, Belgium
Email: leygue@mema.ucl.ac.be

Keywords - Polymer melts - Irreversible thermodynamics - complex flows

Abstract - In this work, we consider the compatibility of a new differential constitutive equation for entangled linear polymer melts proposed in [1] by Marrucci, Greco and Ianniruberto (called here the MGI model) with the non-equilibrium thermodynamics formalism of incompressible isothermal flows [2]. This constitutive equation is an approximation of an integral form proposed as a modification of the basic Doi-Edwards theory. Its major features are the introduction of the convective constraint release (CCR) mechanism, leading to a variable relaxation time, and a new strain measure accounting for force balance requirements on the entanglements.

Our contribution is twofold. First, we show that the MGI model needs to be modified in order to be consistent with irreversible thermodynamics, and that the modified version of the model is in even better agreement with available rheometrical data than the original model. Second, we study the behaviour of the modified MGI model in a benchmark complex flow, the flow through a 4:1:4 constriction, using the Backward-tracking Lagrangian Particle Method [3].

References

[1] G. Marrucci, F. Greco and G. Ianniruberto, *Integral and Differential Constitutive Equations for Entangled Polymers with Simple Versions of CCR and Force Balance on Entanglements*, submitted to Rheol. Acta. January 2000.

[2] A.N. Beris, B.J. Edwards, *Thermodynamics of Flowing Systems with internal Microstructure*, Oxford University Press (1994).

[3] P. Wapperom, R. Keunings, V. Legat, *The Backward-tracking Lagrangian Particle Method (BLPM) for Computing Transient Viscoelastic Flows*, J. Non-Newtonian Fluid Mech. 60 (2000) 273-295.

MHD flow of a power-law fluid over a rotating disk

H.I. Andersson and E. de Korte
Division of Applied Mechanics, Department of Mechanical Engineering
Norwegian University of Science and Technology, Trondheim, Norway
Email: helge.i.andersson@mtf.ntnu.no

Keywords - Non-Newtonian Fluids - Von Karman Swirling Flow - Similarity Solutions

Abstract - Magnetohydrodynamic flow of an electrically conducting power-law fluid in the vicinity of a constantly rotating infinite disk in the presence of a uniform magnetic field is considered. The steady, laminar and axi-symmetric flow is driven solely by the rotating disk, and the incompressible fluid obeys the inelastic Ostwald de Waele power-law model. In spite of the severe non-linearities introduced by the rheological model, the three-dimensional boundary layer equations transform exactly into a set of ordinary differential equations in a generalized similarity variable. These ODEs, together with appropriate boundary conditions at the disk and infinitely far away, constitute a two-parameter problem in n and m, n being the power-law index and m the magnetic parameter. The two-point boundary value problem was first solved by shooting and parallel shooting techniques. However, due to the sensitivity to the initial values, a finite-difference approach was eventually adopted.

After first having reproduced the accurate solutions provided by Rogers & Lance (J. Fluid Mech. 1960) of the classical Von Karman swirling flow; i.e. $n = 1$ and $m = 0$, the non-magnetic case $m = 0$ was considered. Earlier results by Mitschka & Ulbrecht (Coll. Czech. Chem. Comm. 1965) was approved for most power-law fluids, showing that the boundary layer thickness decreases monotonically as the power-law index n is increased. This is accompanied by a reduction in the radial outflow, which in turn is compensated by a reduction of the axial inflow towards the disk. For highly shear-thinning fluids ($n < 0.5$), however, a severe ambiguity in the determination of this inflow was revealed.

The MHD flow problem was solved numerically for values of the magnetic parameter m up to 4.0. The effect of the magnetic field is to reduce, and eventually suppress, the radially directed outflow. An accompanying reduction of the axial flow towards the disk is observed, together with a thinning of the boundary layer adjacent to the disk. Consequently, the wall shear stress in the circumferential direction turns out to increase monotonically with increasing m-values, thereby increasing the torque required to maintain rotation of the disk at the prescribed angular velocity. These major effects of the imposition of a magnetic field are found both for shear-thinning ($n < 1$) and shear-thickening ($n > 1$) fluids. The influence of the magnetic field is, however, more pronounced for shear-thinning than for shear-thickening fluids. The magnetic field therefore makes the difference between the various fluids, i.e. between different values of n, more distinct than in the non-magnetic case $m = 0$.

Elastic energy vs. elongational viscosity in wall turbulence for viscoelastic flows

E.De Angelis, C.M.Casciola and R. Piva
Dipartimento di Meccanica e Aeronautica
Universitá di Roma "La Sapienza" - Italy
Email: betta@flu5.ing.uniroma1.it

Keywords - Wall turbulence - Dilute polymers - Drag reduction

Abstract - The effect of dilute polymers on the structure of wall turbulence is well known and deeply studied since a long ago. The main issue in recent years has been finding a full explanation of the intimate mechanisms which interfere with the regeneration of wall turbulence thus modifying its structure. Two possible explanations have been taken into consideration. The first, proposed by Lumley, assumes that the polymers molecules properly excited (i.e. time scale of the strain rate smaller than the relaxation time) become significantly extended contributing locally to a very large elongational viscosity.
The other approach, proposed by De Gennes, is focused on the idea that polymers can interfere with the classical turbulent cascade at those scales where the elastic energy stored by the partially stretched polymers becomes comparable with the turbulent energy.
To evaluate the respective roles of the elastic energy and of the extra-dissipation due to the polymers, we have performed a decomposition of the stress power due to the polymer as

$$T^p_{ij} D_{ij} = \Phi + \frac{DE_p}{Dt} \qquad \frac{DE_p}{Dt} = \frac{1}{2}\frac{\eta_p}{De} f(\mathcal{R}_{ii}) \frac{D\mathcal{R}_{ii}}{Dt}. \tag{1}$$

where Φ is the viscous dissipation and the last term is the rate of elastic energy accumulation, whose expression is specified in the case of a FENE-P model for the polymer solution.
As shown in the figure, a strong event in the buffer layer causes a significant effect on the istantaneus behaviour of the rate of change of the elastic energy (green) and in the extradissipation(yellow). In fact, it is very difficult to reach any definite conclusion from the inspection of instantaneus turbulent fields. Hence, as it will be discussed, we base our analysis on the idea of conditional sampling, where the relevant fields (e.g. extra-dissipation and elastic energy) are averaged under the condition of a given event (e.g. bursting).

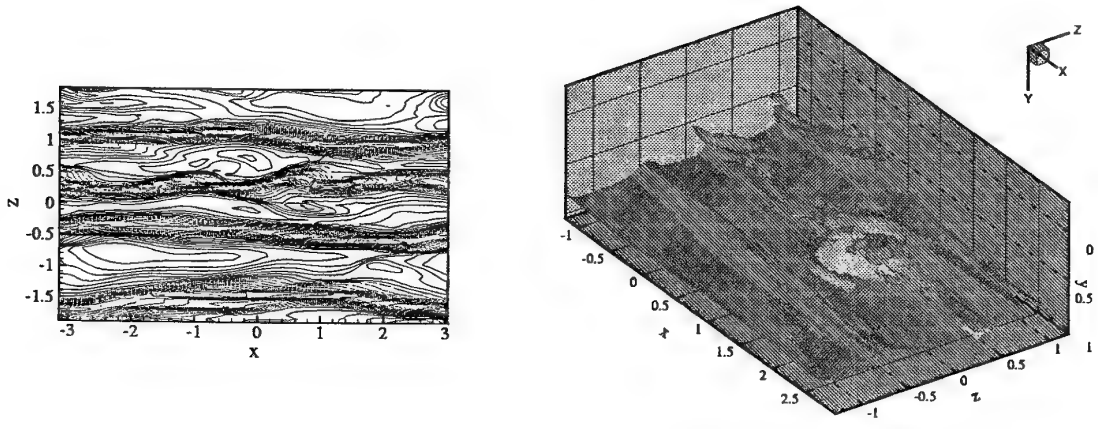

Instantaneus field: left low & high speed streaks during a typical bursting event, right vortical structures (pink), extra-dissipation(yellow) and rate of change of the elastic energy(green).

Thermally induced flow front instabilities in injection moulding

H.J.J. Gramberg and A.A.F. van de Ven
Section Applied Analysis, Department of Mathematics and Computing Science
Eindhoven University of Technology, The Netherlands
Email: h.j.j.gramberg@tue.nl

Keywords - injection moulding - flow front instability - boundary layers - polymers

Abstract - A two-dimensional injection moulding process, in which a molten polymer is injected into a narrow gap between two parallel plates (the cavity) is considered. The two plates (the walls of the cavity) are cooled at a temperature much lower than that of the injected melt.

Experiments show that under certain circumstances an instationary, asymmetric flow front may occur during the injection moulding process. The flow front then changes continuously its asymmetric shape by wobbling between the upper and lower wall. We refer to this wobbling of the flow front as a flow front instability, and it originates from the interaction between the flow field, the temperature distribution and the elastic stresses in the viscoelastic fluid. In this presentation, we focus on the influence of the temperature, especially near the walls of the mould.

The instabilities are studied by using analytical methods, such as perturbation methods and asymptotics, neglecting viscoelastic effects in the fluid. In first instance, the system is assumed to be weakly coupled, meaning that the temperature and velocity are in zeroth order uncoupled.

The velocity problem near the flow front, being an unknown free surface, can be solved using the theory of conformal mapping. The (2-dimensional) velocity problem is formulated in terms of complex variables. The area of the cavity behind the flow front, which is filled with polymer, is mapped onto the unit circle, using a conformal mapping $m(\zeta)$. Since the flow front is a free boundary, its shape and therefore $m(\zeta)$ is in first instance unknown, and its solution leads to a Hilbert problem. As a result, the shape of the front is determined, and the flow lines and velocities behind the flow front can be calculated.

To solve the temperature problem, the problem is considered in three distinct areas inside the mould: far behind the flow front (where a narrow gap approximation is used), near the flow front, and in a transitional area between the latter two. At the inlet of the cavity, the temperature is taken equal to the inlet temperature T_i. The walls of the cavity are kept at a lower temperature $T_w (< T_i)$. Since diffusion is low in comparison to convection in the main part of the cavity, the temperature of the polymer will be equal to T_i there. Only in boundary layers near the walls of the cavity, the temperature will be lower than T_i. By using asymptotic approximations, the thickness of and the temperature distribution inside these boundary layers can be calculated.

The stability of the zeroth order (symmetric) solution is studied using perturbation methods. The perturbations are based on an initially asymmetric flow front, causing different temperature distributions at the upper and lower wall, resulting in different viscosities at these walls. In regions where the temperature is low, and thus the viscosity high, the flow will slow down with respect to regions of higher temperature. We will explain how this can cause the wobbling of the front.

Direct numerical simulation of interfacial waves of two-layer Poiseuille flow

R. Valette, Y. Demay, P. Laure and A. Fortin
Institut Non-Linéaire de Nice, UMR 6618 - CNRS & UNSA
1361 route des Lucioles, 06560 Valbonne, France.
Email: laure@inln.cnrs.fr

Keywords - Interfacial instability - Two-layer plane Poiseuille flow - Non Newtonian fluids

Abstract - This paper deals with two fluids having different viscosities and elasticity which move in a horizontal plane channel. This configuration is related to the industrial coextrusion process which allows to put together polymers having different optical, mechanical and barrier properties. At certain operating conditions, wavy interfaces are observed and are classified as interfacial instabilities.

The shape and the non-linear behavior of these interfacial waves are studied by means of finite elements simulations. We restrict our study to the motion of two viscoelastic fluids which follow Maxwell constitutive law. The position of the interface is fixed by the initial flow rate of each layer. For a fixed viscosity ratio, a flat interface related to the two-layer Poiseuille flow is computed.

First, this flat interface is perturbed by a pulse-like disturbance and we find that the interfacial instability is always convective. That means that the interfacial wave takes the shape of a wave packet which moves towards the die exit as it is amplified or damped. The strength of the interfacial perturbation is measured by looking at the maximum deviation observed at the die exit. We find that in the unstable cases, the maximum deviation increases with elasticity (or the Weissenberg number). It important because the Reynolds number in the coextrusion process is almost null (it is due to very high viscosity of polymers). On the other hand, the elastic stratification between the two layers can prevent the unstable wave due to viscous stratification. Second, a small periodic fluctuation is added to the initial flow rate and we look at the influence of this period on the spatial amplification of interfacial wave.

Finally, the results of direct simulations are compared with informations given by the theoretical studies on the stability of the two-layer Poiseuille flow. The maximal deformation at the die exit seems well evaluated for pulse-like disturbances. For moderate periodic forcing, the Gaster's relation gives good indications of interface deformations.

References

[1] R. VALETTE, P. LAURE, A. FORTIN, and Y. DEMAY. Convective instabilities in coextrusion process. *Int. Poly. Process*, submitted 2000.

[2] P. LAURE and A. FORTIN. Direct simulation of interfacial instabilities of two-layer Poiseuille flow in a coextrusion die. comparisons with linear stability analysis. *Eur. J. Fluid Mech./B*, submitted, 2000.

[3] P. LAURE, H. Le MEUR, Y. DEMAY, J.C. SAUT, and S. SCOTTO. Linear stability of multilayer plane Poiseuille flows of Oldroyd-B fluid. *J. Non-Newtonian Fluid Mech.*, 71:1–23, 1997.

Alexander L. Yarin
Faculty of Mechanical Engineering
Technion

Bending Instability of Electrically Charged Liquid Jets of Polymer Solutions in Electrospinning of Nanofibers

Nanofibers of polymers were electrospun by my collaborators experimentalist by creating an electrically charged jet of polymer solution at a pendent droplet. After it flowed away from the droplet in a nearly straight line, the jet bent into a complex path and other changes in shape occurred, during which electrical forces stretched, and thinned it by very large ratios. After the solvent evaporated, nanofibers that were birefringent left. Observation of the jet with a high frame rate camera showed a rectilinear segment that became unstable and bent. In the present work the bending instability was analyzed. The reason for the instability was explained. The rheological complexity of the polymer solution was included, which allowed consideration of viscoelastic jets. It was shown that the longitudinal stress caused by the external electric field acting on the charge carried by the jet stabilized a straight jet for some distance. Then a lateral perturbation grew in response to the repulsive forces between adjacent elements of charge carried by the jet. The motion of segments of the jet grew rapidly into an electrically driven fractal-like bending instability. The three-dimensional paths of continuous jets were calculated, both in the nearly straight region where the instability grew slowly and in the region where the bending dominated the path of the jet. The highly nonlinear mathematical model developed in the work provided a reasonably good representation of the experimental data, particularly of the jet paths determined from high speed videographic observations. Possible applications of electrospun nanofibers in modern technologies are also discussed.

Buoyancy Driven Flows

Laminar wakes behind flat plates in density stratified flow

Ian P Castro
School of Engineering Sciences
University of Southampton, Highfield, Southampton SO17 1BJ, Great Britain
Email: i.castro@soton.ac.uk

Keywords - bluff body wakes - stratified flow - laminar flow asymptotics

Abstract: A comprehensive set of numerical computations of the symmetric, two-dimensional, laminar, density stratified flow past cascades of flat plates has been undertaken. The fundamental controlling parameters are the Reynolds number Re (based on the unit plate width), the Richardson number Ri (defining the strength of the stratification, with the buoyancy force normal to the approach flow), the Schmidt number Sc (the ratio of density diffusivity to kinematic viscosity) and the blockage ratio H (the ratio of plate width to channel width). A multi-grid, finite-difference method was used, with particular attention given to the convective scheme's accuracy and to grid resolution as the Reynolds number increased. Grid sizes up to around 1000 x 300 were used. In this paper, some salient results are presented for a range of these parameters, encompassing regimes of 'narrow' and 'wide' wakes and cases in which $Sc = 1$ and $Sc = \infty$. For the latter case, the density equation was not solved directly; rather, the fact that constant density and stream-surfaces coincide in that limit was exploited to avoid the practical impossibility of maintaining adequate grid resolution for the density equation.

The results are compared with asymptotic theory (see Reference), whose qualitative features are generally confirmed. In some cases (at large enough Re) multiple solutions, on the same grid and with the same numerical scheme, are identified. One of these two sets of solutions has characteristics very similar to classical Prandtl-Batchelor wakes, but the existence of such wakes behind bluff bodies has never been conclusively demonstrated. The possibility that the solutions are merely numerical artefacts is addressed in the light of more recent theoretical work and earlier numerical computations. Attention is also given to the nature of the flow around the critical Ri region, marking the beginning of lee-wave motions behind the obstacle and beyond which the computations could not extend significantly.

Chernyshenko SI & Castro IP (1996) High-Reynolds number weakly stratified flow past an obstacle. *J. Fluid Mech.* 317, 155-178.

The influence of baroclinic vorticity production on the *3D*-transition of the flow around a heated cylinder

R. Kieft, C.C.M. Rindt and A.A. van Steenhoven
Section Energy Technology, Department of Mechanical Engineering
Eindhoven University of Technology, The Netherlands
Email: c.c.m.rindt@wtb.tue.nl

Keywords - Heated Cylinder Flow - Baroclinic Vorticity Production - *3D*-transition - *3D*-PTV

Abstract - In the present study the attention is focussed on the *3D*-transition of a horizontal cross-flow around a heated cylinder. The Reynolds number is set to $Re_D = 75$ and the Richardson number (a measure for the importance of buoyancy) is varied between $0 < Ri_D < 1.5$. Experiments are carried out in a towing tank configuration with water as the working fluid. Visualization experiments are performed using fluorescence dye injection with a multiple-needle probe. Besides, both *2D* and *3D* Particle Tracking experiments are carried out. In the figure below vorticity surfaces are shown of the span-wise component as deduced from the measured *3D* velocity field for $Ri_D = 1.3$. It can be seen that near the negative upper vortex a patch of fluid is located which contains positive vorticity. This volume of positive vorticity is linking with the negative vorticity of the primary upper vortex resulting in a secondary structure. From subsequent time samples and from the visualization experiments it appeared that this secondary structure moves in upward direction and escapes from the primary upper vortex as a mushroom-type structure. Numerical results obtained with a *2D* Spectral Element code revealed that the onset of this process is a result of baroclinic vorticity production. Due to temperature differences an area of positive vorticity is growing within the negative upper vortex. In the present study the *3D*-transition process will be discussed together with a detailed analysis of the influence of buoyancy on this transition process.

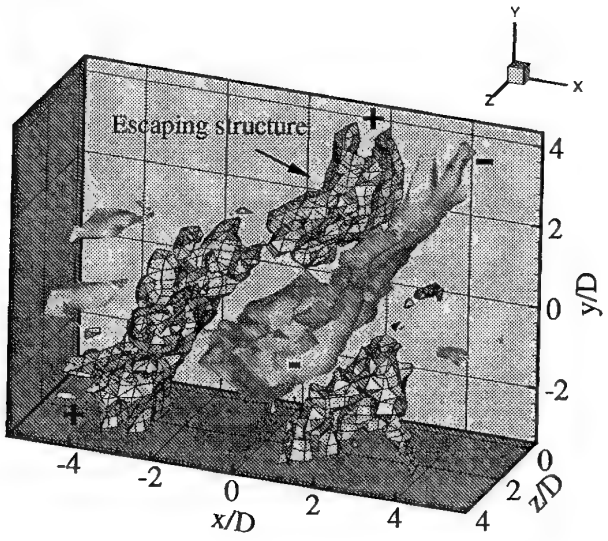

Iso-vorticity contours of the span-wise component as derived from the 3D PTV measurements for $Re_D = 75$ and $Ri_D = 1.3$. Negative vorticity is presented with a shaded surface, positive vorticity with a meshed surface.

Scaling in thermal convection: A unifying theory

Detlef Lohse[1] **and Siegfried Grossmann**[2]

[1] Univ. of Twente, Applied Physics, P. O. Box 217, 7500 AE Enschede, Netherlands
[2] Univ. of Marburg, FB Physik, Renthof 6, 35032 Marburg, Germany

Recent measurements by Ciliberto's group [1] with turbulent mercury Rayleigh-Benard cells revealed an unexpected Prandtl number dependence of the heat transfer. Moreover, the experiments by Chavanne et al. [2] with turbulent thermally driven helium beyond $Ra = 10^{11}$ showed a much stronger increase of Nu with increasing Ra than previously thought.

Here, a systematic theory for the scaling of the Nusselt number Nu and of the Reynolds number Re in strong Rayleigh-Benard convection is suggested [3].

The key idea is to split the total kinetic energy dissipation rate ϵ_u and the total thermal dissipation rate ϵ_θ into boundary layer and bulk contributions, $\epsilon_u = \epsilon_{u,BL} + \epsilon_{u,bulk}$, $\epsilon_\theta = \epsilon_{\theta,BL} + \epsilon_{\theta,bulk}$. The estimates for the individual contributions are based on the dynamical equations in the bulk and in the boundary layers.

Several regimes are identified in the Rayleigh number Ra – Prandtl number Pr phase space, defined by whether the boundary layer or the bulk dominates the global kinetic and thermal dissipation, respectively, and by whether the thermal or the kinetic boundary layer is thicker.

In the regime which has most frequently been studied in experiment ($Ra \lesssim 10^{11}$) the leading terms are $Nu \sim Ra^{1/4}Pr^{1/8}$, $Re \sim Ra^{1/2}Pr^{-3/4}$ for $Pr \lesssim 1$ and $Nu \sim Ra^{1/4}Pr^{-1/12}$, $Re \sim Ra^{1/2}Pr^{-5/6}$ for $Pr \gtrsim 1$. In most measurements these laws are modified by additive corrections from the neighboring regimes so that the impression of a slightly larger (effective) Nu vs Ra scaling exponent can arise. The scaling of those regimes can be seen from below table. In particular, a linear combination of the $1/4$ and the $1/3$ power laws for Nu with Ra, $Nu = 0.27Ra^{1/4} + 0.038Ra^{1/3}$ (the prefactors follow from experiment), mimicks a $2/7$ power law exponent in a regime as large as ten decades.

Two very recent experimental data sets of extreme precision [4] and of extremely high Ra up to 10^{17} [5] can be accounted for within our theory, but *not* with the standard $2/7$ power law.

---

[1] S. Cioni, S. Ciliberto, and J. Sommeria, J. Fluid Mech. **335**, 111 (1997).
[2] X. Chavanne, F. Chilla, B. Castaing, B. Hebral, B. Chabaud, and J. Chaussy, Phys. Rev. Lett. **79**, 3648 (1997).
[3] S. Grossmann and D. Lohse, "Scaling in thermal convection: A unifying theory", J. Fluid Mech. 407, 27-56 (2000).
[4] G. Ahlers et al., submitted to Phys. Rev. Lett. (2000).
[5] Niemela, L. Skrebek, K. R. Sreenivasan, and R. Donelly, submitted to Nature (2000).

Convection in horizontal fluid layers with internal heat generation

O. Morii and M. Nagata
Division of Aeronautics and Astronautics, Graduate School of Engineering,
Kyoto University, Japan
Email: nagata@gas.kuaero.kyoto-u.ac.jp

Keywords - Convection - Internal Heating - Nonlinear Numerical Analysis

Abstract - A nonlinear analysis for convection in horizontal fluid layers with a homogeneously distributed heat source is performed numerically when the upper boundary is at a constant temperature while the lower boundary is thermally insulated. It is well known by the linear stability analysis that the conductive state becomes unstable at the critical Rayleigh number $R_c = 2772.28$ to a perturbation with the horizontal wave number $a_c = 2.629$ when the Prandtl number of the fluid is 7. Because of the horizontal degeneracy pertinent to the problem the planform of convection is not determined by the linear theory. In order to determine the spatial structure of the convection nonlinear investigations were carried out using the mean field approximation by Roberts(1967), a finite difference numerical scheme by Thirlby(1970) and the amplitude expansion method by Tveitereid & Palm(1976). However, they did not fully explain the two-dimensional roll type of convection observed by Tritton & Zarraga(1967).

Our primary motivation of the present study is to find out whether stable two-dimensional roll solutions exist at all or not. First, we obtain finite amplitude two-dimensional roll solutions by the pseudo-spectral method combined with a Newton-Raphson iteration scheme. It is found that these solutions bifurcate supercritically when the Rayleigh number takes its critical value. Next, we examine the stability of the obtained two-dimensional roll solutions by superimposing the general three-dimensional perturbations on the nonlinear solutions. It is shown that although the two-dimensional roll solutions are unstable to a hexagonal type of perturbations at and slightly above the bifurcation point they do recover stability as the Rayleigh number is increased to about twice its critical value. We also find that the stable two-dimensional roll solutions tend to have larger wavelengths as the intensity of the internal heat source increases. These findings compare favourably with the experimental observation by Tritton & Zarraga(1967). Lastly, by considering triad interactions we analyse the hexagonal pattern of convection near the linear criticality. It reveals that down-hexagons are stable whereas up-hexagons are unstable for large Prandtl numbers. The stability properties of the two types of hexagonal solutions interchange when the Prandtl number is less than 0.25.

Transient Natural Convection within a Horizontal Cylindrical Enclosure

M. C. Hort and A. Packwood
School of Mechanical and Materials Engineering
University of Surrey, U.K.
Email: m.hort@surrey.ac.uk

Keywords - Internal Natural Convection, Heat Transfer, DNS

Abstract - The transient behaviour of natural convection within a horizontal cylindrical enclosure subjected to a uniform and constant wall temperature has been investigated numerically and experimentally. Here we shall solely consider the numerical solutions. The instantaneous 2D Boussinesq set of equations are solved directly through spectral approximation. Non-slip boundary conditions are applied at the wall along with a constant uniform temperature. The flow is initiated through the application of a step change in the uniform boundary condition temperature.

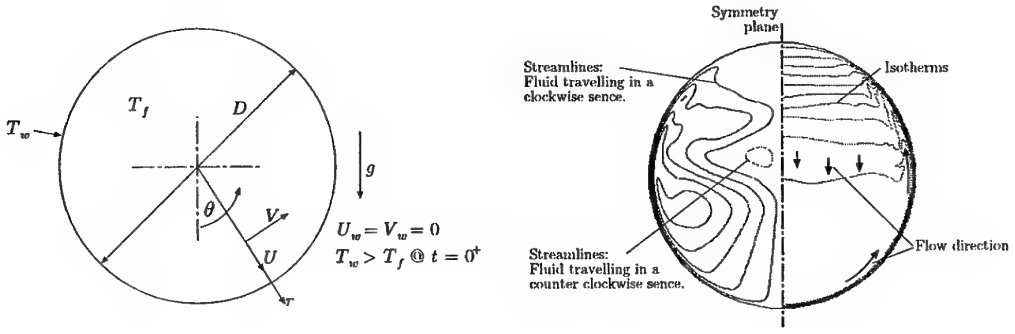

The numerical set-up (left) and a annotated stream line and isotherm image (right).

The problem is considered over the Rayleigh number range of $10^4 \leq Ra \leq 10^8$ for Prandtl numbers $Pr = 0.71$, 7.1 and 100, where Ra is based on the cylinder diameter D. This is extended to $Ra = 10^9$ for $Pr = 7.1$ and 100. The range of Ra considered here covers a variety of flow structures. Streamline and isotherm images clearly show the transition of the flow, with increasing Ra, from the conduction to the boundary layer regime. With increasing Pr the flow structure is found to asymptote to a base solution, rapidly becoming independent of Pr.

The flows evolution was found to be devisable in time into two regimes. The early regime, extending over the conduction time period, scales, classically, as $Ra^{-1/2}L^2/\alpha$. The latter time regime, encompassing the convective flow, scales as $Ra^{-1/4}L^2/\alpha$. The magnitude of the average Nusselt number is seen to be almost Pr independent, and is found to scale like $Ra^{1/4}$. For large Ra motion within the core of the enclosure is found to evolve in an oscillatory manner due to internal wave motion. The structure of these waves is Pr dependant. For $Pr = 0.71$ they appear stationary while for the two higher Pr cases the waves appear to travel through the core, from the top of the cavity to the bottom. The boundary layer is found to posses a two layer structure only over the very early time period. This is quickly superseded by a single layer, where both the thermal and dynamic boundary layers are of the same thickness. This latter single layer structure scales as $Ra^{-1/4}$.

ABSTRACTS
POSTERS

BDP & MPF & NN

The inertial lift on a small particle in a weak-shear channel flow at large channel Reynolds number

Evgeny S. Asmolov
Central Aero-Hydrodynamic Institute
Zhukovsky, Moscow region, 140160, Russia
Email: aes@an.aerocentr.msk.su

Keywords - Small Sphere - Inertial Lift

Abstract - The lateral migration of a small spherical particle translating within a vertical channel flow with large channel Reynolds numbers R_c is investigated. The weak-shear case is studied when the ratio of the slip velocity to maximum velocity of the channel flow, V_s, is finite, while two other dimensionless groups, particle Reynolds number R_s and R_c^{-1} are asymptotically small. The disturbance flow at large distances from the sphere is governed by Oseen-like equations. The ratio of Oseen length to channel width is $\varepsilon = l_s/l = (R_c |V_s|)^{-1} \ll 1$, i.e. the Oseen region is only a small part of the channel while the major portion of the disturbance flow is inviscid. The undisturbed velocity profile within Oseen region is close to the uniform flow. The linear term in the profile is $O(\varepsilon)$, and the parabolic one is $O(\varepsilon^2)$.

Solution of governing equations is constructed in terms of two-dimensional Fourier transform of disturbance field in a plane parallel to the channel walls. The ordinary differential equation for Fourier transform of lateral velocity $\Gamma_z(\mathbf{k}, z)$ is solved using the method of matched asymptotic expansions based on ε. Several domains in $(\mathbf{k}, z)-$ space are distinguished which correspond to different regions in physical space: Oseen region, inviscid region, viscous wake, boundary and critical layers. For the weak-shear case the dominant contribution to the lift gives not velocity disturbances within Oseen region but the large-scale inviscid disturbances. For such disturbances both effects due to inviscid interaction with the walls and the curvature of the undisturbed velocity profile should be taken into account.

The asymptotic theory is employed to modify the previous numerical method (Asmolov 1999) for calculating the lift for the weak-shear limit. At large R_c and $|V_s| > 1$ the two-term asymptotic solution for the lift agrees well with exact numerical solution. For the flow with critical layers, $|V_s| < 1$, the agreement is worse. The particle equilibrium position arises for both negative and positive slip velocities at the distances from the wall compared with the channel width.

The research was supported by Russian Foundation for Fundamental Research (Grant No. 99-01-00419).

References

ASMOLOV, E. S. 1999 The inertial lift on a spherical particle in a plane Poiseuille flow at large channel Reynolds number. *J. Fluid Mech.* **381**, 63–87.

Experiments on the effect of acceleration on the drag of spherical bubbles

C.W.M. van der Geld, H van Wingaarden and B.A. Brand
Department of Mechanical Engineering
Technische Universiteit Eindhoven, The Netherlands
Email: c.w.m.v.d.geld@wtb.tue.nl

Keywords - Drag force - bubble - acceleration

Abstract - 3D Trajectories of spherical bubbles passing through a converging part of a rectangular channel have been measured. Bubble diameters, d_b, were less than 1 mm and the Reynolds numbers, Re_b for stagnant water and for mean liquid velocity $\overline{v}_L = 0.25$ m/s were in the same range because of two counteracting phenomena affecting the relative velocity at $\overline{v}_L = 0.25$ m/s:

- the acceleration in the converging flow area, increasing drag;
- the $\overline{v}_L$-dependent concentration of surface active agents at the bubble interface.

The concentration is lower at $\overline{v}_L = 0.25$ m/s than in stagnant water because the time of travel from the injection point is less and because the concentration is determined by diffusion. At this liquid velocity, the turbulence is of intermediate scale with weak intensity and therefore essentially hardly affecting bubble trajectories in the converging flow area.

The dependency of the drag coefficient, c_D, on Re_b is determined in stagnant water by varying d_b, yielding a correlation $c_D(Re_b, 0)$. The dependency of c_D on the acceleration number, A_c, is subsequently deduced from 3D trajectories at $\overline{v}_L = 0.25$ m/s. The result is the empirical correlation

$$c_D = (1 + 1.79A_c)0.61c_D(Re_b, 0) + 1.29A_c$$

where the factor 0.61 accounts for the decrease in concentration of surface active agents. Numerical computations of Magnaudet et al. (1995) for a spherical, rigid sphere in steady straining flow show a similar, although somewhat weaker, dependency on A_c. Discrepancies are attributed to differences in flow conditions, e.g. the presence of shear in the actual flow experiments.

EXPERIMENTAL DETERMINATION OF MOTION PARAMETERS OF GAS BUBBLES RISING IN A LIQUID METAL

B. Hofmann and E. Kaiser
Technical University of Dresden, Institute of Energiemaschinen und Maschinenlabor,
D-01062 Dresden, Germany; e-mail: hofmann@mal.mw.tu-dresden.de

The topic of this paper is the determination of motion parameters of argon bubbles rising in a liquid metal by using ultrasonic waves. Bubbles can be generated by different sparkling facilities on the bottom of circular-cylindrical vessels consisting of stainless steel, mineral or plastical glass (perspex). Bubble motion is caused by buoyancy forces. Liquid metal having a melting point of about 283,7°K (+10,5°C) is an eutectic alloy of In, Ga and Sn. Therefore, it is liquid at normal laboratory temperatures in general. The aim of the investigations is the measurement of the bubble detaching frequencies and the estimation of the void and bubble size distributions over the cross section of the vessels at different levels above the vessel bottom as functions of the typ of the sparkling facility. The investigations are of interest to MFD applications especially.

For the experimental determination of these two-phase flow parameters the ultrasonic pulse-echo method well known from the non-destructive material testing technology is used. A piezoceramic narrow band straight-beam probe is clamped outside of the vessel by means of a special assembling device allowing a comfortable installation of the probe at different positions on the external vessel wall. This probe having an ultrasonic resonance frequency of 15 MHz transmits short ultrasonic bursts with regular intervalls of about 2 kHz. The triggering pulses are generated by an special electronic device. The ultrasonic waves penetrate the wall and the liquid metal as a slender sonic cone perpendicularely to the inner wall of the vessel. They are reflected partially by the phase boundary between liquid metal and a gas bubble moving inside the sound cone. The echoes are received by the probe again and amplified electronically. The amplitude and the time of flight of the ultrasonic echo signals are transfered into two analogue electric voltages U_S and U_P (see Fig. 1), where U_S is a measure for the bubble sizes and U_P to the bubble positions inside the vessel, respectively. These signals are pre-storaged and recorded as functions of time t_M by a digital storage oscilloscope (DSO). For further data processing using the software tool FAMOS and final storing the measured signal data are transfered to a PC using the software code TRANSITION. By means of different FAMOS functions like *FFT, HISTOGRAM* and others the distribution of the echo amplitudes of bubbles, the detaching frequencies at the bubble generating process and the distribution of the bubble positions inside the vessel can be determined approximately. From this results, to the relative bubble sizes, bubble shapes, bubble velocities, local bubble positions and void distributions in the vessel can be suggested. The detectibility of the bubbles is limited by their minimal size, by the sound attenuation in the liquid metal, by the unavoidable signal noise (see „grass" between bubble peaks in Fig.1) and other effects.

Keywords: bubbles, liquid metal, ultrasonics, two-phase flow

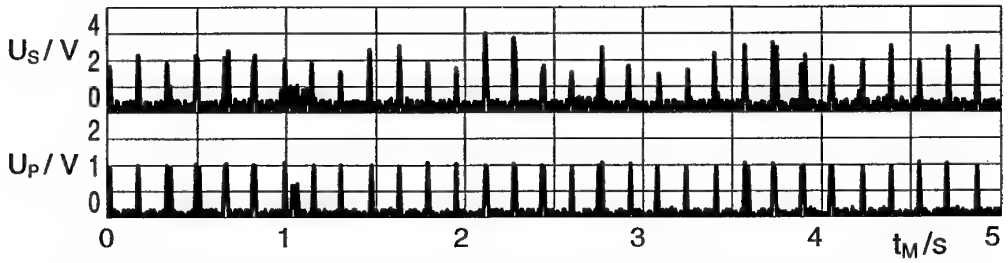

Fig. 1: Ultrasonic echo signals of an argon bubble sequencc having a frequency of about 6,2 Hz generated by a nozzle of 0,3mm in diameter

(upper plot - bubble sizes: varying, lower plot - bubble positions: constant nearly)

(The research project has been done in collaboration with the Research Center Rossendorf e.V., Germany)

Angular Momentum in homogeneous and in biphase and micropolar flows

M. Iovieno and D. Tordella
Department of Aerospace Engineering, Politecnico di Torino, Italy
Email: tordella@polito.it

Keywords Angular momentum - asymmetric stress - spatial averages

Abstract - When the flow is not homogeneous and owns internal structures on which external forces and couples do operate, it may be necessary to introduce a balance of angular momentum, which presence may affect the symmetry property of the stress tensor. In this condition the moment of the momentum balance is no more equivalent to the angular momentum balance and a new variable, the intrinsic angular momentum per unit volume, must necessarily brought in.

We have carried out an analysis about the structure of the angular momentum balance over finite volumes of linear dimension δ. In case of an homogeneous fluid, introducing volume averaged quantities, the intrinsic angular momentum $\mathbf{h}$ of each element about its centre of mass is obtained from the moment of the momentum balance. Through a power series development in δ^2, we showed that the balance for $\mathbf{h}$ is equivalent to the infinite succession of equations obtained applying the following operators:

$$\mathcal{A}_{ik}^m = \varepsilon_{ilk} \frac{\partial^{2m+1}}{\partial x_l^{2m+1}} \quad \forall m \in \mathbf{N}$$

to the momentum equation. While the first order relation is the vorticity equation (Chatwin, *Proc.Cam. Phil.Soc.*, 1973), the higher order relations are not reducible to it. In general $\mathbf{h}$ cannot be described as a function of $\boldsymbol{\omega}$ only. Anyway if $\delta \to 0$, $\mathbf{h}$ contains the same amount of information as $\boldsymbol{\omega}$, but it goes to zero as δ^2.

In case of an inhomogeneous flow we carried out a comparative analysis of the models up to now developed. A description based on power series developments cannot anymore be used since the velocity field, even if continuous, shows discountinuous derivatives at the frontiers separating different phases. The flow of momentum and angular momentum must be represented in integral form. The density ratio α between different phases is a control parameter for the system. When α is different from zero or one it is necessary to associate to the momentum and angular momentum balances, averaged over both phases, the balances averaged over one phase only. When $\alpha \to 1$ Batchelor's theory applies (*JFM*,1970), where collision events among suspended elements are excluded and an external moment acting selectively on the suspended phase is assumed, leading to a non symmetrical flow of momentum. When $\alpha \to 0$ the system becomes a discrete granular flow and the relevant model would be Enskog-like. Recently Goldshtein and Shapiro (*JFM*,1995) tried to transfer the granular flow to a countinuum description that must include angular momentum balances to allow for a quantitative contrast with observations.

There exist as well axiomatic theories that foresee the presence of an angular momentum non linked to the presence of different phases as the micropolar theory (Eringen,*J.Math.Mech.*,1966; Łukaszewicz, *Micropolar Fluids*, Birkhäuser,1999). The flow is here viewed as a collection of material basic systems, the micro elements, owning momentum, intrinsic angular moment and energy. The theory is developed under the approximation of rigid motion inside each micro element and implies that the intrinsic angular momentum will not vanish with the volume, thus the basic elements should be characterized by a finite volume. The evolutive equations are continuous, but the field does not foresee the continuity of the first derivatives at the level of the polar elements. Since a feature of this theory is the presence of two very different scales, the external and the local one, it would seem reasonable to derive the model by means of a limiting process to respect to their ratio. This passage would lead to Eringen's equations only if a singular vorticity field is allowed.

Eringen's model was applied to turbulent fields under the assumption that it should remain valid after the adoption of space averages and of a turbulent viscosity, but this leads to flow terms not equivalent to those deducible filtering the Navier-Stokes equation, as it is the equation here presented. Analog approaches, confined to turbulent application, were proposed in times past by Mattioli (*C.R.Acad.Sci.*,1933), Ferrari (*Acad.Sci.USSR*,1972), where an intrinsic angular momentum was used to represent the turbulent transport, and by Nicolaevky (*P.M.M.*,1970,1973), who tried to approximate the average of the spatial derivatives in terms of differences of surface integrals in such a way introducing spurious asymmetry property to the turbulent flow. The idea by Mattioli about the modeling of the turbulent viscosity may be exploited in the framework of the LES method using a correct moment of momentum balance.

Flow visualization experiments of cellular flows induced by rotation of a cylinder variously positioned inside channels of different shapes

E.F. Kent
Department of Thermodynamics and Heat Transfer
Faculty of Mechanical Engineering
Istanbul Technical University
80191, Gumussuyu, Istanbul, Turkey
Email: fkent@burgaz.mkn.itu.edu.tr

Keywords - Flow Visualization - Cellular Flow

Abstract - In this work, flow visualization experiments of cellular flows induced by rotation of a circular cylinder variously positioned inside channels of different shapes have been performed and high quality visualization photographs have been presented. Flow visualization experiments have been carried out inside V-shaped (having different wedge-angles) and rectangular channels.

In the experiments, these channels are filled with silicon rhodorsil oil of different viscosities (Newtonian fluid) and CMC (Non-Newtonian fluid). Flow visualization experiments are carried out using solid tracers of magnesium for the Newtonian fluid and Rilsan for the Non-Newtonian fluid. They are illuminated by a thin sheet of light coming from a laser device and the visualization photographs are obtained by means of long time exposure photography.

A series of experiments have been performed at different rotational speeds of the circular cylinder. In the experiments, silicon rhodorsil oils having different viscosity values have been used. Thus the Reynolds number of the flow has been changed. The visualization experiments are carried out inside channels of different wedge angles. This permits to investigate the influence of the wedge-angle on the flow structure inside the channel. The shape of the separating streamline and the details of the flow structure in the channels are visualized in the photographs.

The inner cylinder is positioned at different locations inside these channels and many interesting flow patterns have been visualized. The visualization photographs are compared each other.

The numerical solutions are obtained for the corresponding channel geometries and compared with the flow visualization pictures. Excellent agreement is found for each comparison.

Validation of an X-ray Based PTV-Method for Multi-Phase Flows and Opaque Media

U. Kertzscher, A. Seeger, K. Affeld, L. Goubergrits, and E. Wellnhofer[+]
Biofluidmechanics Lab, Humboldt University Berlin, E-mail: axel.seeger@charite.de
[+]German Heart Center Berlin

Keywords - 2D-PTV - X-ray - Bubble column - Multi phase flow

Abstract - The in many flows successfully applied optical methods such as Particle Image Velocimetry (PIV), Particle Tracking Velocimetry (PTV), and Laser Doppler Velocimetry (LDV) fail in some flows. They cannot be applied for the assessment of

- the velocity of liquid and solid phase in multi-phase flows for a large void fraction
  The cause is the different refraction index of liquid phase and void fraction, which leads to reflection and dispersion.
- flow velocities in opaque media, such as sewage water flows
- flow velocities in areas having no optical access

The new x-ray based PTV-method - called "XPTV" - presented here permits to obtain the liquid velocity and velocity of the solid phase of these flows. The problem of light reflection, light dispersion on phase boundaries and light absorption of opaque media is solved by the use of x-rays instead of light. X-rays penetrate multi-phase flows in straight lines.

The purpose of this study was to validate the new method by comparing XPTV with above mentioned optical methods in a flow, where both methods are applicable. A two-dimensional flat bubble column having a small void fraction was used. The experimental set-up is shown below. One x-ray source (point source) generates x-rays, which are received and amplified by the image intensifier. Behind the image intensifier, a CCD-camera digitizes the images. 50 images are taken per second. The liquid is seeded with small x-ray absorbing particles. Water was used as liquid phase and air as gaseous phase.

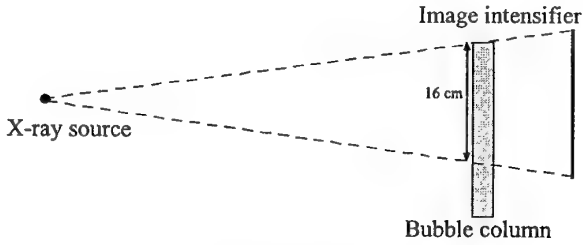

Experimental set-up

The results showed very good agreement with the results obtained by LDV and PIV.

It was shown that it is possible to analyze the three-dimensional velocity of the liquid phase of a bubble column with the new x-ray-based method.

A new kind solitary wave in liquid containing gas bubbles

Kim Din Cher
United Institute of Semiconductors Physics of SB RAS
and Institute for Water and Environmental Problems SB RAS
2, Morskoy Prospekt, Novosibirsk 630090, Russia
Email: iwep@ad-sbras.nsc.ru

Keywords - Oscillatory soliton - Solitary wave oscillations - Bubbly liquid

Abstract - Despite the contribution of many researchers, the description of two-phase liquid flow is still vague. After studying the existing theories and comparing them with each other and with experiments it is not difficult to see that the most limitation of these theories is the linearization of the equation of bubble motion. In many two-phase flows of practical interest such as propagation of sound and shock wave, cloud cavitation on hydrofoils, cooling devises of nuclear-reactor systems, and etc., the amplitude of bubble-radius perturbations is not small. At the same time it has been found out that hydrodynamics nonlinearity is much less than nonlinearity caused gas bubbles. This fact makes it possible to linearize the hydrodynamics velocity field but does not permit to linearize the bubble dynamics. To avoid this and other restrictions a new approach has been put forward. The Lighthill-Crighton-Ffowcs Williams inhomogeneous wave equation [D.G. Crighton and J.E. Ffowcs Williams, J. Fluid Mech. vol. 36, 585 (1969)], generalized by us, for carrier liquid where gas phase is represented by monopole sources and a complete bubble dynamics equation (e.g. as Rayleigh-Plesset) are in its basis:

$$\begin{aligned} \frac{\partial^2\rho}{\partial t^2} - c^2\frac{\partial^2\rho}{\partial x^2} &= \frac{\partial}{\partial t}\left[\rho\frac{\partial}{\partial t}\lg(1+\frac{\phi_0\bar{\rho}\bar{R}^3}{1-\phi_0})\right], \\ \rho\left(R\ddot{R}+\frac{3}{2}\dot{R}^2\right) &= P_{gas}(R,t) - P(x,t) - P_0 - 4\mu\frac{\dot{R}}{R} - \frac{2\sigma}{R} + \frac{R}{c}\frac{d}{dt}\left[P_{gas}(R,t)\right] \end{aligned}$$

A range bubble motion equation we used in our study. New finite difference technique for exact solving these equations has been developed as evolution-boundary-value problem. The predictions of our model agree well with experiments [D.Ch. Kim, in Abstracts of the International Conference "Fluxes and Structures in Fluids". Sanct Peterburg, Russia, pp. 58-60, 1999].

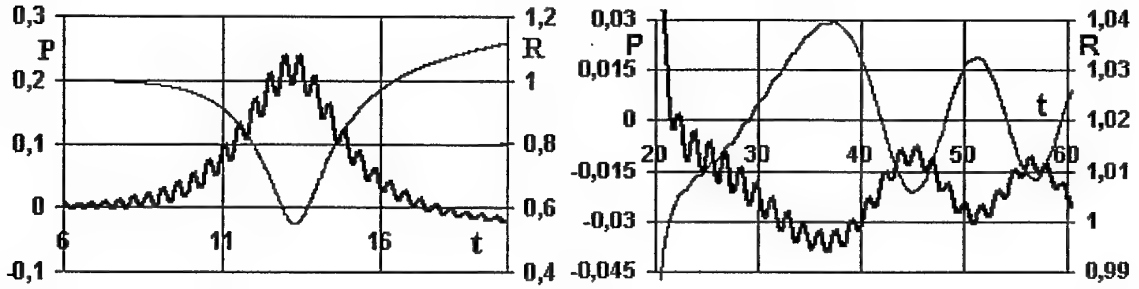

The oscillatory soliton (left) and subharmonic generation on solitary-wave tail (right)

The fundamentally new type solitary wave called oscillatory soliton is discovered. Its profile is amplitude-modulated with frequency of precursor. The nature and mechanisms of solitary-wave tail, solitary wave oscillations, solitary wave with oscillatory structure, and precursor in bubbly liquid are clarified. Similar the oscillatory solitons are to be expected in general for other mechanical and physical problems.

I wish to express my hearty thanks to corresponding member of the RAS G.A. Mikhailov.

IN SEARCH OF A PLANAR WORTHINGTON JET

Sophie Nigen & Ken Walters

Department of Mathematics, University of Wales, Aberystwyth, Ceredigion SY23 3BZ, UK.

ABSTRACT

When a solid sphere is dropped through the free surface of a liquid, a fascinating sequence of events can occur, the most notable being a vertical jet, which can often reach extravagant heights in Newtonian liquids, given the right experimental conditions. This jet has been called the "Worthington jet", after the scientist who first investigated the effect a hundred years ago.

A rheological interest in the Worthington jet emanated from the realization that very low levels of viscoelasticity in the liquid could result in a spectacular decrease in the height of the jet (Cheny and Walters, 1999). Specifically, concentrations of high molecular weight polymers as low as 10ppm, added to a Newtonian solvent, lead to jets which can be an order of magnitude lower than that found in the equivalent Newtonian liquid. This reduction has been tentatively linked to the high uniaxial extensional viscosity of very dilute polymer solutions (Cheny and Walters, 1999).

In order to determine whether the *planar* extensional viscosity is similarly affected, the present work investigates the case when long rods are dropped horizontally onto the free surface of a liquid. In the process, several new flow features emerge, but the main (tentative) conclusion of the work is that the planar jet arising in the rod experiments is not greatly affected by the addition of polymer and we are tempted to conclude that the planar extensional viscosity is not as significantly affected by polymer addition as the uniaxial extensional viscosity.

KEYWORDS: VERY DILUTE POLYMER SOLUTIONS, EXTENSIONAL VISCOSITY, WORTHINGTON JET.

Motion of Granular Material on a Travelling Grate

B. J. Peters and A. Džiugys
Institute of Nuclear- and Energy Technology
Research Centre Karlsruhe, Germany
Email: b.peters@iket.fzk.de

Keywords - Particle Motion - Numerics - Travelling Grate

Abstract - The objective of this contribution is to describe numerically the motion of granular material on a travelling grate. The method works in a Lagrangian frame of reference which uses the position and orientation of particles as independent variables. These are obtained by time integration of the dynamics equations for each particle. The forces and torques are due to gravity and visco-elastic contact forces, which include normal and tangential components with visco-elastic models for energy dissipation and friction. The implementation is carried out with object-oriented techniques, which renders the software less complex and, therefore, easier to maintain and to re-use.

Particles are transported on a travelling grate by displacing every second grate element forward and backward. Thus, particles in front of a step are pushed over the edge of the following step, so that the packed bed moves down the grate. In addition to the particle load, fig. 1 shows the direction and magnitude of the particle velocity.

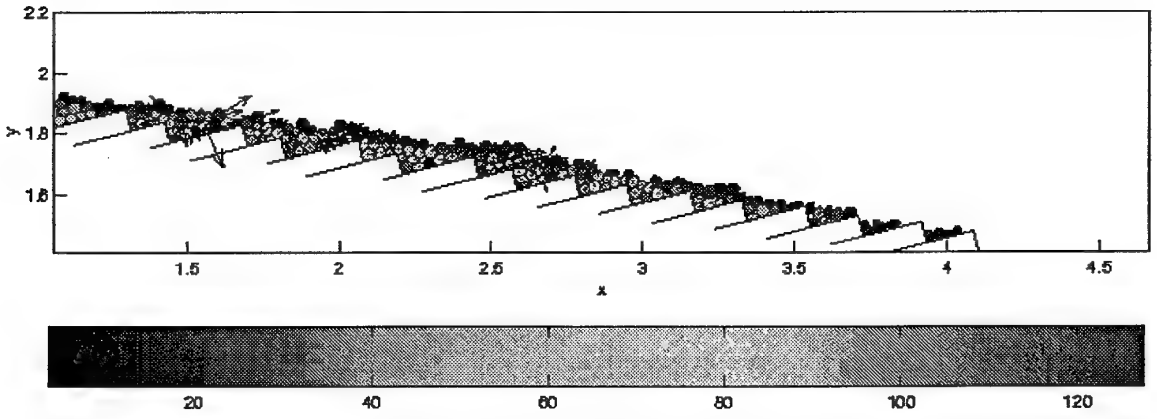

Figure 1: Motion on a moving grate and distribution of particle forces [N]

Due to the kinematics of the moving grate, the weight and the collisions of the particles, maximum velocities of approximately $v \approx 9\ cm/s$ occur. Although, several velocity vectors point into diffrent directions, a global transport along the steps of the grate takes place. This characterisctic emphasizes horizontal motion and prevents vertical dispersion of particles. It implies for commonly used grates in combustion devices, that bottom particles are always protected by an upper layer of particles, which allows generally only a downward propagating conversion front and thus, reduces the thermal capacity.

An X-ray Based PTV-Method to Assess the Three-dimensional Velocity in Bubble Columns and Opaque Media

A. Seeger, K. Affeld, L. Goubergrits, U. Kertzscher, and E. Wellnhofer[+]
Biofluidmechanics Lab, Humboldt University Berlin, E-mail: axel.seeger@charite.de
[+]German Heart Center Berlin

Keywords - 3D-PTV - X-ray - Bubble column - Opaque fluid

Abstract - For the investigation of the flow structures in bubble columns it is necessary to measure the local liquid velocity. Common optical methods such as Particle Image Velocimetry (PIV), Particle Tracking Velocimetry (PTV), and Laser Doppler Velocimetry (LDV) fail in a bubble flow with a large void fraction. The cause is the different refraction index of liquid phase and gaseous phase, which leads to reflection and dispersion. Other methods based on point measurement yield only limited information about the whole flow field and are invasive. The new x-ray based PTV-method - called "XPTV" - presented here permits to obtain the liquid velocity three-dimensionally, touch-free and for any large void fraction. The problem of light reflection and light dispersion on phase boundaries is solved by the use of x-rays instead of light. X-rays penetrate a gas/liquid flow in straight lines.

The new method for velocity measurements in a bubble column works as follows:

1. X-ray-absorbing particles are added to the fluid.
2. Two x-ray images from two different angles are taken. After a short time lag a second image pair is acquired.
3. The three-dimensional position of the particles is calculated from the two image pairs. With the time difference, the three-dimensional velocity of the fluid phase can be obtained from the displacement of the particles.

The three-dimensional XPTV method was applied to two cylindrical bubble columns having one an inner diameter of 110 mm and the other of 150 mm. Injection needles with an inner diameter of 0.55 mm at the bottom were used for the generation of bubbles. Different liquids such as water, glycerin, and silicon oil were used. A medical biplane x-ray device having two x-ray sources and two cameras (including the image intensifiers) was used to assess the particle motion. 25 images for each direction were taken per second. A particle tracking method was developed for the observation of the particle motion.

Particle trajectories and their properties (velocity in three dimensions, curvature of trajectory) were obtained for different flow conditions (void fraction, liquid viscosity).

It was shown that it is possible to analyze the three-dimensional velocity of the liquid phase of a bubble column with the new x-ray-based method.

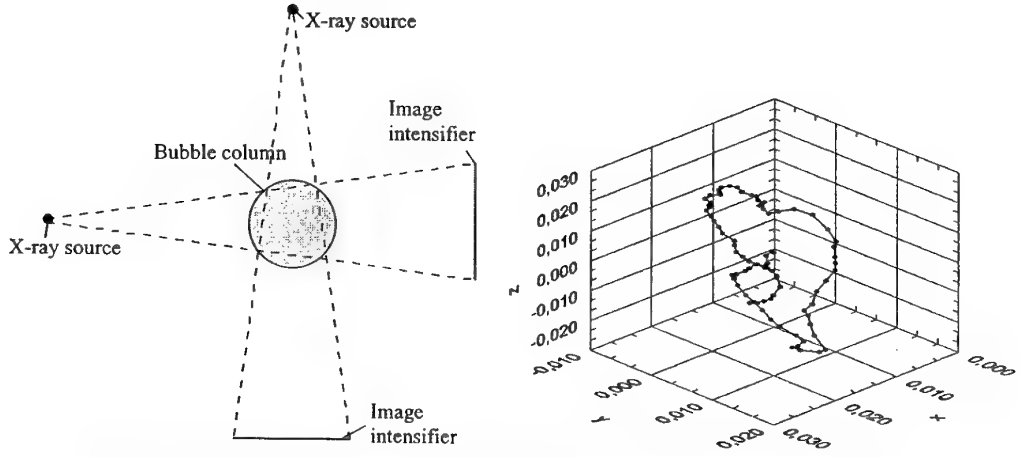

The experimental set-up, top view (left) and a typical particle trajectory (right)

Bubble dynamics in a water-gas solution

P. Zima F. Maršík
Deparment of Thermodynamics, Intitute of Thermomechanics CAS
Dolejškova 5, 182 00 Prague, Czech Republic
Email: zimap@it.cas.cz

Keywords -Cavitation - Bubble dynamics

Abstract The classical approach to the Rayleigh-Plesset dynamics of a single bubble in a liquid originates from the widely used assumption of non-permeability of the bubble boundary. Such assumption, however, discounts any possibilities for mass transfer across the gas-vapor-liquid interface, although evaporation and gas diffusion appear to be the driving forces of bubble growth in many cases. In our work we rederive the Rayleigh-Plesset equation and study the impact of the modifications on the ability of the Rayleigh-Plesset equation to render bubble growth driven by gas diffusion and/or evaporation. The revised Rayleigh-Plesset equation for bubble radius R and various components α now has the following form containing mass flow j_B:

$$\frac{p_B - p_{l\infty}}{\rho_l} = R\ddot{R} + \frac{3}{2}\dot{R}^2 + \frac{2\sigma}{\rho_l R} + (4\nu_l - \frac{2R\sum_\alpha j_{B\alpha}}{\rho_B})\frac{\dot{R}}{R}, \quad j_{B\alpha} = -\frac{\rho_l D_{l\alpha}(c_{l\alpha\infty} - c_{l\alpha B})}{R\sum_\beta(c_{v\beta B} - c_{l\beta B})}. \quad (1)$$

ρ_l, ρ_B, p_l, p_B are densities and pressures of the liquid and the bubble contents. $\rho_{l\alpha} = \rho_{l\alpha}/\rho_l$, $c_{v\alpha} = \rho_{v\alpha}/\rho_v$, p_l, p_v are mass concentrations in the liquid and in the vapor, respectively. Index ∞ denotes infinity, ν_l is liquid kinematic viscosity. $D_{l\alpha}$, $D_{v\alpha}$ are diffusion coeficients in the liquid and in the vapor, respectively. In thermal equilibrium, the energy flux on the bubble is $j_q = -\sum_\alpha h_{lv\alpha} j_{B\alpha}$, where $h_{lv\alpha}$ is evaporation heat.

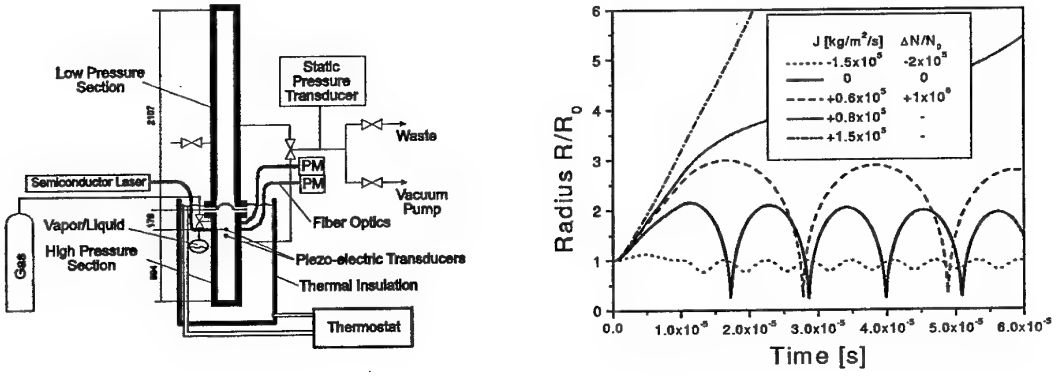

The experimental setup for the nucleation pulse technique (left) and bubble dynamics modes for various levels of mass flux J (right). $J > 0$ means that mass goes into the bubble.

The solution of the revised Rayleigh-Plesset equation (see Fig. (right)) reveals the effect of mass flux density on the behavior of a stable bubble. The model of bubble growth based on the revised Rayleigh-Plesset equation is to complement the experimental study of gas-contaminated water solutions which is being carried out in the Institute of Thermomechanics using the nucleation pulse technique (see Fig. (left)).

BFM

Computational Fluid Dynamics and Experimental Validation of a Microaxial Blood Pump Model

J. Apel, F. Neudel and H. Reul
Cardiovascular Biomechanics Group, Helmholtz-Institute for Biomedical Engineering University of Technology Aachen, Germany
Email: apel@hia.rwth-aachen.de

Keywords - CFD - Blood Pump - Image Velocimetry

Abstract - Intravascular application of microaxial blood pumps in heart assist requires a maximum in size reduction of the pump components. These limitations affect the design process in many ways and restrict suitable experimental procedures. Nevertheless, a detailed knowledge of the hemodynamics of the pump is of great interest for efficiency enhancement and reduction of blood traumatization and thrombus formation. Computational Fluid Dynamics (CFD) offers a convenient approach to reach this goal. In this study, the inlet, vane and outlet regions of a microaxial blood pump for application in intraaortal left ventricular assist are analyzed by CFD and 3-D Particle tracking velocimetry (PTV). For this purpose a mock loop was set up which allows monitoring of static pressure at different inlet and outlet locations as well as 3-D flow visualization. Flow in the main part of this testing device is modelled and computed by means of CFD. Pump HQ-characteristics, axial pressure distribution as well as particle and ink images taken from inlet and outlet regions are compared to numerical flow data. This study also focusses on crucial considerations regarding an appropriate match of measured and numerically implemented boundary conditions (esp. in- and outflow regions). Results show that the pump performance characteristics as well as inlet and outlet spin predicted by the CFD model are very accurate compared to measured data. However, the accuracy depends on proper boundary condition setup and computationol grid quality. Appropriate boundary condition specifications and spatial discretisation topologies required for satisfactory results are discussed.

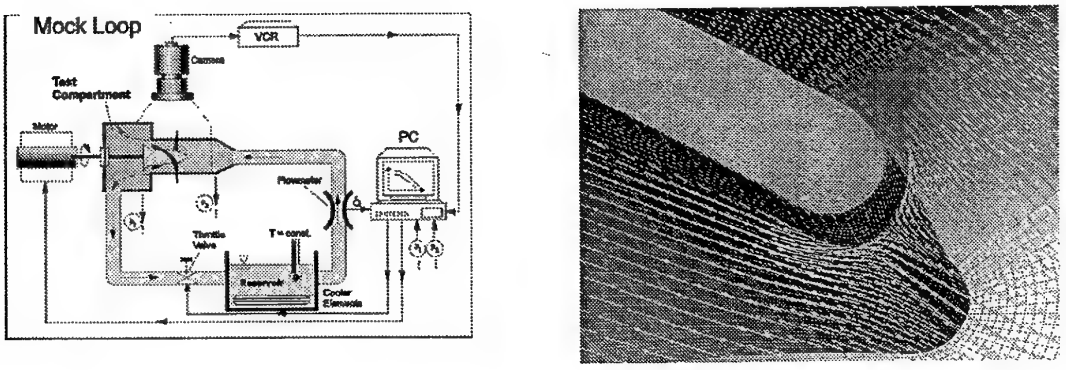

The experimental set-up (left) and a computed vector plot at front blade (right)

EXPERIMENTAL INVESTIGATION OF A BOUNDARY LAYER OVER ELASTIC PLATES MODELING OF SKIN COVERS FOR SOME MARINE ANIMALS

V.V.Babenko, V. I. Korobov, V. V. Moros

Institute of Hydromechanics National Academy of Sciences of Ukraine
8/4 Zheljabov str, 252057 Kiev, Ukraine

The designs of elastic plates were developed based on of analysis of fast swimming water animals, and also based on of modern representations about a structure and parameters of coherent vortical structures in near wall area of a turbulent boundary layer.

Classical researches of a hydrodynamic stability on various kind of an elastic surface in the beginning were carried out. For the first time experimental way obtains classical neutral curves, and also performance of disturbing motion. The development of disturbing motion across a boundary layer is investigated. The physical picture of a disturbing motion development at various stages of transition is developed at a flow over elastic surfaces. The development of disturbing motion on curvilinear elastic surfaces is investigated. The technique of an experimental construction Gertler's diagram of instability is developed. The Gertler's experimental diagram is constructed for the first time at a flow of an elastic surface.

The physical substantiation of the mechanism of interaction of a stream with an elastic surface is developed. The structural and kinematics-dynamic principles of interaction of a boundary layer with elastic surfaces are formulated. The researches of interaction of various perturbations in a boundary layer are carried out at a flow of elastic plates.

The classical experimental researches of a turbulent boundary layer on elastic plates are carried out. Thus were studied two kind of elastic plates: resonance and dissipative. Is constructed experimental profiles of average velocities in various types of semilogarithmic coordinates. The empirical formulas of average profiles of velocities are obtained. The analysis longitudinal and cross-sectional pulsation of velocities is carried out. The obtained outcomes are analyzed in near wall area. The associations of maximum longitudinal pulsating of a velocity and of the Reynolds stresses from factor of oscillation frequency of an elastic plate surface, and also distribution of length of a path of mixing on a thickness of a boundary layer are obtained. The methods of the concentrated and distributed forming of longitudinal vortical systems on elastic plates are investigated.

The experimental outcomes of an dependence of a drag friction coefficient of elastic plates from a Reynold's number in a range $3 \cdot 10^6 \div 4 \cdot 10^7$ are obtained.

THEORETICAL MODEL OF PRESSURE PULSE PROPAGATION IN THE HUMAN SPINAL CSF SYSTEM

By

K. Berkouk[1], P.W. Carpenter[2] and A. D. Lucey[2]

Abstract

This work is motivated by an attempt to explain the origins of *syringomyelia*. This serious disease is characterized by the appearance of cavities, called *syrinxes*, in the central canal of the spinal cord resulting in partial or complete paralysis. Syringomyelia has an incidence of 8.4 new cases per 100,000 per year. The causes of syringomyelia are unknown but pressure propagation is probably implicated. Previous theories about the origin and the mechanisms of syringomyelia progression have been subject to controversy. Gardner and colleagues postulated that the outflow of cerebrospinal fluid (CSF) is transmitted by means of venous pulsatile flow from the fourth ventricle down to the syrinx via the central canal. Williams then proposed two theories: the *suck* mechanism (or cranio-spinal pressure dissociation theory) and the *slosh* theory where a resistance to flow in the central canal is required. The main difference between Gardner's theory and the *suck* mechanism of Williams is that in the latter case, the pressure driving the fluid from the fourth ventricle down to the syrinx originates in the spinal part rather than the cerebral part. Oldfield argued that no evidence of communication between the fourth ventricle and the syrinx is found in most of patients. The *slosh* theory, however, does not imply such communication, and is therefore more convincing. Pressure pulses, caused by coughing, sneezing and similar activities, propagate up the cerebrospinal fluid (CSF) in the spinal subarachnoid space. Williams (1990) suggested a possible cause of syrinx formation is that when such pressure pulses encounter a partial or total blockage a large pressure rise would be generated in the spinal central canal. Our theoretical model modeling was undertaken to investigate Williams' *slosh* hypothesis.

Essentially, we model the spinal system as a channel separated into two parts by a flexible diaphragm representing the spinal cord. The upper part represents the subarachnoid space while the lower part, which has a much smaller cross-sectional area, represents the central canal. A theory for pressure wave propagation in such a two-chamber system has been developed. It has been used to study the wave characteristics of the two-chamber system. In this way it has been found that the leading edge of a pressure pulse/wall bulge tends to steepen into a shock-like wave or elastic jump. When such a pressure pulse is incident on a blockage in the subarachnoid space, a large pressure rise is generated in its vicinity. We showed that this pressure rise could be momentary or permanent depending on whether the pressure pulse bulge is positive or negative. This provides a possible mechanism for the formation of the syrinxes.

Keywords: Elastic jump, syringomyelia, pressure propagation, flow in elastic tubes

[1] School of Engineering, University of Exeter, k.berkouk@exeter.ac.uk
[2] Fluid Dynamics Research Centre, University of Warwick

Unstead flow throug a new mechanical heart valve prosthesis analyzed by High-speed Digital-Particle-Image-Velocimetry (DPIV)

Ch. Brücker*, U. Steinseifer**, W. Schröder*,
* Aerodynamisches Institut, RWTH Aachen, Germany
** Triflo-GmbH Germany, Aachen, Germany
Email: bruecker@aia.rwth-aachen.de

Keywords - artificial heart valve flow - DPIV

Abstract The design of modern artificial heart valves is increasingly optimized on the basis of detailed flow analysis with modern numerical simulation and measurement techniques. It is well known, that any flow separation in addition with regions of high shear are critical with respect to blood clotting and therefore reasons of malfunction after clinical implantation. Therefore, a detailed analysis of these fluid-mechanical aspects is required if a new type of artificial heart valve is in test. Due to the complexity of the geometry with moving objects and the high Reynolds-number of about 5000 numerical simulations are not yet feasible.

In this report we present results of time-resolved flow measurements through a new type of a mechanical heart valve prothesis in aortic position using Digital-Particle-Image-Velocimetry. The measurements are carried out in a pulsating flow circuit with an optical transparent model of the aortic root and a transparend model of the valve. The valve itself has three leaflets similar to the natural aortic heart valve. Pulsating flow is reproduced with a piston motor which is controlled by a PC according the physiological variation of the flow in time, whereby typical values of the pressure ratio p_A/p_V of the diastolic to systolic phase and duration are used. A water-glycerin mixture is used as working fluid to achieve a best match of refractive index of fluid and model to reduce any image destortion. The three-dimensional and unsteady flow field is recorded chronologically with a high-speed camera. In addition, a high-resolution CCD camera is used to obtain phase-locked PIV records to certain phase points in the cycle. This allows to analyze the flow evolution and the cycle-to-cycle variations in detail. The chronological PIV recordings offer to observe the coupling between the leaflet cinematics and the fluid dynamical aspect of the flow around the leaflets. With an electronic synchronization we can also detect cycle-to-cycle variations over a large number of PIV records to compare the results with phase-averaged turbulence properties. An example of a multiexposed flow visualization picture and a result of the measured flow field is given in the figure below. It shows the flow immediately after the valve is complete open. From the multiexposed picture and the measured velocity field one can recognize the wash-out of the bulbi (the three circular shaped exclusion in the aorta). Further results will be provided in the full paper.

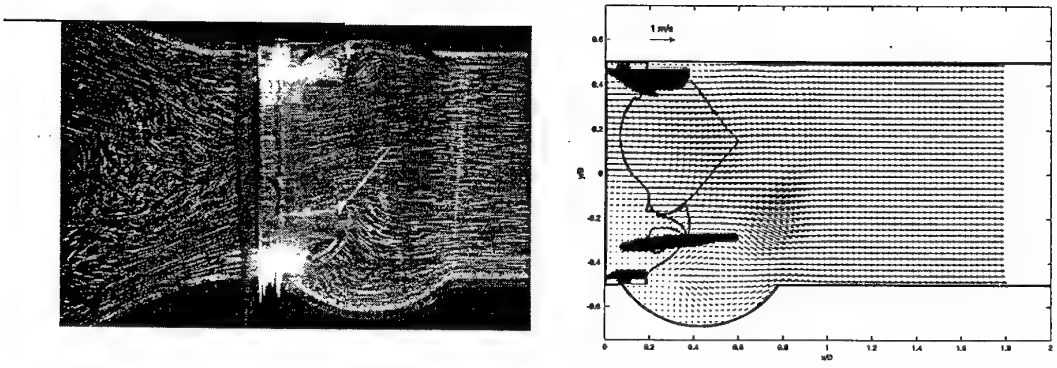

Figure 1: Multiexposed flow picture (left) and velocity field (right) after opening of the valve

References

Brücker, Ch.: Dual-camera DPIV for flow studies past artificial heart valves. *Experiments in Fluids* 22(6), pp. 496-506, 1997

NUMERICAL SIMULATION OF FLOW IN COLLAPSIBLE CHANNEL USING A FLUID-BEAM MODEL

Z.X. Cai, X.Y. Luo & T.J. Pedley†

Department of Mechanical Engineering, University of Sheffield, Sheffield, S10 2TN, UK

†DAMTP, University of Cambridge, Silver Street, Cambridge, CB3 9EW, UK

Flow in collapsible tubes has a number of applications in physiological flows and medical devices. To understand such a fluid-structure interaction system, numerical studies have been carried out on a two- dimensional model in which the collapsible tube is represented by a membrane in one wall of a channel. These studies have shown rich dynamical behaviour(Luo Pedley, 1996) but the model involves several ad hoc assumptions because the membrane equation alone cannot determine the movement of material points of the elastic wall. In the present paper, a study is carried out on a new model in which a plane strained elastic beam with large deflection and incrementally linear extension is used to replace the membrane. A finite element code is developed to solve the coupled fluid-beam equations simultaneously. To make the mesh adaptive to the moving boundary, a new spine method similar to that in Luo Pedley (1996) is introduced which not only allows nodes to move along the spines, but also allows each spine to rotate around a fixed point. The code is validated with different grids and preliminary results are compared with those from the previous model when the bending stiffness is small.

Key words: Collapsible flow, fluid-beam interaction, finite element methods

Reference:
Luo, X. Y. & Pedley, T.J., A numerical simulation of unsteady flow in a 2-D collapsible channel. J. of Fluid Mechanics. Vol. 314,, 191-225, 1996.

Investigation of the Flow in Carotid Arteries with Authentic Geometries

L. Goubergrits, K. Affeld, J. Fernandez-Britto[+] and L. Falkon[+]
Biofluidmechanics Lab, Humboldt University Berlin, E-mail: Leonid.Goubergrits@charite.de
[+]Pathology, Dr. Finlay Hospital, Havana, Cuba

Keywords – Carotid artery- Atherosclerosis – Geometric reconstruction - Flow – CFD

Abstract – The influence of blood flow on the depositions on the vessel wall has been observed and described already in the 19th century. Observations have shown that depositions at the inner vessel wall correlate with regions of low or oscillating wall shear stress, which correlate with regions of separated and stagnant blood flow. These flow phenomena are observed in the vicinity of the bifurcation. However the exact correlation between depositions, vessel geometry and flow parameters is not yet known.

First, at the post mortem the arteries excised and vessel casts are produced. After the cast polymer (Technovit 7143) is hardened, the arteries are analyzed pathomorphologically and morphometrically. The analysis follows rules described 1958 by the WHO group of experts on atherosclerosis. The locations of the wall alterations are transformed by planar mapping. The vessel casts are digitized a render 3-dimensional mathematical models of the arteries. Each set of data is a cloud of about 25.000 points, which define the shape of the vessel. These data are imported by the computational fluid dynamics (CFD) flow program packet FLUENT, which creates an unstructured tetrahedral computational mesh and well suited for incompressible flow. The hardware basis is a Pentium II 350 MHz with 512 Mb RAM.

An example of reconstructed carotid artery.

With this method the blood flow of the deceased patient is reconstructed in a computer model based on the individual geometry of the vessels. The flow parameters, such as velocity, pressure and wall shear stress are computed. At the same time the geometrical parameters and wall alterations are assessed and analyzed. This permits the comparison of the anatomical shape and its flow to the distribution of the wall alterations.

Twenty individual carotid arteries were investigated and used for the comparison. The great variation of the anatomical shape and the great many factors do not permit an exact correlation of the deposition and flow. Using a larger number of arteries and some additional information about objects can only solve this problem.

Modeling the sound of snapping shrimp

Anna von der Heydt[1,2], **Detlef Lohse**[1], **Barbara Schmitz**[3], **and Michel Versluis**[1]

[1]*Fluid Mechanics and Heat Transfer, University of Twente, P.O. Box 217, 7500 AE Enschede, The Netherlands*
[2]*Department of Physics, Philipps-Universität Marburg, Renthof 6, 35032 Marburg, Germany*
[3]*Institut für Zoologie, TU München, Lichtenbergstr. 4, 85747 Garching, Germany*

Email - a.vonderheydt@tn.utwente.nl
Keywords - Snapping shrimp - Cavitation

Abstract - Snapping shrimp (*Alpheus heterochaelis*) produce a snapping sound by an extremely rapid closure of their snapper claw. It generates sound so loud that it disturbs submarine communication. Hydrophone measurements indicate intensities up to 180 dB re 1 µPa at a distance of 1 m. Our experiments showed that the sound is generated by the collapse of a cavitation bubble, and not by the two claw surfaces hitting each other as was previously believed. When rapidly closing its snapper claw, a high-velocity water jet is emitted from the claw with a speed exceeding cavitation conditions. Hydrophone measurements, in conjunction with time-controlled ultra high-speed imaging of the claw closure demonstrate that the sound is emitted at the same time when the cavitation bubble collapses.
In this work we develop a theoretical model for a bubble under such conditions. The dynamics of the bubble radius and the emitted sound can be described by an equation of the Rayleigh-Plesset type together with a diffusion equation for water vapor entering the bubble. The calculated results are compared with the experimental data. The model for spherical bubbles is able to reproduce the dynamics of the non-spherical cavitation bubble size as well as the time dependence and order of magnitude of the emitted sound.

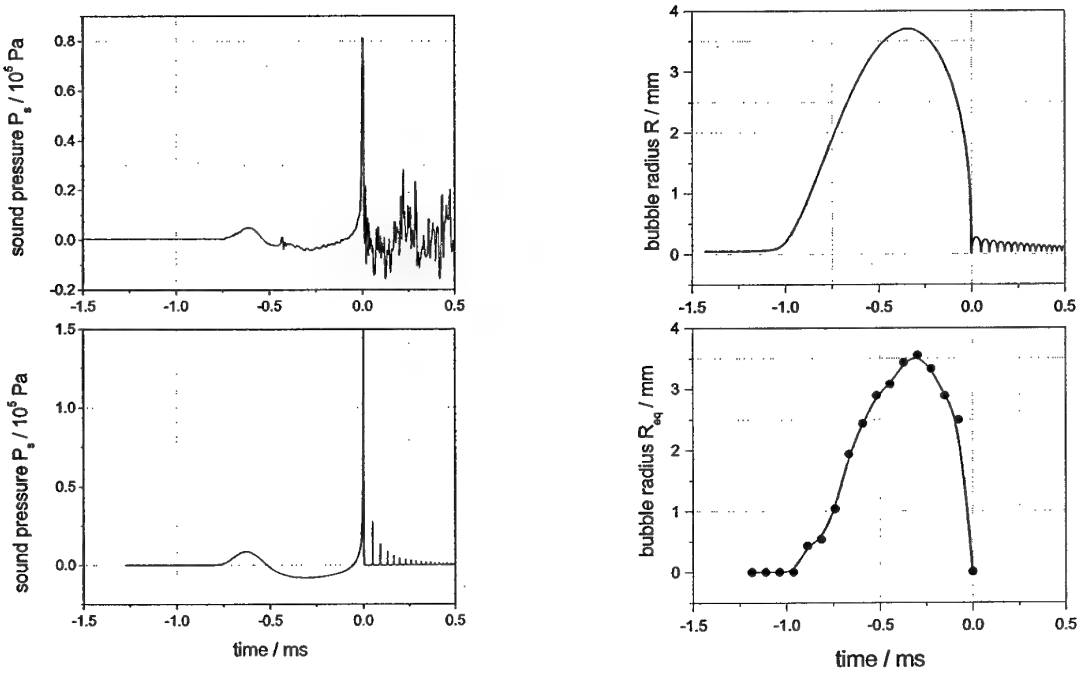

Left: *Sound signal emitted by the bubble as measured in the experiments (upper) and as calculated from the theory (lower).* ***Right:*** *Time dependence of the calculated (upper) and the measured bubble radius (lower).*

The role of hemodynamics in the development of the outflow tract of the heart

Berend Hillen[1], Erwin Loots[2], Hendrik Hoogstraten[2] and Arthur Veldman[2]

[1]Departments of Functional Anatomy, Utrecht University, and [2]Computational Mechanics, University of Groningen, The Netherlands

The question whether and if so, to what extent hemodynamic forces mechanical stimuli do modulate the morphogenesis of the vascular system is a century old, especially in the outflow tract where a spiralling septum develops in and after a strong bend in the tube. Spirallinge patterns of the flow in bends are well known. Of the mechanical stimuli that can potentially exert an effect on morphogenesis is wall shear stress the most likely candidate, a number of genes that are expressed in the cardiovascular system, have shear stress-responsive elements in their regulatory units. Recent investigations have clearly shown that the disturbance of normal hemodynamic conditions results in maldevelopment of the heart. However, an experimental model alone is necessary, but not sufficient to identify the intermediate steps of the interaction between blood flow and tissue remodelling in the developing cardiovascular system, certainly at Reynolds numbers that are very small.

Therefore we created a model with a very simple geometry, using the ComFlo software that was recently developed by the Computational Mechanics Group in Groningen. ComFlo is a fully 3D computational fluid dynamics code that solves the Navier-Stokes equations in a Cartesian grid. A first assessment of the possible influence of a strong curvature, with biological realistic dimensions, was made using steady flow conditions.

Since both the Reynolds number and the Womersley number (indicating the influence of the pulsatility on the velocity profile of the flow) are extremely low it is likely that these flow patterns do not differ significantly from those under pulsatile conditions. A first assessment of the effects of the strong curvature on the flow under the given circumstances, showed only very small secondary velocities and negligible heterogeneity of the wall shear stress, indicating that the (time dependent) geometry may be an important factor.

Theoretical and experimental study of non-linear pumping effects in the peripheral vessels, based on the concept of valveless pumps

Ch. G. Manopoulos, D. Mathioulakis, S. Tsangaris
Fluid Section, Department of Mechanical Engineering
N.T.U.A., P.O. Box 64070, 157 10 Zografos-Athens, Greece
Email: manopoul@central.ntua.gr

Keywords - Unsteady Flow - Distensible tubes - Circulation - Valveless Pumping

Abstract - The effective functioning of valveless pumps has been suggested by G. Liebau (1955), who has studied the idea of a distal auxiliary pump mechanism, where a pulsating arteriole is compressing a neighbouring venule. Under certain conditions a directed flow is possible, which helps the return flow of blood. Liebau has proposed flexible tube models without valves, while H. J. Bredow's experimental study (1968) has further developed Liebau's suggestions. In giving a physical description of this phenomenon O. Mahrenholtz (1974) investigated the interaction of the different parts of the tube considered as vibroelements, and the influence of the periodic changes of the tube geometry and pressure gradient on the flow. In his case, the significant increase in flow resistance of a collapsed cross-section of the tube works like a hydrodynamic valve. Furthermore H. J. Rath (1976) has developed a mathematical model for this flow problem. The equations for his one-dimensional model have been solved by a numerical method. Mahrenholtz as well as Rath show that only a non-linear description of the flow-vessel-system leads to a pumping effect, which may occur in the venous part of systemic circulation under physiological conditions. The object of the present study is to validate and improve the models above, on the basis of the results of a theoretical and experimental model. The theoretical model has been developed in order to represent and confirm pumping phenomena through cylindrical distensible tubes. The model consists of two rigid reservoirs filled with fluid and communicating with a distensible tube (figure). Between the spout of a reservoir and the tube, there is a gate valve. Pumping is achieved by inducing a progressive wave of expansion and shrinkage of the cross section area along the whole length of the above distensible tube. The unsteady-laminar flow, thus established, is predicted by considering the flow as one-dimensional, employing the momentum and continuity equations, leading up to one non-linear ordinary differential equation, solved numerically by a fourth order Runge-Kutta's scheme. It is also considered that the fluid is incompressible and that the viscous terms correspond to a Poisseuille type flow. According to the described above theoretical model, the experimental apparatus included two communicating reservoirs by a rigid pipe, containing a balloon inflated periodically by an oscillating piston, which pushed (and removed) water into (and from) the balloon, respectively. It is noted that the displacement volume is constant for all the examined parameters of the experiment. A valve comes in between the spout of a reservoir and the rigid pipe, in order to introduce an intense asymmetry in the hydraulic installation. The flow-rate towards one of the two reservoirs is calculated indirectly by recording the motion of the free surface of this reservoir to videotape, as a function of the frequency of the balloon oscillation and the valve opening. Based on the theoretical model, the mean flow-rate resulting from the asymmetry of the reservoirs under constant frequency, constant excitation amplitude of the cross section area and zero local losses is presented. Mean flow-rate variation with frequency is also presented. The influence of the local losses on the non-linear term is presented, where maximum flow-rate is achieved varying the opening and consequently the local loss of the valve. The results show that the only way to have non-zero mean flow-rate is to conserve the influence of non-linear term in the equation of the model. This can be achieved if there are asymmetries in the system of the distensible tube. The results of this theoretical model are in good agreement with the experimental ones.

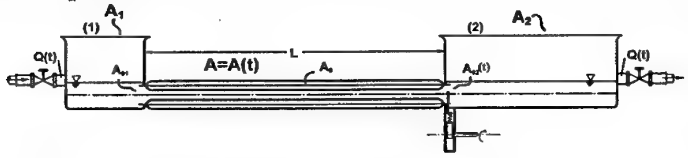

Schematic of experimental apparatus representing the model of communicating reservoirs

Computational Fluid Dynamic (CFD) analysis of blood flow through arterial grafts with distensible walls

T. P. O'Brien, T. McGloughlin

Department of Mechanical and Aeronautical Engineering, University of Limerick, Limerick, Ireland. *E-mail: thomas.obrien@ul.ie*

Introduction

Local hemodynamic factors have been found to play a significant role in the development of atherosclerosis and intimal thickening at the distal end of arterial grafts. The formation of disease at the distal end, in particular at the heel, toe and floor of the junction, reduces graft patency and may lead to occlusion of the junction. The investigation of junction hemodynamics serves to promote the understanding of how the blood flow patterns influence disease formation, thereby permitting optimisation of the graft-artery junction design to result in increased graft patency and to reduce the contribution of hemodynamics to disease formation.

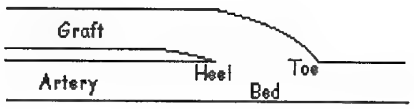

Fig 1 Schematic of End-to-Side Graft Artery Junction

Previous studies [1,2] have found that the formation of disease along the artery floor is influenced by the abnormal wall shear stresses (WSS) resulting from the blood flow patterns in the junction. Flow separation, recirculation and stagnation are the principle flow phenomena which result in these abnormal wall shear stresses. Intimal hyperplasia at the heel and toe of the junction occurs due to the effect of material mismatch and surgical injury at the anastomosis, and the local hemodynamics.

The primary objective of this study was to investigate the effect of distensible walls on the blood flow through an arterial graft and to determine how compliant walls affect the wall shear stress distributions. Computational Fluid Dynamics (CFD) was used to simulate the hemodynamics of the graft-artery junction for various geometries and anastomosis configurations. The CFD package Fidap 8.5 (Fluent Europe) was used to model the flow. The fluid-structure interface of Fidap 8.5 allows numerical modelling of distensible walls. The effect of varying the wall and graft elasticity was also investigated.

Results

Two types of graft geometry were investigated in this study. The first geometry investigated was the basic end to side anastomosis. Both rigid and compliant models were examined. The second geometry involved incorporating a Miller cuff.

The results of the study indicated that distensible walls do have a significant effect on the hemodynamics of the grafts. The elasticity of the walls were found to have an effect on the wall shear stress distributions and magnitude. Less stagnation point movement resulted from the inclusion of a Miller cuff into the geometry. The stresses along the suture line were reduced due to the presence of the compliant cuff.

References

[1] D. Y. Fei, J. D. Thomas, S. E. Rittgers (1994) J. Biomech. Eng. 116: 331-336.

[2] F. Loth, S. A. Jones, D. P. Giddens, H. S. Bassiouny, S. Glagov, C. K. Zarins (1995) Bioengineering Conference 29: 9-10.

EFM

Ye.A. Gayev[*], **E. Savory**[**]
[*] *Institute of Hydromechanics, UNAS, Kiev, Ukraine;*
[**] FMRG, University of Surrey, Guildford, UK

Canopy vorticity seen from spectrum measurements

The terms "***canopy***" or "***penetrable roughness***" (PR) flow express common features of air or water flows interacting with forest and agricultural plants (Meroney, Dubov ea, Raupach & Thom), vegetation in river beds (Kouwen, Nuding, Bennovitsky) or large-scale atmospheric spraying system (Porter & Chen, Gayev ea [1,2]). Recent knowledge about the canopy (or PR) flows has been quite sufficient, mathematical models developed so far may generally be employed in practical problems until one deals with mean flow quantities. However, for explaining some paradoxes found in natural forests (Shaw, Raupach & Thom), for solving canopy turbulence and diffusion problems, the kind and the nature of vorticity being born within the canopy and spreading outside in the external flow must be taken into consideration. While some fluid mechanics disciplines are only about to understand these requirements for the PR of their kind, meteorologists have already undertaken a number of investigations devoted to canopy vorticity (Brunet ea, Finnigan & Brunet, Shaw ea). Present work being continuing our previous experimental canopy research [3,4] concentrates on vorticity flow features represented through spectrum measurements of longitudinal flow fluctuations.

The canopy with the total height $h=h_1+h_2=120$ mm was formed from an staggered array of obstacles ("trees"), each constructed with a cylindrical "stem" (h_1) and a slotted flat-plate "crown" in the shape of an equilateral triangle (h_2). The spacing Δx and Δy between the "trees" was varied in models investigated. This arrangement allowed for detailed flow field diagnostics within the canopy by means of thermal anemometry.

Drastic change of longitudinal fluctuation spectrum shape over long distance through canopy flow has been found. The finding confirms some recent conclusions of previous researchers (Brunet, Finnigan, Raupach and Shaw, 1994) that flow vorticity above the canopy significantly differs from that within the canopy.

Our theoretical model with an algebraic turbulence closure [1 - 4] gives generally good agreement with many mean flow characteristics. However, unexpected vorticity behaviour must encourage researchers for developing advanced theoretical models of the canopy turbulence.

References

1. Gayev Ye.A., Melenevsky V.V., Nickittin I.K., Tsimbal V.S., Prokhorov V.N. Turbulent flows in and above a permeable roughness layer. *Fluid Mechanics, Soviet Research.* 1990, **19**, *N* 6:79-89.
2. Gayev Ye. Aerothermal theory of easily penetrable roughness: Particular application to the atmospheric flow in and over longscale spray cooling system, *Il Nuovo Cimento, 1997.* 20C, *No.* 3: 331-342.
3. Gayev Ye. A., Savory E., Toy N. Wind tunnel investigation of a complex canopy shear flow. *Wind Engineering into the 21th Century.* (A. Larsen e.a. editors). Balkema Publ., 1999, 191 – 198.
4. Gayev Ye. A., Savory E., Toy N. Investigation of a inhomogeneous penetrable roughness in wind tunnel. *Applied Hydromechanics* (Kiev), *No.*1, *2(74), 2000 (in Russian).*

Modeling the Pollutant Dispersion in Convective ABL with used PDF Construction

Boris B. Ilyushin
Institute of Thermophysics, Novosibirsk, Russia
ilyushin@itp.nsc.ru

Experimental and theoretical investigations confirm the formation of Coherent Large Scale Eddy Structure (CS) in convective atmospheric boundary layer (ABL). They contain the main part of the turbulence energy and the turbulent transfer is achieved mainly by the action of CS. Such non-local turbulent transfer cannot be described within "standard" turbulent diffusion models of gradient type. The turbulent transport models of third- and second- order closure are presented in the paper (Ilyushin & Kurbatskii, 1997). These models describe the statistic structure of ABL adequately of the experimental data. The results of ABL modeling have been used for pdf construction in this work. The results of modeling of the pollutant turbulent transfer in convective ABL are presented. The approach based on accounting the influence of the CS by accentuation of the periodic properties of motions, which is analogous to VLES is used. But in this paper the accentuation of periodic motions are obtained for the pdf of vertical velocity field.

The pdf of turbulent fluctuations of the vertical velocity is represented as a superposition of two independent distributions: inertial interval of turbulent spectrum (background turbulence) $P_b(u)$ and large-wave region of pdf spectrum $P_c(v)$ (u and v are the vertical velocity fluctuations of background turbulence and the vertical velocity field of CS, correspondingly)

$$P(u,v) = P_b(u)P_c(v) = \underbrace{\frac{1}{2\pi\sigma_b}exp\left\{-\frac{u^2}{2\sigma_b^2}\right\}}_{\text{Background Turbulence PDF}} \underbrace{\left[\underbrace{\frac{a^+}{\sigma_c^+}exp\left\{-\frac{(m^+-v)^2}{2(\sigma_c^+)^2}\right\}}_{\text{upflow}} + \underbrace{\frac{a^-}{\sigma_c^-}exp\left\{-\frac{(m^--v)^2}{2(\sigma_c^-)^2}\right\}}_{\text{downflow}}\right]}_{\text{Coherent Structures PDF}} \quad (1)$$

where σ_b is the dispersion of background turbulence; a^+ and a^- are the weight coefficients, $\sigma_c{}^+$ and $\sigma_c{}^-$ are the dispersions, m^+ and m^- are the centers of distributions of upflow and downflow of CS, correspondingly. Considering the total turbulent velocity fluctuation w as the sum of u and v, one can obtain the total pdf. The distributions parameterizes are obtained from the normalization conditions and from the denotations for average, dispersion $\sigma = <w^2>^{1/2}$, skewness factor $S_w = <w^3>/<w^2>^{3/2}$. Necessary additional conditions for pdf construct are found from the wavelet model (Tennekes & Lumley, 1972). We suppose here that the main part of the energy-containing interval of the fluctuations spectrum is defined by a single main wavelet with the typical wave number corresponding to the spectrum maximum. The horizontal size of LSES ($\lambda_{max} = 2\pi(2a/E)^{-3/2}/\varepsilon$, a - is the Kolmogoroff coefficient) and the ratio ($\sigma_b^2/<w^2>$) are determined from second-order moment distributions with using of this approach. Obtained algebraic equations with distribution of ratio $\sigma_b^2/<w^2>$ and with accounting the condition for the values place $m^+>0$ and $m^-<0$ have exclusive solution. The results reconstruction of pdf correspond to the observed data. For horizontally homogeneous convective ABL the size of horizontal region of the LSES (where the vertical velocity is equal to $\widetilde{w}$) is taken to be proportional to the probability $P_c(\widetilde{w}) : P_c(\widetilde{w})d\widetilde{w} = dx/(\lambda_{max}/2)$. The vertical velocity field of the coherent structures $\widetilde{w}(x,z)$ can be found from this differential equation. The horizontal velocity field $\widetilde{u}(x,z)$ is determined from the equation of mass conservation. For describing the process of substance dispersion in the convective PBL, it is used the model which takes into account directly an effect of the substance transfer by LSES (in advection terms of the equation for concentration) is used. For accounting of the substance turbulent diffusion under the effect of background turbulence, the "standard" gradient diffusion model is applied. The results of simulation of the pollutant jet spreading from sources placed both on the ABL ground surface and in the middle of the mixed layer are presented. The averaging (over one period λ_{max}/U) crosswind integrated concentration fields are shown in fig.1. The calculated behavior of the plume centerline with a source situated both near the ground and in the middle of the mixing layer corresponds to the Willis and Deardorff's tank experiments.

REFERENCES

Boris B. Ilyushin & Albert F. Kurbatskii. 1997. Modeling of turbulent transport in PBL with third-order moments // Proc. Symposium on Turbulent Shear Flows. Grenoble, France. Vol.2, pp. 2019.

Tennekes H.,Lumley J.L. 1972. A First Course in Turbulence. MIT Press, Cambridge, Massachusetts.

Willis, G.E., & J.W.Deardorff. 1976. A laboratory model of diffusion into the convective boundary layer. *Quart. J. Roy. Meteor. Soc.* **102**, 427.

Willis, G.E.,& J.W.Deardorff. 1981. A laboratory study of dispersion from a source in the middle of the convective boundary layer. *Atmos. Environ.* **15** 109.

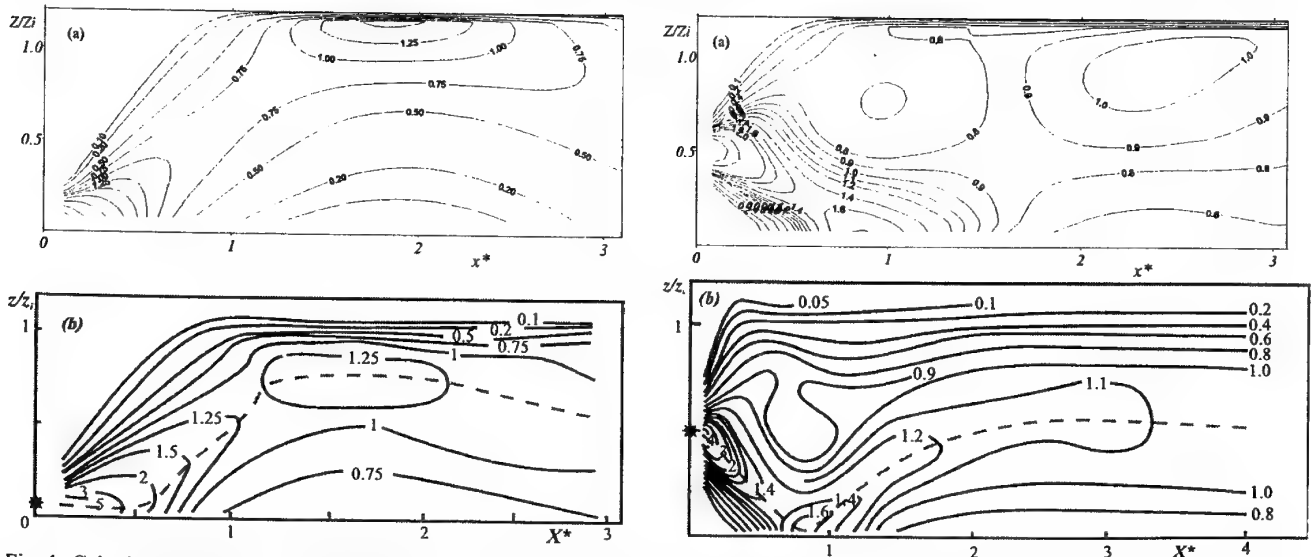

Fig. 1. Calculated (a) and measured (Willis & Deardorff, 1976, 1982) (b) non-dimensional crosswind integrated concentration $C_y z_i U_x/q_0$ for point sources of height $z/z_i=0.067$ and $z/z_i=0.5$..

Research of a nonlinear wave interaction in a rotating liquid of a variable depth

A.A. Kurkin
Department of applied mathematics,
Nizhny Novgorod State Technical University, Russia
kurkin@kis.ru

Keywords - Nonlinear interaction - Hamiltonian formalism - Rotating ocean – Trapped waves

Abstract - In dynamics of waves in shelf zone of ocean the noticeable role is played the special class of own waves, - so-called trapped waves - type of long-wave motions of rotated ocean located in the coastal zone, and also in areas with the prolated and rather strong and sharp heterogeneities of a bottom configuration. The Kelvin waves, including edge Stoks waves, barotropic and baroclinic Rossby waves, concern to them. Their fissile research began two decades back and is prolonged now with reinforced concern, as they play the extremely relevant role in borderline fields of ocean. Near to beaches on waves of this class it is necessary 95-98 % of energy, and last can be transmitted along pattern of acquisition to large distances without essential losses. The observation of the last years have shown, that such heterogeneous phenomena, as topographic curls, inshore circulation, upwelling are intimately connected to trapped waves. The linear theory of these waves at some particular bottom configurations represents enough detailed section wave theories in ocean. A nonlinear wave theory in a shelf zone of constant depth on the basis of the hamiltonian formalism of a beginning to develop some years back. The research of a nonlinear wave interaction in basin of a variable depth is more composite problem and merits the special consideration.

In the present study with the help of methods of the hamiltonian formalism the canonical theory of interacting waves of a Kelvin and Poincare in rotated ocean of an arbitrary bottom configuration in transversal to a coast a direction is constructed. The obtained canonical theory is utilised for research of nonlinear resonant interaction and self-effects Kelvin waves at the presence of waves of open ocean (Poincare waves), including processes of generation on a resonance frequency of two Poincare waves, decay and modulation instabilities. For the considered processes the increments of instabilities of excited waves are constructed and their relation to an angle of incidence of a wave of pumping is researched, and also the estimated comparison to known experimental data and matching of efficiency of this gear with considered earlier is conducted. Alongside with it, the consideration of stabilization arising at the maiden phase of interaction of decay instability Kelvin waves at the expense of phase misalignment of excited waves, resulting four-wave wave coupling of a Kelvin is conducted.

Erosion and sedimentation of a bump in fluvial flow

Pierre-Yves Lagrée
Laboratoire de Modélisation en Mécanique
Université PARIS VI, FRANCE
Email: pyl@ccr.jussieu.fr

Keywords - Interacting Boundary Layer - Sedimentation - Erosion

Abstract - In the present study the erosion and sedimentation of a dune in a fluvial flow is investigated. Here we use the framework of the "Interacting Boundary Layer theory" which allows a strong coupling between the boundary layer and the perfect fluid to compute the flow (assumed 2D, laminar, quasisteady because erosion and sedimentation is a slow process). The displacement of the dune occurs as follows: it is assumed that if the skin friction goes over a threshold value, the bump is eroded:

$$if \quad \frac{\partial \tilde{u}}{\partial \tilde{y}}|_0 > \tau_s \quad then \quad -\frac{\partial \tilde{c}}{\partial \tilde{y}}|_0 = \beta(\frac{\partial \tilde{u}}{\partial \tilde{y}}|_0 - \tau_s)^\gamma, \quad else \quad -\frac{\partial \tilde{c}}{\partial \tilde{y}}|_0 = 0. \qquad (1)$$

Then, the concentration of sediment in suspension is convected but falls at a constant settling velocity $-\tilde{V}_f$ (the equation of transport of concentration is solved in Boundary Layer variables). In adimensionalised variables, the dune changes at a slow time scale according to the balance law:

$$\frac{\partial \hat{f}}{\partial \tilde{t}} = S_c^{-1} \frac{\partial \tilde{c}}{\partial \tilde{y}}|_0 + \tilde{V}_f \tilde{c}|_0. \qquad (2)$$

An example of displacement toward a final equilibrium state is presented on the left figure.

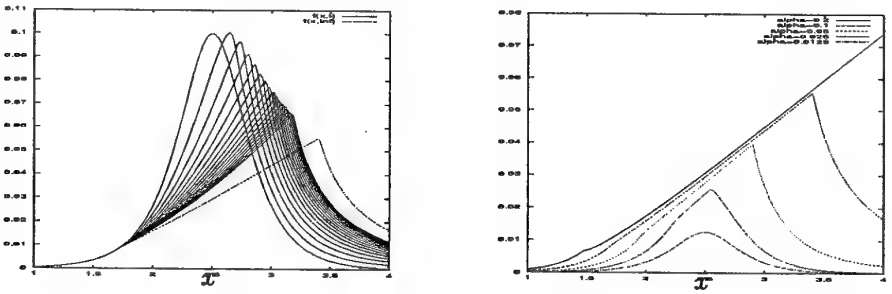

The dune shape ($\hat{f}(\bar{x}, \tilde{t})$ of maximum $\alpha = 0.1$) as a function of time $\tilde{t} = 0, 1, 2, 3..., 16, \infty$ (left) and final dune shapes for different starting values of α (right)

The final calculated stationnary bed profile is caracterized by a constant skin friction equal to τ_s. The upstream side is nearly linear, the lee side has a bigger slope (right fig.).

The advantage of this model is that a lot of hydrodynamical mecanisms have been considered without usual integral (or 1D) simplifications. Of course, the first hypotheses to introduce in the model would be a turbulent stress viscosity and diffusivity and for the river bed it would be interesting to introduce the slope limitation.

The flow around a surface-mounted cube in a simulated stably stratified atmospheric boundary layer

C.S. Maré and A.G. Robins
Environmental Flow Research Laboratory
School of Mechanical and Materials Engineering
University of Surrey, United Kingdom
Email: C.Mare@surrey.ac.uk

Keywords - atmospheric boundary layer - stable stratification - wind tunnel simulation - building wake

Abstract - Pressure measurements are currently being made on the surface of a cube in a simulated stably stratified atmospheric boundary layer. Together with velocity field measurements it will help the present understanding of the effects of stable stratification on building wakes in atmospheric boundary layers. Thermally stratified stable boundary layers in the EnFlo atmospheric wind tunnel are set up by heating the inlet air and cooling the floor of the wind tunnel. Boundary layers varying from neutrally stable to very stable can be set up in this way. Boundary layer characterisation measurements are carried out with a Laser Doppler Anemometer synchronised with a cold wire probe.

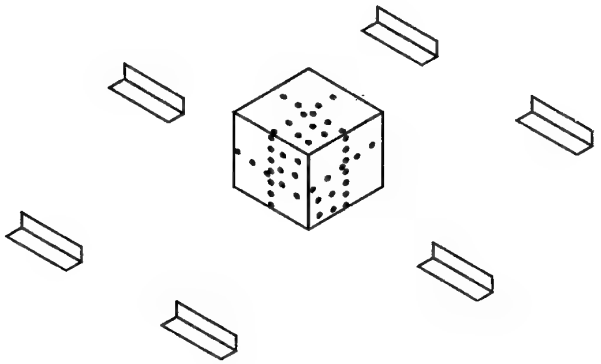

Arrangement of cube with pressure tappings and surrounding roughness elements

Rather large roughness elements relative to the model are used to set up simulated atmospheric boundary layers with the required characteristics. The influence of individual roughness elements on the wakes of obstacles are still unclear. The surface pressure distribution can serve as a bulk indication to study this effect by comparing pressure distributions with individual roughness elements in place or removed close to the obstacle.

Previous work conducted at EnFlo relating to this study included velocity field measurement behind a surface-mounted cube and concentration measurements behind the cube for an upstream source. The proposed talk will focus mainly on velocity field and surface pressure measurements.

Near field investigation of a buoyant jet by means of Laser Induced Fluorescence

G. Querzoli[1] and A. Cenedese[2]
[1] DIT - University of Cagliari - Italy
E-mail: querzoli@unica.it
[2] DITS - University of Rome "La Sapienza", Italy
E-mail: icola@dits.ing.uniroma1.it

Keywords - Buoyant jet - LIF - Mixing

Abstract - The behaviour of buoyant jets has been investigated in the past in the frame-work of the similarity theory based on the assumption that the phenomenon is axisymmetric (Wood et al., 1993). Nevertheless, if the buoyant fluid is released horizontally, the stability conditions at the upper and lower boundary of the jet are very different. Since the fluid released from the source is less dense than the fluid above, an unstable stratification is generated at the upper boundary. Conversely, at the lower boundary a stable stratification is present since the ambient fluid is heavier than the fluid released within the jet. The coherent structures generated at the edge of the jet remain confined where the stratification is stable, and tend to diverge, becoming plume-like at the unstable boundary. This asymmetrical behaviour is responsible both for the curvature of the axis of the jet and the non-symmetrical profile of the mean velocity.

The effect of the buoyancy on the structure of a jet at moderate Reynolds numbers has been investigated by means of Laser Induced Fluorescence (LIF). A laminar jet is generated through a convergent and circular pipe (diameter D = 1.0 cm) 200 D long and released in a tank with water at rest. The buoyancy of the water is changed by changing the jet temperature of few degrees. The illumination is provided by a 300mW Argon-Ion Laser that is used to generate a light sheet by means of a rotating mirror. Series of images are acquired and digitised both in the longitudinal and transversal plane. These frame sequences are used to investigate the generation and the time evolution of the coherent structures at the edges of the jet.

In figure 1 a longitudinal section is shown, with R_e=1100 and F_r=10. The jet axis is bent upwards due to the buoyancy and it is apparent that the structures remain coherent only at the lower boundary.

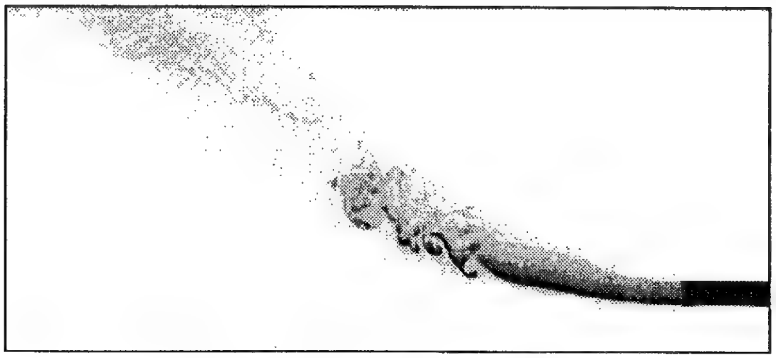

Figure 1 - Longitudinal section of the jet

The evolution of the structures can be observed from the sequence of images shown in figure 2. These images gives the evidence that the buoyancy drive the instability to develop only in the vertical direction since no horizontal mushrooms are observed unlike in the experiments with the simple jet.

Figure 2 - Cross section at 10D. Frame rate 12.5 Hz.

A simple model of up-valley winds

G. Rampanelli, D. Zardi, M. Tubino
Department of Civil and Environmental Engineering, University of Trento, Italy
Email: garampan@tin.it

Keywords - Atmospheric boundary layer - Up-valley wind - potential temperature

Abstract - A hydrodynamic bulk flow model for the evolution of the convective boundary layer in a valley and the consequent development of an up-valley wind is proposed. The model extends previous results on the diurnal evolution of an inversion capped convective boundary layer (Nieuwstadt & Glendening 1989, Park & Mahrt 1979, Driedonks 1982) to include the effects of a sloping valley bottom and adjacent slopes. Assuming the layer to be well mixed, suitable evolution equations are derived for the cross-averaged values (over any valley section Ω) of the along-valley wind velocity U, potential temperature Θ and averaged boundary layer depth $\tilde{Y}$ up to the inversion height h:

$$\frac{\partial h}{\partial t} + U\frac{\partial h}{\partial x} + \tilde{Y}\frac{\partial U}{\partial x} = \tilde{w}_e - \frac{U}{b}\left.\frac{\partial \Omega}{\partial x}\right|_h \tag{1}$$

$$\frac{\partial U}{\partial t} + U\frac{\partial U}{\partial x} + \frac{g}{\theta_{00}}\left[\delta_\Theta \frac{\partial h}{\partial x} - H\frac{\partial \Theta}{\partial x}\right] = \delta_U \frac{\tilde{w}_e}{\tilde{Y}} - \tilde{C}_D U^2 \frac{B}{\Omega} \tag{2}$$

$$\frac{\partial \Theta}{\partial t} + U\frac{\partial \Theta}{\partial x} = \frac{\tilde{F}B}{\Omega} + \frac{\tilde{w}_e \delta_\Theta}{\tilde{Y}} \tag{3}$$

where t is time, x is the along-valley coordinate, w_e is the *entrainment velocity* at the inversion top, g is the acceleration due to gravity, θ_{00} is a reference ground value for the potential temperature profile in the free atmosphere, H is a typical height depending on valley shape, δ_U and δ_Θ are the velocity and temperature jumps across the inversion layer, $\tilde{F}$ is the sensible heat flux averaged along the perimeter B of the valley cross section and C_D is a drag coefficient. Various possible solutions are found, depending on different boundary conditions. The results are compared with experimental evidences from ground and airborne measurements in test cases.

References

Nieuwstadt, F.T.M. & Glendening, J. W., 1989, Mesoscale dynamics of the Depth of a Horizontally Non-Homogeneous, Well-Mixed Boundary Layer, *Beitr. Phys. Atmosph.*, **62**, 275-288.
Park, S. U. & Mahrt, L., 1979, Oscillating, stratified boundary layers driven by surface temperature variations, *Tellus*, **31**, 254-268.
Driedonks, A. G. M., 1982, Models and observations of the growth of the atmospheric boundary layer, *Boundary-Layer Meteorol.*, **23**, 283-306.

Stratification of a gas layer flowing inside a channel

D. Telle and O. Vauquelin
Laboratoire de Mécanique et d'Energétique
University of Valenciennes, France
Email : damien.telle@univ-valenciennes.fr

Keywords - Stratified layer, Richardson number

Abstract - The study relates to the flow of a stratified layer of gas inside a rectangular channel. A numerical study using the Fluent software was carried out and compared with the measurements carried out on a 1/40 scale model. The apparatus comprises of a rectangular channel of section 0.125*0.125 m and a length of 5 m. A mixture of air and helium is injected at ceiling level at one of the ends. A stratified layer is formed, which then runs out, in the absence of longitudinal draught, towards the other end of the channel where it emerges into the surrounding air. Two types of measurements were carried out in the vertical plane in the center of the section: a measurement of helium concentration and a measurement of velocity by PIV (Particle Image Velocimetry). The objective was to determine a parameter which would make it possible to quantify the rate of stratification of the gas layer. This is realised using the local Richardson number which quantifies the relationship between the shear forces and the forces of gravity being exerted locally on the stratified layer. It is defined by: $Ri(z) = \frac{-g\frac{d\rho}{dz}}{\rho_0\left(\frac{du}{dz}\right)^2}$.

The profiles of density, speed and Richardson number are presented in Figure 1. The section at which the measurements were taken was 1.7 m from the point of injection, and the volume fraction of helium was 0,6. A parametric study relating the mass flowrate, the concentration of the mixture injected and the influence of a longitudinal draught in the channel was carried out to correlate the layer characteristic with the vertical evolution of Ri(z). This study was motived by the problems of tunnel safety in case of fire.

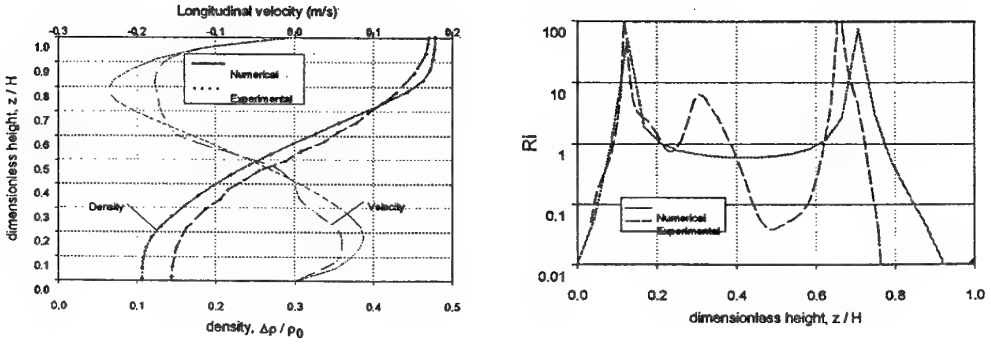

Figure 1: *Profils of density, velocity and Richardson number*

BDF & RFVD

Vortex ring in the post – formation stage

F. Kaplanski and Ü. Rudi
Department of Aeromechanics,
Estonian Energy Research Institute, Tallinn, Estonia
Email: fkaplan@online.ee

Keywords - Vorticity - Vortex Ring – Transitions in Flows

Abstract - This study involves the unsteady process of vortex ring development in an unbounded viscous fluid. In addition to the existing analytical solution of the Stokes equations in the form of vorticity distribution, a new integral expression for stream function is derived and the time-depended properties of a viscous vortex ring are obtained. A new expression is found for the velocity of the ring, which agrees both with the long-time asymptotic drift velocity (Rott and Cantwell, 1993) and the propagation speed for rings with small cross-sections (Saffman, 1970). The result is compared with the experimental data and the obtained velocity of the trajectory of maximum vorticity. In order to take into account the Reynolds number dependence, the method of entrainment diagrams is employed. The system for pathlines of fluid particles is examined as a bifurcation of an autonomous system with the initial Reynolds number as a parameter. It is shown that for high value of R_0/L (ratio of external and internal radii of the ring) for large initial Reynolds numbers three regimes of particle motion exist, and for small R_0/L there are only two regimes. In the additional regime the particles trajectories are divided into two parts: some of them move towards a critical point lying in the axis of symmetry while other part begins to be involved in the core of a ring due to the growth of concentration of vorticity. This separation manifests the influence of nonlinearity and can result to a shedding of impulse into the wake, which is typical for turbulent motion. The modification of offered model for a turbulent vortex ring is also discussed.

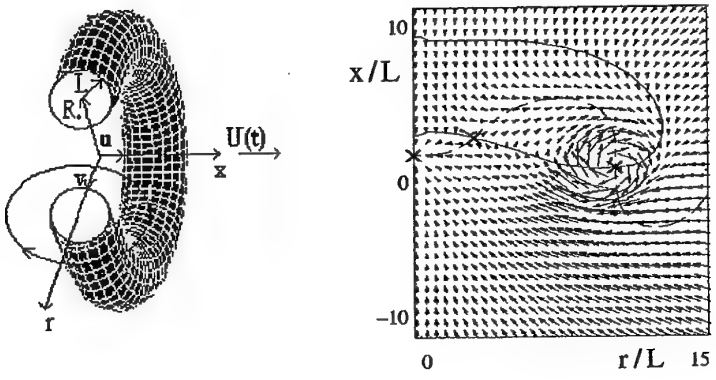

Schematic representation of the vortex ring (left) and the pattern of critical points for $R_0/L=10$ and $Re_0=600$ (right).

Spatial behaviour of inertial waves in a rectangular basin with a sloping boundary

A.M.M. Manders, M.H. Rienstra, L.R.M. Maas
NIOZ, PO Box 59, 1790 AB Den Burg, The Netherlands,
manders@nioz.nl

Inertial waves in a homogeneous, rotating fluid travel along rays with a fixed angle with respect to the rotation axis, depending on the frequency as compared to twice the rotation frequency. These waves were examined in a rectangular basin with one sloping wall on the 13 m diameter rotating platform at Laboratoire Coriolis, Grenoble. PIV-data were collected in horizontal and vertical cross sections. For an infinitely long channel, in a vertical cross-section the waves are predicted to get focused after downward reflection at the sloping wall. They may, after several reflections, end up in a periodic orbit, the 'wave attractor', where the wave energy is concentrated. Indeed attractors were found in the laboratory. But there must be an adaptation at the vertical front and end walls of the basin since inertial wave have a component of motion perpendicular to these walls. We experimentally studied the effect of the finite dimension of the tank on the inertial wave (attractor) behaviour regarding the spatial extension of the attractor and the amplitude and phase propagation of the waves through the basin.

Experimental determination of self-similar regimes in gravity-driven flows

B.M. Marino and L.P. Thomas
Instituto de Física Arroyo Seco, Facultad de Ciencias Exactas
Universidad Nacional del Centro, Pinto 399, 7000 Tandil, Argentina
Email: bmarino@exa.unicen.edu.ar

Keywords - gravity currents, self-similarity

Abstract – It is well known that the behaviour of gravity currents may be described by analytic self-similar solutions which provide the main features of the flow developed in the experiments or in natural events and the corresponding scaling laws. Nevertheless, some theoretical and practical questions remain unsolved when a careful comparison between experimental and theoretical results is needed.

Density distributions indicate that the mixing between the dense and ambient fluids is important throughout the flow evolution and affects the whole current. In consequence it must be considered in the processing of the information obtained in the laboratory. However, the dynamics of gravity flows is not substantially affected by mixing because of the kind of relationship between the density and the volume of the current. Mixing diminishes the reduced gravity and increases the volume almost in the same extent, so that the average hydrostatic pressure in the current remains approximately constant.

By employing the concept of hydrostatic pressure we define an "equivalent" height of the current and estimate the "effective" reduced gravity near the front. We carefully compare the theoretical self-similar solutions in which mixing is ignored and the experimental results based on the measurement of the density distributions of inertial gravity currents generated in a rectangular cross-section channel. This comparison gives us a better idea of the agreement between the self-similar theory and real flows. In addition we find new practical forms to determine the regimes of gravity flows and some parameters usually employed as, for instance, the height profiles and the Froude number at the current front.

We also show that:

+ The velocity and the head height are better parameters than the current front position $x_f(t)$ to determine the regime of the flow.

+ The initial conditions seem to influence the dynamics of the current up to $x_f/x_0 = 25$ (x_0: lock length).

+ When the inertial self-similar regime is developing, the "equivalent" height profile of the head is approximately 0.6 times the head height profile measured experimentally (this is valid for fractional depth $\phi = 1$).

+ The mass of the dense fluid contained in a gravity current head is an important fraction of the whole mass of the current.

Scenarios of boundary layers development and transport processes effected by buoyancy

Eugene Nikiforovich
Department of Thermohydrodynamical Modeling
Institute of Hydromechanics, National Academy of Sciences
Ukraine
Email: nikif@gu.kiev.ua

Keywords - Body Forces - Transition - Stratified Boudary Layer

Abstract - The development of a temperature stratified boundary layer (SBL) over a flat plate is investigated. There are two aspects of the problem which were studied practically independent from each other. The first one deals with the buoyancy effects on the 2D boundary layer structure and heat transfer. The second one concerns the boundary layer stability, transition to 3D motion, its structure and heat transfer peculiarities. Experimentally 3D motion of the longitudinal vortical type was found to be certainly preferable in boundary layers over heated surfaces; space scales of this structure and its downstream observed position were estimated but not determined through the basic parameters. In this report using the asymptotic analysis of Navier-Stokes equations the following conclusions were obtained:
— buoyancy forces in a SBL result in the appearance of the new type of space-time scales which explicitly depends on the value of these forces;
— longitudinal vortices, as an essential flow structural feature, were shown to originate from the interaction of two vorticity sources (due to viscous and buoyancy forces. Available buoyancy forces were proved to result in essentially 3D nature of boundary layers. Obtained results can be used for optimal ways of SBL control using basic parameters.

Three-dimensional structure and decay properties of vortices in shallow fluid layers

M.P. Satijn, R. Verzicco, H.J.H. Clercx and G.J.F. van Heijst
Dept. of Physics, Fluid Dynamics Laboratory
Eindhoven University of Technology, The Netherlands
Email: m.p.satijn@tue.nl

Keywords - Shallow water flows, vortex dynamics

Abstract - Laboratory experiments on quasi two-dimensional vortex structures have been performed in thin (stratified) fluid layers. Commonly, it is tacitly assumed that vertical motions, giving rise to a three-dimensional character of the flow, are inhibited by the limited vertical dimension. However, shallow water flows, vertically bounded by a no-slip bottom and a free surface, necessarily show a three-dimensional structure due to shear in the vertical direction. This shear may lead to significant secondary circulations. Here, the three-dimensional (3D) structure and the decay properties of vortices in shallow fluid layers, both homogeneous and stratified, have been studied in detail by performing 3D direct numerical simulations. The quasi two-dimensionality is an important issue if one is interested in a comparison of experiments of this type with purely two-dimensional theoretical models. The influence of several flow parameters, like the depth of the fluid and the Reynolds number, has been investigated. In general, it can be concluded that the flow loses its two-dimensional character for larger depth and larger Reynolds number. A flow with a 3D character demonstrates stronger secondary circulations which deform the radial profile of axial vorticity of vortex structures. In the limiting case of quasi two-dimensional flow, the vorticity profiles can be scaled according to a simple diffusion model. In a two-layer stratified system, three-dimensional motions are significantly inhibited compared to the corresponding flows in a homogeneous layer.

ANTICONVECTION IN SYSTEMS WITH HEAT RELEASE ON THE INTERFACE

Alexander A. Nepomnyashchy, Ilya B. Simanovskii

Department of Mathematics, Technion – Israel Institute of Technology, 32000 Haifa, Israel

It can be found in any textbooks that in fluids with positive heat expansion coefficient the buoyancy convective instability of equilibrium appears only by heating from below. Paradoxically, it is not actually correct in the presence of *an interface* between two fluids. It was shown by Welander [1], that the thermal and hydrodynamic phenomena on the interface may lead to a buoyancy convective instability by heating from above (" anticonvection "). Anticonvective mechanism of instability appears only under specific conditions: the fluids with considerably different physical properties must be taken.

During a long time it was a common opinion that the phenomenon of anticonvection is rather exotic. It turns out however that the appearance of anticonvection can be simplified when the interface serves as a source or sink of heat. Specific examples of an active influence of the interface on the heat transfer are absorption of light, evaporation, mass transfer through the interface and so on.

In the present work the anticonvection, generated by the joint action of the external heating and heat sources (sinks) homogeneously distributed on the interface in the layers with finite thicknesses is studied. Nonlinear regimes of anticonvection in a real system of fluids with the interfacial heat release are considered. Anticonvective structures for the fluid system, *that have no anticonvection in the absence of heat sources (sinks) on the interface,* have been obtained. This new type of the anticonvective motion appears in the case where one layer is strongly heated from above, while the temperature gradient in another layer is very weak.

References.

1. P. Welander. Convective instability in a two-layer fluid heated uniformly from above, Tellus 16 (1964) 349.

Tu & BL

On a relation between the spectrum of turbulence of noise it radiates.

L.M.B.C. CAMPOS
Seco de Mecnica Aeroespacial, Departamento de Engenharia Mecnica
Instituto Superior Tcnico, Portugal
Email: lmbcampos.aero@popsrv.ist.utl.pt

The generation of sound by turbulence is represented by the Lighthill (1952) tensor, of which the main term is the Reynolds stresses. Thus the acoustic pressure depends on the two-point turbulent velocity correlation and the acoustic power on its four-point correlation. The space-time Fourier transform the latter is the four-point turbulence spectrum. The acoustic power spectrum of sound generated by turbulence, is calculated in terms of the four-point turbulence spectrum in general, and then simplified for incompressible, isotropic turbulence. The method of evaluation of acoustic radiation integrals involving multi-point turbulence spectra is demonstrated first by calculating the acoustic pressure from two-point turbulence spectra, and then applied to the calculation of acoustic power spectra from four-point turbulence spectra. The present results allow a prediction of the power spectrum of noise emitted by turbulence, using as input only the turbulence spectra. This is a distinct approach from the Corcos (1963) type schemes which use semi-empirical functions.

The simplest case of sound generation by turbulence concerns isotropic, incompressible turbulence in a fluid in a mean state of rest. An extension is the case when the mean state is an uniform stream, thus convecting both the sound and the turbulence. In the latter case the turbulence may become axially anisotropic, i.e. its spectrum may depend on the angle of the wavevector with the mean flow. In the present paper the two and four-point spectra of incompressible, axially anisotropic turbulence are introduced, and are used to calculate respectively the acoustic pressure and power spectra of radiated sound, taking into account convection, at low Mach number, of both turbulence and sound. It is shown that turbulence generates sound with the same wavenumber k and with a frequency ω such that the phase speed ω/k equals the sound speed, projected in the observer direction, and divided by a Doppler factor. The acoustic pressure and power spectra are expressed as functions of the wavenumber and angle to the observer direction, and also of the Mach number and angle of the mean flow with the wavevector.

Experimental investigation of transition in pipe flow

C.W.H. van Doorne, M. van der Voort, E.C.J. Hendriks
J. Westerweel and F.T.M. Nieuwstadt
Laboratory for Aero and Hydrodynamics
Department of Mechanical Engineering and Marine Technology
Delft University of Technology, The Netherlands
Email: c.w.h.vanDoorne@wbmt.tudelft.nl

Keywords - Transition - Pipe Flow - LDA and PIV

Abstract - In continuation of the experimental work carried out by Draad et al. [1] we have carried out transition measurements in a pipe facility which is 33 meters long and has a 4 cm inner diameter. The water flow can be kept laminar up to very high Reynolds numbers ($Re \approx 60.000$) and a fully developed parabolic profile can be reached up to $Re = 15.000$. Transition is triggered by introducing disturbances from the wall.

To check the facility we have repeated part of the experiments carried out by Wygnanski &Champagne [2], Darbyshire & Mullin [3], Eliahou et al. [4] and Draad et al. [1].

During these experiments the velocities have been measured with LDA. First we used a strong flow disturbance at the inlet of the pipe and we studied the appearance of puffs and slugs at several downstream locations. The result is a detailed picture of the main bifurcations in pipe flow and the corresponding critical Reynolds numbers.

Second, we have studied the transition from Poisseuille flow to turbulence, triggered by periodic blowing and suction from the wall. Using phase averaging we measure the (mean) development of the disturbance after its initiation. In addition, we aim to carry out experiments for other disturbances, e.g. introduced in the centre region of the pipe.

At this very moment we also set up a stereoscopic PIV system which has the capability to measure all 3 velocity components in a plane perpendicular to the flow. Repeated measurements in one plane could give insight in the spatial structure of the flow. It is our objective to show the first results at the conference.

References

[1] A.A. Draad, G.D.C. Kuiken and F.T.M. Nieuwstadt, 1998, Laminar-turbulent transition in pipe flow for Newtonian and non-Newtonian fluids, *J. Fluid Mech.* **377**, 267-312.

[2] I.J. Wygnanski and F.H. Champagne, 1973, On Transition in a pipe. Part 1. The Origin of puffs and slugs and the flow in a turbulent slug, *J. Fluid Mech.* **59**, 281-335.

[3] A.G. Darbyshire and T. Mullin, 1995, Transition to turbulence in constant-mass-flux pipe flow, *J. Fluid Mech.* **289**, 83-114.

[4] S. Eliahou, A. Tumin and I. Wygnanski, 1998, Laminar-turbulent transition in Poiseuille pipe flow subjected to periodic perturbation emanating from the wall, *J. Fluid Mech.* **361**, 333-349.

Separation and relaxation of supersonic boundary layer behind shock wave and expansion fan

M. A. Goldfeld
Institute of Theoretical and Applied Mechanics, Novosibirsk, Russia
Email: gold@itam.nsc.ru

Keywords - Boundary Layer - Interaction - Velocity Profile - Skin Friction

Abstract - The results of experimental investigation of a turbulent boundary layer relaxation are presented. They include the study of the shock wave and/or expansion fan action upon the boundary layer. **The main aims** of the investigation were: **a.** separation and relaxation of boundary layer, **b.** skin friction and integral parameters, **c.** pulsation characteristics, **d.** successive interaction and mutual effects. Schemes of models test conditions and types of measurements are shown in table. Three groups of models were studied: 2D and 3D models with

N	MODELS	Mach number Geometric Data	Types of measurement
1	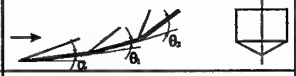	M_∞=2-6 θ_1=11°-25° θ_2=12°-25° α=0°,6°	$P_0(y)$, $P_w(x)$, $U(y)$, C_p δ^*, δ^{**}, δ
2	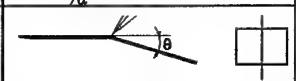	M_∞=2-4 θ=10°-25°	$P_0(y)$, $P_w(x)$, $U(y)$, C_p δ^*, δ^{**}, δ
3	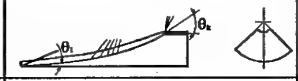	M_∞=2-6 θ_1=5° θ_2=20°	$P_0(y)$, $P_w(x)$, $U(y)$, C_p δ^*, δ^{**}, δ
4	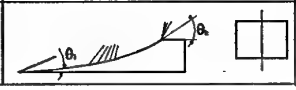	M_∞=2-6 θ_1=5° θ_2=20°	$P_0(y)$, $P_w(x)$, $U(y)$, C_p δ^*, δ^{**}, δ
5		M_∞=2-6 θ=90°	$P_0(y)$,$P_w(x)$
6	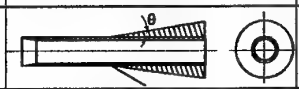	M_∞=2-4 θ=10°-25°	$P_0(y)$, $P_w(x)$, $U(y)$, C_p δ^*, δ^{**}, δ
7	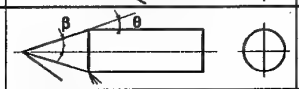	M_∞=2-4 β=15° θ=-15°	$P_0(y)$, $P_w(x)$, $U(y)$, C_p $\langle\rho U\rangle(x, y)$
8	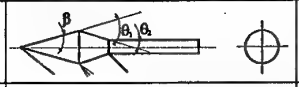	M_∞=2-4 β=7.5° θ_1=-15° θ_2=7.5°	$P_0(y)$, $P_w(x)$, $U(y)$, C_p $\langle\rho U\rangle(x, y)$
9	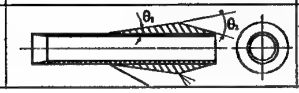	M_∞=2-4 θ_1=12°,20° θ_2=-15°,-25°	$P_0(y)$, $P_w(x)$, $U(y)$, C_p $\langle\rho U\rangle(x, y)$

shock waves, expansion fan or with distributed pressure gradient. These groups include also complex paired interactions. The tests was performed at the Mach numbers from 2 to 6 and Reynolds numbers from 8 to 80 million per meter. The boundary layer relaxation was studied in detail over a large distance behind the interaction region.

The influence of the adverse and favourable pressure gradient on the boundary layer state is also very substantial. The action is different in these two cases. A skin friction increases behind the shock wave and decreases behind expansion fan. These results conform to transformation of velocity profile and its fullness. The length of the boundary layer relaxation behind the shock wave and expansion fan is considerably different (20 and 200 boundary layer thickness) and the boundary layer remains cinematically non-equilibrium (in the sense of Klauser) over the all length. This can be related to specific features of the flow structure behind the expansion fan and a possibility of complete or partial relaminarization of the boundary layer behind the corner point. The conducted studies allowed us to obtain the systematic experimental data on the turbulent boundary layer evolution in flows with large pressure gradients The action of the shock wave and expansion fan leads to considerable changes in integral thicknesses of the boundary layer skin friction and pulsation characteristics. These changes become larger as the action intensity increases, especially in separated flows. Complex interactions cannot be considered as a simple superposition of two individual actions of the opposite pressure gradients. The process is substantially nonlinear and depends on a wide range of parameters.

Two Ways of Manipulation with the Onset of Boundary Layer By-pass Transition

P. Jonáš, O. Mazur and V. Uruba
Institute of Thermomechanics AS CR, Prague, Czech Republic
E-mail: jonas@it.cas.cz

Keywords - By-pass Transition - Scales of Turbulence - Control of Transiton Onset

Abstract - The effect of the intensity of the outer stream turbulence fluctuations on the position of the transition region is well known since the forties. Recently, the effect of the length scale of the outer stream turbulence on the course of the flat plate boundary layer transition has been clearly demonstrated (e.g. [1]) in the framework of experiments carried out for the COST/ERCOFTAC Test Case T3A+. (This test case is characterised by flat-plate boundary layer, mean velocity 5 m/s, intensity = 3% and different length scales of outer stream turbulence at the origin of the layer.) Apparently, there are two ways how to move, in certain limits, with the onset of by pass transition. Either, to maintain the length scale constant and to control the velocity scale of outer stream turbulence, or to make it conversely. The second way was undertaken in the framework of Test Case T3A+ study. Derived correlation of Reynolds numbers corresponding to the onset and termination of by-pass transition with the dissipation length parameter (e.g. [2]) are valid at boundary conditions relating to the COST/ERCOFTAC Test Case T3A+ only. To receive correlation of more general validity, further experiments are necessary.

Results of a new series of experiments, their analysis and an effort to find a more universal dimensionless parameter, describing the onset and termination of the process with regard to turbulence scales of velocity and length, are going to be presented in the contribution. Presently, five transitional boundary layers are investigated at very different turbulence intensity (from 2,8 to 16,3 percent) and dissipation length parameter (from 1 to 4 mm) in the leading edge plane. Experimental facility, measuring technique and boundary conditions were the same as at the measurements dedicated to Test Case T3A+. The incoming flow was turbulized by means of the grid/screen turbulence generator (one from the generator family used in Test Case T3A+ study). In this way, the region of the occurrence of onset positions observed in the course of present experiments overlaps the relevant region in the framework of Test Case T3A+. Moreover, there are planned several complementary measurements at boundary conditions producing the onset of transition at values of the momentum thickness Reynolds number between 100 and 400 to condense the data in this interval.

References:

[1] Jonas P., Mazur O., Uruba V.: Experiments on by-pass boundary layer transition with several turbulent length scales, ImechE 3rd European Conference on Turbomachinery, 2 –5 March 1999, London, Conference Transactions, Vol.A, 179-188.

[2] Jonas P., Mazur O., and Uruba V.: Example of the onset and termination of by-pass transition correlation with turbulence length scale, In: Proc. Colloquium "Fluid Dynamics'99", Jonas P., Uruba V. (Eds.), Institute of Thermomechanics AS CR, Prague, 1999, 95-102

Evaluation of three turbulence models on swirling flows from two counter-rotating burners in a furnace

S Kucukgokoglan, A Aroussi, M Menacer, S.J Pickering

School of Mechanical, Materials, Manufacturing Engineering and Management
University of Nottingham, Nottingham, NG7 2RD, UK

Keywords: *CFD, Turbulent Modelling, Swirling Flow, Burner, Furnace*

Abstract

This paper presents the performance of three different turbulence models for the prediction of turbulent isothermal swirling flows, from two counter-rotating burners enclosed in furnace type geometry. The numerical models being used are: standard k-ε, RNG k-ε, and realisable k-ε. The realisable k-ε, model is a new model to be used in this type of application that needs to be compared with well-established models. The grid for the enclosed furnace-type geometry of the rig was achieved using the GAMBIT V.1.0.4 package, and the predictions from the CFD models have been obtained using the commercial CFD code FLUENT version 5.0.2

Predictions of two counter-rotating burners on a three-dimensional axisymmetric mesh show the near burner region is accurately predicted by increasing the mesh density. In full furnace simulations a fine mesh has been used within the near burner region to eliminate mesh dependency. This is because flame ignition generally occurs within one and a half burner diameters downstream of the exit with this type of burner design, and in this region a substantial amount of the total nitrous oxides emissions (NOx) is produced.

The standard k-ε and RNG k-ε are well established models in predicting turbulent isothermal swirling flows, which have been compared successfully to experimental results. Comprehensive comparisons of the three models show that good agreement is achieved with a high mesh resolution. Overall, the velocity profiles, contours and flow patterns of the realizable k-ε, model are in general good agreement with the standard k-ε, RNG k-ε, models, indicating that the general flow-field within the furnace has been predicted accurately.

Interaction between Tollmien-Schlichting wave and strong longitudinal irregularity of boundary-layer flow

Sergei V. Manuilovich
Central Aero-Hydrodynamics Institute (TsAGI), Russia
Email: manu@recp.aerocentr.msk.su

Keywords - Stability - Boundary layer - Benjamin-Ono equation

Abstract - Stability and receptivity of boundary layer with strong local or periodic longitudinal irregularities are investigated. Both acoustic and vibration receptivity problems are considered. For mathematical description of the phenomena in question we use four-deck approximation (Zhuk & Ryzhov, 1982; Smith & Burggraf, 1985) describing the behavior of large-sized short-scaled disturbances. Within the framework of this approximation the above 2D problems are reduced to the solution of forced Benjamin-Ono equation. The exact solution of the stability problem for periodic flow corresponding to Tollmien-Schlichting (TS) wave of finite amplitude is found. On the base of this solution the problem on interaction between TS wave and Benjamin solitary wave is solved. The scaled displacement thickness A corresponding to the process involved is given by the following equation:

$$A = \frac{4c}{1+c^2\theta^2} + \left[\varepsilon\varphi(\theta)\, e^{ix-it} + c.c.\right] + O\left(|\,\varepsilon\,|^2\right), \quad \varphi = \frac{\left(c\theta + i\frac{3c+2}{c+2}\right)(c\theta - i)}{(c\theta+i)^2}, \quad \theta = x + ct$$

In this expansion the first term describes solitary wave of finite amplitude (Benjamin, 1967) propagating in upstream direction with phase velocity $c > 0$. The second term represents the small disturbance corresponding to scattering of TS wave by this finite unsteady irregularity. This disturbance is normalized by condition $\varphi(\theta) \to 1$ as $\theta \to \pm\infty$. If the TS wavelength is large as compared to characteristic length of Benjamin soliton, the magnitude of pulsations in the centre of irregularity is three times greater than in upstream (or downstream) region.

References

BENJAMIN, T.B. 1967 Internal waves of permanent form in fluids of great depth. *J. Fluid Mech.*, **29**, No. 3, 559-592.

SMITH, F.T. & BURGGRAF, O.R. 1985 On the development of large-sized short-scaled disturbances in boundary layers. *Proc. R. Soc. Lond. A* , **399**, 25-55.

ZHUK, V.I. & RYZHOV, O.S. 1982 Locally nonviscous perturbations in a boundary layer with self-induced pressure. *Sov. Phys. Dokl.*, **27**, No. 3, 177-179.

Probing structures in channel flow through $SO(3)$ and $SO(2)$ decomposition

L. Biferale[1,2], D. Lohse[3], I. Mazzitelli[3] and F. Toschi[2,3]
[1]Dipartimento di Fisica, Universitá di Tor Vergata,
Via della Ricerca Scientifica 1, I-00133 Roma, Italy.
[2]INFM-Unitá di Tor Vergata,
Via della Ricerca Scientifica 1, I-00133 Roma, Italy.
[3]Department of Applied Physics, University of Twente,
P.O. Box 217 7500 AE, Enschede, The Netherlands.
Email: i.mazzitelli@tn.utwente.nl

Keywords - Turbulence - Intermittency - Anisotropies

Abstract - We study the properties of anisotropic turbulence by using the projection of longitudinal structure functions into their irreducible representations of $SO(3)$ and $SO(2)$ symmetry groups, which are, respectively, characterized by j, m and m indexes. We consider a numerical simulation of a turbulent channel flow, this system is mainly homogeneous and isotropic in plane parallel to the walls, on the contrary, it is strongly inhomogeneous and anisotropic in the direction perpendicular to the walls, especially in the boundary layer. The decompositions are used to probe, characterize, and quantify the anisotropic structures in the flow. Close to the wall the $SO(3)$ modes with $j \geq 2$ are dominant and reveal the flow geometry. The isotropic amplitude of the SO(2) decompositions shows nice scaling with the standard intermittency exponents up to very close to the wall. The larger intermittency found in the shear layer for the longitudinal structure function originates from the non SO(2) symmetric amplitudes with $m \geq 2$. The SO(3) decomposition does not converge for large scales as expected. However, in the shear BL it also does not converge for small scales, reflecting the lack of small scale isotropization in that part of the channel flow.

In Figure 1 we show the kind of informations which can be extracted from the $SO(2)$ decomposition. We plot the amplitude of the $m = 2$ sector divided by the $m = 0$ (isotropic projection): this ratio is a first hint of the relevance of anisotropies. This quantity, evaluated at three different scales, is plotted for all distances from the two walls of the channel flow. As it can be seen, larger scales are much more affected by the presence of anisotropies near to the walls.

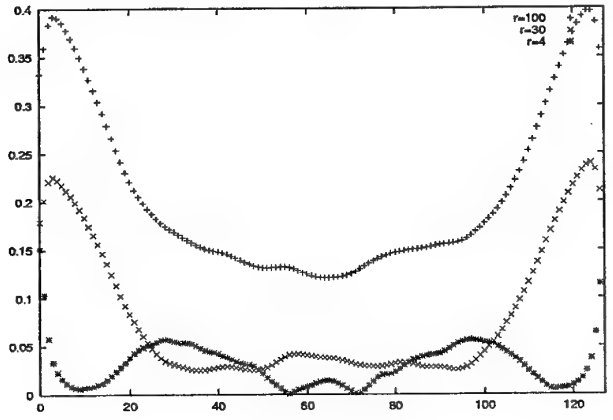

Figure 1: $a_2^{(2)}(z,r)/a_0^{(2)}(z,r)$ as a function of z for $r = 100$ (outer length scale), $r = 30$ (inertial subrange), and $r = 4$ (viscous subrange).

Effects of compressibility on thermal recovery in laminar boundary layer flow

B.W. van Oudheusden
Department of Aerospace Engineering
Delft University of Technology, The Netherlands
Email: B.W.vanOudheusden@LR.TUDelft.nl

Keywords: compressible flow - recovery temperature - laminar boundary layers

Abstract - Because of the analogy between the diffusive transport of momentum and heat that exists in boundary layer flow, the local values of velocity and temperature (enthalpy) are closely coupled. This relation is usually referred to as the Crocco(-Busemann) relation. In particular, for steady boundary layer flow over an adiabatic wall, the total enthalpy is found to remain constant throughout the boundary layer when the fluid Prandtl number (Pr) is equal to one. Under this condition the mechanical and thermal diffusion mechanisms are identical, so that a complete thermal recovery (i.e. the conversion of kinetic energy into enthalpy) occurs in the viscous flow, just like in non-diffusive (inviscid) flow. As a consequence, the adiabatic wall temperature is identical to the free-stream stagnation temperature. The validity of this relation is not compromised by effects of pressure gradient, compressibility (including temperature dependence of the viscosity) or three-dimensionality of the flow.

In the case that the Prandtl number is smaller than one, as in a real gas, only partial thermal recovery occurs. The effect of Pr in this, is commonly incorporated by applying a direct generalisation of the Crocco relation, in which a constant recovery factor is assumed throughout the entire boundary layer. A fundamental objection to such a modification, however, is that the resulting enthalpy distribution is in disagreement with the integral conservation of energy in the boundary layer. According to this, the reduction of the total enthalpy near the wall due to the incomplete heat recovery needs to be balanced by a flow region near the outer flow where $H > H_e$, whereas with a constant recovery factor $H \leq H_e$ everwhere in the boundary layer (assuming $u \leq u_e$).

An asymptotically complete first-order correction to the Crocco relation, for Prandtl numbers near one, is obtained from a perturbation approach, with respect to the parameter $\epsilon = Pr - 1$ (see [1]). With constant-property flow, an analytic first-order extension of the Crocco relation can be formulated:

$$h = h_e + r\frac{1}{2}(u_e^2 - u^2) - (r-1)\frac{\psi}{\rho}\frac{\partial u}{\partial y} + \mathcal{O}(\epsilon^2) \qquad (1)$$

where ψ is the stream function. The result has generally validity, in that it applies to *any* laminar boundary layer solution. Also, the analysis confirms the asymptotic validity of the square root dependence of the recovery factor r on Prandtl number, as:

$$r = \frac{h_w - h_e}{\frac{1}{2}u_e^2} = 1 + \frac{Pr-1}{2} + \mathcal{O}(\epsilon^2) = Pr^{1/2} + \mathcal{O}(\epsilon^2) \qquad (2)$$

The particular subject of the presentation is the investigation of the effect of compressibility (i.e., variable density and viscosity) on this extension of the Crocco relation. For this, the boundary layer equations are studied in the form obtained by the Levy-Lees compressibility tranformation. This reveals that the general validity of the extended Crocco relation is affected by: 1) variable properties (a purely thermal effect) and 2) a direct Mach number effect in combination with the pressure gradient. The constant-property result remains strictly valid, only when the viscosity-temperature relation is linear and for a zero pressure gradient. Numerical results for (quasi-)self similar solutions are used to evaluate and illustrate the extent of these effects.

[1] B.W. van Oudheusden: A complete Crocco integral for two-dimensional laminar boundary layer flow over an adiabatic wall for Prandtl numbers near unity. *J. Fluid Mech.*, vol. 353, pp.313–330, 1997.

ON SUPERSONIC BOUNDARY LAYER RECEPTIVITY OVER FLAT PLATE IN CONTROLLED CONDITIONS

N.V. Semionov

Institute of Theoretical and Applied Mechanics SB RAS, Novosibirsk, Russia

e-mail: semion@itam.nsc.ru

keywords: receptivity, supersonic.

The paper is devoted to the experimental study of a supersonic boundary receptivity layer on a flat plate to external controlled disturbances. The measurements were performed in a supersonic low noise wind tunnel Ò-325 of the Institute of Theoretical and Applied Mechanics of the Russian Academy of Sciences with the test section dimensions 600*200*200 mm at Mach number Ì=2 and 3.5. The model consists of two plates, established under a zero angle of attack. A generator of periodic disturbances, based on electrical discharge, was mounted on the plate *1*. As a result of the electric discharge, initiated at frequency f, the disturbances appeared in the boundary layer and propagated downstream. This process was accompanied by the sound radiation into the free stream. More precisely this radiation was used as external controlled disturbances. Disturbances in free stream and in the boundary layer of plate *2* were registered by the hot-wire anemometer.

The forced disturbance field in free stream was investigated. The acoustic nature of the radiation was obtained. Several characteristic zones were distinguished corresponding to the various types of amplitude and phase functions.

Two cases of receptivity process were considered. In the first experiments the source of controlled disturbances (plate *1* with surface electric discharge) was placed above the model. Disturbance wave structure in the boundary layer was investigated for the case when the maximum of the sound radiation fell on the leading edge of the plate *2*. In the second experiments the controllable disturbances fell on the leading edge of the plate 2 from below. In this case generation of disturbances in the boundary layer by the external controlled acoustic field takes place only in a vicinity of leading edge of the plate *2*. Disturbances in the flat plate boundary layer, excited by external controlled acoustic oscillations in a vicinity of sharp or blunted leading edge were measured. Quantitative comparison of levels of initial acoustic disturbances and eigen oscillations excited by them of a supersonic boundary layer was carried out. Transformation coefficients (ratio of generated disturbances in the boundary layer to the amplitude of the acoustic waves falling on the leading edge) were obtained. Influence of leading edge bluntness and Mach number of flow were considered. It was found, that the excitation of disturbances in the boundary layer by external disturbances at the sharp leading edge grow with Mach number increasing and the transformation coefficients for the oblique waves in the boundary layer are more, than for the plane wave at $\beta \approx 0$. the excitation of disturbances in the boundary layer by external disturbances at the blunted leading edge occurs considerably more heavily than at the sharp leading edge.

Obtained experimental data were compared with theoretical results and some correlations and contradictions were discussed.

Turbulence at the magic angle

Adrian Daniel Staicu and Willem van de Water

Physics Department, Eindhoven University of Technology,
P.O. Box 513, 5600 MB Eindhoven, The Netherlands

We employ multipoint hot-wire anemometry to investigate various fully developed turbulent flows generated in a recirculating windtunnel. We compute generalized structure functions using long time series from the 10 hot-wire anemometers arranged perpendicular with respect to the mean flow:

$$S_p(r,\theta) =< (\Delta u(r,\theta)^p) > \quad (1)$$

Recent theoretical research predicts the generalized structure functions dependence on the separation r and angle θ; the procedure is based on decomposing the structure functions on the irreducible representations of the symmetry group SO(3). The nature of the symmetry group is determined by the property of the flow, in this case homogeneity and isotropy. When the symmetry group changes, similar relations can be obtained. We investigate the differences which occur when we measure structure functions in a turbulent flow which has an axial symmetry, simplifying the relations which determine the generalized structure functions.

EFFECT OF PIPE LENGTH ON THE CHARACTERISTICS OF ISSUING HELICAL JET

J.Wojciechowski, A. Szumowski
Warsaw University of Technology
ul. Nowowiejska 24
00-665 Warsaw, Poland
e-mail: jan@meil.pw.edu.pl

Key words: helical jet, swirling flow

Axisymmetric flow with tangential velocity component is defined as the swirling flow. Swirling flows exist in aircraft engines, cyclones, pneumatic conveying systems and suchlike. Much effort has been devoted in last years to study the characteristic of turbulent swirling flow in pipes. The experiments were conducted with the use of swirl generators prepared to have the axisymmetric flow of high quality, i.e. characterised by uniform flow velocity distribution on concentric circles. Very frequently, however, the swirling flow is generated by a jet from a single nozzle inflowing tangentially into a pipe. Due to the asymmetric supply, a screw – like jets superimposed on the mean swirling flow appears in the pipe.

This complex flow pattern, the helical flow, is investigated experimentally in the present paper. The goal of these investigations is to find the characteristics of the jet issuing from the pipe depending from the distance from its tangential inlet to its axial outlet. The azimutal and radial velocity distributions at the outlet of the pipe are measured by means of a hot wire probe. The free jet was visualised using the laser light knife and CCD camera. It was find that the distance travelled by the helical jet inside the pipe affects considerably the issuing free jet. This reveals in the changing of the asymmetric axial and tangential flow velocity distributions. For the short pipe, the strongest asymmetry exists for a part of the pipe cross-section near the pipe wall. Contrary to this, for a long pipe the largest deviation from axisymmetry appears in the middle part. In this result, the total effect of the asymmetry expressed by the root-mean-square of the swirl number considerably decreases.

Figure shows two photographs of the free jet, cuted perpendicularly to its axis: at one2(left) and two pipe diameters (right) downstream of the pipe exit. The aluminium powder was added to the air inflowing tangentially into the pipe to make the flow visible. The rotation of the jet can be noted in these photographs.

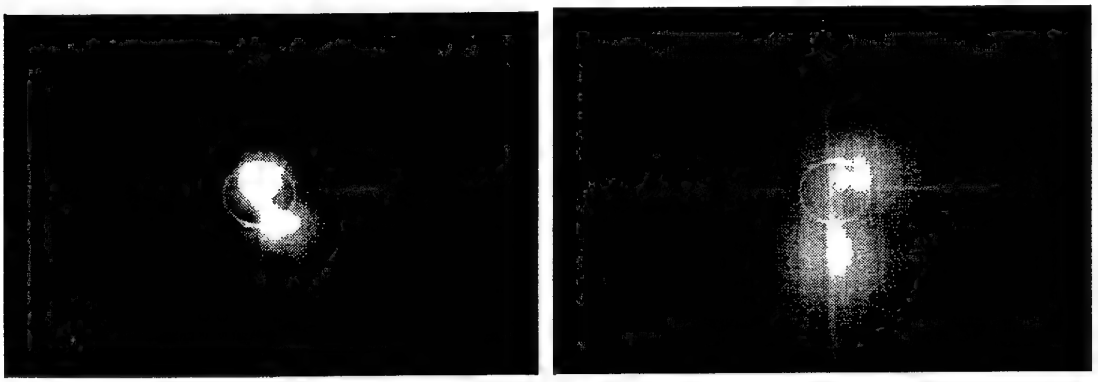

SNM

DNS of non-premixed combustion using simple chemistry

R.J.M. Bastiaans, L.M.T. Somers and H.C. de Lange
Section of Internal Combustion Engines and Energy Technology,
Department of Mechanical Engineering,
Eindhoven University of Technology, The Netherlands
Email: R.J.M.Bastiaans@wtb.tue.nl

The present study is concerned with the direct numerical simulation of realistic turbulent mixing and exothermic reaction of fuel and oxidiser. The flow is compressible (a typical Mach number for in-cylinder engine flows is $Ma = 0.1$) but more severe density changes are generated by the combustion. Therefore, in contrast to many numerical combustion studies, a fully compressible DNS code is taken. The disadvantage of the time-step restriction due to the acoustic propagation speed can be circumvented by employing acoustic sub-steps.

The compressible DNS/LES code (de Lange and Bastiaans [1]) was validated using a time developing three-dimensional compressible mixing layer at $Ma = 0.2$ and $Re_\delta = 50$ as investigated by Vreman [3] (temporal case, four vortex mode). For the non-premixed combustion case a flow domain containing a single vortex was taken at the same Ma and Re numbers. The combustion of methane was considered having air (O_2 and N_2) at the upper side of the mixing layer and a CH_4 and N_2 mixture at the bottom side of the initial shear layer. The amounts of species were taken such that the methane/oxygen ratio in the free-streams is stoichiometric, though separated. A one-step arrhenius reaction was taken to model the chemistry with realistic reaction parameters and Lewis numbers according to van Maaren [2]. Furthermore the thermodynamic properties of the species were evaluated with GriMech 3.0.

In a two dimensional case with initial temperature of 1200 K it was found that first mixing occurs in the developing vortex before the chemical source term became large enough. Then a fast premixed combustion takes place in the vortex core. In the case of an initial temperature of 1400 K the roll-up of the shear layer was heavilly suppressed by the simultaneous reaction. The figure displays an instantaneous temperature field of the latter simulation for the reacting and non-reacting case (temperature contour increments of 5 K). At the moment three-dimensional simulations are in progress.

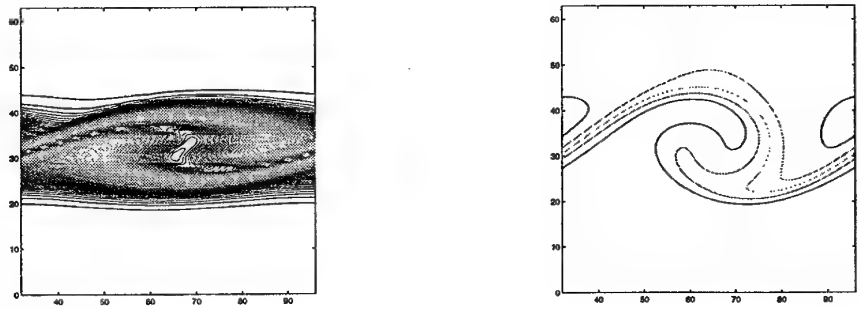

References

[1] H.C. de Lange and R.J.M. Bastiaans. Simulation of the intrusion of coherent free-stream perturbations in a subsonic boundary layer. In C. Dopazo et al., editor, *Advances in Turbulence VIII*, page 964. CIMNE, 2000.

[2] A. van Maaren. *One-step chemical reaction parameters for premixed laminar flames.* PhD thesis, Eindhoven University of Technology, the Netherlands, 1994.

[3] A.W. Vreman. *Direct and Large-Eddy Simulation of the Compressible Turbulent Mixing Layer.* PhD thesis, University of Twente, the Netherlands, 1995.

Dynamics of point vortices and vortex patches in a magnetized plasma

J. Bergmans[a], B. N. Kuvshinov[a], P. W. C. Vosbeek[b], and T. J. Schep[a]

[a] FOM-Instituut for Plasmafysica 'Rijnhuizen', Association Euratom-FOM, TEC, Postbus 1207, 3430 BE Nieuwegein, The Netherlands
[b] KNMI, Postbus 201, 3730 AE De Bilt, The Netherlands

The fluid equations for a dissipationless plasma in a strong background magnetic field are quasi-2D and can be written as a set of three Lagrangian equations. They have the same structure as the vorticity form of the Euler equation; three generalized vorticity fields each incompressibly advected by its own streaming potential. The three conserved fields are combinations of the magnetic flux function, the electrostatic potential, the current along the background field direction, the vorticity, and the plasma density.

Like in ideal hydrodynamics the model has exact point vortex solutions. The three types of vorticity result in three "flavors" of point vortices, whose interaction depends on the type of the vortex. The motion is Hamiltonian and the interaction potential is a mixture of the Eulerian and geostrophic potentials, i.e. the Hamiltonian consists of a logarithmic part and a modified Bessel function K_0, the latter is known from the Charney–Obukhov and Hasegawa–Mima equations. The mixed interaction leads to new orbit topologies. An example is the existence of point vortex collapses that are not self-similar. There also exists a collapse of an integrable four vortex system where the total vorticity of each field vanishes: a point vortex "annihilation".

The pointwise conservation of the generalized vorticities implies that the dynamics of a system of piecewise uniform patches of vorticity is completely determined by the dynamics of the boundaries of the patches. This contour dynamics (CD) method has proven to be very suitable for calculating vortex dynamics in ideal fluids. The important difference between CD in hydrodynamics and in the present plasma model is that patches carrying different types of vorticity *are allowed to overlap*. We will show some results of CD calculations in the plasma model, in particular the resolution of the point vortex collapse for vortices with a finite size.

Dynamic Simulation of the Gas-Assisted Injection Molding Process

Y. Dimakopoulos and J. Tsamopoulos
Laboratory of Computational Fluid Dynamics, Department of Chemical Engineering
University of Patras, Greece
Email: tsamo@chemeng.upatras.gr

Keywords: - Free Surface Flows - Gas-Assisted Injection - Dynamic Simulations

Abstract –The Gas Assisted Injection Molding is a forming process of great importance for the polymer industry, in which basic and fundamental physical phenomena, such as fingering instability in the gas/liquid interface, instability in the liquid/solid interface and motion of a gas-liquid-solid contact line arise. A typical process consists of the displacement of a polymeric melt by air in a cylindrical contraction, under isothermal or non-isothermal conditions. Neglecting the flow in the air, we define as control volume the melt that is being displaced (see figure). At first approximation, the melt is assumed to behave as a Newtonian fluid and the Navier-Stokes and the continuity equation, in their axisymmetric form, together with appropriate boundary conditions govern its motion. At the free surface, an interfacial balance between viscous stresses, surface tension and gaseous pressure is imposed, while no slip and no penetration of fluid apply at the solid wall. Far downstream, in the contraction region, we assume a fully developed flow.

The presence of a highly deformable free surface, which rearranges the control volume in time and the stress-singular points at the three phase contact line and the contraction corner demands an accurate, robust and flexible numerical method. The preferred one is the fixed Finite Element Method for all the dependent variables, together with a system of elliptic partial differential equations, capable of generating boundary-fitted finite element discretizations, which retain mesh orthogonality and uniformity as much as possible. The boundary conditions imposed on the PDEs that generate the mesh are the physical bounds of the geometry and the kinematic condition at the moving interface. Grid points become finite element nodes mapped subparametriaclly from a patched computational domain. The implicit Euler method is used for time integration. The dimensionless parameters which arise in the equations are the Suratman number, Su, which measures the importance of inertial and surface tension forces relative to the square of viscous forces, the Bond number, Bd, which measures the importance of body forces against surface tension forces, the dimensionless gaseous pressure and geometrical ratios. The original mesh generation scheme works for displacements of the center of the tube as large as 2.5 times the inner radius in the entrance, but for subsequent calculations it must be replaced. Depending on the operating conditions and the fluid properties a finger that may evolve all the way to the contracted part of the tube is observed. A complete parametric study will be presented.

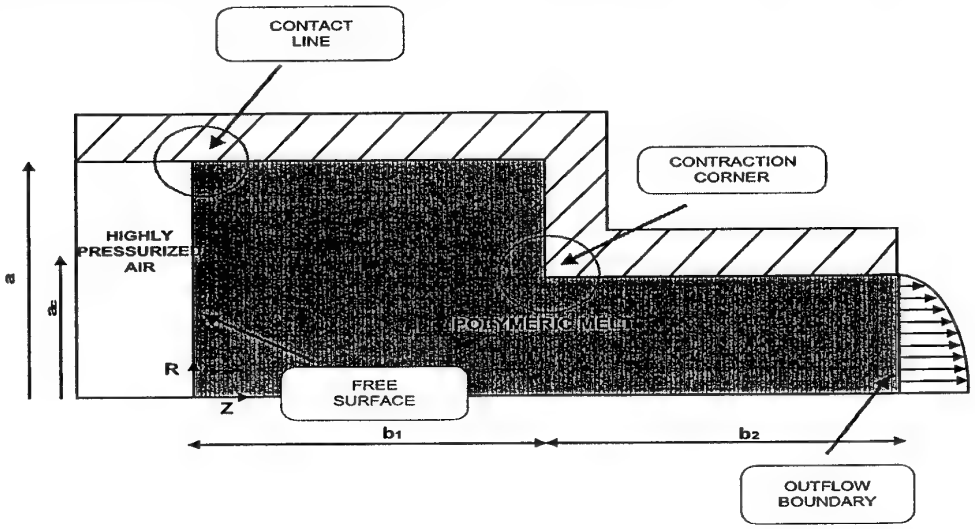

Numerical Simulation of a Single Blade Centrifugal Wastewater Pump

J. Keays and C. Meskell
Department of Mechanical & Manufacturing Engineering
Trinity College, Dublin, Ireland
Email: keaysj@tcd.ie

Keywords - Wastewater pump - 2D unsteady turbulent CFD

Abstract - Traditionally wastewater pumps have been designed with a single spiral shaped blade and a constant height volute, since a multi-vane centrifugal pump would become blocked due to the insoluble solids in the fluid. This design provides a large passage through which the solids can pass without clogging the pump. However, a single vane pump will have a lower hydrodynamic efficiency compared to multi-vane designs. The design and modification of these pumps is almost entirely based on heuristics and simplistic analysis, thus necessitating expensive experimental work. This paper presents a 2D, fully unsteady analysis of a particular commercially available wastewater pump using the CFD package Fluent 5.1. The fluid is modelled as incompressible pure water with a simple two equation turbulence model. A sliding mesh technique is employed to model the variation in flow domain geometry as the impeller rotates. It is necessary to calculate the flow field variables at small intervals of blade rotation angle and to allow several revolutions before the solution can be said to be time periodic. Therefore the simulations are computationally expensive. The CFD predictions are used to calculate the instantaneous torque on the impeller and the total instantaneous specific energy at the outlet. Using these two parameters along with the specified impeller rotational speed, the hydrodynamic efficiency has been calculated. An extensive database of experimental results exists against which the predicted efficiency is compared. It can be seem from figure 1(a) below that the predicted efficiency compares favourably with the experimental results. It should also be noted that the estimates of the torque on the blade and the energy at the outlet are reasonable. From a design viewpoint regions of high turbulent kinetic energy, which are circled on figure 1(b), suggest areas where the geometry might be improved. Although the fluid flow through a centrifugal pump is inherently 3D, a full 3D unsteady analysis would be excessively computationally expensive. Furthermore, the 2D results presented here are promising, and so this approach warrants further investigation.

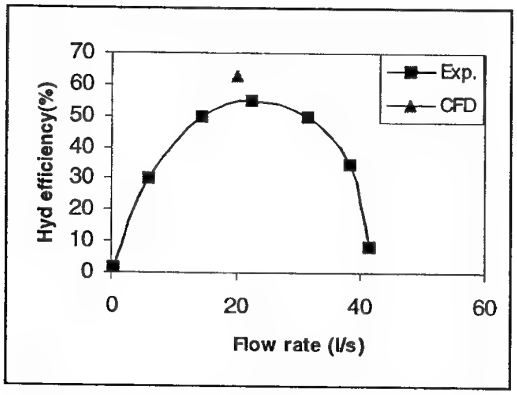

Fig 1(a) Hydraulic efficiency against flow rate.

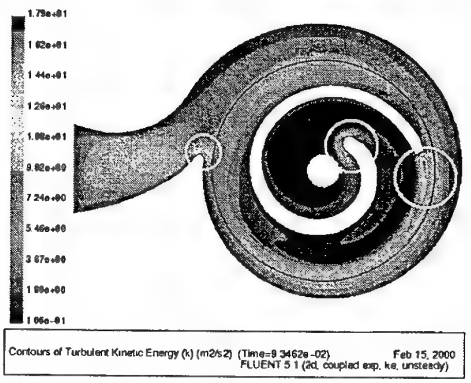

Fig 1(b) Instantaneous turbulent kinetic energy.

Vibration absorber of floating beam subject to wave loads

T.I. Khabakhpasheva and A.A. Korobkin
Lavrentyev Institute of Hydrodynamics, 630090, Novosibirsk, Russia
Email: TANA@hydro.nsc.ru, KAA@hydro.nsc.ru

Keywords - Hydroelasticity - Floating structures

Abstract - An approach to reduce vibrations of floating elastic plate in wave is presented. The approach is based on the concept of *vibration absorber* which is well-known in engineering application. The idea is to add to the main floating structure an auxiliary floating plate and to select the plate size and its characteristics which provide reduction of the main structure deflections for a given frequency of incident wave.

The plane linear problem of two floating beams is considered. The beams are connected with the help of a torsional spring. Vibrations of the beams are caused by periodic incident wave of small amplitude. The longer beam is referred to as the main structure, characteristics of which are prescribed. The shorter beam is referred to as the auxiliary plate, length of which is given. We determine both characteristics of the auxiliary plate and the torsional spring stiffness which essentially reduce the vibration amplitude of the main structure. The auxiliary plate can be adjacent either in front of the structure (fig. a) or at the rear side of it (fig. b). Analysis of floating plate behaviour in waves is based on hydroelasticity, in which the coupled hydrodynamics and structural dynamics problems are solved simultaneously. Different basic functions to represent the pressure distribution and the beam deflection are used. This makes it possible to simplify treatment of the hydrodynamic problem and at the same time to satisfy accurately the beam boundary conditions.

Calculations were performed for the conditions of experiments [1] with a narrow elastic plate in a channel. The plate draft is 8.36mm, the plate thickness 38mm and the plate length 10m. The bending stiffness EJ of the plate is 471Nm^2/m. Period of the incident wave is T=1.429s. It was revealed that: 1) auxiliary plates adjacent in front of the main structure (case a) decrease the structure vibrations; 2) vibrations of the main structure are increased with auxiliary plates attached to its rear side (case b); 3) reduction of the vibration is strongest if the plates are simply connected; 4) short auxiliary plates of length 1.5m decrease the deflections by 20% (case a) and increase them by 10% (case b); 5) essential reduction (35%) of the structure vibrations was detected in the case of rigid auxiliary plates of length 2.5m simply connected in front of the main structure (fig. c: solid line is for single homogeneous plate, dash – for auxiliary plates in front of the main plate, dotted – at the rear side).

Roughly speaking, in order to reduce the floating plate vibrations, a rigid plate of smaller length has to be simply connected in front of the main structure. The effect of the vibration reduction is well pronounced and can be utilized at the design stage.

This work was supported by RFBR (grants 00-01-00850, 00-15-96162).

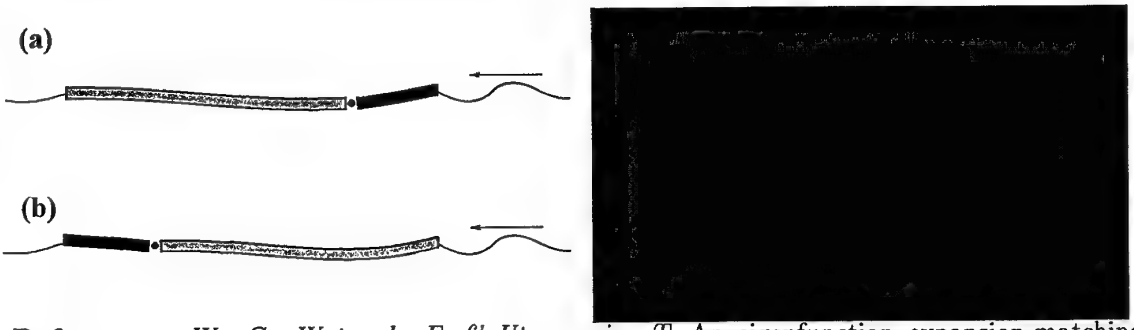

References: *Wu C., Watanabe E. & Utsunomiya T.* An eigenfunction expansion-matching method for analyzing the wave-induced responses of an elastic floating plate. *Appl. Ocean Res.* 1995. V.17(5). pp.301-310.

Statistical simulation of viscous flows in 2D/3D micronozzles

G.N. Markelov and Mikhail S. Ivanov
Institute of Theoretical and Applied Mechanics
Siberian Division of Russian Academy of Sciences
Novosibirsk, Russia
Email: markelov@itam.nsc.ru

Keywords - Statistical simulation - micronozzle - viscous losses

Abstract -

Low-thrust propulsion systems are required to provide a very accurate attitude control of small satellites, micro satellites or even nano satellites, for drag-free motion of larger spacecraft or the outmost accurate pointing capabilities for deep-space planetary probes. To obtain these low thrust values (0.1-10 mN), a small nozzle scale and low chamber pressures are usually used. This results in the throat Reynolds number within the range between 10 and 100. Due to such low levels of Reynolds numbers, the viscous losses are significant in small scale nozzles.

The technology used in micromachined cold gas thruster opens new possibilities for creating effective low thrust propulsion systems. This is due to a possibility of manufacturing nozzles with a throat size of 10μm and using a high chamber pressure (1-10 atm). This permits obtaining a low thrust level for rather high Reynolds numbers. For instance, for axisymmetric or three-dimensional nozzles with a fixed expansion ratio, a ten-fold change in the linear dimensions requires a 100-fold increase in the chamber pressure to preserve a prescribed thrust level. However, the problem of taking into account viscous losses remains because the throat Reynolds number increases only by an order of magnitude.

The main objective of the present paper is a detailed numerical study of flows in micronozzles by Direct simulation Monte Carlo method. The influence of the shape of the micronozzle throat and the flow three-dimensionality on the micronozzle performance is examined and compared with experiment.

Numerical simulation of the flows in a viscous shock layer on the pointed bodies

T.V. Poplavskaya
Hypersonic Flows Laboratory Institute of Theoretical and Applied Mechanics SB RAS
Novosibirsk, Russia
Email: popla@itam.nsc.ru

Keywords - Hypersonic flow- Viscous shock layer - Simulation

Abstract - This investigation are devoted theoretical study of hypersonic flow on bodies with sharp edge.

At high Mach numbers ($M > 10$) and moderate Reynolds number ($Re_x \sim 10^4 - 10^5$) the boundary layer thickness is comparable with the shock wave stand-off distance. Thus, a good approximation for such flows is the full viscous shock layer (FVSL) model suggested, which is an intermediate level of asymptotically approximation between the boundary layer equations and the full Navier-Stokes equations. Apart from all terms of the boundary layer equations, the FVSL equations include the conservation equation for momenta projected onto the normal to the plate and all terms of the Euler equations in the hypersonic approximation. The FVSL model, therefore, describes the entire disturbed flow region of viscous gas between the shock wave and the body surface.

The slip and temperature drop conditions are used on the body surface. The shock wave is assumed to be thin, and, the boundary conditions on the shock wave are taken as the generalized Rankine-Hugoniot conditions.

It is assumed that the flow in the initial cross- section x_0 is described by the boundary layer equations and the shock wave has a constant inclination between the leading edge of the body and cross-section $x = x_0$. The viscous shock layer equations are solved by the marching method with respect to the x coordinate. The iteration process in each cross-section continues until the condition of the massflow conservation when passing through the shock wave is satisfied. The profiles of velocity, temperature, density and pressure in the entire shock layer are obtained while solving the problem. The skin friction coefficient and the heat transfer coefficient (Stanton number) are calculated on the body surface.

The results of calculations of the hypersonic flow around a plate with a sharp leading edge and cone are presented. Step-by-step verification of the numerical model of the full viscous shock layer is performed: the calculated density profiles, shock wave inclinations, and the Stanton numbers are compared with experimental data obtained in ITAM SB RAS and found in other papers. Using the above algorithm of the FVSL equations with obtaining the shock wave position from the condition of constant flow rate, we performed parametric calculations in a wide range of governing parameters: $15 < M < 25, Re_x = 10^4 - 10^6, \alpha = 0^\circ - 15^\circ, 0.05 < T_w/T_0 < 0.26$. When analyzing the parametric FVSL computations, we obtained an empirical function approximating the results for the heat transfer coefficient on the plate and surface pressure on the cone.

Numerical aspects of particle-mesh methods and PDF computation of turbulent flows

J. Pozorski and J.P. Minier
Institute of Fluid Flow Machinery, Polish Academy of Science, Gdańsk, Poland
Email: jp@imp.pg.gda.pl
Research & Development Division, Electricité de France, Chatou, France

Keywords: particle-mesh methods, statistical averages, turbulence, PDF method

Abstract

The Probability Density Function (PDF) method represents a statistical tool for description and computation of turbulent flows (Pope 1994, *Annu. Rev. Fluid Mech.* **26**:23). From the numerical standpoint, it is usually implemented as a stochastic particle method. Particle dynamics is described with stochastic differential equations that have the generic form of a diffusion process

$$d\Phi = \mathbf{D}(\Phi, \langle\Phi\rangle, \langle\phi\phi\rangle, \ldots; \mathbf{x}, t)\, dt + B(\Phi, \langle\Phi\rangle, \langle\phi\phi\rangle, \ldots; \mathbf{x}, t)\, d\mathbf{W} \qquad (1)$$

where $\Phi = \langle\Phi\rangle + \phi$ is a vector of particle properties, decomposed into the mean and fluctuation, $\mathbf{D}$ is the drift vector, B stands for the diffusion matrix, and $\mathbf{W}$ is the Wiener process.

As written above, some moments of the actual PDF are present in the SDE. In the numerical solution process, the moments (like $\langle\Phi_i\rangle$ and $\langle\phi_i\phi_j\rangle$) need to be found from the particle data. The correct computation of these quantities is crucial for the PDF method, for the moments are put back into the SDE and serve to advance the particle properties to the next time step of the simulation. These ingredients of the algorithm, i.e. computation of mean fields and their projection to (or interpolation at) particle locations, will be of major concern here. Even though both factors are classical in so-called particle-mesh methods (Hockney & Eastwood 1981, *Computer simulations using particles,* McGraw-Hill), there are, however, some features specific to the PDF method for turbulent flows. First peculiarity of the PDF particle approach relates to the computation of statistics: not only mean fields have to be obtained, but also (at least) their second-order moments. Next, the computational domain is usually bounded, so some boundary conditions must be prescribed.

In the proposed paper, the issue of mutual correspondence between particle data and mesh-averaged variables is addressed. The particle-mesh coupling is analysed in the numerical solution of position-dependent stochastic differential equations. A development of the Cloud-in-Cell (CIC) computation of statistical averages is proposed in order to account for boundary conditions in the PDF computation of turbulent flows (Minier & Pozorski 1999, *Phys. Fluids* **11**:2632).

Development of a Numerical Method for Simulation of Condensating Real Gas Flows

F. Put and P.H. Kelleners
Section Engineering Fluid Dynamics, Department of Mechanical Engineering
University of Twente, The Netherlands
Email: f.put@wb.utwente.nl; p.h.kelleners@wb.utwente.nl

Keywords - Condensation - Multiphase flow - Separation - Computational method

Abstract - Currently the process industry is using very complicated and large installations to separate components in gas–vapour mixtures. To reduce the high costs involved in this process, there is an ongoing effort to design and develop smaller devices and more efficient processes.

One of such a separation process is based on the differences in saturation pressure of the different components in the mixture. This is implemented in a process in which vapour components are made to condense, as liquid droplets, which are subsequently removed from the gas–vapour mixture, by a separate vortical flow process.

The predominant flow features in the process considered are:

- high speed vortical multiphase flow in a complex geometry
- the fluid is in thermodynamic non–equilibrium
- high stagnation pressures in the flow cause real–gas effects

For this type of flow a numerical tool is being developed to support the design and analysis of flow devices that utilize this process. In the computational method the following models are applied:

- Euler equations to describe advection of the flow
- droplet nucleation and droplet growth models
- integral description of the condensating phase
- real–gas equations of state
- The models are discretized on a non–structured grid to allow for the easy application to complex geometries

At present results have been obtained with a quasi one–dimensional version as well as a three-dimensional version of the computational method. In the proposed paper the computational method will be described and results of numerical simulations for air/water–vapour and nitrogen/water–vapour will be discussed.

Discrete vortex method using a cloud-in-element technique

C. Sweeney, C. Meskell & J.A. Fitzpatrick
Department of Mechanical & Manufacturing Engineering
Trinity College, Dublin, Ireland
Email: pasweene@tcd.ie

Keywords - discrete vortex method - cloud in finite element - unsteady 2D flow

Abstract-

The discrete vortex method for solving unsteady flow around bluff-bodies has been widely used [1,2]. This Lagrangian technique involves solving the stream function-vorticity formulation of the Navier-Stokes equations. Discrete vortex particles, which have are at the surface to satisfy zero slip, are convected in the inviscid flow, while diffusion is modeled as a random walk. Thus, each time step consists of three operations, none of which are iterative and so the flow may be solved with less computational effort than required by other approaches. The interaction of the discrete vortices can be computed more efficiently by use of a cloud-in-cell technique. Here the vorticity of the particles is spread onto a fixed Eulerian mesh, providing a source term for the Poisson equation which can be easily solved to provide the stream function (and hence velocity) field on the mesh. The cloud-in-cell technique has traditionally been used with regular polar or Cartesian grids, thus requiring conformal transformation and/or multi-grid methods for application to complex geometries. This paper presents a new approach to the cloud-in-cell technique which allows a single unstructured mesh to be used for arbitrary geometry. This paper develops the algorithm and presents results for the standard case of impulsively started flow over a circular cylinder for a range of Reynolds numbers. Post-critical Reynolds numbers are achieved by employing a simple eddy viscosity turbulence model. Excellent agreement is achieved between the current predictions and experimental data available in the literature. Figure 1 depicts typical results which have been obtained for impulsively started flow over a circular cylinder.

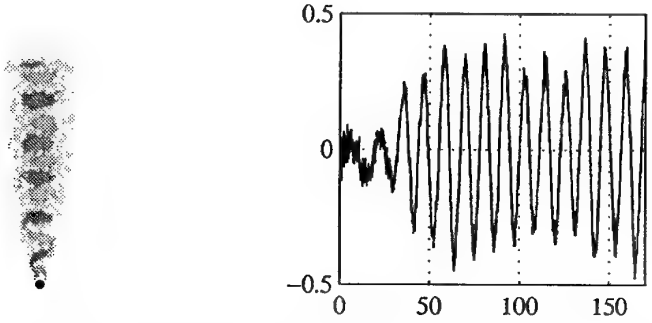

(a) Instantaneous vorticity field (b) Time dependent lift coefficient

Figure 1: Impulsively started flow around a circular cylinder $Re = 200$

[1] A. Leonard, *Vortex methods for flow simulation*, J. Comput. Phys., 37 (1980). pp. 289-335.
[2] J. Sethian, A brief overview of vortex methods, in *Vortex methods and vortex motion*, SIAM (1991) pp. 1-32. Philadelphia

St & Wa

Self-sustained tones reduction achieved by a flow bifurcation to a 'silent' path

A. Coiret, S.Guérin, A. Sakout, R. Henry
Laboratoire L.E.P.T.A.B.
Université de La Rochelle, Avenue M.Crépeau, 17042 La Rochelle
Email : acoiret@univ-lr.fr

Keywords – Hysteresis-like behaviour -Self-sustained tones – Flow bifurcation

Abstract – Intense self-sustained tones can be encountered in air flows, even for low velocities. In the case of two obstacles in a duct, a feedback loop can be established between vortex shedding of the upstream obstacle and acoustical field. This feedback loop is linked to the transfer of energy from the vortices to the acoustical field, as the downstream obstacle diverts them, according to phase and direction conditions. A first experimental set-up contains two «standard » diaphragms in a duct and generates intense self-sustained tones, providing that $L/D_0<1$.

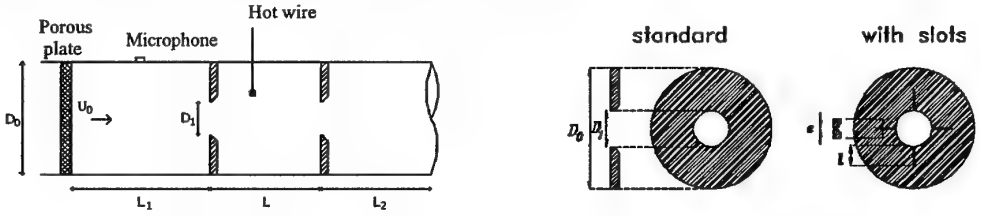

Experimental setup (left) ; standard and modified diaphragms (right)

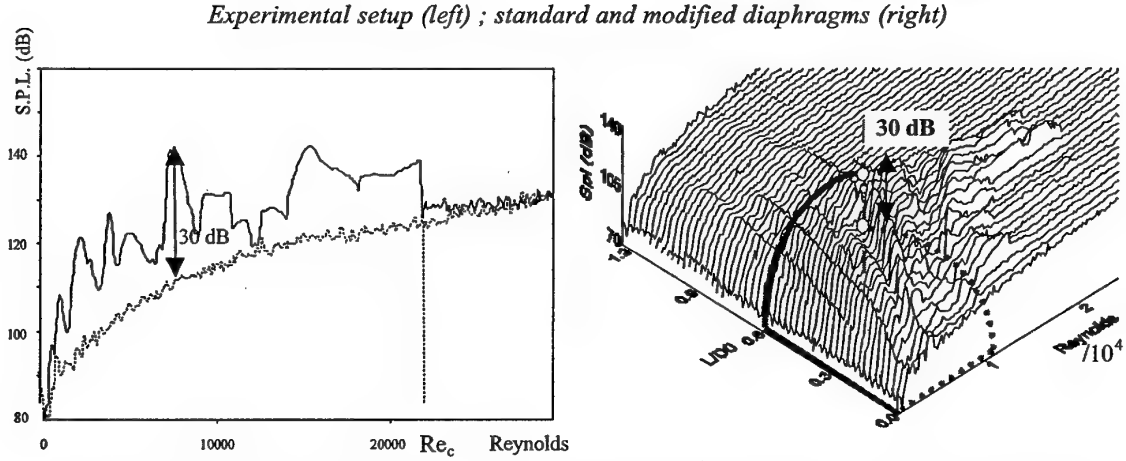

Bifurcation from a 'noisy' to a 'silent' path, with $L/D_0=0.3$ (left) and application to the reach of the silent path (right)

An original method for self-sustained tone reduction has been achieved by adding thin slots on the upstream diaphragm. Secondary plan jets interact with the axisymetric jet and reduce the efficiency of the feedback loop. Indeed the energy transfer from vortices to acoustic field is lowered since incidence angle and phase conditions of the vortices are modified as they reach the downstream diaphragm. When the Reynolds is raised, the noise reduction becomes fully operative at a bifurcation point Re_c, from the « noisy » path to a « silent » path. Furthermore, the sound level stays on the silent path when the Reynolds is then decreased, showing an hysteresis behaviour. The same type of bifurcation is obtained, for a given Reynolds number, when the spacing ratio L/D_0 is varied instead of the Reynolds number. Both these bifurcations to a silent path allow to determine an order of variation of the parameter to reach a given point of the domain (R_e ;L/D_0) on the silent path, avoiding the generation of self-sustained tones…

Temporal Evolution of Periodic Disturbances in Two-Layer Couette Flow

J.E. Dillingh and H.W.M. Hoeijmakers
Section Engineering Fluid Dynamics, Department of Mechanical Engineering
University of Twente, The Netherlands
Email: j.e.dillingh@wb.utwente.nl

Keywords - Two-layer Couette Flow - Interface Mode - Level Set Approach

Abstract - In the present study the temporal development of periodic disturbances in a two-layer Couette flow is investigated. Besides the Tollmien-Schlichting mode found in the classical hydrodynamical stability theory an additional interfacial mode (Yih mode) exists due to the two-fluid interface. The driving mechanism of this instability is the jump in velocity gradient over the interface caused by the difference in viscosity.

In this study numerical simulations are performed using the level set approach (Sussman et al [1994]). This method has originally been designed for surface tension-driven flows. To resolve the interface mode in this viscosity-driven flow a physically correct interpolation of the dissipation terms over the interface is essential. An interpolation method is presented. The initial condition for the computation is the eigenmode derived from the linearized analysis of the base Couette flow. Results are obtained within the linear regime of wave development and are validated against linear theory. Calculations are continued into the nonlinear regime to address the nonlinearity effects.

Bound states of topological defects in Faraday ripples

A.B.Ezersky, S.V.Kiyashko, and A.V.Nazarovsky
Institute of Applied Physics, 46 Uljanov Str., Nizhny Novgorod 603600, Russia
Email: ezer@appl.sci-nnov.ru

Keywords - Waves - Hydrodynamic instabilities - Interaction of defects

Abstract – Bound states of two topological defects of the same sign appearing in parametrically excited ripples on a liquid surface are investigated. Unlike the well known edge dislocations observed in thermo-convection and liquid crystals the topological charge of which is equal to $1(2\pi)$, in the case considered we found stable bound states with the topological charge equal to $2(4\pi)$ (see Fig. 1 a). Such a state appears due to an external homogeneously oscillating field. Parametric forcing results in excitation of a pair of counterpropagating surface waves. The topological defect belonging to one wave due to the coupling with parametric pump introduces phase distortions into counterpropagating wave. Therefore, strong interaction between topological charges takes place.

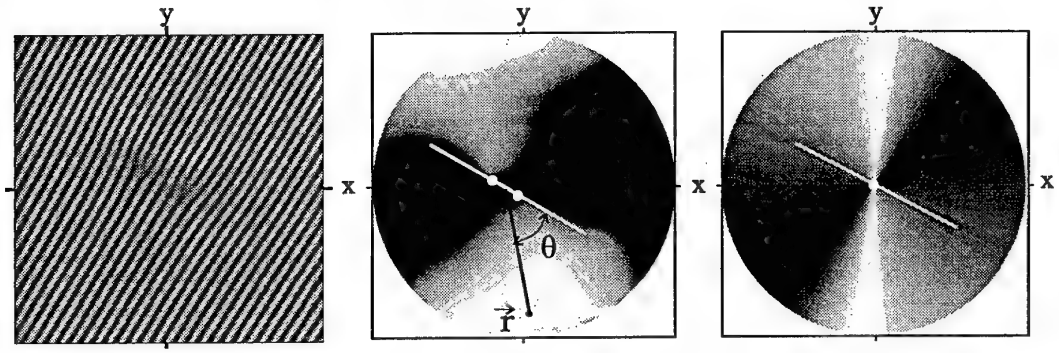

Figure 1: (a) Field of two topological defects constituting bound state; (b) phase field of bound state ($\phi - 2\theta$), the bright line corresponds to the direction of wave propagation, the points are the positions of topological charges; (c) theoretically calculated phase field.

It was revealed that such bound states possess the properties of particles: they may be scattered at each other, annihilate, and form quasistable domain walls. It was elucidated that the distance between the topological defects in bound state depends on supercriticality and on the thickness of the liquid layer. To characterise the interaction of the topological charges constituting the bound state we extract the phase field of spatially periodic structure presenting the field as $u = A(r,\theta)expi((\vec{k}\vec{r} + \phi(r,\theta)) + c.c.$ where $\vec{k}$ is the wavenumber of the structure, A and ϕ are the amplitude and phase of the structure, θ is the azimuthal angle, and $\vec{r}$ is the radius vector, like it is shown in Fig. 1 b. It was found experimentally that the phase field of bound state at a large distance $r = |\vec{r}|$ from topological charges has a form:

$$\phi = 2\theta + Dsin2\theta + \Phi(\theta),$$

where D is a value of order 1, $\Phi(\theta)$ is the sum of harmonics with amplitudes much less than 1, and the term 2θ means that the topological charge of this bound state is 2. An asymptotic theory was constructed that enables us to explain the experimental dependences. In particular, the phase field obtained theoretically is shown in Fig. 1 c. It coincides well with experimentally observed field (cf. Fig. 1 b). Thus, the interaction of topological defects leads to arising of quadrupole component in the phase field of the bound state of two topological defects existing in spatially periodic structure.

This work was supported by the Russian Foundation for Basic Research, grant N 99-02-16493.

Transition between Regular and Mach Reflection of Shock Waves: New Numerical and Experimental Results

M.S. Ivanov, A.N. Kudryavtzev, G.N. Markelov, D.V. Khotyanovsky,
S.B. Nikoforov, A.M. Kharitonov, V.M. Fomin
Institute of Theoretical and Applied Mechanics
Siberian Division of Russian Academy of Sciences
Novosibirsk, Russia
Email: ivanov@itam.nsc.ru

Keywords - Regular and Mach reflection - Transition - Numerical and Experimental study

Abstract - New numerical and experimental results on the transition between regular and Mach reflections of steady shock waves between two inclined wedges are presented.

An existence of two distinct theoretical criteria, von Neumann criterion and the detachment criterion, that predict the transition between regular and Mach reflection of strong shock waves, implies that this transition could be attended by a hysteresis. The possible hysteresis phenomenon predicted by Hornung et al. (1979) encouraged extensive experimental and numerical studies of this problem. The hysteresis was indeed observed experimentally by Chpoun et al. (1995), and later by Ivanov et al. (1997), and also numerically by Ivanov et al. (1995). However, there exist discrepancies between the experimental results and the results of computations, and also between the experimental results obtained at different wind tunnels. One of the possible reasons for these discrepancies may be the flow three-dimensionality, which is always present in the experiments where the models have a finite span.

In this study we investigate in detail the effects of three-dimensionality. Characteristic features of 3D shock wave configuration, such as peripheral Mach reflection, non-monotonous Mach stem variation in transverse direction, the existence of combined Mach–regular–Mach shock wave configuration, have been revealed in the numerical simulations. The application of laser sheet imaging technique in streamwise direction allowed us to confirm all the details of shock wave configuration predicted numerically in our experiments. Close agreement of the numerical and experimental Mach stem heights is also shown.

REFERENCES

[1] H.G. Hornung, H. Oertel, and R.J. Sandeman, "Transition to Mach reflection of shock waves in steady and pseudosteady flow with and without relaxation," *J. Fluid Mech.*, Vol. **90**, pp. 541–560 (1979).

[2] A. Chpoun, D. Passerel, H. Li, and G. Ben-Dor, "Reconsideration of oblique shock wave reflections in steady flows. Part 1. Experimental investigation", *J. Fluid Mech.*, Vol. **301**, pp. 19–35 (1995).

[3] M.S. Ivanov, G.P. Klemenkov, A.N. Kudryavtsev, S.B. Nikiforov, A.A. Pavlov, V.M. Fomin, A.M. Kharitonov, D.V. Khotyanovsky, and H.G. Hornung, "Experimental and numerical study of the transition between regular and Mach reflection of shock waves in steady flows", *Proc. 21st International Symp. Shock Waves*, Vol. **2**, pp. 819-824 (1997).

[4] M.S. Ivanov, S.F. Gimelshein, A.E. Beylich, "Hysteresis effect in stationary reflection of shock waves," *Phys. Fluids*, Vol. **7(4)**, pp. 685–687 (1995).

STABILITY 0F A POINT BLAST WAVE IN AN IDEAL GAS OF A RADIUS-DEPENDING DENSITY

V.M.Ktitorov

Theoretical Division, Russian Federal Nuclear Center (VNIIEF), Arzamas-16, 607190, Nizhnii Novgorod Region, Russia,

Tel (07) 8313045778, Fax (07) 8313042729, E-mail : ktitorov@md08.vniief.ru

Stability of a point blast wave in an ideal gas is considered in the case when gas density before shock front is a power function of radius: $\rho \sim r^k$. The spherical ($s=3$) and cylindrical ($s=2$) blast waves are considered in the unified manner. The perturbations are expanded into spherical harmonics. Perturbations R_1 of shock wave radius R are expanded too. We suppose that the components of expansion are power functions of time t for each harmonic number:

$R_{1nm} \sim R^{\lambda+1} \sim t^{\frac{2(\lambda+1)}{k+s+2}}$ Where λ is a complex number.

The components of expansion of perturbations of hydrodynamic values are presented in the self-similar form (Ref.1,2).

The eigenvalue problem is formulated. This problem is solved, complex values of power exponent λ are calculated as eigenvalues. These eigenvalues are calculated in a wide region of values of γ and n (Fig.1). The eigenvalues are calculated numerically in the general case of arbitrary values of harmonic number n and gas adiabatic exponent γ and analytically in some special cases: $n=1$, $n>>1$, $\gamma-1<<1$.

Instability region on n-γ plane (here γ stands for a gas specific heat ratio and n stands for a harmonic number) is determined in all cases considered (Fig.2). Critical values of γ_c determining the blast wave stability are calculated. For k equal to $-2,-1,0,1,2$ corresponding values of γ_c for spherical blast wave are equal to $1.12,1.17,1.20,1.21,1.22$.

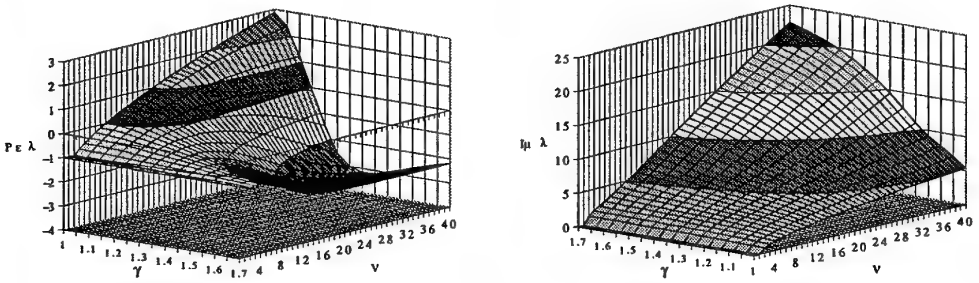

Fig.1 Values of complex exponent λ in the case of spherical blast wave in a gas of constant initial density ($s=3$, $k=0$). For the case $\gamma=1$ values are calculated using analytic expressions.

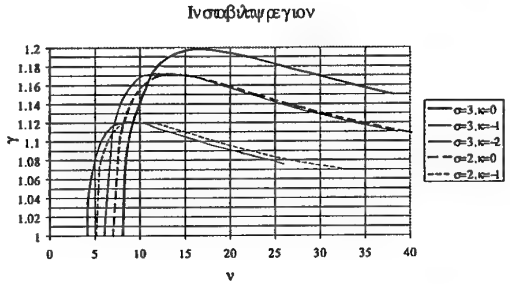

Fig. 2 Instability region on the plane n-γ for spherical and cylindrical blast waves in the case when gas initial density is decreasing with radius.

References

1.V.M.Ktitorov, "Asymptotical development of point blast wave small perturbations," Voprosy Atomnoi Nauki i Tekhniki, Ser.Teoreticheskaya i Prikladnaya.Fizika (Atomic Science and Technique Issues, Ser. Theoretical and Applied Physics), No2, p.28, (1984);

2.D.Ryu and E.T.Vishniac, "The growth of linear perturbations of adiabatic shock waves," Astrophys.J. 313, 820 (1987);

Singularities in 1D nonlinear traveling waves

L. Pastur, M.T. Westra and W. van de Water

Physics Department, Eindhoven University of Technology, P.O. Box 513,
5600 MB Eindhoven, The Netherlands

Spontaneous supercritical bifurcations towards nonlinear traveling waves (TW) may occur in several systems driven out of equilibrium by an external constraint (as in hydrodynamics, optics, chemics, etc). In a one-dimensional spatially extended system, domains of right and left TW may develop independently in different spatial area. The collisions between such domains lead to singularities called sources (emitting singularity) or sinks (receiving singularity). Universal theoretical predictions has been performed in the frame of nonlinear amplitude equations, based on symmetry arguments. We present the first experimental results on the singularities of 1D hydrothermal traveling waves at the free surface of a fluid, and compare them to the theoretical predictions.

Inviscid stability of a jet, application to sound production in a recorder.

Koen Goorman (1), Pierre-Yves Lagrée (2), Claire Ségoufin (3), Benoît Fabre (3)
(1) T.U.E. Eindhoven (NL), (2) LMM / (3) LAM, Univ. Paris VI (F)
Email: segoufin@ccr.jussieu.fr

Keywords - Boundary Layer - Jet - Stability - Musical Instruments -

Abstract - In a recorder like instrument, sound is produced by interaction between an air jet and an acoustical field. Instability models of jets usually consider the velocity profile in the jet at the flue exit as the input for calculations of amplification factor and phase velocity of perturbations. These two factors are obtained by solving Rayleigh's vorticity conservation equation in a potential description. Therefore, the jet velocity profile is assumed to be constant along the jet axis. Here, we investigate the effect of the spreading of the jet on the unstable behavior.
First, the jet profiles are computed using the boundary layer approximation (stationary 2D, laminar incompressible Prandtl equations with constant pressure). As an example, starting from a flat profile at $x = 0$ (distance along the jet axis is adimensionalized by $h(hU_0/\nu)$ where $2h$ is the width of the slit), we see on the left figure some profiles. Enough downstream ($x > 0.5$) of the slit, the Bickley profile is obtained (as expected).

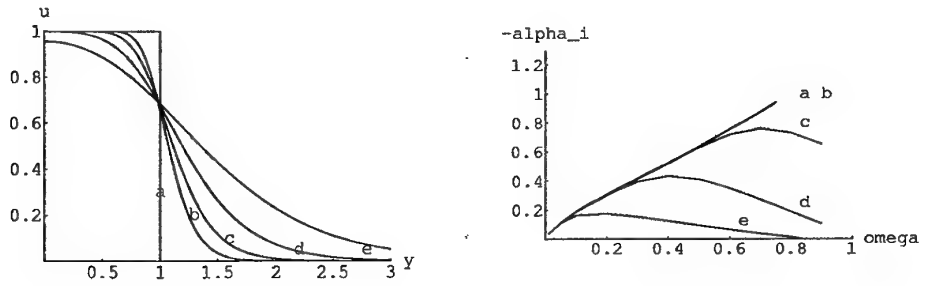

Example of some velocity profiles in the jet (left) and the associated curves of imaginary wave number ($-\alpha_i$) as a function of the (real) pulsation (ω) (right). Positions are: a: $x = 0$, b: $x = 0.01$, c: $x = 0.02$, d: $x = 0.05$, e: $x = 0.15$.

Second, to account for the convective instability of the jet, a spatial analysis is done (ω is real and given), the resulting complex wave number $\alpha = \alpha_r + i\alpha_i$ ($\alpha_i < 0$) is obtained. This analysis is justified by the fact that $(hU_0/\nu) >> 1$, and that the length wave scales with h, which is smaller than the spreading length of the jet $h(hU_0/\nu)$. The amplification factors corresponding to the previous family of profiles are ploted on the right figure.
Third, the global jet oscillation under acoustical perturbation will be determined by integration from the flue exit and compared to results obtained considering the profile at the flue exit. This will be compared to experimental amplification factors obtained by means of visualization of the flow.

References

[1] A.W. Nolle, JASA 103 (6) june 1998.
[2] C. Ségoufin & al. Acta Acustica january 2000 *to be published.*

Wave Propagation along a Jet in Stratified Fluid

I. Selezov[†], P. Huq[‡] and S. Shpakova[†]

[†] Institute of Hydromechanics, National Acad. of Sci., Kiev, Ukraine
[‡] College of Marine Researches Robinson Hall, Delaware University, Newark, USA

The statement and solution of a new problem are presented for wave motions along the vertical axisymmetric jet injected into a stable stratified fluid the density of which linearly increases with the depth. Flow in the jet is assumed to be potential, the motion of stratified fluid is governed by Boussinesq's approximation. The dispersion equation is derived and analysed. The conditions of wave existence are found and the analysis of phase and group velocities and wave modes is presented. It is shown that in external medium the wave disturbances propagate along the jet which have been observed in experiments.

Experimental results obtained by Huq [1] indicate that close to the jet exit z=0, the potential zone of the jet maintains a constant vertical axisymmetric form in accordance with Pratte et al. [2]. Further from the exit the jet is turbulent and grows in scale due to entrainment of ambient fluid. Additionally, the trajectory of the jet is bent due to the crossflow.

It is shown that for real values of the circular frequency omega and the wave number k solutions for traveling waves propagating in stratified fluid from the jet in radial direction do not exist. However, there are wave disturbances localized near and propagating along the jet. These disturbances were observed in the experiments of Huq [1].

The group velocity is shown to be negative, that is the energy is transported in the direction counter to that of wave propagation. In addition, the energy transport in the jet is sufficiently less than in the external region near the jet.

References

[1] Huq P. Observations of jets in density stratified crossflows. Atmospheric Environment, 1997, 31, N13, 2011-2022.

[2] Pratte B.D., Baines W.D. Profiles of the round turbulent jets in a crossflow.J. Hydraulic Division, ASCE, 1967, 93, N1, 53-64.

Generation of barotropic and baroclinic wave packets coupled in the common nonlinear critical layer of a weakly supercritical zonal flow

S.V. Shagalov
Department of Nonlinear Dynamics
Institute of Applied Physics RAS, Russia
Email: reutov@appl.sci-nnov.ru

Keywords - Zonal Flow - Nonlinear Critical Layer - Explosive Instability

Abstract - This paper deals with the problem of generation of barotropic and baroclinic nonlinear wave packets in a horizontally sheared and continuously stratified (along the vertical direction) zonal flow within the framework of the beta-plane approximation. Dissipation in the flow is supposed to be asymptotically small, i.e. the Reynolds number is large and weak bottom damping due to the presence of a thin Ekman layer is taken into account. The basic flow is assumed to have the form of a free shear layer and hence in the inviscid limit (in accordance with the Kuo theorem [1]) it is unstable with respect to barotropic and baroclinic disturbances whenever the gradient of the Coriolis parameter is taken below threshold value. Dynamics of the weakly dissipative flow is studied within the limit of weak supercriticality defined through the departure of the Coriolis parameter gradient from its marginal value in the ideal flow and the Ekman dissipation parameter. In this case just two modes having different wave numbers, namely the barotropic mode and the main baroclinic one, is shown to excite due to the interaction with the common critical layer (CL) in the flow if some restrictions are imposed on the range of the internal deformation radius value.

An asymptotic approach based on the method of the matched asymptotic expansions with respect to the small supercriticality was employed to derive the system of the three coupled equations describing dynamics of the relative vorticity in the nonlinear CL and the evolution of the complex amplitudes of the barotropic and the baroclinic wave packets. Similarly to [2] the effects of finite bandwidth of the instability range for both modes are incorporated in the governing equations. For the moderate supercriticality the CL was proved to be quasistationary and the vorticity equation was solved approximately by expanding the vorticity profile in small wave amplitude in the framework of the quasilinear approximation taking into account distortion of the mean vorticity profile as the main effect responsible for the instability saturation. In the case when modes frequencies were chosen to be incommensurate mutual suppression of the barotropic and the baroclinic modes (competition) leading to mode selection in the established regime was revealed. Resonant modes coupling through the condition of the second harmonic resonance (this is true for the certain value of the internal deformation radius) was shown to cause an explosive instability. In this case jump-like simultaneous excitation of the both modes at certain value of the supercriticality was revealed and the dependence of the established waves amplitudes on the supercriticality was analysed.

1.Pedlosky,J., Geophysical Fluid Dynamics, Springer-Verlag (1982). 2.Reutov V.P., Shagalov S.V., Rybushkina G.V. Advances in Turbulence (ed. U.Frish). Kluwer,1998, p. 483-486.

This work was supported by the Russian Foundation for Basic Research (project code 98–05–64686).

Excitation of acoustic waves in shear flows: vortex-wave mode conversion

G. D. Chagelishvili[1,2], A. G. Tevzadze[1,3], G. Bodo[4], P. Rossi[4] and G. T. Gogoberidze[1]
[1] Abastumani Astrophysical Observatory, Tbilisi, Georgia
[2] Space Research Institute, Moscow, Russia; georgech@mx.iki.rssi.ru
[3] Centre for Plasma Astrophysics, KULeuven, Belgium; alexander.tevzadze@wis.kuleuven.ac.be
[4] Osservatorio Astronomico di Torino, Pino Torineze, Italy; bodo@to.astro.it

Keywords - Wave dynamics - Vortex dynamics - General acoustics

Abstract - In the present study velocity shear induced phenomenon of the vortex-wave mode conversion is investigated. Found in Chagelishvili et al. 1997 (Phys.Rev.Letters **79**, 3178) this linear phenomenon is non-resonant by nature and occurs abruptly. Linear character of the phenomenon allows to identify the perturbation modes and interpret the acoustic wave excitation process in terms of the mode conversion. In this sense presented mechanism differs in principle from the Lighthill's stochastic mechanism of the aerodynamic sound generation. We study the unbounded compressible flow with linear shear of velocity. Linear dynamics of the spatial Fourier harmonics of perturbations allows to reveal the basic properties of the mode conversion phenomenon. Excitation of acoustic waves is more efficient in high shear flows, but is not restricted by the threshold (minimal) value of the shear parameter. We use numerical analysis to simulate the nonlinear dynamics of the shear flow with initially input vortex mode perturbation package. We study the spatial appearance of the acoustic wave generation as well as the nonlinear development of the process. Excitation of waves clearly occurs at times, when the spatial characteristics of the perturbation package (wave-numbers) change in sign during its variation resulted by the shearing background effect on the wave-crests. Generated waves may be identified by several characteristic features: nonzero group velocity (see Fig.1c-h), characteristic periodic phase difference between the wave-packages propagating in the opposite directions (see Fig.1e-f) and potential velocity field (see Fig.2). Presented phenomenon deals with fundamentals of wave excitation theory and makes acoustic waves the natural ingredient of the turbulent flows.

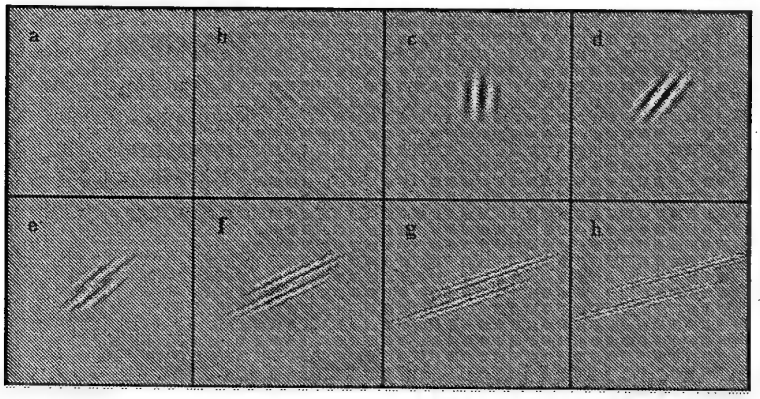

Fig.1 *The evolution of the shear flow density. Initial perturbations are composed by the superposition of the horizontal flow with vertical shear of velocity and vortex-density perturbation field. Conversion of the vortex-density to the acoustic density field occurs at times shown on graph* **c**. *Generated waves spread in the opposite directions (see* **c**–**h**).

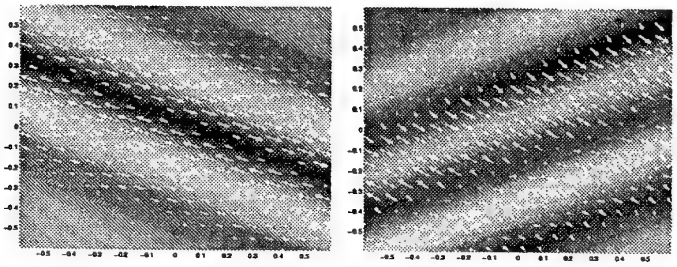

Fig.2 *The velocity field of the perturbations is shown on the background shading of the flow density in the equal time intervals before (left) and after (right) the mode conversion. Change of the nonpotential character of the perturbations is clearly seen.*

Interfacial instabilities of the axisymmetric core-annular flow in a constricted tube[1]

Ch. Kouris and J. Tsamopoulos
Laboratory of Computational Fluid Dynamics, Department of Chemical Engineering
University of Patras, Greece
Email: tsamo@chemeng.upatras.gr

Keywords: - Two phase Core-Annular Flow - Constricted Tube – Steady & Dynamic Analysis

Abstract – In this study we investigate the time evolution of the axisymmetric core-annular flow of two immiscible fluids in a cylindrical tube whose radius varies sinusoidally with the axial distance. The governing equations are the complete radial and axial momentum balances, the incompressibility of both fluids and the usual conditions of no-slip, no penetration at the solid wall, finiteness at the axis of symmetry and periodicity of all variables in the axial direction. We also require the normal and the tangential force balances, taking into account the effect of surface tension, at the fluid/fluid interface, which is determined by a kinematic condition. In order to reduce the computational cost we solve these equations using the streamfunction-vorticity formulation. Time integration is performed using the implicit Euler method, while each variable is approximated by a Pseudo-spectral method with Chebyshev polynomials in the radial direction and Fourier modes in the axial one.

The dimensionless form of these equations shows that the flow is controlled by seven dimensionless numbers: 1) the viscosity and 2) the density ratio of the fluids, 3) the Reynolds, 4) the Weber and 5) the Froude numbers, 6) the constriction ratio, which is the ratio of the minimum to the maximum radius of the tube, 7) the aspect ratio, which is the ratio of the maximum tube radius to the axial wavelength of the tube. Furthermore, we have shown (Kouris & Tsamopoulos, J. Fluid Mech., submitted, 2000) that it is important to retain as many undulations of the tube as computationally possible in order to obtain dynamic results that are independent of their number. The initial condition that we use in each case is the steady solution of the above equations and, first, we reproduced the growth rates computed independently by using linear stability theory. Under steady flow conditions, we have found that, when the total flow rate is against gravity and the core fluid is more viscous and lighter than the annular one, counter current flow takes place with the annular fluid flowing in the direction of gravity. However, integrating the equations of motion using as initial condition this steady solution we have found that in the non-linear, dynamic regime the fluid/fluid interface becomes wavy (figure on the right) and, as a result it carries along more of the annular fluid inside its troughs. Simultaneously the core fluid decelerates (figure in the left), and the striking characteristic of the new regime is that both the core and the annular fluid flow in the same direction against gravity. The flow rate versus time as well as the wave form at dimensionless time t=22.707 and the flow geometry can be seen in the following figures. A complete parametric study will be presented.

[1]Research partially supported by the Ministry of Education of Greece (EPEAEK, Grant # 51)

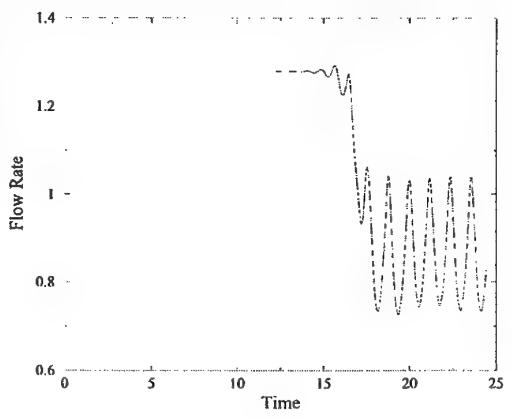

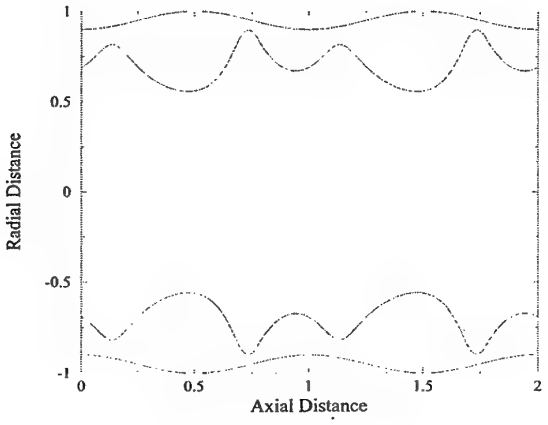

On the instability of non-isothermal flow between coaxial rotating disks

Ewa Tuliszka-Sznitko*, Chyi-Yeou Soong**

*Institute of Thermal Engineering, Technical University of Poznan, ul.Piotrowo 3, 60-965 Poznan, Poland, e-mail:sznitko@sol.put.poznan.pl.

**Rotating Fluids and Vortex Dynamics Laboratory, Chung Cheng Institute of Technology, Tahsi, Taoyuan, Taiwan 33509, Rapublic of China, e-mail cysoong@ccit.edu.tw

Keywords-Rotating disks systems - Flow instability

Abstract-The rotating-disk flows are of fundamental and practical interests and have long been one of the most important topics in the fluid dynamics. The fluid flow between rotating disks are very complicated in nature due to the possibilities of flow reversal, unsteadiness and instability. For the case of the non-isothermal fluids, however, the thermal effects induce more complexities in the flow fields. In the past decades, numerous studies on hydrodynamic characteristics of rotating disk flows have been conducted. Relatively, less effort has been done on this class of rotating non-isothermal flows. The objective of the present study is to investigate the flow stability of the non-isothermal fluids between two rotating disks. The buoyancy effects stemmed from the non-uniformity of the temperature field with the presence of the rotational forces, including centrifugal and Coriolis, are taken into account. A similarity model of the thermal flow with the assumption of Boussinesq fluids is formulated for generating basic solutions of the axially symmetric flows. The disturbance equations are derived by expressing the velocity, pressure and temperature fields as a superposition of the basic state and perturbed flow. The resultant linear stability equations are then solved by a spectral collocation method based on Chebyshev polynomials. Linear stability equations and boundary conditions create eigenvalue problem. The global solution method utilised for solving the eigenproblem yields the full spectrum of the least damped waves.

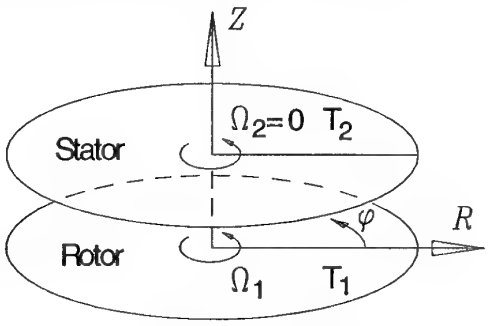

Schematic picture of the rotating disks system

The major concern of the present work is the influence of the rotational-induced buoyancy on the flow instability characteristics, which was not considered in the previous stability analyses. For all cases studied in the frame of this paper, two different types of instability have been observed on Disk 1 and Disk 2 (Type I and Type II). We have found that the boundary layer of the slower rotating disk is more unstable than that on the faster rotating disk. For the case without thermal buoyancy effect, the present results have been compared with available experimental data.

Some aeroelastic and dynamic characteristics of the cylinder elastically supported in the axially symmetric channel with a fluid flow

Václav Vlček a Martin Luxa
Institute of Thermomechanics, Czech Academy of Sciences
Prague, Czech Republic
Email: vlcek@it.cas.cz,luxa@it.cas.cz

Keywords - Aeroelasticity - Vibration - Internal Flow

Abstract - Aerodynamic excitation of plug vibrations in control valves have been simulated in a set-up pictured below. A fixed cylinder with a short elastically mounted cylindrical afterbody is placed in an axisymmetric channel. This elastic support is materialized by a flexible joint, permitting oscillations around the point S (see Figure), and transmitting the afterbody oscillations to the exterior ring k. This design provides a possibility to influence the afterbody vibrations via the ring k, namely to change the stifness, or to fix the afterbody. Light emitted by a laser diode built inside the afterbody at the axis is recorded by photodetector (8×8 mm), and can thus visualize movement of the afterbody in a plane normal to its axis. The diameter of the channel was 120 mm, the diameter of the vibrating body was 80 mm, $Re \approx (1 \div 20).10^4$, the eigenfrequency of the body in the still air $f_o = 11$ Hz, the dimensionless dumping coefficient was 0,017.
A high speed (blow-down) wind tunnel has been used for higher velocities, an Eifel type wind tunnel has been used for lower velocities. A special sealed modification of the test section had to be used in order to enable optical measurements at higher velocities.
During some tests controlled disturbances (pressure pulsations, turbulence) have been introduced in the oncoming flow.

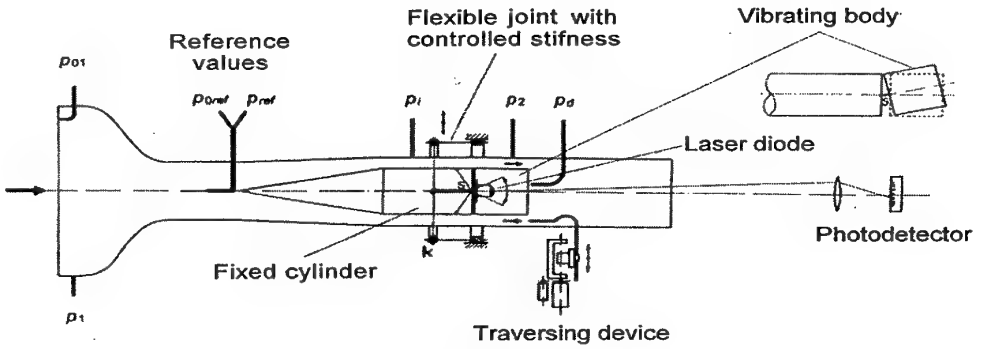

The experimental set-up

The base pressure coefficient $c_{pd} = (p_d - p_2) / (\rho_2 v_2^2/2)$, frequency and amplitude changes has been plotted against flow velocity. Both the trajectory of the cylinder base centre and interferogrammes of the near wake of the cylinder were recorded, however interferogrammes were not evaluated.
The results obtained were used for validation of numerical simulation and for analyzing the near wake structure of cylinders located coaxially in the channel flow.

The trajectory and stability of a spiraling liquid jet

I. Wallwork, S.P. Decent and A.C. King
School of Mathematics and Statistics, The University of Birmingham,
United Kingdom
email: wallwoim@for.mat.bham.ac.uk

We examine a spiraling liquid jet which emerges from a rotating orifice. This work is in part motivated by Norsk Hydro, a Norwegian company who manufacture fertiliser pellets. In their process, a sieve-like cylindrical drum spins rapidly about a central axis. Molten fertiliser is pumped into the top of the drum, and emerges from the holes in the curved surface of the drum in the form of thousands of spiraling liquid jets.

In this poster we present results on the trajectory and stability of such curved liquid jets. Our initial calculations have concentrated on the flow of inviscid jets. The trajectory of such jets is examined using asymptotic methods, since the jet is assumed to be slender. The stability can then be examined using a multiple scales approach.

Since the rate of rotation is large, the jets do not fall under gravity significantly before breaking up into droplets. Therefore, in this presentation we will concentrate on results where gravity is 'switched-off' and the jets move in a horizontal plane. However, some work has been carried out on spiraling liquid jets which fall under gravity, and these results will also be briefly discussed.

Latecomers

Numerical solution of flow of a second-order fluid over an enclosed rotating disc

H.G.SHARMA[1] AND K.S.BIRADAR[2]
[1]Department of Mathematics, University of Roorkee, Roorkee, India
[2]P.D.A. Engineering College, Gulbarga, India

Finite difference method is used to obtain the solution of non-linear boundary value problem arising due to the steady motion of an incompressible second-order fluid (flowing with a small mass rate of symmetrical radial outflow) over a finite rotating disc enclosed within a coaxial cylindrical casing. The resulting equations are converted into a set of difference equations. Starting from the known values of flow functions for small values of the Reynolds numbers, the solution is extended for larger Reynolds number, by making use of Newton-Raphson iterative method and Gauss-elimination method. The second-order effects on the velocity components have been investigated in detail in the regions of and inflow and illustrated graphically. Such flows are useful in Chemical and Mechanical industries.

Author Index

A

Adams N.A. 5
Afenchenko V.O. 104
Affeld K. 218, 222, 230
Aikawa H. 52
Alekseenko S. 102
Andersen A. 193
Anderson P.D. 117
Andersson H.I. 7, 184, 201
Angelis E. De 202
Anne-Archard D. 157
Anthore R. 15
Antipin V. 102
Aoki K. 52
Apel J. 225
Arina R. 113
Aristov V.V. 45
Armenio V. 65
Aroussi A. 165, 253
Asmolov E.S. 17, 213
Auteri F. 150
Azzopardi B.J. 174

B

Babenko V.V. 226
Babiano A. 110
Bake S. 62
Barenblatt G.I. 1
Barthès-Biesel D. 2, 140
Bastiaans R.J.M. 63, 261
Bastian H. 195
Basu A.J. 112
Belcher S.E. 85
Bergmans J. 262
Beris A. 200
Berkouk K. 227
Biesheuvel A. 21
Biferale L. 255
Bijl H. 123
Billingham J. 103, 164
Biradar K.S. 285
Bisset D.K. 31
Blondeaux P. 100
Blyth M.G. 129
Bobylev A. 102
Bodo G. 280
Bognetti L. 37
Bøhler E.M. 54
Bohr T. 193
Bokhove O. 77
Bontozoglou V. 105, 106
Booij R. 82
Borée J. 115
Bostel F. 15
Brand B.A. 214
Braza M. 157
Brenn G. 27
Brocchini M. 100
Brouwers J.J.H. 46
Brücker Ch. 228
Brule B.H.A.A. van den 196
Bury Y. 115
Buyze R. 192

C

Cai Z.X. 229
Campos L.M.B.C. 249
Cancelli C. 113
Caramiello C. 147
Caro C.G. 127, 132
Carpenter P.W. 66, 154, 158, 227
Casciola C.M. 202
Castro I.P. 86, 207
Cenedese A. 240
Chagelishvili G.D. 280
Charnay G. 115
Charru F. 160
Cheng H. 86
Chernov V.V. 84
Chorda J. 90
Clercx H.J.H 34, 53, 118, 247
Cohen J.E. 111
Coiret A. 96, 271
Colin C. 14
Colley A.J. 158
Cooper R.J. 164
Cortis A. 163
Costa M. 147
Coutsias E.A. 34
Cox E.A. 61
Crespo A. 24
Creuse E. 55

D

Dahlhaug O.G. 184
Dalziel S.B. 76, 79
Dartus D. 90
David T. 137
Davies C. 154
Decent S.P. 25, 284
Decré M.M.J. 192
Demay Y. 204
Dequand S. 58, 97
Diaz A. 140
Dillingh J.E. 272
Dillman A. 6
Dimakopoulos Y. 263
Ding Z. 134
Dizès S. Le 187
Doinikov A. 26
Domenichini F. 64
Dongen M.E.H. van 169
Doorewaard M.A.T. 188
Doorly D.J. 127, 132
Doorne C.W.H. van 250
Dreyer M.E. 152

Duck P.W. 72
Duhar G. 14
Dušek J. 146
Džiugys A. 221

E

Eames I. 189
Eich T. 199
Ellingsen K. 173
Eloy C. 187
Exner A. 61
Ezersky A.B. 84, 91, 104, 273

F

Fabre B. 145, 277
Falkon L. 230
Falossi M. 113
Favini B. 37
Fekken G. 49
Fernandez-Britto J. 230
Fernández-Feria R. 56
Fernholz H.H. 42, 62
Fessant A.L. Le 90
Feuillebois F. 13, 15
Finnigan J.F. 85
Firdaouss M. 163
Fitzpatrick J.A. 270
Flór J.-B. 189
Fomin V.M. 274
Fortin A. 204
Franceschi M. de 87
Frank A.M. 29
Franke P.T. 127
Friedman M.H. 134
Früh W.-G. 88

G

Gaki A. 26
Gal P. Le 187
Galaktionov O.S. 117
Galiev Sh.U. 99
Galiyev T.Sh. 99
Gampert B. 199
Gayev Ye.A. 235
Geers L.F.G. 41
Geld C.W.M. van der 19, 214
Gerrits J. 47
Ghidersa B. 146
Gogoberidze G.T. 280
Gökçöl O. 167
Goldfeld M.A. 251
Gomez T. 80
Goorman K. 277
Goubergrits L. 218, 222, 230
Gramberg H.J.J. 203
Grossmann S. 209
Grota B. 171
Guérin S. 96, 271
Guermond J.L. 163
Guiot C. 119
Gunawan A.Y. 159
Gunnarsson J. 191

H

Haas P.C.A. de 53
Halpern D. 124
Hanjalić K. 32, 35, 41
Härtel C. 75
Heel A.P.G. van 196
Heijst G.J.F van. 109, 118, 179, 180, 186, 188, 247
Heiler M. 168
Hendriks E.C.J. 250
Henry R. 96, 271
Hewitt R.E. 156
Heydt A. von der 139, 231
Higginson R.C. 79
Higuera F.J. 151
Hill N.A. 136
Hillen B. 232
Hinch E.J. 160
Hirsch Ch. 40
Hirschberg A. 58, 97, 125, 145
Hoarau Y 157
Hoeijmakers H.W.M. 144, 272
Hofmann B. 215
Holford J.M. 76
Homsy G.M. 50
Hoogstraten H.W. 122, 232
Horsburgh M.K. 124
Hörschler I. 126
Hort M.C. 211
Housiadas K. 161
Hulsen M.A. 196
Hulshoff S. 58
Hunt J.C.R 31, 81
Huq P. 278

I

Ilyushin B.B. 236
Iollo A. 153
Iovieno M. 216
Ivanov M.S. 266, 274
Ivanov N.G. 190

J

Jensen O.E. 124
Jiménez-Fernandez J. 24
Jonáš P. 83, 252

K

Kaiser E. 215
Kalliadasis S. 50

Kalse S. 123
Kaplanski F. 243
Kaykayoğlu C.R. 167
Keays J. 264
Keirsbulck L. 71
Kelleners P.H. 269
Kenjereš S. 32
Kent E.F. 217
Kerr O.S. 149
Kerswell R.R. 44
Kertzscher U 218, 222
Keunings R. 200
Khabakhpashev G.A. 98
Khabakhpasheva T.I. 265
Kharitonov A.M. 274
Khatir Z. 66
Khotyanovsky D.V. 274
Kieft R. 208
Kim D.C. 219
King A.C. 25, 164, 284
King G.P. 114, 177
Kiyashko S.V. 91, 104, 273
Kleiser L. 5
Kluwick A. 61
Koehler R. 23, 155
Kogan M.N. 68
Kolodziej J.A 51
Konijnenberg J. van de 39
Konstantinov M. 170
Kooner S. 177
Korobkin A.A. 265
Korobov V.I. 226
Korte E. de 201
Kouris Ch. 166, 281
Krams R. 133
Krasnopolskaya T.S. 179, 180
Krogstad P.-Å. 38
Kruijt P.G.M. 117
Ktitorov V.M. 275
Kucukgokoglan S. 165, 253
Kudryavtzev A.N. 274
Kuerten J.G.M. 19
Kuibin P.A. 183
Kurkin A.A. 237
Kuvshinov B.N. 262

L

Labraga L. 71
Lafarge D. 163
Lagrée P.-Y. 128, 238, 277
Lakehal D. 175
Lally C. 131
Lamanna G. 169
Lammers J.H. 192
Landrini M. 54
Lange H.C de. 63, 261
Laure P. 204
Lebon G. 108
Lecoq N. 15
Lee K.W. 121
Legros J.C. 108
Leneweit G. 23, 155
Lesniak B. 130
Leuprecht A. 134, 135
Levêque E. 43
Leweke T. 148
Leygue A. 200
Liepsch D. 130
Liñán A. 10
Litvinenko A.A. 98
Lohse D. 18, 139, 181
209, 231, 255
Loots G.E. 122, 232
Lorthois S. 128
Luca L. de 147
Lucey A.D. 227
Luchini P. 4, 33
Luo X.Y 229
Luxa M. 283

M

Maanen H.R.E. van 174
Maas L.R.M. 95, 244
Maeder T. 5
Magnaudet J. 3
Manopoulos Ch.G. 233
Manders A.M.M. 244
Manuguerra M. 28
Manuilovich S.V. 69, 254
Maré C.S. 239
Marino B.M. 245
Markelov G.N. 266, 274
Markovich D. 102
Maršik F. 223
Mårtensson G.E. 191
Masmoudi K. 15
Mathew J. 112
Mathioulakis D. 233
Matsuo T. 130
Mattheij R.M.M. 53
Mazouz A. 71
Mazur O. 83, 252
Mazzitelli I. 255
McGloughlin T. 131, 234
Meijer H.E.H. 117
Meinke M. 126
Meleshko V.V. 109
Menacer M. 165, 253
Meskell C. 264, 270
Mestel A.J. 16, 129
Metcalfe A.M. 141
Meunier P. 148
Meyer D.G.W 62
Mezić I. 114
Michalski C. 143
Miladinova S. 108
Milelli M. 175
Minier J.P. 268

Molenaar J. 159
Montabone L. 110
Morii O. 210
Moros V.V. 226
Mortazavi I. 55
Müller U.K. 138
Murakhtina T.O. 185

N

Nagata M. 210
Naulin V. 39
Nazarovsky A.V. 84, 91, 273
Neemann K. 67
Nepomnyashchy A.A. 248
Neudel F. 225
Nielsen A.H. 34
Nieuwstadt F.T.M. 11, 81, 250
Nigen S. 198, 220
Nikoforov S.B. 274
Nikiforovich E. 246
Nørgaard Nielsen M. 193

O

Obermeier F. 170
O'Brien T.P. 234
Ohl C.D. 20
Okulov V.L. 184, 185
Ooms G. 174
Ortega Casanova J. 56
Oudheusden B.W. van 256

P

Packwood A. 211
Panfilov S.V. 172
Parolini N. 150
Pasquero C. 28
Pastur L. 276
Pearson B.R. 38
Pedley T.J. 141, 229
Pedrizzetti G. 120
Peiró J. 127, 132
Pelekasis N.A. 26, 73
Pelorson X. 125
Peregrine D.H. 9
Perktold K. 134, 135
Peters B.J. 221
Peters E.A.J.F. 196
Peters G.W.M. 117
Phillips T.N. 197
Pickering S.J. 165, 253
Pietrzak J.D. 94
Pigeonneau F. 13
Piva R. 202
Politano H. 80
Poplavskaya T.V. 267
Pouquet A. 80
Pozorski J. 268
Pozzi A. 70
Pribaturin N.A. 176
Prooijen B.C. van 89
Prosi,M. 134
Prosperetti A. 20
Provansal M. 143
Provenzale A. 8, 28, 110
Put F. 269

Q

Quadrio M. 33
Querzoli G. 240

R

Rampanelli G. 22, 87, 241
Rasmussen J.J. 39
Rath H.J. 152
Read P.L. 88
Rensink D. 27
Repetto R. 93
Reul H. 225
Reynolds A.M. 111
Ribe N.M. 59
Richter J. 193
Riddell G.D. 177
Rienstra M.H. 244
Rindt C.C..M. 208
Risso F. 173
Rist U. 62
Robins A.G. 78, 239
Rodes P. 157
Roesner K.G. 155
Rogers M.M. 31
Roos M.E. 81
Rosendahl U. 152
Rossi P. 280
Rowlands G. 114
Rubio P. 195
Rudi Ü 243
Rudman M. 114
Ruiz-Chavarria G. 43

S

Sakout A. 96, 271
Saudreau M. 115
Satijn M.P. 186, 247
Savory E. 235
Sbresny H. 57
Schep T.J. 262
Schmitt F. 40
Schmitz B. 139, 231
Schnerr G.H. 168
Schoemaker R.M. 53
Schouveiler L. 143
Schram P.P.J.M. 179, 180
Schram-Christensen M. 193
Schröder W. 126, 228

Seeger A. 218, 222
Ségoufin C. 145, 277
Selezov I. 278
Seminara G. 22
Semionov N.V. 257
Shagalov S.V. 279
Sharma H.G. 285
Sherwin S.J. 127, 132
Shikhmurzaev Y.D. 30
Shpakova S. 278
Shumilkin V.G. 68
Simanovskii I.B. 248
Slager C.J. 133
Slavtchev S. 108
Smeulders D.M.J. 163
Smirnaios D.N. 73
Smirnov E.M. 190
Smith B.L. 175
Somers L.M.T. 261
Soong C.-Y. 282
Speetjens M.F.M. 118
Spendiff M.K. 136
Staicu A.D. 258
Stamhuis E.J. 138
Steenhoven A.A. van 208
Stefes B. 42
Steijl R. 144
Steinseifer U. 228
Stenum B. 39
Stolz S. 5
Strauss K. 171
Sweeney C. 270
Szumowski A. 259

T

Tagliazucca M. 87
Takata S. 52
Tampieri F. 87
Taylor T.J. 78
Telle D. 242
Tevzadze A.G. 280
Thielen L. 35
Thomas L.P. 245
Thomas P.J. 177, 178
Toegel R. 18
Tognaccini R. 70
Tordella D. 216
Toschi F. 43, 255
Tournier C. 71
Trieling R.R. 188
Trifonov Yu.Ya. 107
Trigger S.A. 179, 180
Tsamopoulos J.A. 26, 73, 161
166, 263, 281
Tsangaris S. 233
Tsirkunov Yu.M. 172
Tubino M. 93, 241
Tuck E.O. 103
Tuliszka-Sznitko E. 282
Tunç M. 167
Tyvand P.A. 54

U

Uijttewaal W.S.J. 89, 92
Uruba V. 83, 252
Ustinov M.V. 68

V

Valette R. 204
Valougeorgis D. 48
Varlamova E.A. 183
Vassilicos J.C. 116
Vauquelin O. 242
Veldman A.E.P. 36, 47, 49
122, 232
Ven A.A.F. van de 159, 203
Versluis M. 139, 231
Verstappen R.W.C.P. 36
Verzicco R. 247
Videler J.J. 138
Vilain C. 125
Visser A. 94
Vittori G. 65, 100
Vlachogiannis M. 105, 106
Vlček V. 283
Volkov A.N. 172
Voort M. van der 250
Vosbeek P.W.C. 262
Voskamp J.H. 179
Vosse F.N. van de 133
Vrieling A.J. 81
Vries A.W.G. de 21

W

Wagner M.H. 195
Walker P. 137
Wallwork I. 284
Walters K. 198, 220
Wapperom P. 200
Water W. van de 38, 101, 258, 276
Waters S.L. 119
Watkins N. 127
Weele J.P .van der 181
Weigand C. 130
Weiss D.A. 27
Wellnhofer E. 218, 222
Wentzel J.J. 133
Werven M. van 174
Westerweel J. 250
Westra M.T. 101, 276
Wijngaarden L. van 21
Wilkes C. 199
Willems J.F.H. 125
Williams A.J. 197
Wingaarden H. van 214
Winkler G. 168

Wojciechowski J. 259
Wolters B.J.B.M. 133
Wonhas A.H.P. 116
Woods A.W. 77

X

Xu X.Y. 121

Y

Yannacopoulos A.N. 114
Yarin A.L. 27, 205

Z

Zannetti L. 153
Zardi D. 22, 87, 241
Zhigulev S.V. 68
Zima P. 223
Zoueshtiagh F. 178